



DEGRADING OUR DEFENSES

*novel features of human cytomegalovirus-induced
HLA class I ERADication*

Anouk Babette Carina Schuren

DEGRADING OUR DEFENSES

*novel features of human cytomegalovirus-
induced HLA class I ERADication*

Anouk Babette Carina Schuren

About the cover

It is not only viruses degrading the things that protect us. This macroscopic ER-like structure was created by human activity. With a far shorter evolutionary history than the herpesviruses, we have yet to find a sustainable balance with our own host – planet Earth.

New oil palm plantations near Pundu, Borneo, Indonesia (1°59' S, 113°06' E).

On the island of Borneo, 1.3 million hectares of virgin rain forest are deforested annually to be replaced by oil palm plantations. These plantations cause the loss of 80% of the original plant life and 80 to 90% of animal species, while the former rain forest served as a carbon sink. The demand for palm oil is growing each year. It is used in food products, detergents, cosmetics and biofuel. More than half of all packaged products contain palm oil. Fortunately, not all palm oil production is associated with deforestation. Products containing sustainably grown palm oil can be recognized by an RSPO certification.

Photo © by Yann Arthus-Bertrand (with permission)

© 2019 Anouk Schuren
ISBN: 978-90-9031492-1
Layout: Anouk Schuren
Printed by: Groenprint



This thesis was printed on 100% recycled FSC-certified Cocoon Offset paper. Two trees were planted to offset the carbon footprint associated with the printing and distribution of this thesis, resulting in a CO₂-neutral printing process.

Printing of this thesis was financially supported by Utrecht Medical Center Utrecht, Infection & Immunity Utrecht, UbiQ Bio B.V., ChipSoft B.V., the Netherlands Society of Medical Microbiology (NVMM) and the Royal Netherlands Society for Microbiology (KNVM).

Degrading our defenses
novel features of human cytomegalovirus-
induced HLA class I ERADication

Het breken van onze bescherming
nieuwe bevindingen in HLA klasse I afbraak door humaan cytomegalovirus
(met een samenvatting in het Nederlands)

Proefschrift

ter verkrijging van de graad van doctor
aan de Universiteit Utrecht op gezag van de
rector magnificus, prof.dr. H.R.B.M. Kummeling,
ingevolge het besluit van het college voor promoties
in het openbaar te verdedigen op
dinsdag 2 april 2019 des middags te 2.30 uur

door

Anouk Babette Carina Schuren

geboren op 19 augustus 1990 te Haren (Gn.)

PROMOTOR: Prof.dr. E.J.H.J. Wiertz

COPROMOTOR: Dr. R.J. Lebbink

Not in our heads but in our hearts
lies the power that leads us to great deeds.

- Charles Dickens

LEESCOMMISSIE:

Prof.dr. I. Braakman
Prof.dr. H. Ovaa
Prof.dr. F. Förster
Prof.dr. W. Stoorvogel
Dr. A.J.A.M. Sijts

PARANIMFEN:

Jery Baan
Ingrid Brak-Boer

TABLE OF CONTENTS

Chapter 1	General introduction	9
Chapter 2	Recent advances in viral evasion of the MHC class I processing pathway	25
Chapter 3	Multiple E2 ubiquitin conjugating enzymes regulate human cytomegalovirus US2-mediated immuno- receptor downregulation	41
Chapter 4	The UFM1 pathway impacts HCMV US2-mediated degradation of HLA class I	63
Chapter 5	Genetic editing of SEC61/62/63 abrogates HCMV US2-mediated HLA-I degradation by regulating US2 expression	93
Chapter 6	P97 association with UBXD8 is essential for HCMV US11-mediated HLA class I degradation	121
Chapter 7	Summarizing discussion	145
Appendices	<ul style="list-style-type: none">- Nederlandse samenvatting voor niet-ingewijden- Dankwoord- Curriculum vitae- List of scientific publications- List of popular-scientific publications	161



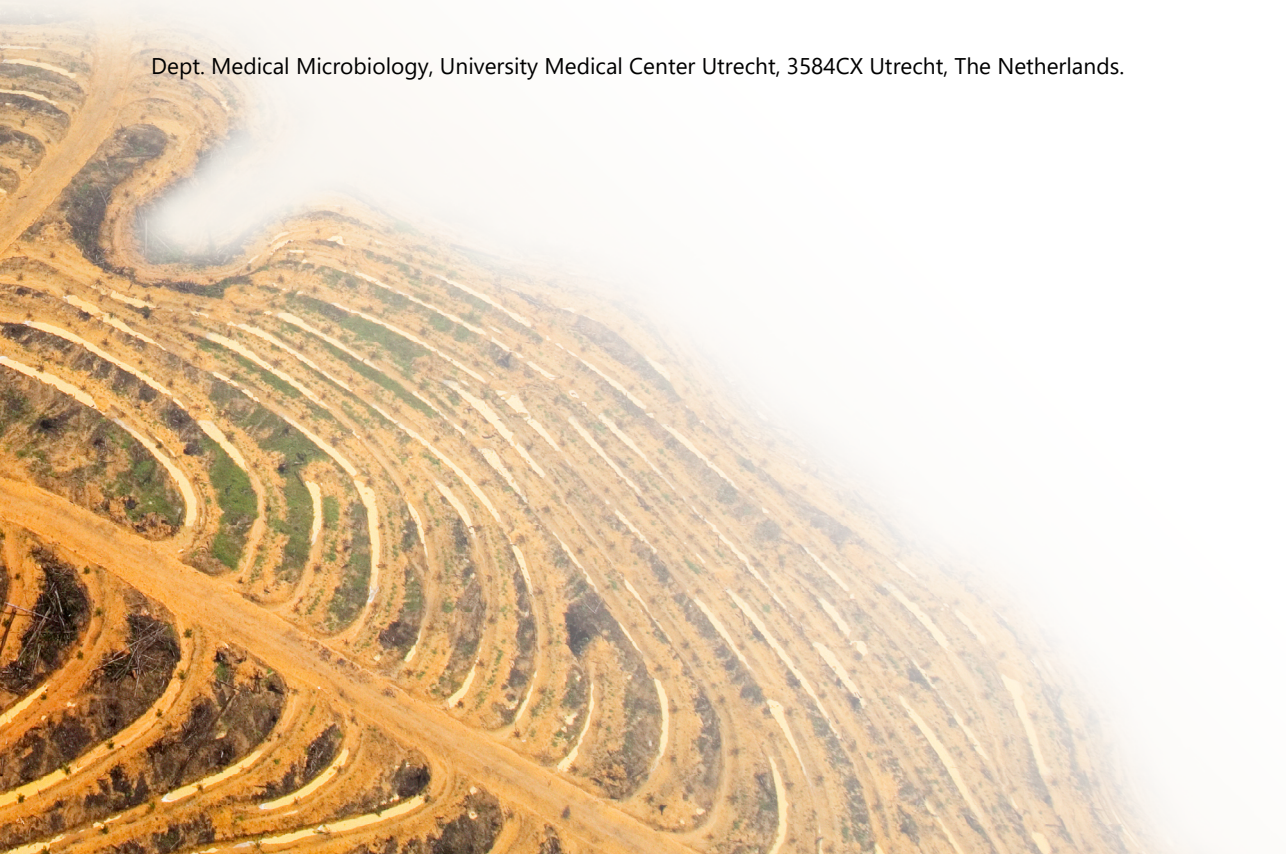
CHAPTER

1

General introduction

Anouk B.C. Schuren

Dept. Medical Microbiology, University Medical Center Utrecht, 3584CX Utrecht, The Netherlands.



Molecular piracy: hit-and-run versus hide-and-seek

For successful replication, viruses rely on the cellular machinery of the host they infect. They transform the cellular homeostasis to their own benefit, while shutting off cellular processes that do not contribute to viral replication. Virus-infected cells often die in this process. As the presence of a viral infection is sensed by the immune system¹, many viruses adopt a ‘hit and run’ strategy, replicating and spreading quickly, before being eliminated by the immune system. Viruses causing the common cold, such as rhinoviruses, exemplify this mechanism. Whether this strategy is successful depends on the characteristics of the virus. An 8- to 12-hour replication cycle makes rhinoviruses very suitable for a quick ‘hit and run’. Other RNA viruses, such as HIV, outsmart the immune system by rapidly accumulating mutations during replication, such that the adaptive immune system lags behind². Interestingly, the most lethal viruses are not necessarily the most successful. It is generally beneficial to the virus when its host remains fit enough to establish contact and infect others, rather than succumbing to the virus shortly after infection³. The *Herpesviridae* have adopted a different and quite unique strategy. Having originated hundreds of millions of years ago⁴, these viruses have co-evolved with their hosts for a long period of time. Extensive host adaptation allows herpesviruses to persist dormant in the body in perpetuity, while occasionally re-activating. This strategy is so successful that >90% of the population is infected with one or more herpesviruses^{3,5}.

Herpesvirus	Symptoms	% infected
Herpes Simplex Virus-1 (HSV-1)	cold sores (mostly oral, also genital), keratitis	~50-70%
Herpes Simplex Virus-2 (HSV-2)	sores (mostly genital, sometimes oral)	~20-30%
Varicella Zoster Virus (VZV)	chickenpox, zoster	~95%
Epstein-Barr Virus (EBV)	mostly asymptomatic; infectious mononucleosis, lymphoid and epithelial malignancies	~90%
Human Cytomegalovirus (HCMV)	mostly asymptomatic or mononucleosis-like; congenital disease, pneumonia, gastroenteritis, organ transplant rejection	~40-60%
Human Herpesvirus-6 (HHV-6)	roseola infantum, mononucleosis syndromes, focal encephalitis, pneumonitis	> 90%
Human Herpesvirus-7 (HHV-7)	mostly asymptomatic; acute febrile respiratory disease, fever, rash, vomiting, diarrhea, febrile seizures	unknown
Kaposi's Sarcoma-associated Herpesvirus (KSHV)	Kaposi's sarcoma	< 5%

Table 1 | Prevalence of human herpesviruses in the Netherlands. The % infected shows the percentage of the Dutch population with humoral immunity against these respective viruses, indicating (a history of) active infection. Source: RIVM.

The family of herpesviruses can be subdivided by tropism, with α -herpesviruses being neurotropic, β -herpesviruses polytropic, and γ -herpesviruses lympho- and epitheliotropic⁶. While most primary herpesvirus infections are mild or even asymptomatic, they can be life-threatening to the immuno-compromised and unborn children^{7,8}. Also in healthy individuals however, latent carriage or reactivation of herpesviruses can result in severe disease, such as Hodgkin's lymphoma in case of EBV⁹, or herpes zoster ('shingles') for VZV¹⁰.

An unusual alliance

As herpesviruses are carried lifelong, they can be seen as part of the host's microbial community, the virobiome, similar to the well-studied bacterial microbiome¹¹. Interestingly, even microbiota-like protective characteristics of latent herpesvirus carriage are observed. As the latent infection raises a permanent low-level activity in the immune system, herpesviruses could be beneficial by providing bystander protection against other pathogens as well as tumorigenesis. In mice, latent infection with the murine γ -herpesvirus 68 (γ HV68) protects against infection with *Listeria monocytogenes*, *Yersinia pestis*¹², and tumor formation¹³, while subclinical corneal HSV-1 infection provides long-lasting local protection against pseudorabies virus¹⁴. If a similar mechanism holds true for human infection, the protective effects of herpesvirus infections may have contributed to the high prevalence seen for many of its virus family members.

HCMV: the mother of birth defects

This thesis will focus on human cytomegalovirus, or HCMV. Its name is derived from the Greek *cyto* (cell) and *megalo* (large) because it generates large cells containing inclusion bodies¹⁵. These so-called "owl's eyes" were first discovered in histology samples from stillbirths around 1910¹⁶ and later around pioneering organ transplants in the 1960's¹⁷.

Although an infection with HCMV is generally asymptomatic, it causes severe disease in organ transplant recipients, AIDS patients, the elderly and particularly neonates¹⁷. In third-world countries, prevalence of HCMV infection is nearly 100%, with most individuals contracting the virus asymptotically during childhood. In developed countries, including the Netherlands, ~40-60% of the population is infected.

Because contact with the virus is less common in countries with a low HCMV prevalence, the average age of primary infection is higher in developed countries¹⁷. This results in an increased risk of contracting the virus at childbearing age. In developed countries, two percent of pregnant women become seropositive for HCMV during pregnancy^{8,18}, although this is often not recognized due to the asymptomatic to mild nature of the infection. HCMV can however cross the placenta to infect the unborn child, leading to congenital infection in 0.6-0.7% of all children in developed countries¹⁹. One in five of these develop symptoms, either at birth (e.g. low birth weight, jaundice) or afterwards, with hearing loss and mental retardation being the predominant outcomes¹⁸. These high numbers make HCMV the most common infectious cause of congenital defects.

A viral infection normally causes immunological memory, thereby preventing re-infection with the virus itself or a related strain. However, preconceptional immunity against HCMV (i.e. in seropositive women) provides only partial protection to mother and child²⁰. Reactivation of latent

virus, or super-infection with a novel virus strain can cause congenital infection as well. 10-30% of seropositive women experience superinfection during pregnancy^{19,20} and 1-3% of seropositive women deliver congenitally infected children. The relative abundance of seropositive women in the population makes secondary infection the predominant source of congenital HCMV infection²¹. These secondary herpesviral infections can occur because of the immune-evading properties of this virus family²².

Going underground: escaping immune surveillance

Herpesviruses, carrying a linear double-stranded DNA genome, are far less variable compared to previously mentioned RNA viruses such as rhinoviruses or HIV. The herpesvirus genome is unusually large for a virus, with HCMV containing the largest genome of the herpesviruses at 235 kilobases²³ – nearly 25 times larger than the HIV genome. This large and stable genome allows HCMV and other herpesviruses to carry a plethora of host-adapted immune-evasive genes²⁴.

While primary viral infection with HCMV can still occur in the absence of immune evasion^{25,26}, super-infection is, at least in rhesus macaques, only possible when immune-evasive proteins (evasins) are active. Immune evasion during primary infection hampers the formation of immunological memory, which in turn allows for follow-up infection events²².

One of the main targets of HCMV's evasins is the HLA class I antigen presentation pathway. HLA class I molecules (HLA-I) present intracellular peptides at the plasma membrane. This way, the presence of a viral infection can be signaled extracellularly to the immune system. The peptide-HLA class I complexes are recognized by CD8⁺ T lymphocytes, which display cytotoxic activity towards the infected cells. By reducing HLA class I levels, HCMV prevents recognition of the infection by CD8⁺ T cells. Interference mechanisms of HCMV and other viruses with HLA class I expression are reviewed in **Chapter 2**.

The unique short (US) region of the HCMV genome contains a family of (potential) evasins, named US2 to US11. While US7 to US9 are not extensively studied²⁷, US2, US3, US6, US10 and US11 are all dedicated to HLA class I downregulation through various mechanisms. US6 blocks the import of antigenic peptides into the ER²⁸, while US3 causes retention of HLA class I molecules inside the ER²⁹. US10 degrades the HLA class I paralogue HLA-G³⁰. Both US2 and US11 degrade ER-resident HLA class I molecules by hijacking a cellular quality control mechanism called ER-associated protein degradation, or ERAD^{31,32}.

The functions of these immune-evasive proteins are synergistic³³, and expression of single evasins does not protect against recognition by CD8⁺ T cells³⁴. The evasion proteins are likely expressed at different stages during HCMV infection, with US3 as immediate-early protein, US2 and US11 expressed during the early phase, and US6 during the late phase of infection^{35,36}. Moreover, each evasin displays specificity to certain HLA class I allotypes, extending the range of targets by combining multiple evasion proteins^{33,37}.

ER-associated HLA class I degradation by both US2 and US11 might seem redundant at first glance. However, the two evasins complement one another. While US11 degrades both mature HLA-I as well as partially unfolded HLA-I heavy chains, the activity of US2 may depend on the conformation of HLA-I³⁸⁻⁴⁰. Although both US2 and US11 bind to the ER-luminal domain of

HLA⁴¹⁻⁴³, the cytosolic HLA-I C-terminus is absolutely required for US11-mediated ERAD⁴⁴, but less so for US2⁴². Other differences between US2 and US11 include the ERAD pathways they hijack (described below), as well as the resulting ubiquitination on HLA class I. While HLA is ubiquitinated on its C-terminal lysines in the context of US2, ubiquitination does not seem to be required for US11-mediated degradation^{39,45}.

The interference with cellular processes by viral proteins is a valuable tool to study cellular functioning. In this thesis, US2 and US11 are used for this purpose. Because HLA class I degradation by US2 and US11 is so potent, this pathway is one of the commonly used model systems to study ERAD. This model has allowed the identification of many key components of mammalian ERAD, such as SEC61³¹, p97^{46,47}, Derlin-1⁴⁸, TMEM129^{49,50} and UBXD8. The functions of these factors are described below.

ERADication of misfolded proteins

Of all proteins synthesized, roughly one-third is directed to the endoplasmic reticulum^{51,52}. This high processing load requires an effective quality control mechanism, as accumulation of aberrant proteins has major pathological consequences⁵³⁻⁵⁵ (see below).

Protein translocation into the ER is facilitated by the SEC61 complex, also called the translocon. Upon entry into the ER, newly synthesized proteins undergo modifications such as glycosylation, formation of disulfide bonds, proteolytic cleavage and, with the help of chaperones, folding into their mature conformation. Should a protein fail one of these processes, it is recognized by ER quality control chaperones, initially for another folding endeavour⁵⁶. When a mature conformation ultimately cannot be reached, the protein is removed from the ER by the ER-associated protein degradation machinery (Fig. 1).

Following recognition of terminally misfolded proteins, ERAD comprises retro-translocation (sometimes called dislocation) towards the cytosol, ubiquitination, and eventually proteasomal degradation. When an ERAD substrate reaches the cytosol during retro-translocation, it is ubiquitinated by a consecutive cooperation of E1, E2 and E3 enzymes⁵⁷. The ubiquitinated retro-translocation intermediate is recognized by the AAA+ ATPase p97 (also called VCP)^{58,59}, which provides the pulling force to complete retro-translocation⁶⁰. However, as the poly-ubiquitin chain causes steric hindrance to p97, the substrate is partially de-ubiquitinated prior to extraction^{59,60}. Finally, the substrate is degraded by the proteasome, which may interact either directly with the ERAD complex at the ER membrane⁶¹ or in a cytosolic environment⁶². The latter requires a cytosolic chaperone complex, comprising Bag6, that guides the substrate towards the proteasome.

Many questions regarding ERAD remain unanswered. The exact composition of ERAD complexes at the ER membrane is only partially understood. They should contain at least a channel through which proteins cross the ER-membrane (the actual retro-translocon), a ubiquitin E2 conjugase and E3 ligase, a recruitment factor for p97, and p97 itself, but accessory factors required for correct positioning of the ERAD constituents and the substrate are possibly also involved.

ERAD is conserved in all eukaryotic cells. Therefore, it is often studied in yeast because the mutability of this model organism allows easy phenotypic screening on knockout strains. In *S. cerevisiae*, two ubiquitin E3 ligases have been described for ERAD. Hrd1 facilitates degradation

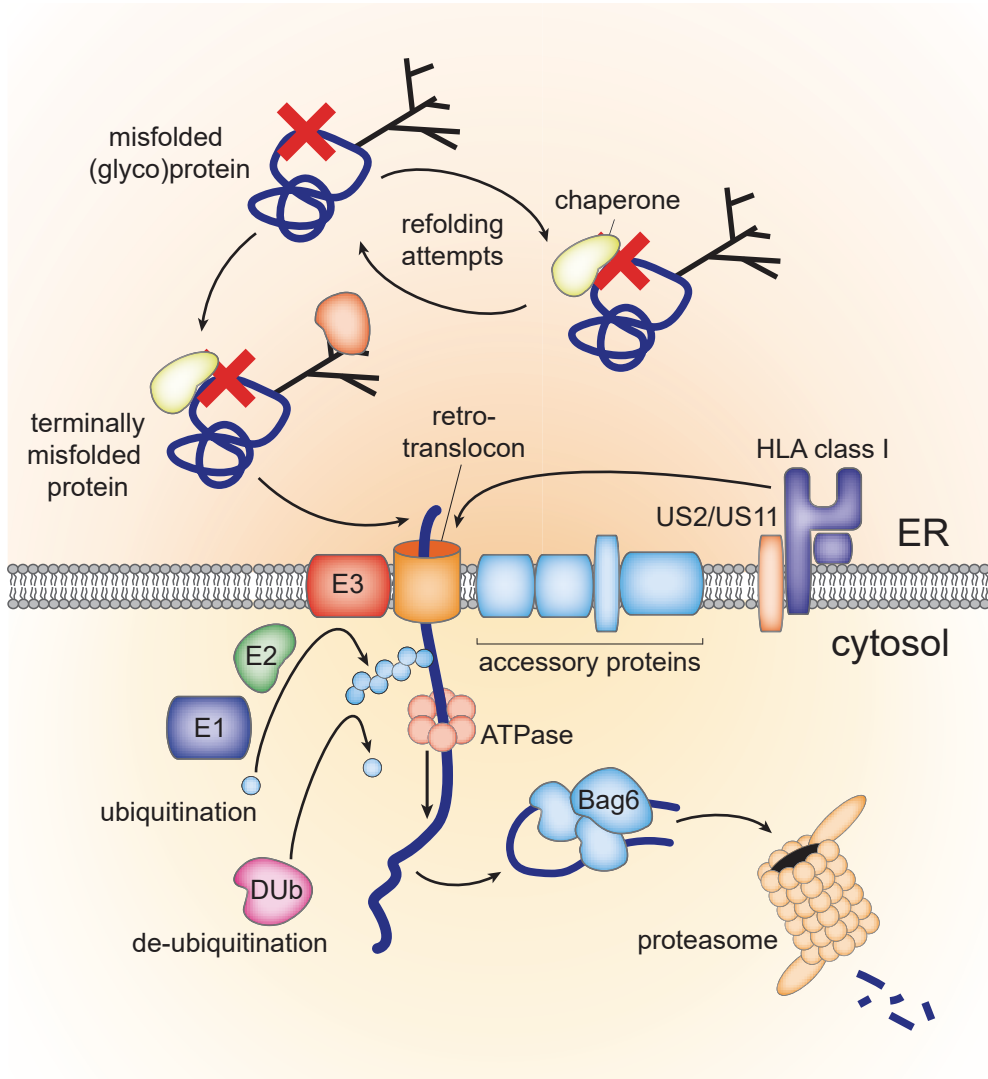


Figure 1 | Schematic overview of ERAD. From top left to bottom right: misfolded ER proteins are recognized by chaperones. After initial refolding attempts, terminally misfolded proteins are targeted for ER-associated protein degradation. The US2 and US11 proteins from human cytomegalovirus may skip these initial steps and directly target HLA class I molecules for degradation. The retro-translocation complex comprises a channel through which ERAD substrates are transported towards the cytosol, as well as many accessory proteins for complex stability and recruitment of crucial ERAD factors. The nature of the retro-translocation channel remains to be identified. Once a degradation substrate reaches the cytosol, it is ubiquitinated by concerted action of E1, E2 and E3 enzymes. The p97 ATPase recognizes ubiquitinated retro-translocation intermediates and provides the energy for completing retro-translocation. However, as the ubiquitin chain causes steric hindrance, partial de-ubiquitination needs to occur prior to p97 action. Once retro-translocated, the ERAD substrate is degraded by the proteasome, to which it may be transported by the Bag6 complex.

of ER-luminal proteins (ERAD-L), whereas Doa10 degrades ER transmembrane proteins with a defect on the cytosolic side (ERAD-C)⁶³. Hrd1 not only provides ubiquitination of the substrate, it may also function as the channel through which substrates are retro-translocated⁶⁴, although other candidates such as SEC61^{61,65–70} have also been suggested as retro-translocon.

In mammalian cells, the ERAD machinery is more complex, with multiple homologues to the basic yeast machinery. For example, 3 homologues of the yeast protein Der1 exist in mammalian cells⁷¹, and at least 12 mammalian ubiquitin E3 ligases have been described in ERAD^{49,72,73}. Many factors, including the retro-translocation complex, remain to be identified or better studied. Similar to yeast, the SEC61 complex has been suggested as retro-translocon³¹, although others suggest that ubiquitin E3 ligases, together with Derlin proteins may form a channel^{74,75}. Most likely, the constituents of an ERAD complex vary between substrates⁷⁶, but also between degradation context of the same substrate: while misfolded HLA class I is degraded via the E3 ligase Hrd1⁷⁷, HLA degradation by US2 requires TRC8⁷⁸, and US11 uses TMEM129^{49,79}.

To study ERAD, we use the HCMV US2 and US11 proteins, that effectively target HLA class I molecules for degradation via this pathway. Importantly, US2 and US11 likely bypass the initial substrate recognition steps in ERAD and directly induce retro-translocation and degradation of HLA-I. This is supported by the notion that HLA-I molecules degraded via US2 and US11 are not misfolded, as they can present peptides at the cell surface when US2- or US11-mediated degradation is suppressed^{80,81}. Furthermore, HLA-I degradation via US2/US11 occurs much faster compared to degradation of misfolded HLA-I. The half-life of a misfolding HLA-I mutant lacking its β 2-microglobulin (β 2M) subunit is approximately 90 minutes⁷⁷. In the context of US2, this is shortened to approximately five minutes³¹, while the presence of US11 shortens the half-life of HLA-I even to approximately one minute³².

When quality control fails...

Gaining a better understanding in ERAD is highly relevant in the context of many diseases. Over 70 pathologies have been attributed to ERAD. For example, mutant ERAD proteins have been identified, which result in aberrant protein accumulation. These mutant proteins encompass particularly E3 ubiquitin ligases, such as BRCA1 in hereditary breast- and ovary cancer, Von Hippel Lindau protein in a broad range of malignancies, and Parkin in Parkinson's disease⁷³. While a role for ERAD is still under debate in other neurodegenerative diseases⁵³, such as Alzheimer's (Amyloid β plaques), and Huntington's (accumulations of mutant Huntingtin), similar protein accumulations are observed.

On the other hand, excessive protein degradation also results in disease. In cystic fibrosis, mutations in the chloride transporter CFTR activate ERAD. CFTR, being a very complex protein, is highly sensitive to folding defects. Even for wildtype CFTR, over 50% of the synthesized protein is degraded. In the most common cystic fibrosis mutation, Δ F508, degradation of CFTR is so effective that cells hardly express this ion channel on their surface, resulting in severe salt and water regulation issues in epithelial tissue^{53,54}. When degradation of ERAD is suppressed and CFTR Δ F508 reaches the cell surface, the protein shows partial activity, which could alleviate disease symptoms⁸². Blocking substrate recognition by molecular chaperones could potentially be a therapeutic target for diseases like cystic fibrosis. Aberrant protein degradation also occurs

in a variety of malignancies, such as HPV-induced degradation of the tumor suppressor protein p53 in cervical cancer, and degradation of the p27 tumor suppressor via overexpression of the E3 ubiquitin ligase Skp2⁷³.

Scope of this thesis

Here, we used the US2 and US11 proteins from human cytomegalovirus to study HLA-I degradation as a model for ERAD. In **Chapter 2**, we reviewed viral interference with the HLA class I antigen presentation pathway, as it is not only HCMV but a variety of viruses that evade CD8⁺ T cell recognition through preventing HLA-I from reaching the cell surface.

The first step for elucidating the mechanisms behind ERAD is the identification of players in the ERAD process. While a genome-wide screen has identified novel players in US11-mediated degradation, including the crucial E3 ligase TMEM129^{49,50}, no such approach had been performed for US2.

In contrast to US11, the ubiquitin E3 ligase for US2 has long been known: TRC8⁷⁸. However, the E2 conjugating enzyme in this process remained unknown. In **Chapter 3**, we therefore systematically knocked out all E2 enzymes using a targeted CRISPR/Cas9 library. We identified UBE2G2 as a crucial factor for US2-mediated ERAD. Interestingly, one of the E2 enzymes required for US11-mediated downregulation, UBE2J2, counteracted US2 function.

Beside the ubiquitin E2-conjugating enzyme, other factors in US2-mediated HLA degradation are likely missing. Many players in ERAD, such as Derlin-1, VIMP⁴⁸ and SEL1L⁸³ are involved in HLA-I downregulation via US11 but not US2, suggesting that alternative proteins are part of the process mediated by US2. To identify these, we performed a genome-wide CRISPR/Cas9 screen (**Chapter 4**). In this screen, we observed that eliminating the UFMylation pathway partially rescued HLA. UFM1 is a recently discovered ubiquitin-like molecule, but unlike ubiquitin, no role in protein degradation is known for this post-translational modification.

The SEC61 complex has previously been described as potential retro-translocon in US2-mediated HLA-I degradation³¹. The overwhelming effect of SEC61 on HLA-I degradation we observed in our genome-wide screen (**Chapter 4**) sparked our interest. Using CRISPR/Cas9-generated mutant cell lines we re-evaluated the role of SEC61 in US2-mediated HLA-I degradation (**Chapter 5**). In contrast to previous research, we observed that SEC61 affects HLA-I degradation indirectly, via downregulation of US2.

For US11, most ERAD players have been identified, with the newest additions being the ubiquitin E2 and E3 enzymes^{49,50}. How it works mechanistically is still poorly understood. The cytosolic p97 ATPase is recruited towards ERAD complexes at the ER membrane in an unknown manner. Therefore, in **Chapter 6**, we tested a panel of potential p97-recruiting factors and show that the p97-binding capacity of UBXD8 is crucial for HLA class I degradation via US11.

The results of these chapters are discussed in **Chapter 7**.

REFERENCES

1. Schuren, A. B. C., Costa, A. I. & Wiertz, E. J. H. J. Recent advances in viral evasion of the MHC Class I processing pathway. *Curr. Opin. Immunol.* **40**, 43–50 (2016).

2. Arcia, D., Acevedo-Sáenz, L., Rugeles, M. T. & Velilla, P. A. Role of CD8⁺ T Cells in the Selection of HIV-1 Immune Escape Mutations. *Viral Immunol.* **30**, 3–12 (2017).
3. Virgin, H. W., Wherry, E. J. & Ahmed, R. Redefining Chronic Viral Infection. *Cell* **138**, 30–50 (2009).
4. McGeoch, D. J., Cook, S., Dolan, A., Jamieson, F. E. & Telford, E. A. R. Molecular phylogeny and evolutionary timescale for the family of mammalian herpesviruses. *J. Mol. Biol.* **247**, 443–458 (1995).
5. Wylie, K. M. *et al.* Metagenomic analysis of double-stranded DNA viruses in healthy adults. *BMC Biol.* **12**, 71 (2014).
6. McGeoch, D. J. The genomes of the human herpesviruses. *Annu Rev Microbiol* **43**, 235–265 (1989).
7. Prockop, S. E. & Vatsayan, A. Epstein-Barr virus lymphoproliferative disease after solid organ transplantation. *Cytotherapy* **19**, 1270–1283 (2017).
8. Yinon, Y. *et al.* Cytomegalovirus infection in pregnancy. *J. Obstet. Gynaecol. Canada* **32**, 348–354 (2010).
9. Flavell, K. J. & Murray, P. G. Hodgkin's disease and the Epstein-Barr virus. *Mol. Pathol.* **53**, 262–9 (2000).
10. Pergam, S., Limaye, A. & the AST Infectious Disease Community of Practice. Varicella Zoster Virus (VZV). *Am J Transpl.* **9**, S108–S115 (2009).
11. White, D. W., Suzanne Beard, R. & Barton, E. S. Immune modulation during latent herpesvirus infection. *Immunol. Rev.* **245**, 189–208 (2012).
12. Barton, E. S. *et al.* Herpesvirus latency confers symbiotic protection from bacterial infection. *Nature* **447**, 326–329 (2007).
13. Raffegerst, S., Steer, B., Hohloch, M. & Adler, H. Prevention of tumor formation by latent gammaherpesvirus infection. *PLoS One* **10**, 1–10 (2015).
14. Rowe, A. M., Yun, H., Treat, B. R., Kinchington, P. R. & Hendricks, R. L. Subclinical Herpes Simplex Virus Type 1 Infections Provide Site-Specific Resistance to an Unrelated Pathogen. *J. Immunol.* **198**, 1706–1717 (2017).
15. Louten, J. in *Essential Human Virology* (ed. Louten, J. B. T.-E. H. V.) 235–256 (Academic Press, 2016). doi:<https://doi.org/10.1016/B978-0-12-800947-5.00013-2>
16. Smith, A. J. & Weidman, F. Infection of a stillborn infant by an amebiform protozoön (*Entamoeba mortinatalium*, N.S.). *Univ Penn Med Bull* **23**, 285–298 (1910).
17. Griffiths, P., Baraniak, I. & Reeves, M. The pathogenesis of human cytomegalovirus. *J. Pathol.* **235**, 288–97 (2015).
18. Kagan, K. O. & Hamprecht, K. Cytomegalovirus infection in pregnancy. *Arch. Gynecol. Obstet.* **296**, 15–26 (2017).

19. Elizabeth C. Swanson, DO and Mark R. Schleiss, M. Congenital cytomegalovirus infection : new prospects for prevention and therapy . Congenital cytomegalovirus infection : current strategies and future perspectives . Antiviral treatment of cytomegalovirus infection . *Pediatr Clin North Am* **60**, 1–17 (2013).
20. Boppana, S. B., Rivera, L. B., Fowler, K. B., Mach, M. & Britt, W. J. Intrauterine transmission of cytomegalovirus to infants of women with preconceptional immunity. *N. Engl. J. Med.* **344**, 1366–71 (2001).
21. Verweij, M. C. *et al.* Viral Inhibition of the Transporter Associated with Antigen Processing (TAP): A Striking Example of Functional Convergent Evolution. *PLoS Pathog.* **11**, e1004743 (2015).
22. Hansen, S. G. *et al.* Evasion of CD8+ T cells is critical for superinfection by cytomegalovirus. *Science* **328**, 102–6 (2010).
23. Davidson, A. J. in *Human Herpesviruses: Biology, Therapy and Immunoprophylaxis* (eds. Arvin, A., Campadelli-Fiume, G., Mocarski, E. & et al., E.) (Cambridge University Press, 2007).
24. Pande, N. T., Powers, C., Ahn, K. & Früh, K. Rhesus cytomegalovirus contains functional homologues of US2, US3, US6, and US11. *J. Virol.* **79**, 5786–98 (2005).
25. Gainey, M. D., Rivenbark, J. G., Cho, H., Yang, L. & Yokoyama, W. M. Viral MHC class I inhibition evades CD8+ T-cell effector responses in vivo but not CD8+ T-cell priming. *Proc. Natl. Acad. Sci.* **109**, E3260–E3267 (2012).
26. Jones, T. R., Muzithras, V. P. & Gluzman, Y. Replacement Mutagenesis of the Human Cytomegalovirus Genome - Us10 and Us11 Gene-Products Are Nonessential. *J. Virol.* **65**, 5860–5872 (1991).
27. Huber, M. T., Tomazin, R., Wisner, T., Boname, J. & Johnson, D. C. Human cytomegalovirus US7, US8, US9, and US10 are cytoplasmic glycoproteins, not found at cell surfaces, and US9 does not mediate cell-to-cell spread. *J. Virol.* **76**, 5748–5758 (2002).
28. Ahn, K. *et al.* The ER-luminal domain of the HCMV glycoprotein US6 inhibits peptide translocation by TAP. *Immunity* **6**, 613–621 (1997).
29. Jones, T. R. *et al.* Human cytomegalovirus US3 impairs transport and maturation of major histocompatibility complex class I heavy chains. *Proc. Natl. Acad. Sci. U. S. A.* **93**, 11327–11333 (1996).
30. Park, B., Spooner, E., Houser, B. L., Strominger, J. L. & Ploegh, H. L. The HCMV membrane glycoprotein US10 selectively targets HLA-G for degradation. *J. Exp. Med.* **207**, 2033–2041 (2010).
31. Wiertz, E. J. H. J. *et al.* Sec61-mediated transfer of a membrane protein from the endoplasmic reticulum to the proteasome for destruction. *Nature* **384**, 432–438 (1996).
32. Wiertz, E. J. H. J. *et al.* The human cytomegalovirus US11 gene product dislocates MHC class I heavy chains from the endoplasmic reticulum to the cytosol. *Cell* **84**, 769–779 (1996).

33. Ameres, S., Besold, K., Plachter, B. & Moosmann, A. CD8 T cell-evasive functions of human cytomegalovirus display pervasive MHC allele specificity, complementarity, and cooperativity. *J. Immunol.* **192**, 5894–905 (2014).
34. Besold, K., Wills, M. & Plachter, B. Immune evasion proteins gpUS2 and gpUS11 of human cytomegalovirus incompletely protect infected cells from CD8 T cell recognition. *Virology* **391**, 5–19 (2009).
35. Jones, T. R. & Muzithras, V. P. Fine mapping of transcripts expressed from the US6 gene family of human cytomegalovirus strain AD169. *J. Virol.* **65**, 2024–36 (1991).
36. Tenney, D. J. & Colberg-Poley, a M. Human cytomegalovirus UL36-38 and US3 immediate-early genes: temporally regulated expression of nuclear, cytoplasmic, and polysome-associated transcripts during infection. *J. Virol.* **65**, 6724–34 (1991).
37. Barel, M. T., Pizzato, N., Le Bouteiller, P., Wiertz, E. J. H. J. & Lenfant, F. Subtle sequence variation among MHC class I locus products greatly influences sensitivity to HCMV US2- and US11-mediated degradation. *Int. Immunol.* **18**, 173–182 (2006).
38. Blom, D., Hirsch, C., Stern, P., Tortorella, D. & Ploegh, H. L. A glycosylated type I membrane protein becomes cytosolic when peptide: N-glycanase is compromised. *EMBO J.* **23**, 650–658 (2004).
39. Furman, M. H., Loureiro, J., Ploegh, H. L. & Tortorella, D. Ubiquitinylation of the cytosolic domain of a type I membrane protein is not required to initiate its dislocation from the endoplasmic reticulum. *J. Biol. Chem.* **278**, 34804–34811 (2003).
40. Barel, M. T., Hassink, G. C., Voorden, S. Van & Wiertz, E. J. H. J. Human cytomegalovirus-encoded US2 and US11 target unassembled MHC class I heavy chains for degradation. *Mol. Immunol.* **43**, 1258–1266 (2006).
41. Gewurz, B. E. *et al.* Antigen presentation subverted: Structure of the human cytomegalovirus protein US2 bound to the class I molecule HLA-A2. *Proc. Natl. Acad. Sci. U. S. A.* **98**, 6794–6799 (2001).
42. Barel, M. T. *et al.* Human cytomegalovirus-encoded US2 differentially affects surface expression of MHC class I locus products and targets membrane-bound, but not soluble HLA-G1 for degradation. *J. Immunol.* **171**, 6757–65 (2003).
43. Story, C. M., Furman, M. H. & Ploegh, H. L. The cytosolic tail of class I MHC heavy chain is required for its dislocation by the human cytomegalovirus US2 and US11 gene products. *Proc. Natl. Acad. Sci. U. S. A.* **96**, 8516–8521 (1999).
44. Cho, S., Kim, B. Y., Ahn, K. & Jun, Y. The C-Terminal Amino Acid of the MHC-I Heavy Chain Is Critical for Binding to Derlin-1 in Human Cytomegalovirus US11-Induced MHC-I Degradation. *PLoS One* **8**, 1–14 (2013).
45. Hassink, G. C., Barel, M. T., Van Voorden, S. B., Kikkert, M. & Wiertz, E. J. Ubiquitination of MHC class I heavy chains is essential for dislocation by human cytomegalovirus-encoded US2 but not US11. *J. Biol. Chem.* **281**, 30063–30071 (2006).

46. Ye, Y. *et al.* Recruitment of the p97 ATPase and ubiquitin ligases to the site of retrotranslocation at the endoplasmic reticulum membrane. *Proc. Natl. Acad. Sci. U. S. A.* **102**, 14132–8 (2005).
47. Ye, Y., Meyer, H. H. & Rapoport, T. A. Function of the p97-Ufd1-Npl4 complex in retrotranslocation from the ER to the cytosol: Dual recognition of nonubiquitinated polypeptide segments and polyubiquitin chains. *J. Cell Biol.* **162**, 71–84 (2003).
48. Lilley, B. N. & Ploegh, H. L. A membrane protein required for dislocation of misfolded proteins from the ER. *Nature* **429**, 834–840 (2004).
49. Van De Weijer, M. L. *et al.* A high-coverage shrna screen identifies TMEM129 as an E3 ligase involved in ER-associated protein degradation. *Nat. Commun.* **5**, 1–14 (2014).
50. van den Boomen, D. J. H. *et al.* TMEM129 is a Derlin-1 associated ERAD E3 ligase essential for virus-induced degradation of MHC-I. *Proc. Natl. Acad. Sci. U. S. A.* **111**, 11425–30 (2014).
51. Wallin, E. & Heijne, G. Von. Genome-wide analysis of integral membrane proteins from eubacterial, archaean, and eukaryotic organisms. *Protein Sci.* **7**, 1029–1038 (2008).
52. Chen, X., Karnovsky, A., Sans, M. D., Andrews, P. C. & Williams, J. A. Molecular characterization of the endoplasmic reticulum: Insights from proteomic studies. *Proteomics* **10**, 4040–4052 (2010).
53. Guerriero, C. J. & Brodsky, J. L. The delicate balance between secreted protein folding and endoplasmic reticulum-associated degradation in human physiology. *Physiol. Rev.* **92**, 537–576 (2012).
54. Zhao, L. & Ackerman, S. L. Endoplasmic reticulum stress in health and disease. *Curr. Opin. Cell Biol.* **18**, 444–452 (2006).
55. Balchin, D., Hayer-Hartl, M. & Hartl, F. U. In vivo aspects of protein folding and quality control. *Science (80-)*. **353**, aac4354 (2016).
56. Araki, K. & Nagata, K. SUP: Protein folding and quality control in the ER. *Cold Spring Harb. Perspect. Biol.* **4**, a015438 (2012).
57. Christianson, J. C. & Ye, Y. Cleaning up in the endoplasmic reticulum: Ubiquitin in charge. *Nat. Struct. Mol. Biol.* **21**, 325–335 (2014).
58. Rabinovich, E., Kerem, A., Fröhlich, K., Bar-nun, S. & Fro, K. Chaperone Required for Endoplasmic Reticulum-Associated Protein Degradation AAA-ATPase p97 / Cdc48p , a Cytosolic Chaperone Required for Endoplasmic Reticulum-Associated Protein Degradation. *Mol. Cell. Biol.* **22**, 626–634 (2002).
59. Bodnar, N. & Rapoport, T. Toward an understanding of the Cdc48/p97 ATPase. *F1000Research* **6**, 1318 (2017).
60. Bodnar, N. O. & Rapoport, T. A. Molecular Mechanism of Substrate Processing by the Cdc48 ATPase Complex. *Cell* **169**, 722–735.e9 (2017).

61. Kalies, K. U., Allan, S., Sergeyenko, T., Kröger, H. & Römisch, K. The protein translocation channel binds proteasomes to the endoplasmic reticulum membrane. *EMBO J.* **24**, 2284–2293 (2005).
62. Wang, Q. *et al.* A ubiquitin ligase-associated chaperone holdase maintains polypeptides in soluble states for proteasome degradation. *Mol. Cell* **42**, 758–70 (2011).
63. Carvalho, P., Goder, V. & Rapoport, T. A. Distinct Ubiquitin-Ligase Complexes Define Convergent Pathways for the Degradation of ER Proteins. *Cell* **126**, 361–373 (2006).
64. Baldridge, R. D. & Rapoport, T. A. Autoubiquitination of the Hrd1 Ligase Triggers Protein Retrotranslocation in ERAD. *Cell* **166**, 394–407 (2016).
65. Tretter, T. *et al.* ERAD and protein import defects in a sec61 mutant lacking ER-luminal loop 7. *BMC Cell Biol.* **14**, 1–14 (2013).
66. Plemper, R. K., Böhmeler, S., Bordallo, J., Sommer, T. & Wolf, D. H. Mutant analysis links the translocon and BIP to retrograde protein transport for ER degradation. *Nature* **388**, 891–895 (1997).
67. Schäfer, A. & Wolf, D. H. Sec61p is part of the endoplasmic reticulum-associated degradation machinery. *EMBO J.* **28**, 2874–2884 (2009).
68. Scott, D. C. & Schekman, R. Role of Sec61p in the ER-associated degradation of short-lived transmembrane proteins. *J. Cell Biol.* **181**, 1095–1105 (2008).
69. Willer, M., Forte, G. M. A. & Stirling, C. J. Sec61p is required for ERAD-L: Genetic dissection of the translocation and ERAD-L functions of Sec61P using novel derivatives of CPY. *J. Biol. Chem.* **283**, 33883–33888 (2008).
70. Wheeler, M. C. & Gekakis, N. Defective ER associated degradation of a model luminal substrate in yeast carrying a mutation in the 4th ER luminal loop of Sec61p. *Biochem. Biophys. Res. Commun.* **427**, 768–773 (2012).
71. Lilley, B. N. & Ploegh, H. L. Multiprotein complexes that link dislocation, ubiquitination, and extraction of misfolded proteins from the endoplasmic reticulum membrane. *Proc. Natl. Acad. Sci. U. S. A.* **102**, 14296–14301 (2005).
72. Mehnert, M., Sommer, T. & Jarosch, E. ERAD ubiquitin ligases: Multifunctional tools for protein quality control and waste disposal in the endoplasmic reticulum. *BioEssays* **32**, 905–913 (2010).
73. Reinstein, E. & Ciechanover, A. Narrative Review: Protein Degradation and Human Diseases: The Ubiquitin Connection. *Ann. Intern. Med.* **145**, 676 (2006).
74. Bernardi, K. M. *et al.* The E3 Ubiquitin Ligases Hrd1 and gp78 Bind to and Promote Cholera Toxin Retro-Translocation. *Mol. Biol. Cell* **21**, 140–151 (2010).
75. Huang, C. H., Hsiao, H. T., Chu, Y. R., Ye, Y. & Chen, X. Derlin2 protein facilitates HRD1-mediated retro-translocation of sonic hedgehog at the endoplasmic reticulum. *J. Biol. Chem.* **288**, 25330–25339 (2013).
76. Brodsky, J. L. & Wojcikiewicz, R. J. Substrate-specific mediators of ER associated degradation (ERAD). *Curr. Opin. Cell Biol.* **21**, 516–521 (2009).

77. Burr, M. L. *et al.* HRD1 and UBE2J1 target misfolded MHC class I heavy chains for endoplasmic reticulum-associated degradation. *Proc. Natl. Acad. Sci. U. S. A.* **108**, 2034–2039 (2011).
78. Stagg, H. R. *et al.* The TRC8 E3 ligase ubiquitinates MHC class I molecules before dislocation from the ER. *J. Cell Biol.* **186**, 685–692 (2009).
79. van den Boomen, D. J. H. *et al.* TMEM129 is a Derlin-1 associated ERAD E3 ligase essential for virus-induced degradation of MHC-I. *Proc. Natl. Acad. Sci.* **111**, 11425–11430 (2014).
80. Hsu, J.-L. *et al.* Plasma Membrane Profiling Defines an Expanded Class of Cell Surface Proteins Selectively Targeted for Degradation by HCMV US2 in Cooperation with UL141. *PLOS Pathog.* **11**, e1004811 (2015).
81. van de Weijer, M. L. *et al.* Multiple E2 ubiquitin-conjugating enzymes regulate human cytomegalovirus US2-mediated immunoreceptor downregulation. *J. Cell Sci.* **130**, 2883–2892 (2017).
82. Dalemans, W. *et al.* Altered chloride ion channel kinetics associated with the $\Delta F508$ cystic fibrosis mutation. *Nature* **354**, 526–528 (1991).
83. Mueller, B., Lilley, B. N. & Ploegh, H. L. SEL1L, the homologue of yeast Hrd3p, is involved in protein dislocation from the mammalian ER. *J. Cell Biol.* **175**, 261–270 (2006).



CHAPTER

2

Recent advances in viral evasion of the MHC class I processing pathway

Anouk B.C. Schuren*, Ana I. Costa* and Emmanuel J.H.J. Wiertz

*These authors contributed equally

Dept. Medical Microbiology, University Medical Center Utrecht, 3584CX Utrecht, The Netherlands.

Curr Opin Immunol 2016, 40:43–50

ABSTRACT

T-cell mediated adaptive immunity against viruses relies on recognition of virus-derived peptides by CD4+ and CD8+ T cells. Detection of pathogen-derived peptide-MHC-I complexes triggers CD8+ T cells to eliminate the infected cells. Viruses have evolved several mechanisms to avoid recognition, many of which target the MHC-I antigen-processing pathway. While many immune evasion strategies have been described in the context of herpesvirus infections, it is becoming clear that this 'disguise' ability is more widespread. Here, we address recent findings in viral evasion of the MHC-I antigen presentation pathway and the impact on CD8+ T cell responses.

INTRODUCTION

Viral proteins, like self-proteins, undergo cytosolic degradation by the proteasome, and the resulting peptides are transported into the ER by the transporter associated with antigen processing (TAP). In the ER, the peptides are loaded onto MHC class I molecules (MHC-I), and the resulting peptide-MHC-I (pMHC-I) complexes will proceed toward the cell surface for recognition by circulating CD8+ T cells (Figure 1a; reviewed in [1]). Viruses are able to tamper with the MHC-I antigen- processing pathway to evade immune recognition (reviewed in [2, 3•]): they may limit the density of pMHC-I complexes at the cell surface by interfering with pMHC-I assembly, by trapping the (mature) molecules in an intracellular compartment, by rapidly re-internalizing the pMHC-I complexes, often followed by degradation, or by masking pMHC-I complexes at the cell surface.

Interference with peptide loading: viral inhibition goes beyond herpesviruses

MHC-I maturation begins in the ER, and includes association of the b2m light chain to an MHC-I heavy chain followed by binding of an antigenic peptide. For peptides to bind to MHC-I molecules, they must gain access to the ER, and this occurs mainly through translocation by TAP. Herpesviruses have devised diverse mechanisms to inhibit TAP transport: blocking peptide binding and/or ATP binding to TAP (Figure 1b), inducing degradation of TAP subunits, or locking TAP in a conformation that does not permit translocation without affecting peptide and/or ATP binding (Table 1; reviewed in [3 •, 4]). Also poxviruses, in particular certain cowpox virus (CPXV) strains, devote a protein to interfering with TAP [5,6]. This protein, CPXV012, has recently been shown to hinder ATP binding to TAP [7•, 8•].

Little is known about the evolutionary origin of viral evasion proteins that interfere with TAP transport, with the exception of CPXV012 [4]. A longer version of this evasion protein is a putative ligand for the NK cell inhibitory receptor NKR-P1 [5]. This CPXV012 homolog may have preceded the TAP-inhibitor in evolution, as it is also found in a strain of the mousepox/ectromelia virus (ECTV), a different species among the Orthopoxviruses [8•].

MHC-I molecules present a small fraction of all peptides that have been imported into the ER by TAP. Some peptides require trimming by ERAAP (mice) or ERAP1 (human; reviewed in [9]) before they can bind to MHC-I (Figure 1b). Interfering with ERAP1 function leads to decreased peptide loading, resulting in reduced pMHC-I expression at the cell surface, as was shown initially in ERAAP KO mice. Human cytomegalovirus (HCMV) encodes a miRNA, miR-US4-1, which downregulates ERAP1 mRNA, thereby interfering with the processing of

antigenic peptides, and the maturation of MHC-I in the ER [10].

Retaining mature pMHC-I in the ER

The murine cytomegalovirus (MCMV) gp40 protein does not interfere with MHC-I maturation, but it binds to mature MHC-I molecules in the ER. Gp40 accompanies pMHC-I through the ER-Golgi intermediate compartment (ERGIC) and *cis*-Golgi, after which it retrieves pMHC-I to the ER, such that it does not reach the cell surface [11] (Figure 1d).

CPXV also prevents cell surface expression of mature pMHC-I complexes (Figure 1d). Its CPXV203 protein binds to mature pMHC-I complexes, and this occurs with particularly high affinity at the slightly lower pH of the ERGIC-Golgi. CPXV203 then exploits the KDEL-receptor-pathway through its C-terminal KTEL sequence to bring pMHC-I complexes back to the ER [12,13]. Curiously, the core structure of CPXV203 (b-sandwich fold) that binds to pMHC-I seems to share secondary structure with poxvirus decoy proteins that bind to chemokines and cytokines (e.g.: vCCI, the viral chemokine inhibitor from cowpox) [13]. This shared structure, thus far not described for eukaryotic or prokaryotic proteins, has been recently proposed as a new domain: Poxvirus Immune Evasion (PIE) domain [14].

Degradation through ERAD

Some viral evasins not only retain MHC-I in an intracellular compartment, but also force its degradation. ER-resident proteins, including MHC-I, can be degraded by the ubiquitin-proteasome system as a result of ER-associated protein degradation (ERAD), a quality control mechanism for misfolded proteins. Hijacking of ERAD by HCMV proteins US2 and US11 to degrade MHC-I has since its discovery in 1996 [15,16] served as a model for studying this protein degradation pathway.

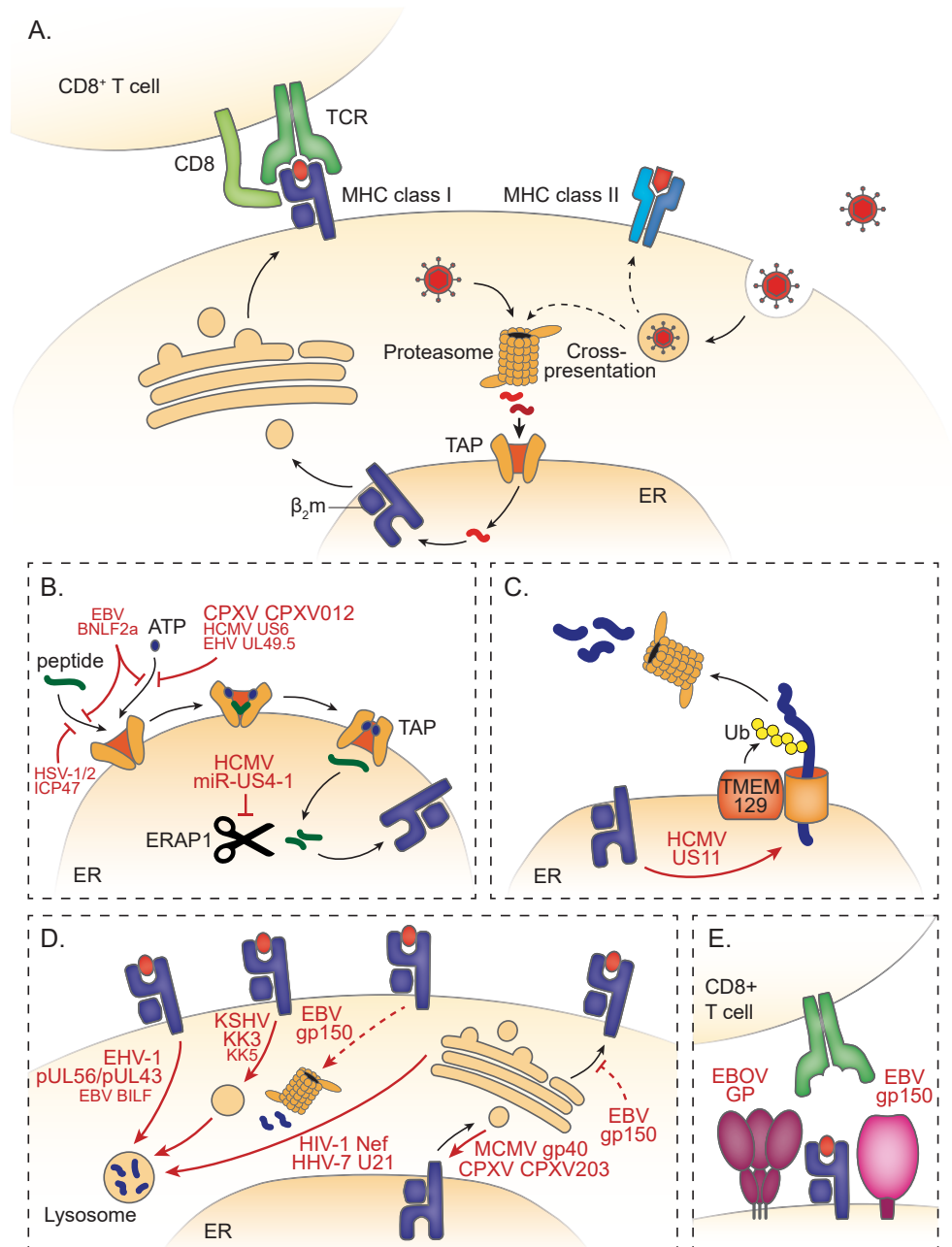
The pathway through which ER proteins are degraded is substrate-specific and involves ubiquitination by a de-fined combination of E2 and E3 enzymes. However, even for a single substrate like MHC-I, degradation may employ different pathways. Both HCMV proteins US2 and US11 induce degradation of MHC-I, but do so in completely different ways. Whereas US2 employs TRC8 as its E3 ubiquitin ligase [17], for US11, the E3 ligase has long been the missing link, but was recently discovered to be TMEM129 (Figure 1c) [18•, 19•]. In the absence of HCMV, misfolded MHC-I is targeted for degradation by yet another E3 ligase, HRD1, as part of the cellular quality control function of ERAD [20].

Viral hijacking of ERAD to degrade MHC-I suggests that it would be a specific mechanism of evasion. In agreement, US11 seems to be specifically downregulating MHC-I molecules. However, US2 turned out to degrade not only pMHC-I, but also a variety of other plasma membrane proteins such as integrins [21•].

Re-routing for degradation or concealment of pMHC-I

Human herpesvirus-7 (HHV-7) also expresses an immune evasion protein, U21, which binds MHC-I in the ER. U21 does not target MHC-I for ERAD, but instead reroutes it toward lysosomes [22], possibly forming complexes with MHC-I in a 4:2 ratio [23]. The mechanism behind the rerouting can either be direct, with pMHC-I traveling from the *trans*-Golgi network

(TGN) directly to the endosomal system, or indirect, if pMHC-I is first expressed at the cell surface, but rapidly re-internalized and degraded. Cellular clathrin adapter proteins (AP)-1 through -4 are involved in targeting proteins to specific cellular compartments. U21-mediated pMHC-I degradation is dependent on AP-1 and AP-3, which sort proteins toward lysosomes,



but independent of AP-2, which is involved in clathrin-mediated endocytosis at the plasma membrane. A direct route from the TGN toward the lysosome has therefore been suggested (Figure 1d) [24]. However, since AP-1 and -3 are cytosolic protein complexes and the cytosolic tail of U21 is dispensable for pMHC-I degradation [22], the search continues for a cellular protein that bridges U21/MHC-I to AP-1 and -3.

HIV Nef-induced downregulation of pMHC-I (Figure 1d) [25], similarly to HHV-7 U21, also involves AP-1 hijacking: Nef redirects pMHC-I from the TGN to lysosomes in clathrin-coated vesicles. It does so by binding the cellular GTPase Arf1, which activates AP-1. The presence of Nef enhances trimerization of AP-1/Arf1 complexes, the first step toward forming hexagons. These hexagons bind to clathrin and activate clathrin cage assembly. Not only did this show the mechanism behind Nef's pMHC-I evasion, it also shed new light on clathrin-mediated vesicular transport [26].

In equine herpesvirus-1 (EHV-1) infected cells, pMHC-I first travels to the plasma membrane before it is degraded in lysosomes. The viral proteins pUL43 and pUL56 cooperate in this process (Figure 1d). pUL56 induces dynamin-mediated endocytosis [27]. pUL43, a non-essential viral protein expressed in the Golgi compartment and degraded by the lysosome [28], possibly escorts pMHC-I.

Endosomal sorting complexes required for transport (ESCRT) are responsible for targeting proteins to specific parts of the endosomal system, including multivesicular bodies (MVB) and lysosomes. This targeting is a sequential process involving ESCRT-0, -I, -II and -III proteins. The Kaposi's sarcoma-associated herpes virus protein K3 (KK3) hijacks ESCRT-0, -I and -III proteins to target pMHC-I for lysosomal degradation [29]. The histidine domain phosphotyrosine phosphatase (HD-PTP), a crucial host factor for KK3-dependent pMHC-I degradation, then performs the role of ESCRT-II [30].

The Epstein–Barr virus (EBV) protein gp150, encoded by BDLF3, has recently been identified as a novel T cell immunoevasin [31, 57]. Different mechanisms of action have been proposed. Quinn et al. [31] suggest that gp150 induces re-internalization of pMHC-I and -II and reduces their trafficking toward the plasma membrane in a process potentially dependent on proteasomal

◀ **Figure 1 | Overview of classical MHC-I antigen processing and presentation and how viruses evade it.**

(a) MHC-I antigen presentation. Endogenous antigens, including viral proteins upon infection, are degraded by the proteasome and enter the ER via TAP, where they bind to MHC-I molecules. Mature pMHC-I complexes then travel to the cell surface via the Golgi and can be recognized by CD8+ T cells. Exogenous antigens degraded in endosomal compartments may be loaded onto MHC-II or cross-presented on MHC-I (for simplification, only the cytosolic pathway of cross-presentation is depicted). (b) Interference with antigen processing. Viruses may interfere with TAP translocation of peptides or with peptide trimming in the ER by ERAP1, hampering antigen supply to MHC-I. Additional mechanisms of interference with TAP transport are listed in Table 1. Evasins that are not mentioned in this review, or only briefly, are shown in a smaller font. (c) ERAD-mediated degradation of MHC-I by US11. Other viral evasins induce degradation of MHC-I through ER-associated protein degradation. The crucial E3 ubiquitin ligase TMEM129 has recently been identified for US11-mediated degradation of MHC-I. (d) Re-routing of pMHC-I. Several viral evasion proteins are able to retrieve pMHC-I to the ER. In addition, viruses may prompt lysosomal degradation of pMHC-I complexes prior to cell surface expression or after internalization from the cell surface membrane. It is not certain whether EBV gp150 decreases surface expression of pMHC-I, and if so, if it involves proteasomal degradation of internalized complexes and/or hindrance of export to the cell surface. (e) Shielding surface pMHC-I from CD8+ T cells. Viral glycoproteins at the surface of infected cells may sterically hinder the interaction between pMHC-I complexes and the T-cell receptor (TCR) of CD8+ T cells.

activity (Figure 1d). They claim that gp150 causes ubiquitination of pMHC-I and -II, which could be a signal for endocytosis (via K63-linked ubiquitination) or proteasomal degradation (via K48-linked ubiquitination). Yet, although surface levels of pMHC-I and -II were strongly decreased by gp150, intracellular levels were hardly affected [31]. It is, thus, uncertain if the mechanism of action of gp150 involves degradation of pMHC-I/II. By contrast, Gram et al. did not observe an effect of proteasomal nor lysosomal inhibition on gp150-associated decrease of cell surface pMHC-I [57]. They propose that the antigen-presenting molecules are not removed from the cell surface, but rather are masked by the extensively glycosylated gp150 molecules by means of a surface glycan shield (Figure 1e). A similar mechanism was reported for the glycoprotein of Ebolavirus to mediate MHC-I immune evasion [32].

Evasins cooperate in decreasing CD8+ T cell recognition...

Differential downregulation of MHC-I alleles by the HCMV evasins US2-11 has been suggested by both biochemical and cell surface analyses of pMHC-I [33, 34] and T-cell recognition studies [35•, 36•]. Different MHC-I alleles are unevenly down-tuned by each of these HCMV evasins. Yet, the evasins cooperate in decreasing CD8+ T cell effector function. This synergy becomes even more important in an inflammatory environment, where cytokines such as IFN γ work against MHC-I downregulation [35•]. CPXV012 and CPXV203 also concur in downregulating cell surface MHC-I and diminishing the magnitude of the total CD8+ T cell response [5,6].

In EBV infection, the evasins BNLF2a and BILF1 may also collaborate in decreasing recognition of EBV epitopes by cognate CD8+T cells: BNLF2a, a TAP inhibitor, seems to become less effective as the lytic cycle progresses; in contrast, BILF1, involved in pMHC-I internalization and targeting to lysosomes for degradation [37], may be more efficient toward the late phase of the lytic cycle. This suggests that these evasins function best at different phases of the lytic cycle, yet synergize in decreasing at least a fraction of the CD8+ T cell responses [38•].

...yet MHC-I downregulation is partial

MHC-I downregulation driven by viral evasins is potent, yet incomplete. Partial downregulation is thought to allow for a tradeoff between evading CD8+ T cell activation as much as possible, while dodging NK cell activation: in the context of HCMV infection, an MHC-I allele that is recognized by the NK-cell inhibitory receptor KIR2DL3 was shown to be incompletely down-regulated. Subjects carrying this allele often mount a dominant CD8+ T cell response toward an epitope of the immediate early protein 1 (IE1), yet the partial expression of the MHC-I likely inhibits NK cell-mediated killing. By contrast, IE1-specific CD8+ T cell responses restricted by MHC-I alleles that are not NK-inhibitory ligands (e.g.: HLA-A*0201) are more strongly down-regulated [36•]. Also, BILF1 does not downregulate HLA-C, presumably as a means to limit NK cell activation [39]. MHC-I immune evasion, thus, cannot be an all-or-nothing process: it is influenced by the window of activity of the various evasins and the variable extent of MHC-I allele downregulation, to reduce both CD8+ T cell and NK cell responses.

CD8+ T cell priming despite MHC-I downregulation

While herpesviruses and CPXV are efficient at targeting the classical MHC-I processing pathway and decreasing the availability of pMHC-I complexes at the cell surface, antiviral CD8+ T cells can still be effectively primed [35•, 40–44]. In fact, no significant differences were reported on the magnitude of virus-specific CD8+ T cell responses upon infection with wildtype (WT) CPXV or MCMV when compared to mutants lacking MHC-I evasins [40, 41, 44]. In the case of CPXV, MCMV and HSV-1, CD8+ T cell priming seems to rely mainly on cross-presentation, and less so on direct presentation through the classical MHC-I pathway [40, 45–47]. In the context of ECTV and vaccinia virus (VV) infection, direct presentation may be the dominant priming pathway [48–50]. So far, no ECTV or VV proteins have been described to play a role in evasion of the MHC-I antigen processing pathway, which might allow for a main contribution of direct presentation on priming of these virus-specific CD8+ T cell responses. Even if not all poxviruses interfere with MHC-I antigen processing to diminish presentation to T cells, some of them (monkeypox and variola viruses, CPXV) encode a protein that suppresses T cell function [51]. However, this mechanism of action is not completely elucidated.

CD8+ T cells primed despite efficient downregulation of pMHC-I are functional: when WT-CPXV-primed CD8+ T cells are transferred into CPXVD012D203-infected mice (without MHC-I downregulation), lesions are more efficiently reduced than in WT-CPXV infection [40]. This illustrates that MHC-I downregulation on target cells at the lesion site interferes with efficient CD8+ T cell killing and control of infection [40]. In fact, deletion of CPXV012 and CPXV203 yields a significantly less pathogenic virus, with the impressive decrease in lethality being dependent on CD8+ T cells. In vivo CPXV infection of WT *versus* an evasin-lacking mutant thus highlights the contribution of MHC-I downregulating proteins to viral pathogenicity [5, 6, 40].

The in vivo benefits of MHC-I evasion do not always translate into a clear difference in disease phenotype during primary infection. Primary infection and establishment of latency still take place in the absence of known herpesviral MHC-I evasins (of e.g. MCMV [41], Rhesus CMV (RhCMV) [42], MHV-68 [52]). However, an RhCMV mutant lacking the US2, US3, US6 and US11 orthologs is unable to superinfect the host unless CD8+ T cells are depleted, suggesting that these evasins are crucial once immunological memory has been formed [42].

Blurring the division between MHC class I and II antigen processing and recognition

In the context of immunization, the RhCMV orthologs of the evasin US11 and UL128-131 (in HCMV) may play a novel role on the development of virus-specific CD8+ T cell responses, violating the classical paradigms of MHC-I antigen presentation and recognition. An SIV-vaccine based on an RhCMV backbone elicited protective immunity against pathogenic SIV [53, 54••] via a broad, unconventional, MHC-II- and MHC-E-restricted CD8+ T cell response [53, 54••, 55••, 56••]. The US11 ortholog was essential for the inhibition of canonical MHC-I-restricted CD8+ T cell responses. Non-canonical CD8+ T cell responses developed only in the absence of the UL128-131 gene ortholog cluster.

In HCMV, UL128-131 in complex with gH/gL allow the virus to infect professional anti-

gen-presenting cells (APCs) [58]. In the absence of the UL128-131 ortholog, RhCMV may thus lose tropism for APCs. According to the classical paradigms, APCs would then cross-present exogenous antigens on classical MHC-I to prime CD8+ T cells, while CD4+ T cells would be activated by MHC-II-restricted antigen. Cross-presentation on classical MHC-I is potentially counteracted by the RhCMV US11 ortholog through depletion of MHC-I molecules. Yet, MHC-E is upregulated by RhCMV [56••], presumably to evade NK cells. The authors suggest that the MHC-E binding groove is unexpectedly permissive in binding requirements: in the vaccinated rhesus macaques, this non-classical MHC allele can bind a broad array of peptides that are recognized to a high frequency [56••].

Also, the establishment of MHC-II-restricted CD8+ T cell responses recognizing virus-specific epitopes does not 'play by the book'. So far, such pathogen-specific CD8+ T cell responses restricted by MHC-II have been shown in CD4^{-/-} mice, and they are probably the by-products of skewed thymic selection [59]. In humans, MHC-II-restricted CD8+ T cells have been reported in the context of alloreactivity [60, 61]. In addition, an HCMV-specific CD8+ T cell clone was shown to cross-react with an HLA-DR4 alloantigen [62]. Yet, unconventional CD8+ T cells recognizing pathogen-derived antigens in the context of MHC-II do not seem to be ordinarily elicited upon infection.

PERSPECTIVES

As illustrated above, the context of antigen presentation (i.e. MHC-I *versus* MHC-II) does not necessarily define which immune cells will respond. Likewise, the source of antigen (intracellular *versus* extracellular) does not definitely dictate whether it will be presented on MHC-I and/or MHC-II at the cell surface. The full picture is even more complex when we take into account that known MHC-I evasins, such as US2 from HCMV [63] and gp150 from EBV [31], additionally downregulate MHC-II and consequently impact MHC-II antigen presentation. The EBV-encoded gp42 protein is dedicated to MHC-II completely: it associates with pMHC-II and hinders pMHC-II/TCR interaction, potentially interfering with CD8+ T cell help [64]. Current research, often focused on single evasins and single antigen-presentation pathways, may therefore not provide the complete picture. Novel, unbiased techniques have already proved valuable in elucidating cellular players in viral evasion [18•, 19•, 21•]. Additional proteomics approaches and genomic screens, complemented by *in vivo* studies, might further elucidate how antigen processing pathways and viral evasion strategies are connected.

ACKNOWLEDGEMENTS

We thank M.E. Ressing, A.M. Gram and R.D. Luteijn for critical reading of this review. A.B.C.S. is funded by The Netherlands Organization for Health Research and Development (NWO; project number NWO 022.004.018).

REFERENCES AND RECOMMENDED READING

Papers of particular interest, published within the period of review, have been highlighted as:

- of special interest

•• of outstanding interest

1. Blum JS, Wearsch PA, Cresswell P: Pathways of antigen processing. *Annu Rev Immunol* 2013, 31:443-473.
2. Hansen TH, Bouvier M: MHC class I antigen presentation: learning from viral evasion strategies. *Nat Rev Immunol* 2009, 9:503-513.
3. • van de Weijer ML, Luteijn RD, Wiertz EJ: Viral immune evasion: lessons in MHC class I antigen presentation. *Semin Immunol* 2015, 27:125-137.
This review gives an extensive overview of immune evasion and the molecular mechanisms behind it.
4. Verweij MC, Horst D, Griffin BD, Luteijn RD, Davison AJ, Rensing ME, Wiertz EJ: Viral inhibition of the transporter associated with antigen processing (TAP): a striking example of functional convergent evolution. *PLoS Pathog* 2015, 11:e1004743.
5. Alzhanova D, Edwards DM, Hammarlund E, Scholz IG, Horst D, Wagner MJ, Upton C, Wiertz EJ, Slifka MK, Fruh K: Cowpox virus inhibits the transporter associated with antigen processing to evade T cell recognition. *Cell Host Microbe* 2009, 6:433-445.
6. Byun M, Verweij MC, Pickup DJ, Wiertz EJ, Hansen TH, Yokoyama WM: Two mechanistically distinct immune evasion proteins of cowpox virus combine to avoid antiviral CD8 T cells. *Cell Host Microbe* 2009, 6:422-432.
7. • Lin J, Eggensperger S, Hank S, Wycisk AI, Wieneke R, Mayerhofer PU, Tampe R: A negative feedback modulator of antigen processing evolved from a frameshift in the cowpox virus genome. *PLoS Pathog* 2014, 10:e1004554.
This paper elucidates that CPXV012-induced inhibition of TAP transport of peptides depends on interference with ATP binding to TAP.
8. • Luteijn RD, Hoelen H, Kruse E, van Leeuwen WF, Grootens J, Horst D, Koorengel M, Drijfhout JW, Kremmer E, Fruh K et al.: Cowpox virus protein CPXV012 eludes CTLs by blocking ATP binding to TAP. *J Immunol* 2014, 193:1578-1589.
This paper elucidates that CPXV012-induced inhibition of TAP transport of peptides depends on interference with ATP binding to TAP.
9. Shastri N, Nagarajan N, Lind KC, Kanaseki T: Monitoring peptide processing for MHC class I molecules in the endoplasmic reticulum. *Curr Opin Immunol* 2014, 26:123-127.
10. Kim S, Lee S, Shin J, Kim Y, Evnouchidou I, Kim D, Kim YK, Kim YE, Ahn JH, Riddell SR et al.: Human cytomegalovirus microRNA miR-US4-1 inhibits CD8(+) T cell responses by targeting the aminopeptidase ERAP1. *Nat Immunol* 2011, 12:984-991.
11. Janssen L, Ramnarayan VR, Aboelmagd M, Iliopoulou M, Hein Z, Majoul I, Fritzsche S, Halenius A, Springer S: The murine cytomegalovirus immunoevasin gp40 binds MHC class I molecules to retain them in the early secretory pathway. *J Cell Sci* 2015.
12. Byun M, Wang X, Pak M, Hansen TH, Yokoyama WM: Cowpox virus exploits the endoplasmic reticulum retention pathway to inhibit MHC class I transport to the cell surface. *Cell Host Microbe* 2007, 2:306-315.
13. McCoy WHt, Wang X, Yokoyama WM, Hansen TH, Fremont DH: Structural mechanism of ER retrieval of MHC class I by cowpox. *PLoS Biol* 2012, 10:e1001432.

14. Nelson CA, Epperson ML, Singh S, Elliott JI, Fremont DH: Structural conservation and functional diversity of the poxvirus immune evasion (PIE) domain superfamily. *Viruses* 2015, 7:4878-4898.
15. Wiertz EJ, Jones TR, Sun L, Bogyo M, Geuze HJ, Ploegh HL: The human cytomegalovirus US11 gene product dislocates MHC class I heavy chains from the endoplasmic reticulum to the cytosol. *Cell* 1996, 84:769-779.
16. Wiertz EJ, Tortorella D, Bogyo M, Yu J, Mothes W, Jones TR, Rapoport TA, Ploegh HL: Sec61-mediated transfer of a membrane protein from the endoplasmic reticulum to the proteasome for destruction. *Nature* 1996, 384:432-438.
17. Stagg HR, Thomas M, van den Boomen D, Wiertz EJ, Drabkin HA, Gemmill RM, Lehner PJ: The TRC8 E3 ligase ubiquitinates MHC class I molecules before dislocation from the ER. *J Cell Biol* 2009, 186:685-692.
18. • van de Weijer ML, Bassik MC, Luteijn RD, Voorburg CM, Lohuis MA, Kremmer E, Hoeben RC, LeProust EM, Chen S, Hoelen H et al.: A high-coverage shRNA screen identifies TMEM129 as an E3 ligase involved in ER-associated protein degradation. *Nat Commun* 2014, 5:3832.
This paper identifies TMEM129, a novel E3 ubiquitin ligase for ER-associated protein degradation, and show its role in HCMV US11- mediated degradation of MHC-I.
19. • van den Boomen DJ, Timms RT, Grice GL, Stagg HR, Skodt K, Dougan G, Nathan JA, Lehner PJ: TMEM129 is a Derlin-1 associated ERAD E3 ligase essential for virus-induced degradation of MHC-I. *Proc Natl Acad Sci U S A* 2014, 111:11425-11430.
This paper identifies TMEM129, a novel E3 ubiquitin ligase for ER-associated protein degradation, and show its role in HCMV US11- mediated degradation of MHC-I.
20. Burr ML, Cano F, Svobodova S, Boyle LH, Boname JM, Lehner PJ: HRD1 and UBE2J1 target misfolded MHC class I heavy chains for endoplasmic reticulum-associated degradation. *Proc Natl Acad Sci U S A* 2011, 108:2034-2039.
21. • Hsu JL, van den Boomen DJ, Tomasec P, Weekes MP, Antrobus R, Stanton RJ, Ruckova E, Sugrue D, Wilkie GS, Davison AJ et al.: Plasma membrane profiling defines an expanded class of cell surface proteins selectively targeted for degradation by HCMV US2 in cooperation with UL141. *PLoS Pathog* 2015, 11:e1004811.
Using proteomics screens, this paper shows that the HCMV evasin US2 degrades multiple proteins, suggesting that it hijacks a broader mechanism of protein degradation.
22. Hudson AW, Blom D, Howley PM, Ploegh HL: The ER-luminal domain of the HHV-7 immunoevasin U21 directs class I MHC molecules to lysosomes. *Traffic* 2003, 4:824-837.
23. May NA, Wang Q, Balbo A, Konrad SL, Buchli R, Hildebrand WH, Schuck P, Hudson AW: Human herpesvirus 7 U21 tetramerizes to associate with class I major histocompatibility complex molecules. *J Virol* 2014, 88:3298-3308.
24. Kimpler LA, Glosson NL, Downs D, Gonyo P, May NA, Hudson AW: Adaptor protein complexes AP-1 and AP-3 are required by the HHV-7 Immunoevasin U21 for rerouting of class I MHC molecules to the lysosomal compartment. *PLoS One* 2014, 9:e99139.
25. Schwartz O, Marechal V, Le Gall S, Lemonnier F, Heard JM: Endocytosis of major histocompatibility complex class I molecules is induced by the HIV-1 Nef protein. *Nat Med*

- 1996, 2:338-342.
26. Shen QT, Ren X, Zhang R, Lee IH, Hurley JH: HIV-1 Nef hijacks clathrin coats by stabilizing AP-1:Arf1 polygons. *Science* 2015, 350:aac5137.
 27. Huang T, Lehmann MJ, Said A, Ma G, Osterrieder N: Major histocompatibility complex class I downregulation induced by equine herpesvirus type 1 pUL56 is through dynamin-dependent endocytosis. *J Virol* 2014, 88:12802-12815.
 28. Huang T, Ma G, Osterrieder N: Equine Herpesvirus 1 multiply inserted transmembrane protein pUL43 cooperates with pUL56 in downregulation of cell surface major histocompatibility complex Class I. *J Virol* 2015, 89:6251-6263.
 29. Bowers K, Piper SC, Edeling MA, Gray SR, Owen DJ, Lehner PJ, Luzio JP: Degradation of endocytosed epidermal growth factor and virally ubiquitinated major histocompatibility complex class I is independent of mammalian ESCRTII. *J Biol Chem* 2006, 281:5094-5105.
 30. Parkinson MD, Piper SC, Bright NA, Evans JL, Boname JM, Bowers K, Lehner PJ, Luzio JP: A non-canonical ESCRT pathway, including histidine domain phosphotyrosine phosphatase (HD-PTP), is used for down-regulation of virally ubiquitinated MHC class I. *Biochem J* 2015, 471:79-88.
 31. Quinn LL, Williams LR, White C, Forrest C, Zuo J, Rowe M: The missing link in EBV immune evasion: the BDLF3 gene induces ubiquitination and downregulation of MHC class I and MHC class II. *J Virol* 2015.
 32. Francica JR, Varela-Rohena A, Medvec A, Plesa G, Riley JL, Bates P: Steric shielding of surface epitopes and impaired immune recognition induced by the ebola virus glycoprotein. *PLoS Pathog* 2010, 6:e1001098.
 33. Barel MT, Pizzato N, Le Bouteiller P, Wiertz EJ, Lenfant F: Subtle sequence variation among MHC class I locus products greatly influences sensitivity to HCMV US2- and US11-mediated degradation. *Int Immunol* 2006, 18:173-182.
 34. Gewurz BE, Wang EW, Tortorella D, Schust DJ, Ploegh HL: Human cytomegalovirus US2 endoplasmic reticulum-lumenal domain dictates association with major histocompatibility complex class I in a locus-specific manner. *J Virol* 2001, 75:5197-5204.
 35. • Ameres S, Besold K, Plachter B, Moosmann A: CD8 T cell-evasive functions of human cytomegalovirus display pervasive MHC allele specificity, complementarity, and cooperativity. *J Immunol* 2014, 192:5894-5905.
This systematic analysis of the HCMV proteins US2, US3, US6 and US11 shows how the evasins have different MHC allele specificity and cooperate in downregulating MHC.
 36. • Ameres S, Mautner J, Schlott F, Neuenhahn M, Busch DH, Plachter B, Moosmann A: Presentation of an immunodominant immediate-early CD8+ T cell epitope resists human cytomegalovirus immunoevasion. *PLoS Pathog* 2013, 9:e1003383.
Ameres et al., exemplify that CD8+ T cell responses to epitopes of the same antigen are differentially affected by HCMV immune evasins, depending on whether they are HLA-C versus HLA-A and -B-restricted. They relate the incomplete downregulation of HLA-C to its function as a ligand to NK-cell inhibitory receptor.
 37. Zuo J, Currin A, Griffin BD, Shannon-Lowe C, Thomas WA, Rensing ME, Wiertz EJ, Rowe

- M: The Epstein-Barr virus G-protein-coupled receptor contributes to immune evasion by targeting MHC class I molecules for degradation. *PLoS Pathog* 2009, 5:e1000255.
38. • Quinn LL, Zuo J, Abbott RJ, Shannon-Lowe C, Tierney RJ, Hislop AD, Rowe M: Cooperation between Epstein-Barr virus immune evasion proteins spreads protection from CD8+ T cell recognition across all three phases of the lytic cycle. *PLoS Pathog* 2014, 10:e1004322. *This paper shows that EBV immune evasion proteins affect CD8+ T cell responses differently, and have different windows of activity, yet they collaborate to limit these responses throughout the lytic cycle.*
 39. Griffin BD, Gram AM, Mulder A, Van Leeuwen D, Claas FH, Wang F, Rensing ME, Wiertz E: EBV BILF1 evolved to downregulate cell surface display of a wide range of HLA class I molecules through their cytoplasmic tail. *J Immunol* 2013, 190:1672-1684.
 40. Gainey MD, Rivenbark JG, Cho H, Yang L, Yokoyama WM: Viral MHC class I inhibition evades CD8+ T-cell effector responses in vivo but not CD8+ T-cell priming. *Proc Natl Acad Sci U S A* 2012, 109:E3260-E3267.
 41. Gold MC, Munks MW, Wagner M, McMahon CW, Kelly A, Kavanagh DG, Slifka MK, Koszinowski UH, Raulet DH, Hill AB: Murine cytomegalovirus interference with antigen presentation has little effect on the size or the effector memory phenotype of the CD8 T cell response. *J Immunol* 2004, 172:6944-6953.
 42. Hansen SG, Powers CJ, Richards R, Ventura AB, Ford JC, Siess D, Axthelm MK, Nelson JA, Jarvis MA, Picker LJ et al.: Evasion of CD8+ T cells is critical for superinfection by cytomegalovirus. *Science* 2010, 328:102-106.
 43. Manley TJ, Luy L, Jones T, Boeckh M, Mutimer H, Riddell SR: Immune evasion proteins of human cytomegalovirus do not prevent a diverse CD8+ cytotoxic T-cell response in natural infection. *Blood* 2004, 104:1075-1082.
 44. Munks MW, Pinto AK, Doom CM, Hill AB: Viral interference with antigen presentation does not alter acute or chronic CD8 T cell immunodominance in murine cytomegalovirus infection. *J Immunol* 2007, 178:7235-7241.
 45. Busche A, Jirmo AC, Welten SP, Zischke J, Noack J, Constabel H, Gatzke AK, Keyser KA, Arens R, Behrens GM et al.: Priming of CD8+ T cells against cytomegalovirus-encoded antigens is dominated by cross-presentation. *J Immunol* 2013, 190:2767- 2777.
 46. Nopora K, Bernhard CA, Ried C, Castello AA, Murphy KM, Marconi P, Koszinowski U, Brocker T: MHC class I cross-presentation by dendritic cells counteracts viral immune evasion. *Front Immunol* 2012, 3:348.
 47. Torti N, Walton SM, Murphy KM, Oxenius A: Batf3 transcription factor-dependent DC subsets in murine CMV infection: differential impact on T-cell priming and memory inflation. *Eur J Immunol* 2011, 41:2612-2618.
 48. Norbury CC, Malide D, Gibbs JS, Bennink JR, Yewdell JW: Visualizing priming of virus-specific CD8+ T cells by infected dendritic cells in vivo. *Nat Immunol* 2002, 3:265-271.
 49. Sei JJ, Haskett S, Kaminsky LW, Lin E, Truckenmiller ME, Bellone CJ, Buller RM, Norbury CC: Peptide-MHC-I from endogenous antigen outnumber those from exogenous antigen, irrespective of APC phenotype or activation. *PLoS Pathog* 2015, 11:e1004941.

50. Xu RH, Remakus S, Ma X, Roscoe F, Sigal LJ: Direct presentation is sufficient for an efficient anti-viral CD8+ T cell response. *PLoS Pathog* 2010, 6:e1000768.
51. Alzhanova D, Hammarlund E, Reed J, Meermeier E, Rawlings S, Ray CA, Edwards DM, Bimber B, Legasse A, Planer S et al.: T cell inactivation by poxviral B22 family proteins increases viral virulence. *PLoS Pathog* 2014, 10:e1004123.
52. Stevenson PG, May JS, Smith XG, Marques S, Adler H, Koszinowski UH, Simas JP, Efsthioiu S: K3-mediated evasion of CD8(+) T cells aids amplification of a latent gamma-herpesvirus. *Nat Immunol* 2002, 3:733-740.
53. Hansen SG, Ford JC, Lewis MS, Ventura AB, Hughes CM, Coyne-Johnson L, Whizin N, Oswald K, Shoemaker R, Swanson T et al.: Profound early control of highly pathogenic SIV by an effector memory T-cell vaccine. *Nature* 2011, 473:523-527.
54. Hansen SG, Piatak M Jr, Ventura AB, Hughes CM, Gilbride RM, Ford JC, Oswald K, Shoemaker R, Li Y, Lewis MS et al.: Immune clearance of highly pathogenic SIV infection. *Nature* 2013, 502:100-104.
- The studies of Hansen et al., demonstrate that the genetic make-up of a vaccination vector can make a difference for control of SIV viral infection. Particular genetic features of the vector, namely evasion proteins and tropism-defining proteins, influence whether a conventional MHC-Ia-restricted or an unconventional MHC-E- and MHC-II-restricted CD8+ T cell response is elicited. Ref #56 also shows that MHC-E is more promiscuous in binding than traditionally thought.*
55. Hansen SG, Sacha JB, Hughes CM, Ford JC, Burwitz BJ, Scholz I, Gilbride RM, Lewis MS, Gilliam AN, Ventura AB et al.: Cytomegalovirus vectors violate CD8+ T cell epitope recognition paradigms. *Science* 2013, 340:1237874.
- See annotation to Ref. [54 ••].*
56. Hansen SG, Wu HL, Burwitz BJ, Hughes CM, Hammond KB, Ventura AB, Reed JS, Gilbride RM, Ainslie E, Morrow DW et al.: Broadly targeted CD8+ T cell responses restricted by major histocompatibility complex-E. *Science* 2016, 351:714-720.
- See annotation to Ref. [54 ••].*
57. Gram AM, Oosenbrug T, Lindenbergh MFS, Büll C, Comvalius A, Dickson KJI, Wiegant J, Vrolijk H, Lebbink RJ, Wolterbeek R et al.: A herpesvirus glycoprotein forms an immune-evasive glycan shield at the surface of infected cells. *PLoS Pathog* 2016, 12:e1005550.
58. Gerna G, Percivalle E, Lilleri D, Lozza L, Fornara C, Hahn G, Baldanti F, Revello MG: Dendritic-cell infection by human cytomegalovirus is restricted to strains carrying functional UL131-128 genes and mediates efficient viral antigen presentation to CD8+ T cells. *J Gen Virol* 2005, 86:275-284.
59. Tyznik AJ, Sun JC, Bevan MJ: The CD8 population in CD4- deficient mice is heavily contaminated with MHC class II-restricted T cells. *J Exp Med* 2004, 199:559-565.
60. Heemskerk MH, de Paus RA, Lurvink EG, Koning F, Mulder A, Willemze R, van Rood JJ, Falkenburg JH: Dual HLA class I and class II restricted recognition of alloreactive T lymphocytes mediated by a single T cell receptor complex. *Proc Natl Acad Sci U S A* 2001, 98:6806-6811.

61. Hirosawa T, Torikai H, Yanagisawa M, Kamei M, Imahashi N, Demachi-Okamura A, Tanimoto M, Shiraishi K, Ito M, Miyamura K et al.: Mismatched human leukocyte antigen class II-restricted CD8(+) cytotoxic T cells may mediate selective graft-*versus*-leukemia effects following allogeneic hematopoietic cell transplantation. *Cancer Sci* 2011, 102:1281-1286.
62. Rist M, Smith C, Bell MJ, Burrows SR, Khanna R: Cross-recognition of HLA DR4 alloantigen by virus-specific CD8+ T cells: a new paradigm for self-/nonself-recognition. *Blood* 2009, 114:2244-2253.
63. Tomazin R, Boname J, Hegde NR, Lewinsohn DM, Altschuler Y, Jones TR, Cresswell P, Nelson JA, Riddell SR, Johnson DC: Cytomegalovirus US2 destroys two components of the MHC class II pathway, preventing recognition by CD4+ T cells. *Nat Med* 1999, 5:1039-1043.
64. Rensing ME, van Leeuwen D, Verreck FA, Gomez R, Heemskerk B, Toebes M, Mullen MM, Jardetzky TS, Longnecker R, Schilham MW et al.: Interference with T cell receptor-HLA-DR interactions by Epstein-Barr virus gp42 results in reduced T helper cell recognition. *Proc Natl Acad Sci U S A* 2003, 100:11583-11588.



An aerial photograph of terraced agricultural fields in a dry, hilly region. The fields are arranged in concentric, curved patterns, following the contours of the land. The soil appears brown and dry, and the vegetation is sparse. The overall scene is one of arid, mountainous terrain.

CHAPTER

3

Multiple E2 ubiquitin conjugating enzymes regulate human cytomegalovirus US2-mediated immunoreceptor downregulation

Michael L. van de Weijer^{1,*,#}, Anouk B. C. Schuren^{1,*,#},
Dick J. H. van den Boomen², Arend Mulder³, Frans
H. J. Claas³, Paul J. Lehner², Robert Jan Lebbink^{1,\$}
and Emmanuel J. H. J. Wiertz^{1,\$,¶}

^{#,§} These authors contributed equally

¹ Dept. Medical Microbiology, University Medical Center Utrecht, 3584CX Utrecht, The Netherlands. ² Cambridge Institute for Medical Research, University of Cambridge, Cambridge CB2 0XY, UK. ³ Dept. Immunohematology and blood transfusion, Leiden University Medical Center, 2333 ZA Leiden, The Netherlands. * Present address: Sir William Dunn School of Pathology, University of Oxford, Oxford OX1 3RE, UK. [¶] Author for correspondence (E.Wiertz@umcutrecht.nl).

ABSTRACT

Misfolded endoplasmic reticulum (ER) proteins are dislocated towards the cytosol and degraded by the ubiquitin-proteasome system in a process called ER-associated protein degradation (ERAD). During infection with human cytomegalovirus (HCMV), the viral US2 protein targets HLA class I molecules (HLA-I) for degradation via ERAD to avoid elimination by the immune system. US2-mediated degradation of HLA-I serves as a paradigm of ERAD and has facilitated the identification of TRC8 (also known as RNF139) as an E3 ubiquitin ligase. No specific E2 enzymes had previously been described for cooperation with TRC8. In this study, we used a lentiviral CRISPR/Cas9 library targeting all known human E2 enzymes to assess their involvement in US2-mediated HLA-I downregulation. We identified multiple E2 enzymes involved in this process, of which UBE2G2 was crucial for the degradation of various immunoreceptors. UBE2J2, on the other hand, counteracted US2-induced ERAD by downregulating TRC8 expression. These findings indicate the complexity of cellular quality control mechanisms, which are elegantly exploited by HCMV to elude the immune system.

KEY WORDS: ERAD, ER-associated protein degradation, E2, Ubiquitin, US2, Cytomegalovirus

INTRODUCTION

Human cytomegalovirus (HCMV) is a member of the β -herpesviridae and carries the largest double-stranded (ds)DNA genome of the human herpesviruses family (McGeoch et al., 2006). HCMV is a common virus with a seroprevalence of 40–100%, depending on the socioeconomic status of the host population. Primary infection of healthy individuals usually is asymptomatic, but in pregnant women and immunocompromised patients, HCMV infection can cause serious disease (Griffiths et al., 2015). HCMV encodes multiple immunomodulatory proteins that facilitate interference with the immune system of the host, thereby facilitating HCMV to establish a lifelong infection (Dunn et al., 2003; Hansen et al., 2010; Mocarski, 2002).

The HLA-I antigen presentation pathway is a major target for the immune-evasive strategies of HCMV, resulting in its effective elusion from CD8-positive cytotoxic T cells (Noriega et al., 2012b; Schuren et al., 2016). At least five unique short (US) regions in the HCMV genome are known to encode proteins that specifically interfere with the expression of HLA-I molecules (van de Weijer et al., 2015). US3 retains newly synthesized HLA-I proteins in the ER and blocks tapasin-dependent peptide loading (Jones et al., 1996; Noriega et al., 2012a; Park et al., 2004). US6 interacts with the transporter associated with antigen processing (TAP) complex and induces conformational changes of TAP that prevent ATP binding, thereby inhibiting TAP-mediated peptide translocation into the ER (Ahn et al., 1997; Hengel et al., 1997; Hewitt et al., 2001; Lehner et al., 1997). US10 specifically targets HLA-G molecules for degradation (Park et al., 2010). US2 and US11 are type 1 transmembrane ER glycoproteins that cause retrograde transport, or dislocation, of newly synthesized HLA-I heavy chains from the ER into the cytosol for proteasomal degradation (Oresic et al., 2009; Wiertz et al., 1996a,b).

As a result of the above process, US2 and US11 hijack the cellular protein quality control pathway in the ER that recognizes misfolded proteins and targets them for degradation via the ubiquitin–

proteasome system. This reaction is referred to as ER-associated protein degradation (ERAD). At the center of this process are multiprotein complexes that combine the various functions essential to this reaction, namely substrate recognition, dislocation, ubiquitylation and degradation (Christianson et al., 2011; Olzmann et al., 2013; Preston and Brodsky, 2017; Ye et al., 2001, 2004). Although US2 and US11 both target HLA-I for degradation, they utilize distinct protein complexes. US11 uses derlin-1 and the E3 ubiquitin ligase TMEM129 in cooperation with the E2 ubiquitinconjugating enzymes UBE2J2 and UBE2K to dislocate HLA-I (Flierman et al., 2006; Lilley and Ploegh, 2004; van deWeijer et al., 2014; van den Boomen et al., 2014). US2, however, does not depend on these proteins but usurps the E3 ubiquitin ligase TRC8 (also known as RNF139) to mediate HLA-I downregulation (Stagg et al., 2009). On the cytosolic side, both US2 and US11 rely on the ATPase p97/VCP to shuttle HLA-I to the proteasome for degradation (Soetandyo and Ye, 2010; Ye et al., 2005). Besides HLA-I, US2 induces downregulation of multiple immunoreceptors to modulate cellular migration and immune signaling, whereas US11-mediated degradation is restricted to HLA-I (Hsu et al., 2015).

In US2-mediated degradation of HLA-I, the function of TRC8 as E3 ligase is well documented (Hsu et al., 2015; Stagg et al., 2009). However, no specific E2 ubiquitin-conjugating enzymes have been implicated in this process. Here, we constructed a lentiviral CRISPR/Cas9-based library targeting all known human E2 enzymes and used this resource to screen for E2 enzymes that regulate US2-mediated HLA-I downregulation. We identify UBE2G2 as an essential E2 enzyme for this process. Upon UBE2G2 depletion, HLA-I molecules are detected in an ER-resident US2- and TRC8-containing complex, possibly because ubiquitylation may be required for extraction of the class I molecules from the ER and their subsequent degradation. Interestingly, our screen also identifies UBE2J2 as a counteracting E2 enzyme, depletion of which further downregulates HLA-I in US2-expressing cells. In line with our findings for HLA-I, the immunoreceptors integrin- α 1, - α 2 and - α 4, the interleukin (IL)12 receptor β 1-subunit (IL12R-B1), and thrombomodulin are also degraded by US2 in a UBE2G2-dependent manner, whereas UBE2J2 counteracts this effect. In conclusion, we show that the E2 ubiquitin-conjugating enzymes UBE2G2 and UBE2J2 are broadly involved in regulating the downregulation of immunoreceptors targeted by HCMV US2.

MATERIALS AND METHODS

Cell culture and lentiviral infection

U937 human monocytic cells and 293T human embryonic kidney cells were obtained from ATCC (American Type Culture Collection) and grown in RPMI medium (Lonza) supplemented with glutamine (Gibco), penicillin/streptomycin (Gibco) and 10% fetal bovine serum (Biowest). For individual transductions using lentiviruses, virus was produced in 24-well plates using standard lentiviral production protocols and third-generation packaging vectors. The supernatant containing virus was harvested 3 days post transfection and stored at -80°C . For lentiviral transductions, 50 μl supernatant containing virus supplemented with 8 $\mu\text{g ml}^{-1}$ polybrene (Santa Cruz Biotechnology) was used to infect $\sim 20,000$ U937 cells by spin infection at 1000 g for 2 h at 33°C . Fully-supplemented medium was added after centrifugation to reduce polybrene concentration.

Generation of the CRISPR/Cas9-based library and selection of clonal E2-knockout cell lines

CRISPR gRNAs and Cas9 were expressed from a lentiviral vector, as described previously (van de Weijer et al., 2014). In short, this vector carried a CRISPR gRNA under control of a U6 promoter as well as a Cas9 gene that was N-terminally fused to a puromycin-resistance cassette by means of a T2A sequence. The region immediately downstream of the U6 promoter contains a cassette with a BsmBI restriction site on each side to allow cloning of gRNA target sites followed by the gRNA scaffold and a terminator consisting of five T residues. gRNAs targeting all known human E2s were designed using an online CRISPR design tool (<http://crispr.mit.edu/>). gRNA sequences are listed in Table S1. The genomic target sites for the gRNAs used in the validation studies and/or in the generation of clonal knockout cell lines are listed in Table S2.

U937 cells stably co-expressing eGFP–Myc–HLA-A2 and HA–US2 or 3xST2–HA–US2 [ST2 is Strep(II)] were transduced with this CRISPR/Cas9 system. At 2 days post infection (dpi), transduced cells were selected by using 2 µg ml⁻¹ puromycin and allowed to recover. Additional CRISPR gRNAs targeting UBE2G2 were expressed from a pKLV lentiviral backbone containing a U6 sgRNA as well as a pGK Puro-2A-BFP cassette. This vector was expressed in THP1 cells already containing US2-IRES–mCherry with hygromycin resistance as well as Cas9 under blasticidin resistance.

Cells were single-cell sorted by fluorescence-activated cell sorting (FACSAriaII, BD Biosciences). The knockout status of the clonal cell lines was confirmed by flow cytometry and immunoblotting (UBE2G2) or genomic target site sequencing (UBE2J2). For genomic target site sequencing of UBE2J2, genomic DNA was isolated using the Quick-DNA Miniprep kit (Zymo Research), and the specific region containing the gRNA-target site was amplified by PCR using primers 5'-CCGACGTCTCTATACTGCC-3' and 5'-GGCCCTTCTGTTTTGTTCC-3'. Subsequently a nested PCR was performed using primers 5'-CCGACGTCTCTATACTGCC-3' and 5'-GACACAGCCTGCAAACGGG-3' to generate more-specific PCR products.

PCR products were prepared according to the manufacturer's guidelines, and subjected to deep-sequencing using the MiSeq Reagent Nano Kit v2 for 500 cycles. Deep sequencing data were analyzed using the Varscan algorithm and are presented in Fig. S2.

Antibodies

Primary antibodies used in our studies were: mouse anti-HLA-I HC HC10 monoclonal antibody (mAb), 1:400; mouse anti-HLA-I HC HCA2 mAb, 1:25; phycoerythrin (PE)-conjugated mouse anti-HLA-A2 mAb (clone BB7.2, no. 558570, BD Pharmingen), 1:20; human anti-HLA-A3 OK2F3 mAb (LUMC, Leiden, the Netherlands), 1:40; mouse anti-TfR H68.4 mAb (no. 13-68xx, Invitrogen), 1:5000; mouse anti-FLAG-M2 mAb (no. F1804, Sigma-Aldrich), 1:10,000; rat anti-HA 3F10 mAb (no. 11867423001, Roche) 1:1000; rabbit anti-UBE2G2 mAb (EPR9248, no. ab174296, Abcam), 1:1000; rabbit anti-TRC8 polyclonal antibody (pAb) (H89, no. sc-68373, Santa Cruz Biotechnology), 1:1000; mouse anti-CD141 (THBD) mAb (clone 1A4, no. 559780, BD Pharmingen), 1:320; mouse anti-CD49b (ITGA2) mAb (clone 12F1, no. 555668, BD Pharmingen), 1:1000; mouse anti-CD49d (ITGA4) mAb (clone 9F10,

no. 555502, BD Pharmingen), 1:1000; rabbit anti-ITGA4 mAb (EPR1355Y, no. ab81280, Abcam), 1:1000; mouse anti-IL12 receptor β 1 subunit (CD212) mAb (clone 2.4E6, no. 556064, BD Pharmingen), 1:1000; and rabbit anti-ITGA2 mAb (EPR17338, no. ab181548, Abcam), 1:1000.

Secondary antibodies used were: F(ab')₂ goat anti-human-IgG+IgM(H+L) conjugated to PE (no. 109-116-127, Jackson ImmunoResearch) 1:500; F(ab')₂ goat anti-mouse-IgG conjugated to PE (no. R0480, Dako) 1:500; goat anti-mouse-IgG conjugated to AlexaFluor647 (no. A21236, Invitrogen/Thermo) 1:500; goat anti-mouse IgG(H+L) conjugated to horseradish peroxidase (HRP; no. 170-6516, Bio-Rad), 1:10,000; goat anti-rabbit-IgG(H+L) conjugated to HRP (no. 4030-05, Southern Biotech), 1:10,000; mouse anti-rabbit-IgG(L) conjugated to HRP (no. 211-032-171, Jackson ImmunoResearch), 1:10,000; goat anti-mouse-IgG(L) conjugated to HRP (no. 115-035-174, Jackson ImmunoResearch), 1:10,000; and goat anti-rat-IgG(L) conjugated to HRP (no. 112-035-175, Jackson ImmunoResearch), 1:10,000.

Plasmids and cDNAs

Several different lentiviral vectors were used in the present studies. The N-terminally eGFP- and Myc-tagged human HLA-A2 vector present in the lentiviral pHRsincPPT-SGW vector was kindly provided by Dr Paul Lehner and Dr Louise Boyle (University of Cambridge, Cambridge, UK). HCMV US2 was N-terminally tagged with either an HA tag only, or three ST2 tags followed by an HA tag. The original leader was replaced by the human (h) CD8 leader sequence in the tagged US2 constructs. US2 and tagged variants were expressed from a dual promoter lentiviral vector, which also included expression of BlastR-T2A-mAmetrine via the hPGK promoter. For E2 rescue and overexpression experiments, gRNA-resistant HA-tagged E2 ubiquitin-conjugating enzymes were generated and cloned into a dual promoter lentiviral vector, which also included expression of ZeoR-T2AmAmetrine via the hPGK promoter, as described previously (van deWeijer et al., 2014). UBE2D3 and UBE2G2 were tagged N-terminally; UBE2J2 was tagged C-terminally. Catalytically inactive E2 mutants were generated using PCR-based site-directed mutagenesis with primers carrying the mutation desired: UBE2D3 C85S, UBE2G2 C89S, UBE2J2 C94S. TRC8 was tagged C-terminally with a FLAG and ST2 tag. The resulting TRC8-FLAG-ST2 was still functional (Fig. S3). All constructs were verified by standard Sanger sequencing (Macrogen, The Netherlands).

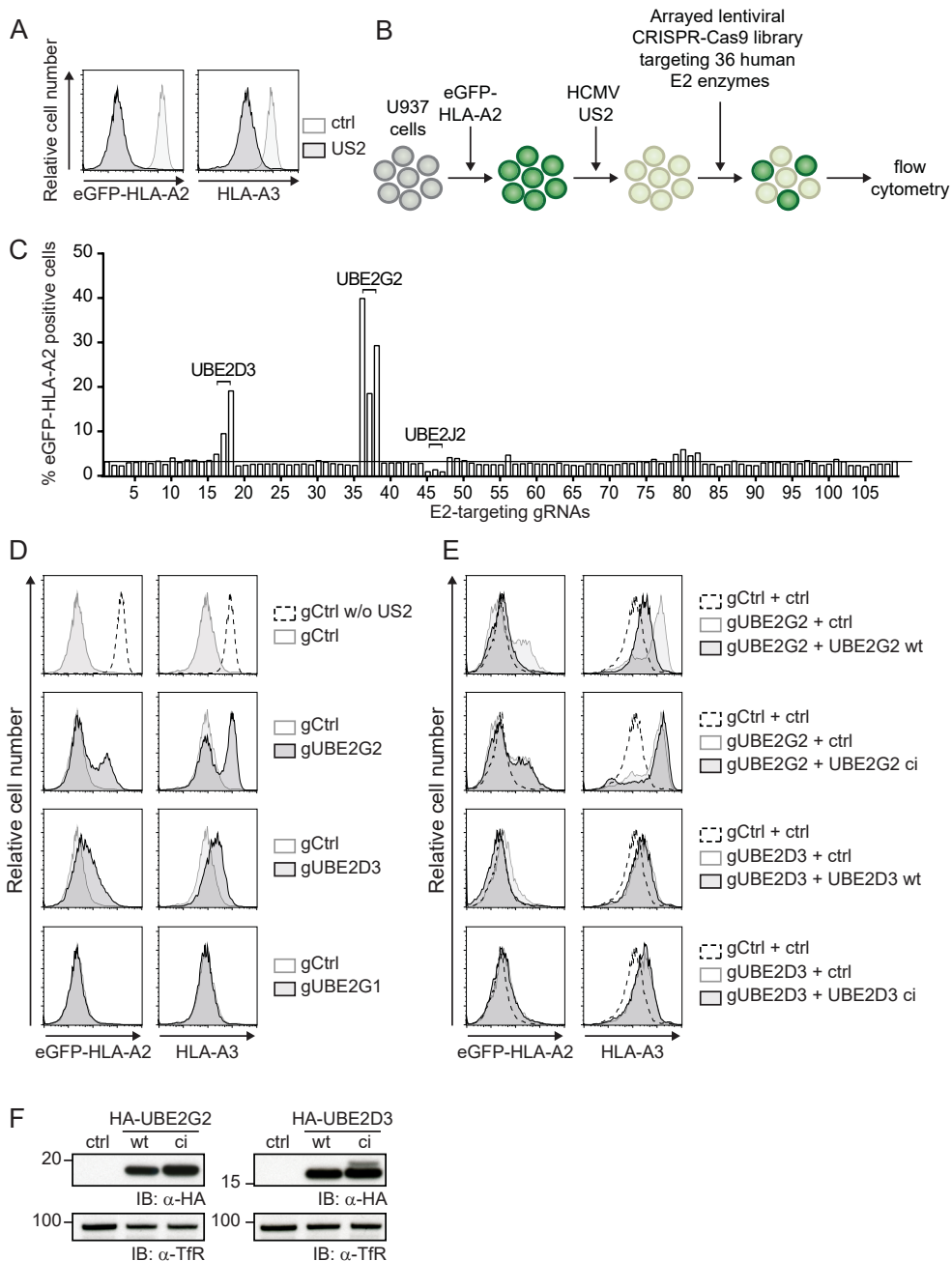
Flow cytometry

Cells were washed in FACS buffer (PBS containing 0.5% BSA and 0.02% sodium azide) and analyzed on a FACSCanto II (BD Bioscience). Flow cytometry data were analyzed using FlowJo software.

Immunoblotting

Cells were lysed in 1% Triton X-100 lysis buffer (1.0% Triton X-100, 20 mM MES, 100 mM NaCl, 30 mM Tris-HCl pH 7.5) containing 1 mM Pefabloc SC (Roche) and 10 μ M leupeptin (Roche). Nuclei and cell debris were pelleted at 12,000 g for 20 min at 4°C. Post-nuclear lysates were denatured in Laemmli sample buffer and incubated at room temperature for 30

min. Proteins were separated by SDS-PAGE and transferred to PVDF membranes (Immobilon-P, Millipore). Membranes were probed with the indicated antibodies. Reactive bands were detected by ECL (Thermo Scientific Pierce), and exposed to Amersham Hyperfilm ECL films (GE Healthcare).



Co-immunoprecipitations

Cells were lysed in digitonin lysis buffer [1% digitonin (Calbiochem), 50 mM Tris-HCl pH 7.5, 5 mM MgCl₂, 150 mM NaCl] containing 1 mM Pefabloc SC (Roche) and 10 μM leupeptin (Roche). Lysates were incubated for 90 min at 4°C. Nuclei and cell debris were pelleted 12,000 g for 20 min at 4°C. Post-nuclear supernatants were incubated overnight with StrepTactin beads (GE Healthcare). After four washes in 0.1% digitonin lysis buffer, proteins were eluted in elution buffer (2.5 mM dethiobiotin, 150 mM NaCl, 100 mM Tris-HCl pH 8, 1 mM EDTA) for 30 min on ice. The eluate was separated from the beads using 0.45 μm Spin-X filter column (Corning Costar), and subsequently denatured in Laemmli sample buffer containing DTT. Immunoblotting was performed as described above.

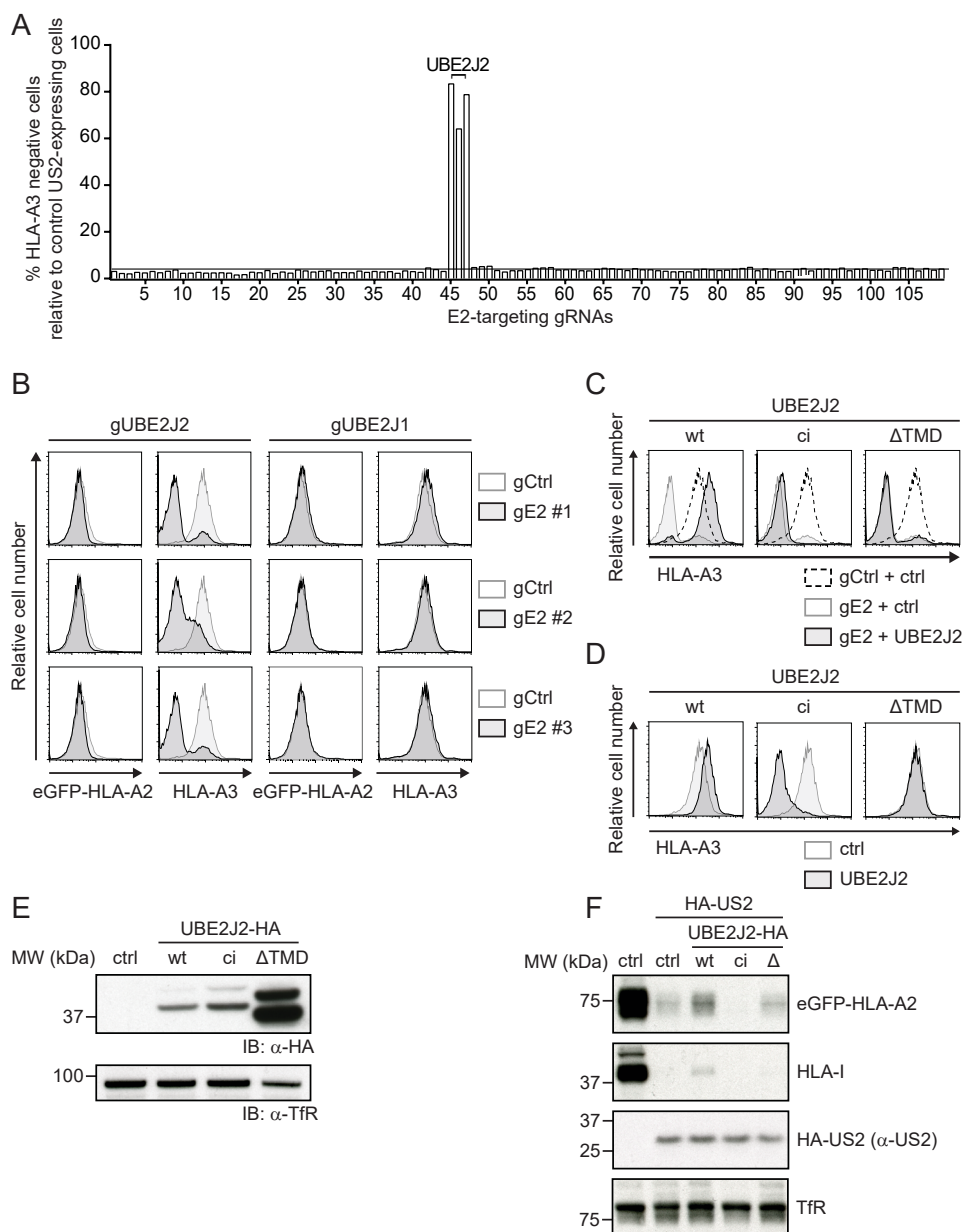
RESULTS

A CRISPR/Cas9 library screen identifies the E2 ubiquitin-conjugating enzyme UBE2G2 to be essential for US2-mediated HLA-I downregulation

To identify E2 ubiquitin-conjugating enzymes required for US2-mediated degradation of HLA-I molecules, we established a lentiviral CRISPR/Cas9-based library targeting all known human E2 ubiquitin-conjugating enzymes. Approximately three guideRNAs (gRNAs) were used per E2 gene. U937 monocytic cells stably expressing an HLA-A2 molecule with an N-terminal eGFP-tag were generated to allow monitoring of HLA-I expression levels by flow cytometry. Upon stable introduction of HCMV US2, the chimeric HLA-I molecules as well as endogenous HLA-I proteins were degraded efficiently (Fig. 1A). These cells were then transduced with the lentiviral E2-targeting CRISPR/Cas9 library, after which eGFP-HLA-A2 expression was evaluated by flow cytometry. Disruption of an E2 gene essential for US2 activity would rescue eGFP-HLA-A2 from degradation and thus increase eGFP-HLA-A2 levels (Fig. 1B).

- ← **Figure 1 | A CRISPR/Cas9 library screen for E2 ubiquitin-conjugating enzymes identifies UBE2G2 and UBE2D3 as essential players in US2-mediated HLA-I downregulation.** (A) Downregulation of eGFP-HLA-A2 and endogenous HLA-A3 mediated by US2 in U937 cells expressing eGFP-HLA-A2. (B) Schematic overview of the CRISPR/Cas9 library screen to identify E2 ubiquitin-conjugating enzymes essential for US2-mediated HLA-I downregulation. U937 cells are transduced with eGFP-HLA-A2 and subsequently transduced with an HCMV US2 expression vector. As a result, cells display low total eGFP-HLA-A2 expression levels, which can be monitored by means of the eGFP tag. Subsequently, cells are lentivirally transduced with CRISPR/Cas9 constructs targeting individual E2 ubiquitin-conjugating enzymes and selected to purity using puromycin. Cells are analyzed by flow cytometry at 10 dpi to assess total eGFP-HLA-A2 levels. (C) Quantification of the percentage eGFP-HLA-A2-positive US2-expressing cells upon transduction with CRISPR/Cas9 constructs targeting individual E2 ubiquitin-conjugating enzymes. gRNAs targeting UBE2D3, UBE2G2 and UBE2J2 are indicated. (D) CRISPR/Cas9-mediated knockout of E2 ubiquitin-conjugating enzymes UBE2G2 (gRNA #1) and UBE2D3 (gRNA #3) rescues expression of chimeric eGFP-HLA-A2 and endogenous HLA-A3 from US2-expressing cells. gRNAs targeting UBE2G1 (gRNA #1) were used as a negative control. eGFP-HLA-A2 and endogenous HLA-A3 surface levels were assessed at 10 dpi by flow cytometry. (E) Reconstitution of UBE2G2 or UBE2D3 expression in UBE2G2- and UBE2D3-knockout cells, respectively, rescues US2-mediated downregulation of HLA-I. The wild-type E2 (UBE2G2 wt or UBE2D3 wt) or a catalytically inactive E2 (UBE2G2 ci or UBE2D3 ci) was introduced in the corresponding polyclonal E2 knockout cells from C, after which flow cytometry analysis was performed to assess total eGFP-HLA-A2 levels and endogenous HLA-A3 surface levels at 7 dpi. (F) The expression of wild-type and catalytically inactive E2 ubiquitin-conjugating enzymes used in D was assessed via immunoblotting (IB). Transferrin receptor (TfR) was used as a loading control.

CRISPR gRNAs targeting UBE2D3 and UBE2G2 induced rescue of eGFP–HLA-A2 expression in US2-expressing cells (Fig. 1C). Expression of gRNAs targeting UBE2G2 induced the strongest rescue of eGFP–HLA-A2. The anti-UBE2G2 and anti-UBE2D3 gRNAs also increased the levels of endogenous HLA-A3 in these US2-expressing cells (Fig. 1D). By contrast, targeting the UBE2G2 homolog UBE2G1 with CRISPR gRNAs did not affect eGFP–HLA-A2 expression. To validate the involvement of UBE2G2 and UBE2D3, their expression was restored by



introduction of gRNA-resistant E2 cDNA constructs into the gRNA-expressing cells (Fig. 1E). For both UBE2G2 and UBE2D3, reconstitution of protein expression restored US2-mediated HLA-A2–eGFP downregulation. For UBE2G2, a similar pattern was also observed for endogenous HLA-A3. On the other hand, introduction of catalytically inactive E2 mutants, in which the active cysteine residue was replaced with a serine, did not result in restoration of US2-mediated HLA-I downregulation. Expression of the HA-tagged wild-type (wt) and catalytically inactive (ci) E2 enzymes was confirmed by immunoblotting (Fig. 1F).

These results indicate that UBE2G2 and UBE2D3 affect US2-mediated degradation of HLA-I. Compared to UBE2G2, the effects of UBE2D3 depletion and reconstitution were limited, especially for the endogenous HLA-A3 molecule. Because UBE2G2 has a stronger effect on HLA-I rescue, mechanistic experiments in this study will focus on this E2 enzyme.

The E2 ubiquitin-conjugating enzyme UBE2J2 counteracts US2-mediated HLA-I downregulation

In contrast to UBE2G2 and UBE2D3, we noticed that targeting UBE2J2 with CRISPR gRNAs resulted in a further downregulation of eGFP–HLA-A2 (Fig. 1C) and endogenous HLA-A3 expression (Fig. 2A). The window to assess reduced eGFP–HLA-A2 levels was low, as US2 downregulates the chimeric eGFP–HLA-A2 molecule to near background levels (Fig. 1A). Downregulation of the endogenous HLA-A3 by US2 was less potent (Fig. 1A), allowing us to study the effect of UBE2J2 depletion in more detail. Indeed, gRNAs targeting UBE2J2 further decreased HLA-A3 levels (Fig. 2B). Depletion of the UBE2J2 homolog UBE2J1 did not affect HLA-A3 expression (Fig. 2B). Reconstitution of wt UBE2J2 expression abolished the enhanced downregulation of HLA-A3 molecules (Fig. 2C, left panel), showing that the gRNA effect was specific for UBE2J2. Expression of the exogenous UBE2J2 even resulted in slightly less downregulation of HLA-A3 by US2 (Fig. 2C, left panel), which could be due to overexpression of the cDNA. In US2-expressing cells with intact endogenous UBE2J2, introduction of this UBE2J2 cDNA increased HLA-A3 expression in a similar manner (Fig. 2D, left panel). These findings indicate that UBE2J2 counteracts US2-mediated downregulation of HLA-I. Reconstitution with a catalytically inactive UBE2J2 (ci) or a UBE2J2 mutant lacking its transmembrane domain (Δ TMD) did not counteract the enhanced HLA-I downregulation (Fig. 2C, middle and right

- ◀ **Figure 2 | UBE2J2 counteracts US2-mediated HLA-I downregulation.** (A) Quantification of the percentage of cells showing enhanced downregulation of HLA-A3 upon transduction with CRISPR/Cas9 constructs targeting individual E2 ubiquitin-conjugating enzymes. gRNAs targeting UBE2J2 are indicated. (B) CRISPR/Cas9-mediated knockout of UBE2J2 decreases endogenous HLA-A3 surface expression in US2-expressing cells. The homolog UBE2J1 is shown as a negative control. Endogenous HLA-A3 surface levels were assessed at 10 dpi by flow cytometry. (C) Reconstitution of UBE2J2 expression in UBE2J2-knockout cells rescues HLA-I from enhanced US2-mediated downregulation. Wild-type UBE2J2 (wt), catalytically inactive UBE2J2 (ci), or soluble UBE2J2 (Δ TMD) was introduced in knockout cells from B (gRNA #1), after which flow cytometry analysis was performed to assess endogenous HLA-A3 surface levels at 7 dpi. (D) Ectopic expression of UBE2J2 increases HLA-A3 expression. Wild-type UBE2J2, catalytically inactive UBE2J2 or soluble UBE2J2 was ectopically expressed in cells similar to those from B, but lacking a gRNA targeting UBE2J2. Endogenous HLA-A3 surface levels were assessed using flow cytometry. (E) Expression of wild-type, catalytically inactive and Δ TMD UBE2J2, as used in C and D, were assessed by immunoblotting. Transferrin receptor (TfR) was used as a loading control. (F) Lysates of U937 cells expressing either wild-type UBE2J2 (wt), catalytically inactive UBE2J2 (ci), or soluble UBE2J2 (Δ) were prepared and immunoblotted for the indicated proteins.

panels). These results indicated that catalytic activity is required for this phenotype. Expression of the catalytically inactive mutant in the absence of gRNAs further stimulated US2-mediated HLA-A3 downregulation (Fig. 2D, middle panel), mimicking the phenotype of CRISPR/Cas9-mediated UBE2J2 disruption. This indicates that the catalytically inactive UBE2J2 acts as a dominant-negative mutant. Expression of the soluble mutant (Δ TMD) did not affect HLA-A3 expression levels (Fig. 2D, right panel). The expression levels of wild-type, catalytically inactive and soluble UBE2J2 were confirmed by immunoblotting (Fig. 2E). The effect of UBE2J2 counteracting US2-mediated HLA-I degradation was not caused by directly affecting US2 expression, as introduction of wild-type, catalytically inactive or soluble UBE2J2 did not alter US2 levels (Fig. 2F). Taken together, our data indicate that UBE2J2 counteracts US2-mediated downregulation of HLA-I through a mechanism that relies on its catalytic activity.

Depletion of UBE2G2 causes accumulation of HLA-I in the US2-TRC8 complex

Next, we investigated the effect of UBE2G2 and UBE2J2 depletion on the composition of the US2 ERAD complex. To this end, clonal UBE2G2- and UBE2J2-null cell lines were established (Fig. S1). Removal of UBE2G2 in these cells caused a growth defect, but was not lethal. HLA-I levels were increased in UBE2G2-null cells as compared to control cells (Fig. 3A, lane 1 and 2 versus lane 5), which was in agreement with the flow cytometry results from Fig. 1C. In addition,

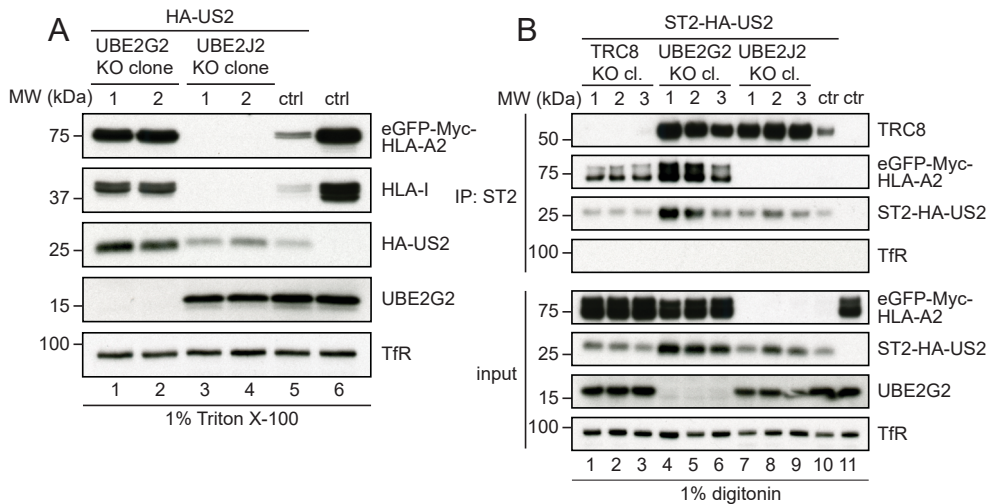


Figure 3 | Loss of UBE2G2 locks the US2-TRC8 complex in a dislocation-incompetent state. (A) Two independent knockout clones of either UBE2G2 or UBE2J2 were established in U937 cells co-expressing eGFP-HLA-A2 and HA-US2. These clones were subjected to immunoblot analysis to assess expression levels of the indicated proteins. (B) ST2-HA-tagged US2 was immunoprecipitated (IP) by using StrepTactin beads from 1.0% digitonin lysates of cells in which TRC8 (lane 1–3), UBE2G2 (lane 4–6) or UBE2J2 (lane 7–9) were knocked out. US2-expressing U937 eGFP-HLA-A2 cells without knockout (lane 9) and cells without US2 (lane 10) were used as controls. Immunoprecipitated complexes were eluted using d-Desthiobiotin, after which immunoblot analysis was performed to detect the indicated proteins.

US2 protein levels were increased, likely due to the stabilization of the US2 ERAD complex in the absence of UBE2G2.

In line with our previous results, immunoblot analysis for UBE2J2-null cells revealed that HLA-I levels were further decreased as compared to control cells (Fig. 3A, lanes 3 and 4 versus lane 5). US2 protein levels were comparable to control conditions (lane 3) or slightly elevated (lane 4), suggesting that the strong increase in HLA-I degradation upon UBE2J2 knockout was not caused by increased US2 levels.

To investigate the effects of UBE2G2 and UBE2J2 depletion on the composition of the US2 ERAD complex, US2 was immunoprecipitated from cell lysates prepared by using digitonin, which preserves most membrane protein complexes. The E3 ubiquitin ligase TRC8 is part of this ERAD complex and is essential for HLA-I downregulation by US2 (Stagg et al., 2009).

Knocking out TRC8 rescues US2-associated HLA-I (Fig. 3B, lanes 1–3 versus 10). In UBE2G2-null cells, HLA-I co-precipitated with US2 as well (lanes 4–6). In addition, increased amounts of TRC8 were co-precipitated from UBE2G2-null cells as compared to control cells (lane 10). Overall US2 expression varied slightly per condition and seemed higher in UBE2G2-null cells. Our data suggest that the US2–TRC8 ERAD complex is stabilized in the absence of UBE2G2, leading to the accumulation of HLA-I prior to the dislocation of US2–TRC8 from the ER membrane.

UBE2J2 counteracts HLA-I degradation by US2 via downregulation of TRC8

Upon UBE2J2 knockout (Fig. 3B, lanes 7–9), HLA-I was not detectable in the US2–TRC8 complex, consistent with the observation that HLA-I degradation is enhanced in these cells. Intriguingly, the amount of TRC8 present in the complex was increased upon UBE2J2 knockout (Fig. 3B, lanes 7–9) compared to control cells (lane 10), while US2 levels were elevated only slightly. This suggests that depletion of UBE2J2 may increase TRC8 levels. Because TRC8 is the rate-limiting factor for US2-mediated HLA-I degradation (Van den Boomen and Lehner, 2015), this TRC8 increase would explain the enhanced HLA-I downregulation. To investigate this, we assessed TRC8 levels in UBE2J2-knockout cells by direct quantitative immunoprecipitation of TRC8 (Fig. 4A), as the ligase could not be detected in lysate directly. Indeed, in US2-expressing cells, TRC8 expression levels were increased upon UBE2J2 knockout compared to what was observed in the control conditions (Fig. 4A). A minor increase in TRC8 expression could also be observed in cells without US2 (Fig. S4A, lane 3 versus 4).

We observed a similar increase in TRC8 expression in US2 cells expressing catalytically inactive UBE2J2 (Fig. 4B). These cells show stronger HLA-I downregulation compared to cells expressing US2 alone (Fig. 2C). Again, TRC8 expression was also elevated in cells without US2 (Fig. S4B, lane 4 versus 2), indicating that the effect of UBE2J2 on TRC8 is independent of US2. Expression levels of US2 (Fig. S4A,B) and UBE2G2 (Fig. 4C; Fig. S4A,B) were not clearly affected by expression of catalytically inactive or wild-type UBE2J2 constructs.

Catalytically inactive UBE2J2 not only raised total TRC8 expression, but also resulted in increased TRC8 levels present in the ERAD complex immunoprecipitated via US2 (Fig. 4C, lane 12 versus 10). By contrast, exogenous expression of wild-type UBE2J2 (lane 11 versus 10) caused decreased TRC8 association. Thus, UBE2J2 depletion or the expression of catalyti-

cally inactive UBE2J2 increases TRC8 expression levels, which in turn enhances US2-mediated HLA-I downregulation.

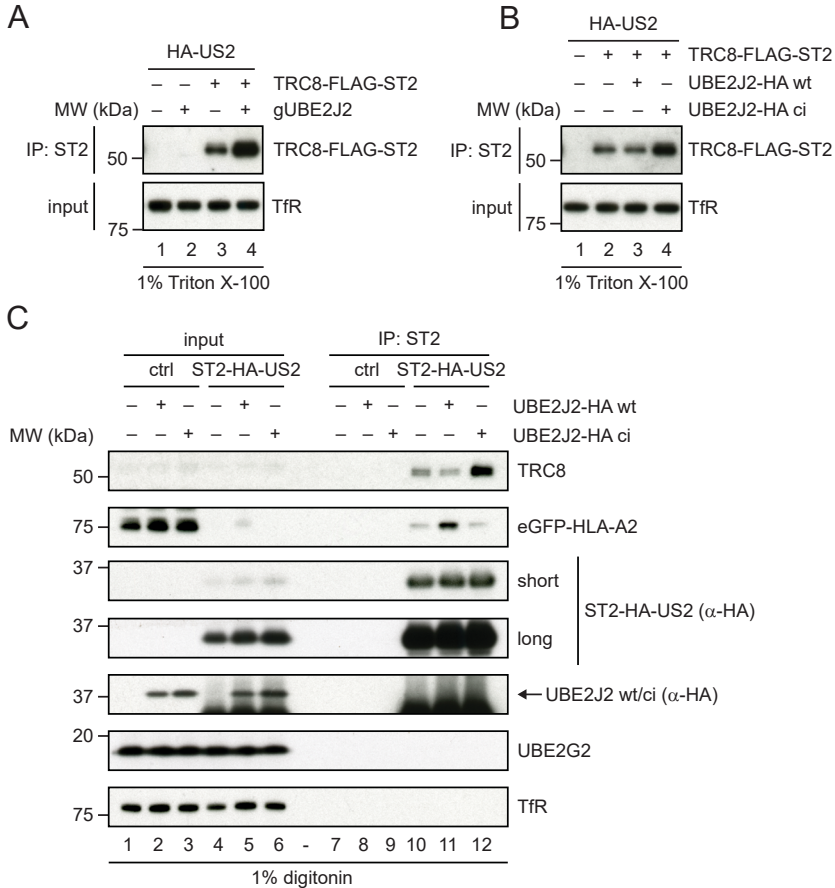


Figure 4 | Impaired UBE2J2 function enhances HLA-I downregulation by US2 via upregulation of TRC8. (A) US2-expressing TRC8-knockout cells were transduced with TRC8-Flag-ST2 or a control vector. To these cells, UBE2J2-targeting CRISPR gRNAs or empty vector were added. TRC8 levels were assessed by direct immunoprecipitation (IP). Upon UBE2J2 knockout, the expression of TRC8 increases. (B) US2-expressing TRC8-knockout cells were transduced with TRC8-Flag-ST2 or a control vector. To these cells, cDNA of wild-type (wt) or catalytically inactive (ci) HA-tagged UBE2J2 or a control vector were added. TRC8 levels were assessed by direct immunoprecipitation. Upon expression of catalytically inactive UBE2J2, the expression of TRC8 increases compared to that seen in control cells without HA-UBE2J2 or in cells with wild-type HA-UBE2J2. (C) Catalytically inactive UBE2J2 increases TRC8 levels in the US2 ERAD complex. A control vector, a vector expressing wild-type UBE2J2 (wt) or catalytically inactive UBE2J2 (ci) was transduced in U937 cells expressing eGFP-HLA-A2 and ST2-HA-US2. After G418 selection, cells were lysed in 1.0% digitonin lysis buffer, after which ST2-HA-US2 was immunoprecipitated by using StrepTactin beads. Immunoprecipitated complexes were eluted using d-Desthiobiotin, after which immunoblot analysis was performed for the proteins indicated. A short and a long exposure of the anti-HA immunoblot are shown.

Degradation of immunoreceptors by US2 is dependent on UBE2G2 and counteracted by UBE2J2

HCMV US2-mediated protein degradation is not limited to HLA-I; US2 also modulates the expression of various other cell surface receptors, including integrin- α 2 (ITGA2), integrin- α 4 (ITGA4) and thrombomodulin (THBD) (Hsu et al., 2015). Similar to HLA-I, the degradation of these cell surface receptors is catalyzed by the E3 ubiquitin ligase TRC8 (Hsu et al., 2015). We tested whether the degradation of these cell surface receptors induced by US2 is also dependent on UBE2G2, and whether their downregulation can be counteracted by UBE2J2. Indeed, TRC8 and UBE2G2 depletion restored the surface expression of these receptors in US2-expressing U937 and THP-1 cells (Fig. 5A, -B), whereas UBE2J2 depletion further decreased the expression compared to that in control US2-expressing cells (Fig. 5A, -B). When looking at HLA-I downregulation, we noticed a difference between the two cell lines used. In contrast to U937 cells, which express the HLA-A3 allele, the HLA-A2-expressing THP-1 cells displayed only partial rescue of this HLA-A protein upon introduction of anti-UBE2G2 gRNAs. Other US2 substrates, including integrin α 1 (ITGA1), ITGA2, ITGA4, the IL12 receptor β 1-subunit (IL12R-B1), and thrombomodulin were upregulated more potently in the THP-1 cells (Fig. 5B,C). The elevated expression of HLA class I, ITGA2, ITGA4 and THBD upon UBE2G2 knockout was confirmed by immunoblotting (Fig. 5D). Thus, UBE2G2 and UBE2J2 not only regulate US2-induced downregulation of HLA-I, but also that of other cell surface receptors, including several integrins and thrombomodulin.

DISCUSSION

HCMV US2 facilitates proteasomal degradation of HLA-I and various other immunoreceptors through a pathway that is poorly characterized (Hsu et al., 2015; Stagg et al., 2009; Wiertz et al., 1996b). Here, we identify multiple E2 ubiquitin-conjugating enzymes involved in US2-mediated immunoreceptor downregulation. Knocking out UBE2G2 in US2-expressing cells by using the CRISPR/Cas9 system rescues HLA-I expression. Loss of UBE2G2 stabilizes HLA-I in a complex that also contains US2 and TRC8, suggesting that UBE2G2 is required for the dislocation to occur. We were unable to show association of UBE2G2 with the US2-TRC8 complex, possibly due to the weak and transient nature of the interaction between E2 ubiquitin-conjugating enzymes and the E3 ubiquitin ligases *in vivo*, as has been reported for other E2-E3 interactions (Duncan et al., 2010; Kleiger et al., 2009; Yin et al., 2009).

In our CRISPR/Cas9 screen, we noticed that the knockout of a second E2 enzyme, UBE2D3, also rescued HLA-I expression. UBE2D3 appears to be an essential gene for U937 cell survival, as we were not able to establish clonal knockout cell lines. UBE2D3 depletion only moderately counteracted US2-mediated HLA-I downregulation in U937 cells, although this low rescue may have been impacted by the lethality of knocking out this E2 enzyme.

Our studies consistently demonstrated a partial rescue of HLA-A2 expression upon depletion of UBE2G2; HLA-A3, as well as other US2 substrates were rescued more strongly. This difference was most apparent when HLA-A-specific antibodies were used in cell lines that carry a single HLA-A locus product. The weaker rescue phenotype observed for HLA-A2 suggests that another E2 enzyme, possibly UBE2D3, may contribute to the downregulation of this HLA protein.

Previous functional studies have associated UBE2G2 with several ER-resident E3 ubiquitin ligases. For example, UBE2G2 interacts with HRD1 (also known as SYVN1) (Kikkert et al., 2004) and TEB4 (also known as MARCH6) (Hassink et al., 2005) to promote K48-linked polyubiquitylation *in vitro*. The E3 ligase gp78 (also known as AMFR) also cooperates with UBE2G2 (Liu et al., 2014). A dedicated UBE2G2-binding region (G2BR) has been identified

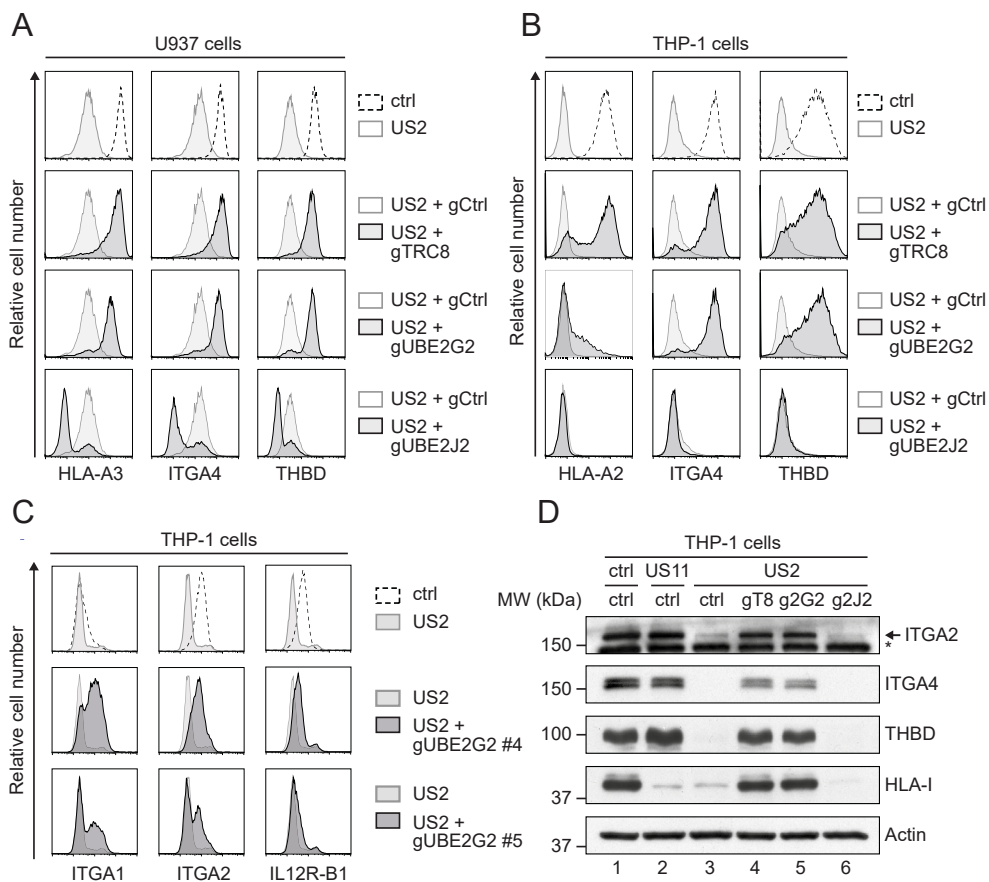


Fig. 5. UBE2G2 and UBE2J2 regulate US2-induced immunoreceptor downregulation.

(A, B) U937 (A) or THP-1 (B) cells expressing US2 were lentivirally transduced with a CRISPR/Cas9 vector targeting TRC8 (gRNA #1), UBE2G2 (gRNA #1) or UBE2J2 (gRNA #1). At 2 days after infection, gRNA-expressing cells were selected using puromycin. Cell surface expression of integrin- α 4 (ITGA4), thrombomodulin (THBD) and HLA-I (HLA-A2 for THP-1 cells, HLA-A3 for U937 cells) was assessed by flow cytometry at 10 days (U937) or 15 days (THP-1) post infection. (C) THP-1 cells expressing US2 were lentivirally transduced with two CRISPR gRNAs (#4 and #5) targeting UBE2G2. At 2 days after infection, gRNA-expressing cells were selected using puromycin, and expression of integrin α 1 (ITGA1), integrin α 2 (ITGA2) or IL12 receptor β 1-subunit (IL12R-B1) was assessed by flow cytometry at 7 dpi. (D) Lysates from cells used in B were prepared and subjected to immunoblotting analysis for total protein expression levels of ITGA2, ITGA4, thrombomodulin, and HLA-I (HCA2). US11-expressing cells were included as a control. Actin was used as a loading control. The asterisk marks an unspecific band.

for gp78 that increases its affinity for UBE2G2 by ~50-fold. The strong interaction between gp78 and UBE2G2 allows for efficient ubiquitylation and degradation of the CD3 δ subunit (Das et al., 2009; Chen et al., 2006). Both gp78 and HRD1 act with UBE2G2 to catalyze cholera toxin dislocation (Bernardi et al., 2010). UBE2G2 has also been proposed to be involved in the turnover of HMGCR (Miao et al., 2010). HMGCR degradation is facilitated by the E3 ligases gp78 (Jo et al., 2011, 2013) and TRC8 (Chen et al., 2006; Jo et al., 2011) as well as the UBE2G2-recruiting protein AUP1 (Jo et al., 2013). Although this suggests that UBE2G2 cooperates with the E3s TRC8 and gp78 to facilitate degradation of HMGCR, a direct role for UBE2G2 has not been established in these studies. Our data show that UBE2G2 is a crucial player in US2-induced dislocation of HLA-I as well as degradation of other immunoreceptors, all of which also require the E3 ubiquitin ligase TRC8 (Stagg et al., 2009). We therefore propose that TRC8 and UBE2G2 indeed cooperate in ubiquitylating ERAD substrates.

Surprisingly, UBE2J2 is able to counteract US2-induced HLA-I degradation. When knocking out UBE2J2, we observed an unexpected further downregulation of eGFP–HLA-A2 as well as endogenous HLA-A3. This phenotype is reversed upon reconstitution of UBE2J2 expression by means of cDNA expression. In contrast to UBE2G2, little is known about the tail-anchored E2 ubiquitin-conjugating enzyme UBE2J2 and its role in protein degradation. Its murine homolog plays a role in ERAD of unassembled T-cell receptor subunits (Tiwari and Weissman, 2001).

Interestingly, UBE2J2 has previously been described to be involved in MHC class I downregulation in the context of herpesviral infection. During infection with γ -herpesvirus 68 (γ -HV68), UBE2J2 is recruited by the viral murine K3 (mK3) E3 ubiquitin ligase and facilitates the degradation of murine MHC class I molecules (Wanget al., 2009). The HCMV protein US11 also cooperates with UBE2J2 to downregulate HLA-I. Similar to US2, US11 causes accelerated ER-associated degradation of HLA-I, but the proteins do so through different degradation pathways. US11 acts in concert with the cellular E3 ubiquitin ligase TMEM129 and recruits UBE2J2 to ubiquitylate and dislocate HLA-I from the ER membrane (van de Weijer et al., 2014; van den Boomen et al., 2014). How UBE2J2 balances HLA-I downregulation during HCMV infection, in which both the UBE2J2-dependent US11 as well as the UBE2J2-counteracted US2 proteins are present, is currently unknown.

The counteracting effect of UBE2J2 on US2-mediated HLA-I degradation may be related to downregulation of the ubiquitin E3 ligase TRC8. We observe increased levels of TRC8 in both

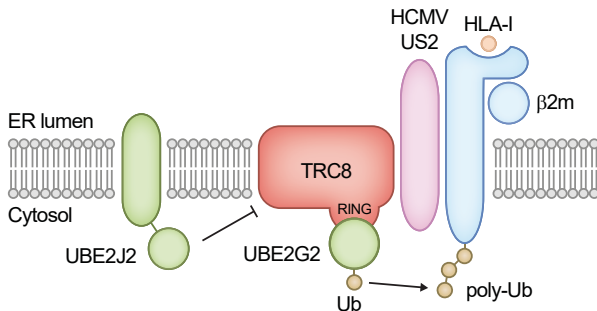


Figure 6 | Schematic overview of the ubiquitylation step in US2-mediated HLA-I downregulation. US2 engages β 2m-associated HLA-I and directs it to the E3 ubiquitin ligase TRC8. In cooperation with UBE2G2, TRC8 facilitates polyubiquitylation of HLA-I. Next, p97 catalyzes the extraction from the ER membrane into the cytosol for proteasomal degradation. UBE2J2 depletion increases TRC8 expression levels in the presence of US2, and in this way, enhances US2-mediated HLA-I downregulation.

clonal UBE2J2-knockout cells and cells expressing catalytically inactive UBE2J2. TRC8 is a crucial player in US2-mediated ERAD, not only for HLA-I degradation (Stagg et al., 2009), but also for degradation of other cell surface receptors, including α - and β -integrins, the NK cell-activating receptor CD112 (also known asnectin-2), thrombomodulin and the IL-12 receptor β 1 subunit (Hsu et al., 2015). In the absence of US2, UBE2J2 depletion or expression of a catalytically inactive UBE2J2 also results in increased TRC8 expression levels, indicating that UBE2J2 might play a general role in the turnover of TRC8. We thus propose that the increased downregulation of HLA-I upon UBE2J2 depletion is primarily caused by increased TRC8 levels in these cells (Fig. 6). Expression of a catalytically inactive UBE2J2 mutant also enhances HLA-I downregulation, mimicking the UBE2J2-knockout phenotype. These results suggest that the catalytic activity of UBE2J2 is required for the downregulation of TRC8 and hence for the increased HLA-I downregulation.

Remarkably, expression of US2 alone was sufficient to induce a dramatic decrease in TRC8 levels. This observation suggests that US2 also induces degradation of TRC8. This reaction is potentially aided by UBE2J2. Why US2 limits TRC8 expression while it relies on this E3 ligase to dispose of HLA-I and other immunoreceptors remains to be determined.

Counteracting mechanisms, such as TRC8 downregulation by UBE2J2 and US2, highlight an interesting regulatory pathway in which ERAD factors themselves influence turnover of the ERAD and ER stress machinery. A similar phenomenon has been described for HERP (also known as HEY2), a key organizer of ERAD complexes in the ER (Leitman et al., 2014). HERP is upregulated under ER stress, when the unfolded protein response (UPR) is activated. Once stress is relieved, HERP levels are reduced again via ERAD, in this case via UBE2G2- and gp78-mediated ubiquitylation (Yan et al., 2014). IRE1 α , a sensor for the unfolded protein response, is also upregulated under conditions of ER stress. This ER-resident transmembrane protein is degraded by an ERAD complex centered around the E3 ubiquitin ligase HRD1, in complex with SEL1L (Sun et al., 2015). For TRC8, no such downregulation has been described to date, although this E3 ligase is known to catalyze auto-ubiquitylation and cause its own downregulation upon sterol abundance (Lee et al., 2010). The existence of negative feedback loops in the life cycle of ERAD- and ER stress-related factors underlines the complexity of these protein turnover pathways. The present study sheds light on the regulation of HCMV-induced immunoreceptor degradation, as well as a feedback loop within this ERAD pathway, a process that involves a multitude of acting and counteracting E2 ubiquitin-conjugating enzymes.

ACKNOWLEDGEMENTS

We thank Jasper Soppe, Ferdy van Diemen and Luan Nguyen from the Medical Microbiology department at UMC Utrecht for their assistance in deep sequencing.

COMPETING INTERESTS

The authors declare no competing or financial interests.

AUTHOR CONTRIBUTIONS

Conceptualization: M.L.v.d.W., A.B.C.S., R.J.L., E.J.H.J.W.; Methodology: M.L.v.d.W., A.B.C.S.; Validation: M.L.v.d.W., A.B.C.S., D.J.H.v.d.B., P.J.L., R.J.L., E.J.H.J.W.; Investigation: M.L.v.d.W., A.B.C.S., D.J.H.v.d.B.; Resources: A.M., F.H.J.C.; Writing - original draft: M.L.v.d.W., A.B.C.S.; Writing - review & editing: M.L.v.d.W., A.B.C.S., D.J.H.v.d.B., P.J.L., R.J.L., E.J.W.; Supervision: R.J.L., E.J.H.J.W.; Project administration: R.J.L., E.J.H.J.W.; Funding acquisition: P.J.L., R.J.L., E.J.H.J.W.

FUNDING

A.B.C.S. is funded by the Graduate Programme of the Nederlandse Organisatie voor Wetenschappelijk Onderzoek (Netherlands Organization for Scientific Research; NWO) (project number 022.004.018), and by a Wellcome Trust PRF (Principal Research Fellowship) to P.J.L. with grant no. 101835/Z/13/Z. Deposited in PMC for release after 6 months.

SUPPLEMENTARY INFORMATION

Supplementary information available online at <http://jcs.biologists.org/lookup/doi/10.1242/jcs.206839.supplemental>

REFERENCES

- Ahn, K., Gruhler, A., Galocha, B., Jones, T. R., Wiertz, E. J. H. J., Ploegh, H. L., Peterson, P. A., Yang, Y. and Fröhlich, K. (1997). The ER-luminal domain of the HCMV glycoprotein US6 inhibits peptide translocation by TAP. *Immunity* 6, 613-621.
- Bernardi, K. M., Williams, J. M., Kikkert, M., van Voorden, S., Wiertz, E. J., Ye, Y. and Tsai, B. (2010). The E3 ubiquitin ligases Hrd1 and gp78 bind to and promote cholera toxin retro-translocation. *Mol. Biol. Cell* 21, 140-151.
- Chen, B., Mariano, J., Tsai, Y. C., Chan, A. H., Cohen, M. and Weissman, A. M. (2006). The activity of a human endoplasmic reticulum-associated degradation E3, gp78, requires its Cue domain, RING finger, and an E2-binding site. *Proc. Natl. Acad. Sci. USA* 103, 341-346.
- Christianson, J. C., Olzmann, J. A., Shaler, T. A., Sowa, M. E., Bennett, E. J., Richter, C. M., Tyler, R. E., Greenblatt, E. J., Harper, J. W. and Kopito, R. R. (2011). Defining human ERAD networks through an integrative mapping strategy. *Nat. Cell Biol.* 14, 93-105.
- Das, R., Mariano, J., Tsai, Y. C., Kalathur, R. C., Kostova, Z., Li, J., Tarasov, S. G., McFeeters, R. L., Altieri, A. S., Ji, X. et al. (2009). Allosteric activation of E2-RING finger-mediated ubiquitylation by a structurally defined specific E2-binding region of gp78. *Mol. Cell* 34, 674-685.
- Duncan, L. M., Nathan, J. A. and Lehner, P. J. (2010). Stabilization of an E3 Ligase-E2-ubiquitin complex increases cell surface MHC class I expression. *J. Immunol.* 184, 6978-6985.
- Dunn, W., Chou, C., Li, H., Hai, R., Patterson, D., Stolc, V., Zhu, H. and Liu, F. (2003).

Functional profiling of a human cytomegalovirus genome. *Proc. Natl. Acad. Sci. USA* 100, 14223-14228.

Flierman, D., Coleman, C. S., Pickart, C. M., Rapoport, T. A. and Chau, V. (2006). E2-25K mediates US11-triggered retro-translocation of MHC class I heavy chains in a permeabilized cell system. *Proc. Natl. Acad. Sci. USA* 103, 11589-11594.

Griffiths, P., Baraniak, I. and Reeves, M. (2015). The pathogenesis of human cytomegalovirus. *J. Pathol.* 235, 288-297.

Hansen, S. G., Powers, C. J., Richards, R., Ventura, A. B., Ford, J. C., Siess, D., Axthelm, M. K., Nelson, J. A., Jarvis, M. A., Picker, L. J. et al. (2010). Evasion of CD8+ T cells is critical for superinfection by cytomegalovirus. *Science* 328, 102-106.

Hassink, G., Kikkert, M., van Voorden, S., Lee, S.-J., Spaapen, R., van Laar, T., Coleman, C. S., Bartee, E., Fröhlich, K., Chau, V. et al. (2005). TEB4 is a C4HC3 RING finger-containing ubiquitin ligase of the endoplasmic reticulum. *Biochem. J.* 388, 647-655.

Hengel, H., Koopmann, J.-O., Flohr, T., Muranyi, W., Goulmy, E., Hämmerling, G. J., Koszinowski, U. H. and Momburg, F. (1997). A viral ER-resident glycoprotein inactivates the MHC-encoded peptide transporter. *Immunity* 6, 623-632.

Hewitt, E. W., Gupta, S. S. and Lehner, P. J. (2001). The human cytomegalovirus gene product US6 inhibits ATP binding by TAP. *EMBO J.* 20, 387-396.

Hsu, J.-L., van den Boomen, D. J. H., Tomasec, P., Weekes, M. P., Antrobus, R., Stanton, R. J., Ruckova, E., Sugrue, D., Wilkie, G. S., Davison, A. J. et al. (2015). Plasma membrane profiling defines an expanded class of cell surface proteins selectively targeted for degradation by HCMV US2 in cooperation with UL141. *PLoS Pathog.* 11, e1004811.

Jo, Y., Lee, P. C. W., Sguigna, P. V. and DeBose-Boyd, R. A. (2011). Sterol-induced degradation of HMG CoA reductase depends on interplay of two Insigs and two ubiquitin ligases, gp78 and Trc8. *Proc. Natl. Acad. Sci. USA* 108, 20503-20508.

Jo, Y., Hartman, I. Z. and DeBose-Boyd, R. A. (2013). Ancient ubiquitous protein-1 mediates sterol-induced ubiquitination of 3-hydroxy-3-methylglutaryl CoA reductase in lipid droplet-associated endoplasmic reticulum membranes. *Mol. Biol. Cell* 24, 169-183.

Jones, T. R., Wiertz, E. J., Sun, L., Fish, K. N., Nelson, J. A. and Ploegh, H. L. (1996). Human cytomegalovirus US3 impairs transport and maturation of major histocompatibility complex class I heavy chains. *Proc. Natl. Acad. Sci. USA* 93, 11327-11333.

Kikkert, M., Doolman, R., Dai, M., Avner, R., Hassink, G., van Voorden, S., Thanedar, S., Roitelman, J., Chau, V. and Wiertz, E. (2004). Human HRD1 is an E3 ubiquitin ligase involved in degradation of proteins from the endoplasmic reticulum. *J. Biol. Chem.* 279, 3525-3534.

- Kleiger, G., Saha, A., Lewis, S., Kuhlman, B. and Deshaies, R. J. (2009). Rapid E2-E3 assembly and disassembly enable processive ubiquitylation of cullin-RING ubiquitin ligase substrates. *Cell* 139, 957-968.
- Lee, J. P., Brauweiler, A., Rudolph, M., Hooper, J. E., Drabkin, H. A. and Gemmill, R. M. (2010). The TRC8 ubiquitin ligase is sterol regulated and interacts with lipid and protein biosynthetic pathways. *Mol. Cancer Res.* 8, 93-106.
- Lehner, P. J., Karttunen, J. T., Wilkinson, G.W. G. and Cresswell, P. (1997). The human cytomegalovirus US6 glycoprotein inhibits transporter associated with antigen processing-dependent peptide translocation. *Proc. Natl. Acad. Sci. USA* 94, 6904-6909.
- Leitman, J., Shenkman, M., Gofman, Y., Shtern, N. O., Ben-Tal, N., Hendershot, L. M. and Lederkremer, G. Z. (2014). Herp coordinates compartmentalization and recruitment of HRD1 and misfolded proteins for ERAD. *Mol. Biol. Cell* 25, 1050-1060.
- Lilley, B. N. and Ploegh, H. L. (2004). A membrane protein required for dislocation of misfolded proteins from the ER. *Nature* 429, 834-840.
- Liu, W., Shang, Y., Zeng, Y., Liu, C., Li, Y., Zhai, L., Wang, P., Lou, J., Xu, P., Ye, Y. et al. (2014). Dimeric Ube2g2 simultaneously engages donor and acceptor ubiquitins to form Lys48-linked ubiquitin chains. *EMBO J.* 33, 46-61.
- McGeoch, D. J., Rixon, F. J. and Davison, A. J. (2006). Topics in herpesvirus genomics and evolution. *Virus Res.* 117, 90-104.
- Miao, H., Jiang, W., Ge, L., Li, B. and Song, B. (2010). Tetra-glutamic acid residues adjacent to Lys248 in HMG-CoA reductase are critical for the ubiquitination mediated by gp78 and UBE2G2. *Acta Biochim. Biophys. Sin. (Shanghai).* 42, 303-310.
- Mocarski, E. S. (2002). Immunomodulation by cytomegaloviruses: manipulative strategies beyond evasion. *Trends Microbiol.* 10, 332-339.
- Noriega, V. M., Hesse, J., Gardner, T. J., Besold, K., Plachter, B. and Tortorella, D. (2012a). Human cytomegalovirus US3 modulates destruction of MHC class I molecules. *Mol. Immunol.* 51, 245-253.
- Noriega, V., Redmann, V., Gardner, T. and Tortorella, D. (2012b). Diverse immune evasion strategies by human cytomegalovirus. *Immunol. Res.* 54, 140-151.
- Olzmann, J. A., Kopito, R. R. and Christianson, J. C. (2013). The mammalian endoplasmic reticulum-associated degradation system. *Cold Spring Harb. Perspect. Biol.* 5, a013185.
- Oresic, K., Ng, C. L. and Tortorella, D. (2009). TRAM1 participates in human cytomegalovirus

US2- and US11-mediated dislocation of an endoplasmic reticulum membrane glycoprotein. *J. Biol. Chem.* 284, 5905-5914.

Park, B., Kim, Y., Shin, J., Lee, S., Cho, K., Fröhlich, K., Lee, S. and Ahn, K. (2004). Human cytomegalovirus inhibits tapasin-dependent peptide loading and optimization of the MHC class I peptide cargo for immune evasion. *Immunity* 20, 71-85.

Park, B., Spooner, E., Houser, B. L., Strominger, J. L. and Ploegh, H. L. (2010). The HCMV membrane glycoprotein US10 selectively targets HLA-G for degradation. *J. Exp. Med.* 207, 2033-2041.

Preston, G. M. and Brodsky, J. L. (2017). The evolving role of ubiquitin modification in endoplasmic reticulum-associated degradation. *Biochem. J.* 474, 445-469.

Schuren, A. B. C., Costa, A. I. and Wiertz, E. J. H. J. (2016). Recent advances in viral evasion of the MHC Class I processing pathway. *Curr. Opin. Immunol.* 40, 43-50.

Soetandyo, N. and Ye, Y. (2010). The p97 ATPase dislocates MHC class I heavy chain in US2-expressing cells via a Ufd1-Npl4-independent mechanism. *J. Biol. Chem.* 285, 32352-32359.

Stagg, H. R., Thomas, M., van den Boomen, D., Wiertz, E. J. H. J., Drabkin, H. A., Gemmill, R. M. and Lehner, P. J. (2009). The TRC8 E3 ligase ubiquitinates MHC class I molecules before dislocation from the ER. *J. Cell Biol.* 186, 685-692.

Sun, S., Shi, G., Sha, H., Ji, Y., Han, X., Shu, X., Ma, H., Inoue, T., Gao, B., Kim, H. et al. (2015). IRE1 α is an endogenous substrate of endoplasmic-reticulum associated degradation. *Nat. Cell Biol.* 17, 1546-1555.

Tiwari, S. and Weissman, A. M. (2001). Endoplasmic reticulum (ER)-associated degradation of T cell receptor subunits. Involvement of ER-associated ubiquitinconjugating enzymes (E2s). *J. Biol. Chem.* 276, 16193-16200.

Van de Weijer, M. L., Bassik, M. C., Luteijn, R. D., Voorburg, C. M., Lohuis, M. A. M., Kremmer, E., Hoeben, R. C., LeProust, E. M., Chen, S., Hoelen, H. et al. (2014). A high-coverage shRNA screen identifies TMEM129 as an E3 ligase involved in ER-associated protein degradation. *Nat. Commun.* 5, 3832.

Van de Weijer, M. L., Luteijn, R. D. and Wiertz, E. J. H. J. (2015). Viral immune evasion: lessons in MHC class I antigen presentation. *Semin. Immunol.* 27, 125-137.

Van den Boomen, D. J. H. and Lehner, P. J. (2015). Identifying the ERAD ubiquitin E3 ligases for viral and cellular targeting of MHC class I. *Mol. Immunol.* 68, 106-111.

Van den Boomen, D. J. H., Timms, R. T., Grice, G. L., Stagg, H. R., Skødt, K., Dougan, G., Nathan, J. A. and Lehner, P. J. (2014). TMEM129 is a Derlin-1 associated ERAD E3 ligase

essential for virus-induced degradation of MHC-I. *Proc. Natl. Acad. Sci. USA* 111, 11425-11430.

Wang, X., Herr, R. A., Rabelink, M., Hoeben, R. C., Wiertz, E. J. H. J. and Hansen, T. H. (2009). Ube2j2 ubiquitinates hydroxylated amino acids on ER-associated degradation substrates. *J. Cell Biol.* 187, 655-668.

Wiertz, E. J. H. J., Jones, T. R., Sun, L., Bogyo, M., Geuze, H. J. and Ploegh, H. L. (1996a). The human cytomegalovirus US11 gene product dislocates MHC class I heavy chains from the endoplasmic reticulum to the cytosol. *Cell* 84, 769-779.

Wiertz, E. J. H. J., Tortorella, D., Bogyo, M., Yu, J., Mothes, W., Jones, T. R., Rapoport, T. A. and Ploegh, H. L. (1996b). Sec61-mediated transfer of a membrane protein from the endoplasmic reticulum to the proteasome for destruction. *Nature* 384, 432-438.

Yan, L., Liu, W., Zhang, H., Liu, C., Shang, Y., Ye, Y., Zhang, X. and Li, W. (2014). Ube2g2-gp78-mediated HERP polyubiquitylation is involved in ER stress recovery. *J. Cell Sci.* 127, 1417-1427.

Ye, Y., Meyer, H. H. and Rapoport, T. A. (2001). The AAA ATPase Cdc48/p97 and its partners transport proteins from the ER into the cytosol. *Nature* 414, 652-656.

Ye, Y., Shibata, Y., Yun, C., Ron, D. and Rapoport, T. A. (2004). A membrane protein complex mediates retro-translocation from the ER lumen into the cytosol. *Nature* 429, 841-847.

Ye, Y., Shibata, Y., Kikkert, M., van Voorden, S., Wiertz, E. and Rapoport, T. A. (2005). Recruitment of the p97 ATPase and ubiquitin ligases to the site of retrotranslocation at the endoplasmic reticulum membrane. *Proc. Natl. Acad. Sci. USA* 102, 14132-14138.

Yin, Q., Lin, S.-C., Lamothe, B., Lu, M., Lo, Y.-C., Hura, G., Zheng, L., Rich, R. L., Campos, A. D., Myszka, D. G. et al. (2009). E2 interaction and dimerization in the crystal structure of TRAF6. *Nat. Struct. Mol. Biol.* 16, 658-666.





CHAPTER

4

The UFM1 pathway
impacts HCMV US2-
mediated degradation of
HLA class I

A.B.C. Schuren¹, I.G.J. Boer¹, E.M. Bouma^{1,2},
M.L. van de Weijer^{1,3}, P. Hubel⁴, A. Pichlmair⁴, R.J.
Lebbink^{1,#,*} and E.J.H.J. Wiertz^{1,#,*}

These authors contributed equally

1 Dept. Medical Microbiology, University Medical Center Utrecht, 3584CX Utrecht, The Netherlands. 2 Current address: Department of Medical Microbiology, University Medical Center Groningen, Postbus 30001, 9700 RB Groningen, The Netherlands. 3 Current address: Sir William Dunn School of Pathology, University of Oxford, Oxford OX1 3RE, UK. 4 Innate Immunity Laboratory, Max-Planck Institute for Biochemistry, Am Klopferspitz 18, D-82152 Martinsried / Munich, Germany. *Correspondence: E.Wiertz@umcutrecht.nl (E.J.H.J.W.); R.J.Lebbink-2@umcutrecht.nl (R.J.L.).

submitted

ABSTRACT

To prevent the accumulation of misfolded proteins in the endoplasmic reticulum, chaperones perform quality control on newly translated proteins and direct misfolded proteins back to the cytosol for degradation by the ubiquitin-proteasome system. This pathway is called ER-associated protein degradation (ERAD). The human cytomegalovirus protein US2 induces accelerated ERAD of HLA class I molecules to prevent immune recognition of infected cells by CD8⁺ T cells. Using US2-mediated HLA-I degradation as a model for ERAD, we performed a genome-wide CRISPR/Cas9 library screen to identify novel cellular factors associated with ERAD. Besides identifying known factors such as TRC8, p97, and UBE2G2, we identify players of the UFM1 pathway to affect degradation of HLA-I. UFMylation is a post-translational modification resembling ubiquitination. Whereas we observe ubiquitination of HLA-I, no UFMylation was detected on ERAD-related proteins, suggesting that the UFM1 pathway impacts ERAD in a different manner than ubiquitin. Mass spectrometry analysis showed that ribosomes are UFMylated in US2-expressing cells. We speculate that UFM1 may affect US2-mediated protein degradation via an indirect mechanism, potentially involving the ribosome.

INTRODUCTION

When newly translated secretory proteins are inserted into the ER, quality control must occur to ensure that misfolded proteins do not accumulate and disturb ER function. In the ER, protein folding is continuously monitored by molecular chaperones. When a protein fails to acquire its correct conformation, it is transferred to the ER-associated protein degradation (ERAD) pathway. Substrates of ERAD are transported over the ER membrane towards the cytosol, where they are ubiquitinated and degraded by the proteasome.

With over 70 diseases associated with ERAD^{1,2}, including cystic fibrosis and Parkinson's disease, a better understanding of this protein degradation pathway is required. Because viruses depend on and manipulate their host cells, they provide useful models to study a wide range of cellular processes. Indeed, many viruses exploit ERAD to facilitate virus replication³ or to evade immune recognition^{4,5}. These manipulation strategies can be exploited to study protein degradation.

Human cytomegalovirus (HCMV) is a herpesvirus that causes severe congenital defects when it infects pregnant women⁶. The virus can successfully evade the immune system, allowing it to persist in the body lifelong. HCMV induces accelerated ERAD of HLA class I molecules to prevent recognition of virus-infected cells by CD8⁺ T lymphocytes. The viral proteins responsible for this, US2 and US11, serve as important models to study the degradation of ER-resident proteins. These HCMV proteins have allowed the identification of many key mammalian ERAD factors, including Derlins, VIMP^{7,8}, and the ubiquitin E3 ligases TRC8⁹ and TMEM129^{10,11}.

Despite the identification of a number of factors involved in ERAD, many questions remain to be answered. It is thought that the protein complexes required for ERAD are (partially) specific to the substrate that is degraded, in combination with some general ERAD players such as p97/VCP and the proteasome. While the ubiquitination machinery for US2-mediated degradation of HLA class I has been identified⁹⁻¹³, knowledge about other ERAD factors is lacking.

Here, we performed a genome-wide CRISPR/Cas9 library screen to identify novel host genes involved in US2-mediated HLA class I degradation. Besides known ERAD-related factors,

we identified all known factors of the UFMylation pathway to affect HLA-I degradation via US2. Under the circumstances used however, we did not detect UFMylation of HLA-I or other proteins involved in ERAD. A mass spectrometry analysis showed that UFMylation may occur on ribosomes in US2-expressing cells. We speculate that UFM1 may affect US2-mediated protein degradation indirectly, via a mechanism potentially involving the ribosome.

MATERIALS AND METHODS

Cell culture and lentiviral transduction

U937 cells (ATCC) were cultured in RPMI 1640 culture medium (Gibco) supplemented with penicillin/streptomycin (Gibco), Ultraglutamine-1 (Gibco) and 10% fetal calf serum (BioWest). Wildtype U937 cells were lentivirally transduced with HLA-A2-eGFP (kindly provided by Dr. Louise Boyle, University of Cambridge UK). This chimera was cloned into a lentiviral pSico vector containing a hygromycin B resistance gene. Successfully transduced cells were selected with Hygromycin B at 3 days post-infection, and subcloned. The HLA-A2-eGFP cells were subsequently transduced with US2 and a clonal cell line was established by fluorescence-activated cell sorting (FACS) of the HLA-A2-eGFP^{low} cells. SpCas9 (Addgene #52962) was stably introduced by lentiviral transduction and selected for by Blastocidin treatment starting at three days post-infection.

Plasmids

HLA-A2-eGFP was expressed from a bidirectional lentiviral vector under control of an EF1a promoter. The vector also contained a Hygromycin B resistance cassette in the other direction, under control of a hPGK promoter. US2 was expressed from an EF1a promoter in a lentiviral backbone. The lentiCas9-Blast vector was a gift from Feng Zhang (Addgene plasmid #52962; <http://n2t.net/addgene:52962>; RRID: Addgene_52962). This vector drives expression of SpCas9 and a Blastocidin resistance gene. CRISPR sgRNAs were cloned downstream of a human U6 promoter in a BsmBI-linearized pSicoR lentiviral vector also containing an EFS (EF1A short) promoter driving expression of a puromycinR-T2A-Cas9Flag cassette. sgRNA-resistant cDNAs for UFM1, UBA5 and UFC1 were expressed from an EF1A promoter on a bidirectional lentiviral vector. This vector also contains a human PGK promoter driving expression of a Zeocin resistance gene.

Genome-wide CRISPR/Cas9 library screen

150 million U937 HLA-A2-eGFP cells co-expressing US2 and SpCas9 were transduced at an MOI of 2 in duplicate with the human GeCKOv2 CRISPR knockout pooled library (gift from Feng Zhang (Addgene, #1000000049)). The library targets 19,050 genes with 6 sgRNAs/gene. Transduced cells were selected by puromycin treatment (2 µg/ml) at 2 days post-infection (d.p.i.) and maintained at high complexity for the duration of the screen. At 7 and 18 d.p.i., 1 billion cells were harvested and subjected to cell sorting via a two-step sort-protocol using a Becton Dickinson Influx cell sorter. First, PE⁺ cells were sorted using an 'enrichment-protocol', which allowed for high-speed cell sorting of the entire population of cells in a short timeframe. Next, we sorted the top ±1% of eGFP⁺/PE⁺ cells to purity selecting for cells that display

enhanced levels of eGFP and HLA-A2 surface staining (stained with BB7.2-PE; BD Biosciences, #558570). As control, the eGFP^{low}/HLA-A2^{low} were sorted. We next isolated genomic DNA from all sorted cell populations by standard phenol/chloroform extraction protocols using the Phase Lock gel heavy tubes (Quantabio; 10847-802) according to manufacturer's instructions. Next, the lentiviral sgRNA inserts were PCR-amplified for 27 cycles using Fw primer 5'-**AATGATACGGCGACCACCGAGATCTACACTCTTCCCTACACGACGCTCTTC-CGATCTNNNNNN**Nctgtggaaggac gaaacacc-3' and Rev primer 5'-**CAAGCAGAAGACG-GCATAACGAGAT**gactcggtgccacttttcaag-3' and Phusion polymerase (NEB) in the presence of buffer GC supplemented with DMSO. Both primers contain an Illumina adapter sequence (displayed in bold) that allows for direct loading on an Illumina NextSeq500 sequencer and a lentiviral-specific primer binding site (lowercase letter) to facilitate amplification of the integrated lentiviral sgRNA sequence. The Fw primer also contains a unique 6nt barcode sequence (NNNNNN) allowing for multiplexed sequencing, and a primer binding site for the Illumina sequencing primer (underlined). The PCR products were purified/concentrated using a PCR purification kit (Qiagen), and subsequently loaded on a 20% polyacrylamide gel in 0.5 × TBE. Bands of the correct size were excised, electro-eluted, purified by phenol-chloroform extraction and subsequently quantified using a Nanodrop quantification device (Nanodrop, Rockland, DE, USA) and an Agilent bioanalyzer (Agilent Technologies, Palo Alto, CA, USA). Deep sequencing was carried out as single 75bp run on a Illumina NextSeq500 machine (performed by the Utrecht Sequencing facility USEQ) using the sequencing primer 5'-ACACTCTTCCCTACACGACGCTCTTCCGATCT-5', in which the Index and sgRNA sequence was sequenced simultaneously. Due to the low complexity at the start of the sequence, a Phix library was mixed with the libraries to 20% of total reads. Sequences were aligned to the sgRNA library by using Bowtie2³² and the counts per sgRNA were calculated. We used the MaGeCk package³³ (available from <https://sourceforge.net/projects/mageck/>) as a computational tool to identify genes that were significantly enriched in the screens by comparing sgRNA read counts of control sorted cells to cells displaying enhanced HLA-A2-eGFP levels. The overlap between the top 300 of the two duplicates was compared and used to select genes for further validation. The hits in this list were ranked, based on the number of sgRNAs that was enriched >5-fold, and the number of sgRNAs that showed >20-fold enrichment. As every gene was targeted with 6 sgRNAs in duplicate, the genes that showed >5-fold enrichment in at least 6 out of the total 12 sgRNAs (from both duplicates) were selected for further validation. In total, this list contained 46 genes. For initial validation studies, two sgRNAs/gene from the GeCKOv2human library that yielded the highest enrichment were selected and cloned into a pSicoR lentiviral vector with an EFS-PuroR-T2A-Cas9 cassette. sgRNA sequences are listed in Supplementary information 1. sgRNAs were transduced in target cells, and transduced cells were selected for by puromycin selection (2 µg/ml). HLA-A2-eGFP rescue of these hits was validated based on eGFP intensity and an HLA-A2-specific antibody staining on the cell surface, using a flow cytometric readout (BD FACS Canto II). When setting up the validation, some gene-knockouts resulted in strong autofluorescence, indicating that these were false-positive hits. We therefore included the irrelevant PE-Texas Red channel to omit PE-Texas Red⁺ cells prior to assessing HLA-A2-eGFP rescue. HLA-A2-eGFP expression was measured using the FITC channel for eGFP and the PE channel

for HLA-A2 cell surface expression (using a PE-conjugated HLA-A2-specific antibody, BB7.2, see 'Antibodies' section). Genes that showed only autofluorescent signal were omitted from further analysis and are not shown in the list from Figure 1B. Validation was performed on day 7, 11, 14, 18 and 28 post infection. For UFM1 and UBA5, two additional sgRNAs (#3 and #4) were designed using an online CRISPR design tool (<http://crispr.mit.edu/>). Target site sequences of these additional sgRNAs are also listed in Supplementary information 1.

Clonal knockout cell lines

sgRNAs targeting UFM1-, UBA5-, and UFC1 were introduced in target cell lines by lentiviral transduction. At 3 days post-infection, transduced cells were selected for by Puromycin treatment (2 µg/ml). At 10 d.p.i., the sgUFM1 and sgUBA5 cells were stained for HLA-A2 cell surface expression and PE⁺/GFP⁺ cells were single-cell sorted by fluorescence-activated cell sorting (FACS) on a FACSAria III. Cells were allowed to recover for ~8 weeks and analyzed by flow cytometry to select cells that displayed enhanced HLA-A2-eGFP and endogenous HLA-A3 expression. The knock-out status was confirmed by Western blot and the genomic target sites of both alleles were sequenced by Sanger sequencing.

Antibodies

Antibodies used in this study were: rabbit anti-UFM1 [EPR4264(2)] (Abcam, ab109305), rabbit anti-UBA5 (Abcam, ab177507), rabbit anti-UFC1 [EPR15014-102] (Abcam, ab189252), rabbit anti-UFL1 (Atlas Antibodies, HPA030559), mouse anti-human transferrin receptor (H68.4) (Invitrogen, 13-6800), mouse anti-p97 (VCP) (BD Transduction Laboratories, 612183), rat anti-HA (3F10) (Roche, 11867423001), mouse anti-HLA class I HCA2, mouse anti-HLA class I HC10, mouse anti-ubiquitin (P4D1) (Santa Cruz, sc-8017), goat anti-rabbit-HRP (light chain-specific) (Jackson, 211-032-171), goat anti-rat-HRP (light chain-specific) (Jackson, 112-035-175), goat anti-mouse-HRP (light chain-specific) (Jackson, 115-035-174), mouse anti-HLA-A2-PE (BB7.2) (BD Biosciences, 558570), human anti-HLA-A3 (OK2F3), goat anti-human-PE (Jackson Immunoresearch, 109-116-127)

Immunoblotting

When indicated, cells were incubated overnight with 500 nM MG132 (Sigma-Aldrich, C2211-5MG), 5 nM Bortezomib (New England Biolabs, 2204S) or DMSO control, prior to preparing cell lysates. To make lysates, cells were counted using a Casy cell counter and an equal number of live cells was subjected to two washes in PBS containing 20 mM N-ethylmaleimide (Sigma-Aldrich, E3876-5G) to block de-ubiquitinating and de-UFMylation activity. Subsequently, cells were lysed on ice in Triton X-100 lysis buffer (1% Triton X-100, 100 mM NaCl, 50 mM Tris, pH 7.5) supplemented with 20 mM N-ethylmaleimide. Samples were spun down at 12,000g for 20 minutes at 4 °C to pellet cell debris and nuclei. Supernatant was transferred to a clean tube and mixed with Lämmli sample buffer containing DTT. Lysates were stored at -80 °C until further use. For Western blot analysis, proteins were separated using SDS-PAGE (Thermo Bolt 4-12% or self-made gels) and subsequently transferred to PVDF membranes (Millipore). Membranes were blocked using 5% milk and incubated with the respective antibodies for specific protein

detection. Protein bands were visualized using ECL (Thermo Scientific Pierce) on Amersham Hyperfilm ECL films (GE Healthcare).

Co-immunoprecipitation

Cells were lysed in 1% Digitonin (Calbiochem) lysis buffer (pH 7.5) containing 50 mM Tris-HCl, 5 mM MgCl₂ and 150 mM NaCl, supplemented with 1 mM Pefabloc SC (Roche), 10 μM Leupeptin (Roche) and 20 mM N-ethylmaleimide (Sigma-Aldrich). Lysates were incubated on ice for 60 minutes and subsequently centrifuged at 12,000g for 20 minutes at 4 °C to remove nuclei and cell debris. Post-nuclear lysates were incubated overnight with StrepTactin beads (GE Healthcare). Beads were washed 4 times with 0.1% Digitonin lysis buffer, after which they were eluted for 45 minutes on ice. Elution buffer contained 2.5 mM d-Desthiobiotin, 150 mM NaCl, 100 mM Tris-HCl and 1 mM EDTA, at a pH of 8.0. The eluate was collected from the beads using SpinX columns (Corning Costar) and was denatured in Lämmli sample buffer containing DTT. Immunoblotting was performed as described before.

Mass spectrometry

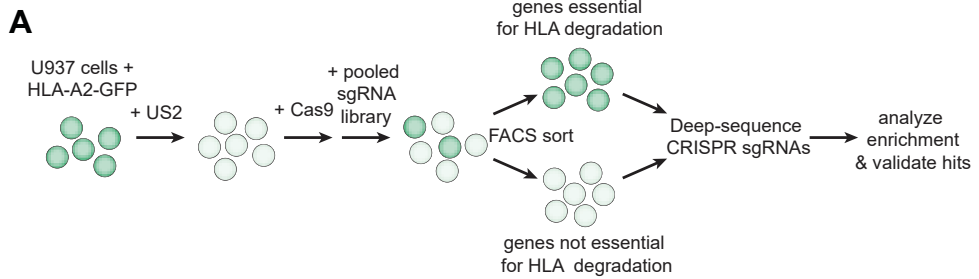
U937 cells containing HLA-A2-eGFP and US2 were transduced with either StrepII-tagged UFM1 wildtype cDNA or one of two control constructs: StrepII-tagged UFM1 ΔVGSC (inactive mutant lacking the 4 C-terminal residues) or StrepII-tagged mCherry. Per cell line, 50 million cells were pelleted in quadruplicate. Cell pellets were stored at -80 °C until lysis and immunoprecipitation. For affinity enrichment, pellets were lysed on ice using TAP lysis buffer (50 mM Tris pH 7.5, 100 mM NaCl, 5% (v/v) glycerol, 0.2 % (v/v) Nonidet-P40, 1.5 mM MgCl₂, 1 μg/ml Avidin (2-0204-015; IBA), 20 mM N-ethylmaleimide, and protease inhibitor cocktail (EDTA-free, cOmplete; Roche)) for 15 min followed by a 5 min sonication step at 4°C. StrepTactin agarose was added to the clarified cell lysates and incubated for 3h at 4°C on a rotary wheel. Beads were washed four times in TAP lysis buffer to reduce the concentration of unspecific proteins and to separate specific binders from background ones. Samples were washed five additional times with TAP washing buffer (50 mM Tris pH 7.5, 100 mM NaCl, 5% (v/v) glycerol, 1.5 mM MgCl₂) supplemented with 20 mM N-ethylmaleimide, to remove remaining detergents. Beads were re-suspended in 20 μl guanidinium chloride buffer (6 M GdmCl, 10 mM TCEP, 40 mM CAA, 100 mM Tris/HCl pH 8), boiled at 95 °C for 5 min and digested by adding 20 μl LysC-Protease-Mix (100 mM Tris/HCl pH 8 and 0.5 μg LysC (WAKO Chemicals USA)) for 3h at 30°C. Samples were diluted 1:5 with Trypsin-Protease-Mix (100 mM Tris/HCl pH 8 and 1 μg Trypsin) (Promega) and incubated for 12h at room temperature. TFA and acetonitrile was added to a final concentration of 0.6% and 2%, respectively. Peptides were desalted and concentrated using C18 Empore filter discs (3M)32. After elution, peptides were analysed employing an EASY-nanoLC system (Thermo Fisher Scientific), which was directly coupled to a Q-Exactive plus HF mass spectrometer (Thermo Fisher Scientific). Peptides were loaded on an analytical 15 cm C18 column (Reprosil-Pur 120 C10-AQ, 3 μM; Dr. Maisch) and eluted using an 115 min acetonitrile gradient starting with 5% to 30% (85 min), 30% to 95% (15 min), a wash out period of 5 min at 95% and a re-adjustment phase to 5% of organic acetonitrile buffer (80% acetonitrile, 0.1% Formic acid) (10 min) at a constant flow of 250 nl/min. The mass

spectrometer was used in a data-dependent acquisition mode with one full MS scan followed by 15 MS/MS scans. Raw files were processed with MaxQuant version 1.5.3.34 using label-free quantification (LFQ) and match between run options and searched against forward and reverse sequences of the human proteome (UniprotKB, release 03.2016) by the built-in Andromeda search engine. Carbamidometylation was set as fixed, methionine oxidation and N-acetylation as variable modification. Precursor ions with a mass tolerance of 6 ppm and fragmented ions with a mass tolerance of 0.5 Da were accepted. Peptide and protein identification were controlled by a False Discovery Rate (FDR) of 0.01. Perseus version 1.5.3.0 was used to analyze the output of MaxQuant. Protein groups identified as known contaminants or reverse sequence matches were excluded from the analysis. Only proteins with a minimum of 2 LFQ quantifications in at least one group of replicate experiments ($N = 4$) for a specific condition were considered for the analysis. Missing values were imputed using normal distribution, whose standard deviation was defined as 30% and the mean was offset by -1.8 standard deviations of the data distribution of the real intensities observed in the corresponding MS run, respectively. The significance of the protein enrichment in the pulldowns of a bait versus the other condition was determined by t-test (two-sided, equal variance, $S0=0.5$) and corrected for multiple hypothesis testing using permutation-based false discovery rate statistics (FDR=0.05, 250 permutations).

RESULTS

A genome-wide CRISPR/Cas9 library screen identifies the UFM1 pathway as essential for HCMV US2-mediated ERAD

To identify novel human genes involved in HCMV US2-mediated degradation of ER-resident HLA class I molecules (HLA-I), we performed a genome-wide CRISPR/Cas9 library screen. U937 cells expressing a C-terminally eGFP-tagged HLA-A2 chimera, as well as HCMV US2 and Cas9, were transduced in duplicate with the GeCKO v2 CRISPR library, targeting 19,050 genes with 6 single guideRNAs (sgRNAs) per gene (Fig. 1A). Knocking out a gene that is crucial for US2-mediated HLA class I degradation is expected to rescue the eGFP-tagged HLA-A2 chimera from degradation, thereby increasing eGFP levels in the cell. We used FACS to select cells displaying enhanced levels of eGFP (rescued eGFP-tagged HLA-A2 expression) as well as PE (cell surface expression of HLA-A2 as detected by an antibody staining) at 7- and 18 days post-transduction. Cells displaying low eGFP- and HLA-A2 cell surface expression were sorted as a control. As ERAD is an important cellular pathway that is essential for cell viability, the 7-day timepoint was included to allow for the identification of ERAD factors that are critical for cell survival. We next sequenced the lentiviral sgRNA sequences from the eGFP⁺/HLA-A2⁺ and control cell populations by Illumina sequencing and used the MaGeCK package to compare the HLA-A2⁺ population *versus* the control at both timepoints. The overlap of the top 300 genes was used to select genes for further analysis, which is presented in Figure 1B. As expected, essential genes such as proteasome subunits were identified only at the early timepoint, whereas others, such as AUP1 and SEC63, were seen only after 18 days. TRC8 (RNF139), the known ubiquitin E3 ligase for US2-mediated HLA-I degradation⁹, was our main hit at both timepoints, and therefore used as positive control for the following studies. We also identified other known players in US2-mediated ERAD, such as the E2 enzyme UBE2G2¹³, p97/VCP¹⁴, various proteasomal

**B**

Gene ID	Gene symbol	Full name	Enriched at:		Included in validation:
			7 dpi	18 dpi	
550	AUP1	Ancient Ubiquitous Protein 1		✓	
567	B2M	Beta-2 Microglobulin	✓	✓	
79587	CARS2	Cysteinyl-tRNA Synthetase 2, Mitochondrial		✓	✓
27235	COQ2	Coenzyme Q2, Polyprenyltransferase		✓	✓
23197	FAF2	Fas-Associated Factor Family Member 2	✓	✓	
192286	HIGD2A	HIG1 Hypoxia Inducible Domain Family Member 2A		✓	✓
6782	HSPA13	Heat Shock Protein Family (Hsp70) Member 13	✓		✓
4528	MTIF2	Mitochondrial Translation Initiation Factor 2		✓	✓
54539	NDUFB11	NADH:Ubiquinone Oxidoreductase Subunit B11		✓	✓
55666	NPLOC4	NPL4 Homolog, Ubiquitin Recognition Factor	✓	✓	
5687	PSMA6	Proteasome Subunit Alpha 6	✓		
5695	PSMB7	Proteasome Subunit Beta 7	✓		✓
5702	PSMC3	Proteasome 26S Subunit, ATPase 3	✓		
5705	PSMC5	Proteasome 26S Subunit, ATPase 5	✓		
5718	PSMD12	Proteasome 26S Subunit, Non-ATPase 12	✓		
5719	PSMD13	Proteasome 26S Subunit, Non-ATPase 13	✓		✓
5709	PSMD3	Proteasome 26S Subunit, Non-ATPase 3	✓		
254958	REXO1L1	RNA Exonuclease 1 Homolog Like 1, Pseudogene	✓		✓
11236	RNF139	Ring Finger Protein 139	✓	✓	✓
29927	SEC61A1	SEC61 Translocon Alpha 1 Subunit	✓	✓	✓
10952	SEC61B	SEC61 Translocon Beta Subunit		✓	✓
7095	SEC62	SEC62 Homolog, Preprotein Translocation Factor	✓	✓	✓
11231	SEC63	SEC63 Homolog, Protein Translocation Regulator		✓	✓
6727	SRP14	Signal Recognition Particle 14	✓		
6728	SRP19	Signal Recognition Particle 19	✓		
6731	SRP72	Signal Recognition Particle 72	✓		✓
6734	SRPR	SRP Receptor Alpha Subunit	✓		✓
58477	SRPRB	SRP Receptor Beta Subunit	✓		✓
90871	TMEM261	Distal Membrane Arm Assembly Complex 1		✓	✓
79876	UBA5	Ubiquitin Like Modifier Activating Enzyme 5		✓	✓
7327	UBE2G2	Ubiquitin Conjugating Enzyme E2 G2	✓	✓	
7353	UFD1L	Ubiquitin Fusion Degradation 1 Like	✓		
51569	UFM1	Ubiquitin Fold Modifier 1	✓		✓
7415	VCP	Valosin Containing Protein	✓		

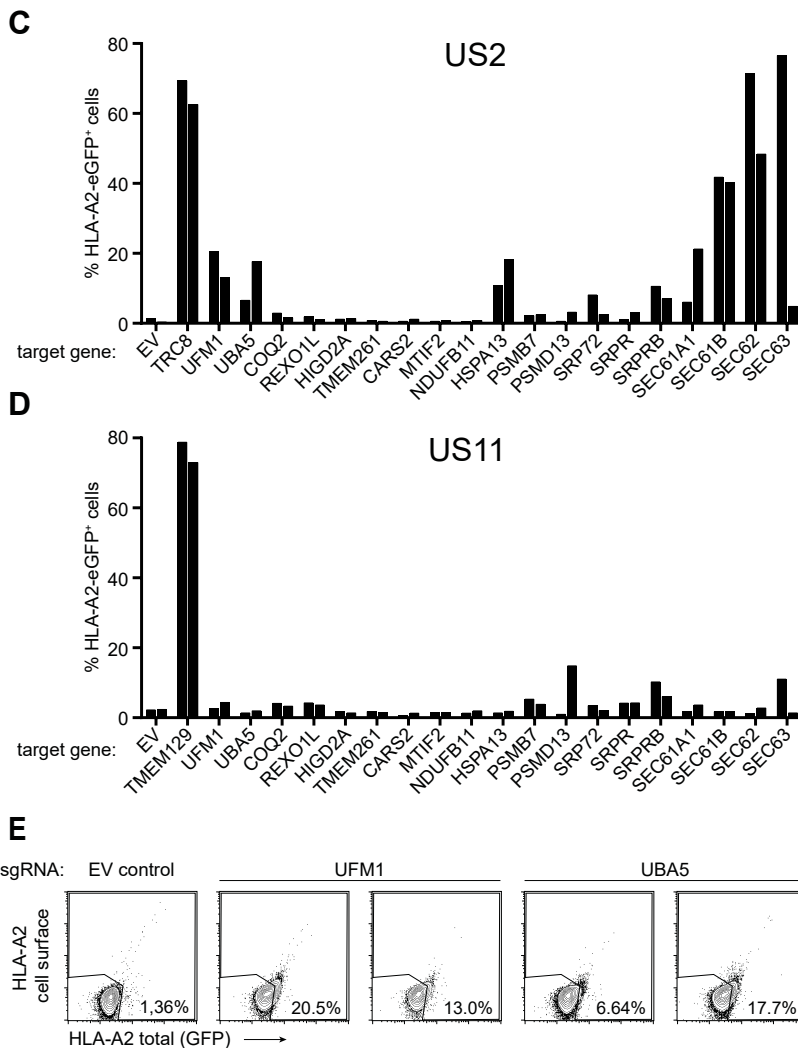


Figure 1 | A genome-wide CRISPR/Cas9 library screen identifies the UFM1 pathway to affect HCMV US2-mediated degradation of HLA class I. A) Schematic overview of the genome-wide CRISPR/Cas9 library screen. B) Overview of hits identified in the library screen and genes selected for validation studies. Flow cytometric analysis for the library screen was performed at 7- and 18 days post-lentiviral transduction with the sgRNA library. The checkmarks indicate at which timepoint the respective genes were identified. C) Validation of the screen at 14 days post-transduction of the sgRNAs. HLA-A2-eGFP U937 cells co-expressing US2 and SpCas9 were transduced with single sgRNAs targeting the presented genes. For each gene, the two most enriched sgRNAs from the screen were validated. The ubiquitin E3 ligase TRC8 was included as positive control, and an empty vector (EV) was included as negative control. Rescue of HLA-A2-eGFP (as measured by assessing eGFP levels and cell surface staining with an HLA-A2-specific antibody) was measured by flow cytometry. Validation was performed at 7, 11, 14, 18, and 28 days post-infection. The other timepoints are shown in Figure S1. D) Same as in C), although US11-expressing U937 cells were tested, instead of US2-expressing cells. HLA-A2 rescue observed in the polyclonal knockout cells are specific to US2 for the majority of genes. TMEM129 was taken along as a positive control for these US11-expressing cells, as this ubiquitin ligase is essential for US11 function. E) Flow cytometry dot plots of UBA5- and UFM1 sgRNA-targeted cells from the cells shown in figure 1C.

subunits¹⁵, and multiple members of the SEC61 complex¹⁵. The role of the SEC61/62/63 complex in US2-mediated HLA-I degradation is studied in more detail in Chapter 5. We also identified multiple components of the signal recognition particle, which may be related to US2 translocation (see Chapter 5). Other hits in this screen have been described in ERAD, but not for US2: the UBE2G2-binding ER-membrane protein AUP1¹⁶, FAF2/UBXD8¹⁷, and the p97 co-factors Npl4 and Ufd1¹⁴ (Chapter 5). A selection of the hits from both timepoints (Fig. 1B) was subjected to further validation (Fig. 1C). To do so, the two most enriched sgRNAs per gene were selected from the library, and were individually transduced into U937 cells co-expressing HLA-A2-eGFP, US2 and Cas9. HLA-A2-eGFP expression was assessed by flow cytometry at 7, 11, 14, 18, and 28 days post-transduction (Figs. S1 and 1C). At 14 d.p.i. hits from both the early and the late timepoint can be observed (Fig. 1C). Most, but not all, sgRNAs showed enhanced eGFP expression in a subset of transduced cells, showing that these were bona-fide hits in the screen. Among these hits were some that could be related to ERAD: the Hsp70 chaperone HSPA13, proteasome subunits PSMB7 and PSMD13, and four subunits of the SEC61 complex. The latter are characterized in Chapter 5. Others hits, such as components of the signal recognition particle (SRP72, SRPR and SRPRB) and COQ2 cannot be directly linked to protein degradation. A control validation using the HCMV protein US11 was performed and showed that most hits were specific to US2-mediated HLA-I degradation (Figs. 1D and S1).

We noted a modest, yet consistent rescue of HLA-A2-eGFP expression upon UFM1 and UBA5 targeting (Figs. 1C and 1E). This rescue was specific to US2-mediated ERAD, as introduction of these same sgRNAs in US11 expressing cells did not enhance HLA-A2-eGFP expression (Fig. 1D). Similar small effects can be observed when other genes known to be essential, such as p97, Npl4 and Ufd1 are knocked out (Chapter 5). UFM1 is a ubiquitin-like molecule, and UBA5 is the E1 activating enzyme that catalyzes the first step in the UFMylation reaction. As ubiquitination of ERAD substrates is required for recognition by the proteasome¹⁸, the identification of two genes involved in a ubiquitination-like post-translational modification pathway is intuiting and suggests that UFMylation plays an important role in ERAD as well.

All known players in UFMylation affect degradation of HLA class I

As two genes from the UFM1 pathway were identified in the genome-wide CRISPR/Cas9 library screen, we tested whether also other players in the UFMylation machinery affect US2-mediated degradation of HLA-I. These factors are related to UFM1 activation and its conjugation to substrates (Fig. 2A). UFM1 is initially expressed as a precursor protein that is cleaved by the UFM1-specific protease 2 (UfSP2) to yield an active UFM1. Similar to ubiquitination, UFM1 is then transferred to E1 (UBA5), E2 (UFC1) and E3 (UFL1, a.k.a. RCAD) enzymes in order to be conjugated to a substrate. UFM1-binding protein (UFBP1, a.k.a. DDRGK1) may function as a scaffold protein to aid the UFMylation reaction¹⁹. The cycle is completed when UfSP2 deUFMylylates the substrate, freeing UFM1 for another round of UFMylation. Another deUFMylyating enzyme, UfSP1, does exist but it is expressed only in murine and not in human cells¹⁹. We designed two sgRNAs targeting each of these genes, and introduced these in U937 cells co-expressing HLA-A2-eGFP and US2. As we observed only a minor HLA-A2 rescue effect at 14 d.p.i. (Figs. 1C and 1E), we first tested which timepoint would be optimal to detect a phenotype

upon sgRNA-targeting the UFM1 pathway (Fig. S2). Targeting any of the genes involved in UFMylation resulted in abrogated US2-mediated HLA-I degradation, thereby enhancing eGFP levels in a significant percentage of the cells (Figs. 2B and 2C). As expected, only UfSP1, the inactive paralog of UfSP2, did not rescue the phenotype.

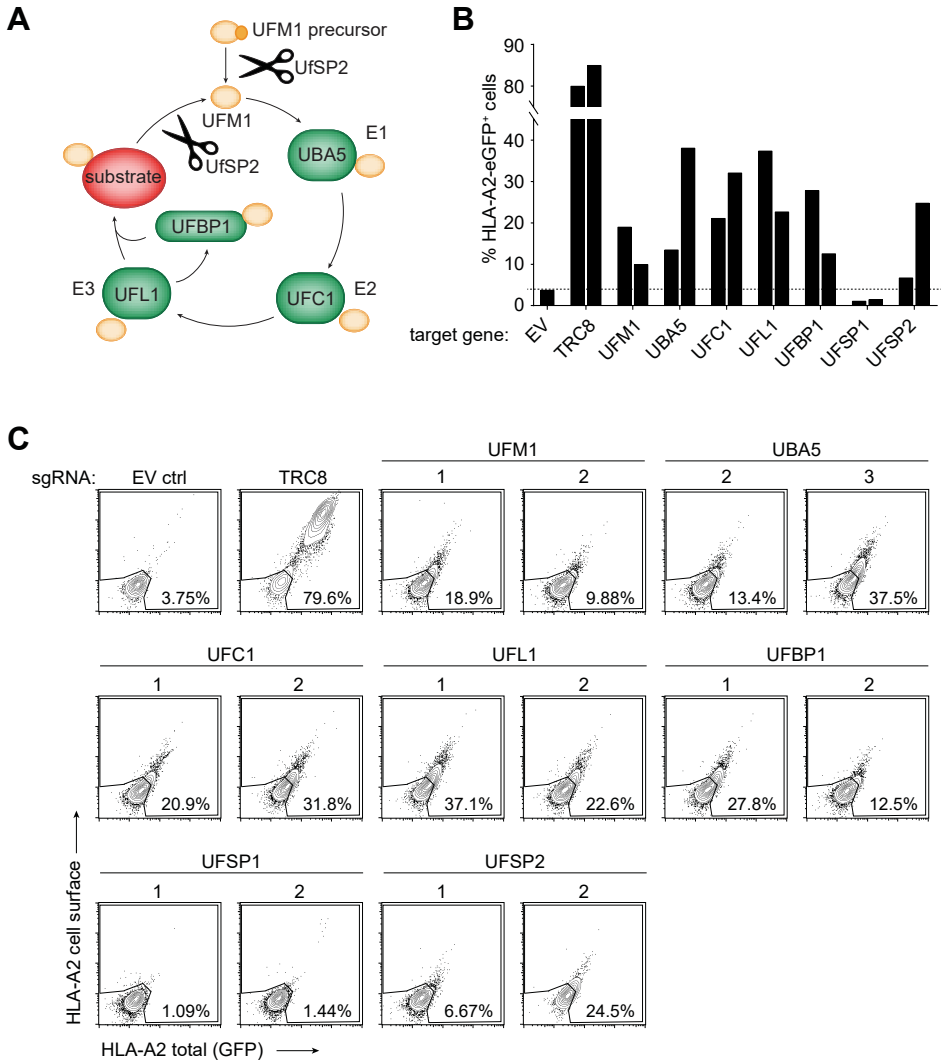


Figure 2 | US2-mediated HLA class I expression is rescued upon knockout of multiple players in the UFMylation pathway. A) Schematic overview of the UFMylation cycle. UfSP2 cleaves UFM1 downstream of its C-terminal glycine, either to create active UFM1 from its precursor, or to release UFM1 from a substrate. UfBP1 is a target of UFMylation but may also aid the UFMylation reaction. B) Individual genes involved in UFMylation were targeted by two sgRNAs and monitored for rescued HLA-A2-eGFP expression at 12 days post-infection. UfSP1 was included as negative control, as this protein is only functional in murine cells but not in human tissue. The experiment was performed three times, of which one representative experiment is shown. C) Flow cytometry plots of the data shown in Fig. 2B.

Clonal knockout cell lines for UFM1 and UBA5 show stable HLA-I rescue in the presence of HCMV US2

Upon targeting of genes important for UFMylation, we observed clear HLA-I rescue at 10-14 days post transduction with the lentiviral CRISPR/Cas9 sgRNA vectors (Fig. S2). The phenotype was much reduced, or even lost, after prolonged culture of the cells (Fig. S1). This suggests that knockout cells are either non-viable or have a growth defect, resulting in loss of these cells from polyclonal cell populations. To assess whether UFMylation knockout cells are viable, we single-cell sorted HLA-A2-eGFP⁺ cells from the polyclonal knockout cultures of UFM1 and UBA5 and allowed these to establish a stable clonal population. Indeed, we were able to establish stable knockout clones for both genes and the cells displayed a moderate increase of both chimeric HLA-A2-GFP and endogenous HLA-A3 expression (Fig. 3A). Protein levels of either UFM1 and UBA5 were undetectable in the respective knockout clones (Fig. 3B). Similar, yet temporal, HLA-A2 rescue results were obtained for a polyclonal UFC1 knockout population (Fig. 3C). The abrogated US2-mediated HLA-I downregulation could be fully rescued by introduction of a sgRNA-resistant cDNA vector for UFM1 (Fig. 3D, top panel, and Fig. 3F). For UFC1, we introduced cDNAs in a polyclonal context (Figs. 3E and 3G). The UBA5 cDNA was expressed at very low levels and no reversal of the HLA-I rescue phenotype could therefore be observed in clonal UBA5 knock-out cells (data not shown). UFM1 and UFC1 cDNAs encoding inactive mutants, lacking the 4 C-terminal amino acids (Δ VGSC) for UFM1, and harboring a C116S mutation for UFC1, could not revert the HLA-I rescue phenotype (Figs. 3D and 3E, lower panels). This shows that the observed abrogation of US2-mediated HLA-I downregulation requires the activity of these proteins, and is not caused by the expression of the proteins alone. To confirm that the Δ VGSC variant of UFM1, lacking the crucial glycine for conjugation to a substrate, was indeed an inactive mutant, we immunoprecipitated this construct from UFM1 KO cells (Fig. S3). Not only can no higher molecular weight bands be observed, we also showed that this mutant was unable to bind UBA5, in contrast to wildtype UFM1.

No UFMylation can be detected on HLA class I, US2 or p97

When cell lysates containing UFM1, or UFM1 immunoprecipitation samples were stained in Western blot, immunoblotting against the 9 kD UFM1 revealed a number of higher molecular weight proteins (Fig. S3, lanes 2 and 6, and Fig. 4A, lanes 1 and 2), suggesting that these higher bands represent UFM1-conjugated target proteins. We performed immunoprecipitation experiments on UFM1 to assess which proteins are UFMylated in US2-expressing cells. For this, we transduced an N-terminally StrepII-tagged UFM1 (ST2-UFM1) in HLA-A2-eGFP- and US2-expressing U937 cells and pulled down UFM1 by using StrepTactin beads. Subsequent immunoblotting for UBA5 (lane 4) and UFC1 (lane 6) confirmed the presence of these proteins in the UFM1 IP samples, showing that our UFM1 IP protocol was able to co-isolate UFMylated proteins from LMNG cell lysates. These UFM1-interacting factors may explain part of the higher molecular weight products observed in the UFM1 staining (Fig. 4A, lane 2). We did not observe an interaction of UFM1 with the E3 enzyme UFL1 (lane 8). We also hypothesized that the ~36 kD band consistently present in all UFM1 stainings performed may represent UFBP1 (predicted weight: 35.6 kD), which was the first identified substrate of UFMylation²⁰. We were however

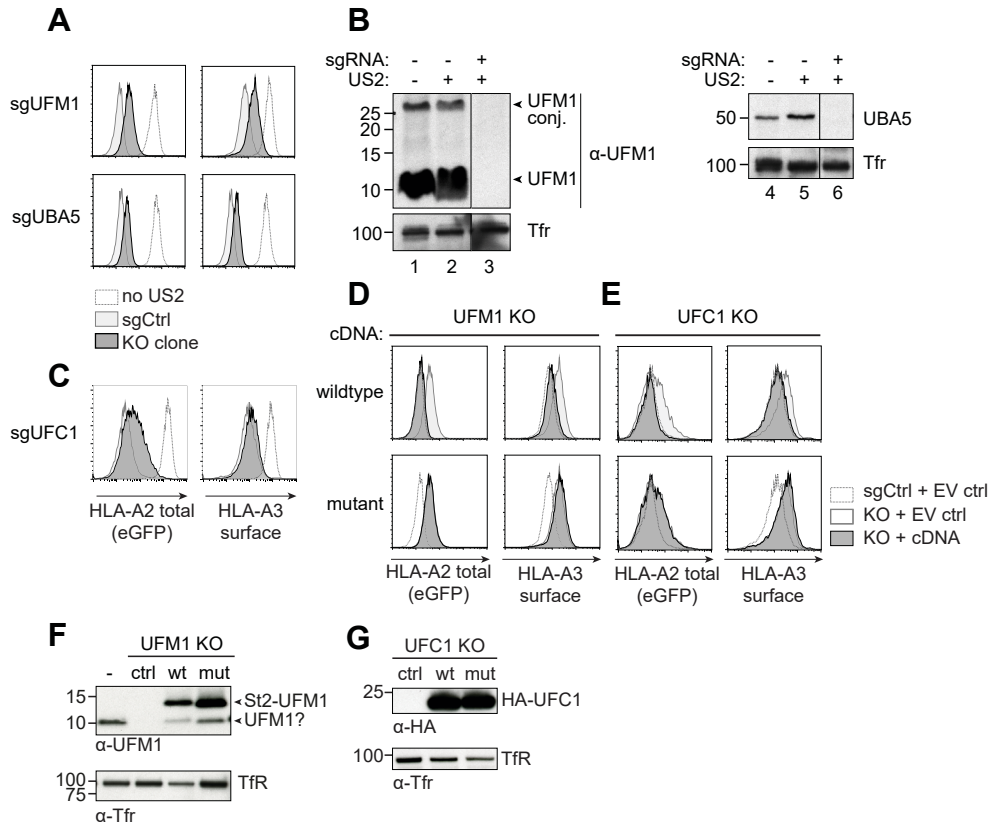
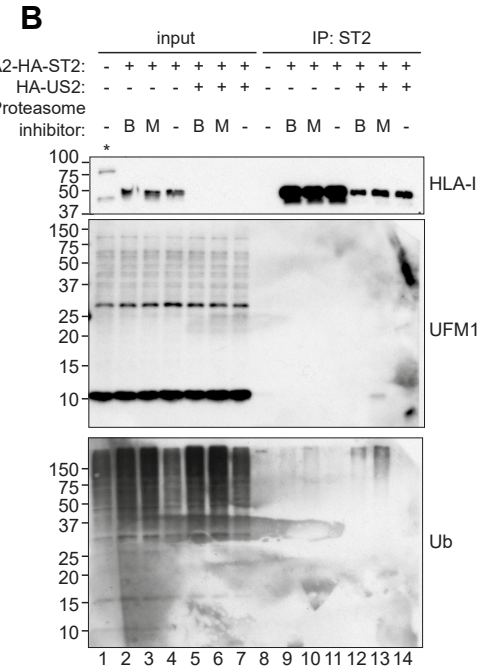
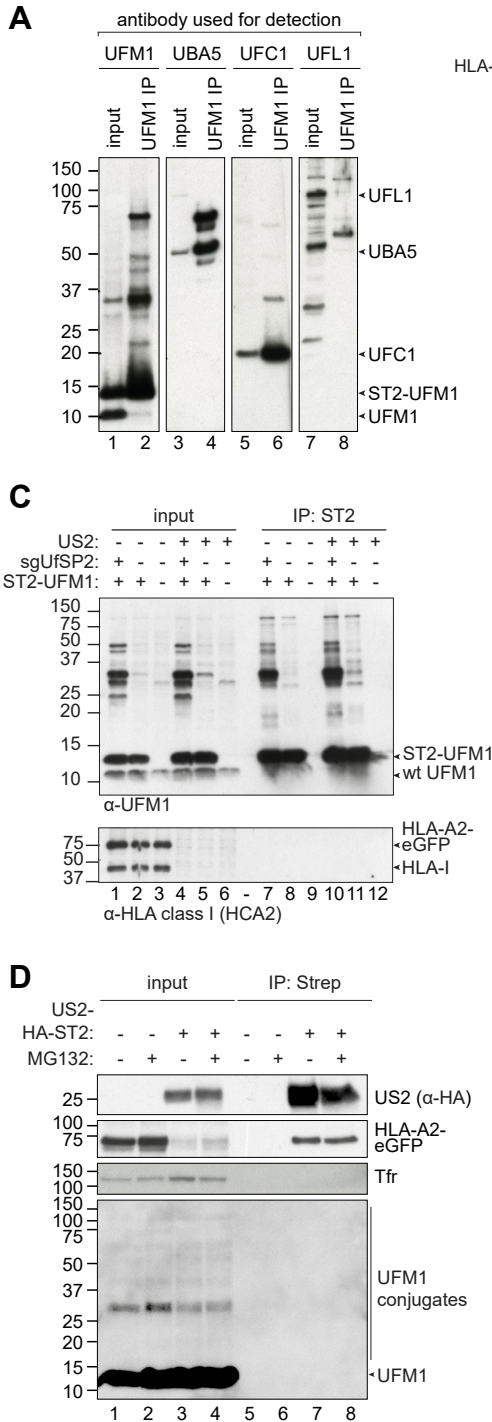


Figure 3 | Clonal knockout cell lines for UFM1 and UBA5 show stable HLA-I rescue in the presence of HCMV US2. A) U937 cells expressing HLA-A2-eGFP and US2 were transduced with sgRNAs targeting UFM1, UBA5, or UFC1. At 12 d.p.i., single HLA-A2-eGFP⁺ cells from the sgUFM1 and sgUBA5 cell lines were cloned by FACS and allowed to expand for ~8 weeks. Expression of HLA-A2-eGFP and endogenous HLA-A3 was assessed by flow cytometry. One representative clone is shown. B) Western blot analysis of the clonal cell lines established for UFM1 and UBA5. Cell lysates from the cell lines shown in A were prepared in 1% Triton X-100 and stained for the gene that was targeted by the CRISPR sgRNAs. Tfr was used as a loading control. C) A polyclonal cell population of UFC1-targeted U937 cells expressing eGFP-tagged HLA-A2 and US2 was also stained for HLA-A3 at 10 d.p.i. These cells show a modest rescue of HLA-A2 and HLA-A3, similar to the clonal lines shown in A. D) sgRNA-resistant wildtype or mutant cDNAs encoding inactive UFM1 were transduced into the knockout clone shown in A and B. Whereas a wildtype cDNA for UFM1 reverts the HLA-A2-eGFP- and HLA-A3 rescue phenotype observed in knockout clones, the inactive mutant cDNA does not. For mutant UFM1, the four C-terminal amino acids, including glycine used for substrate conjugation, were deleted (Δ VGSC). UBA5 cDNAs did not express well, therefore this cDNA was excluded from the experiment. E) Similar to figure D, wildtype or inactive sgRNA-resistant cDNAs for UFC1 were introduced in the polyclonal UFC1 knockout cell population. For the inactive UFC1 cDNA, the active site cysteine essential for catalytic activity was mutated into alanine (C53A). F) Immunoblots showing UFM1 protein expression in the knockout clones following the introduction of the cDNAs expressed in D. The UFM1 construct is detected using a UFM1-specific antibody. Upon expression of StrepII-tagged UFM1, a product migrating at the molecular weight of untagged UFM1 is consistently observed, suggesting this product may be a truncated variant of the ST2-UFM1 construct. G) Immunoblotting of the UFC1 cDNAs used in E. The HA-tagged UFC1 construct is detected using an anti-HA antibody.



unable to detect UFBP1 in Western blot with any of the antibodies tested (data not shown). We subsequently aimed at identifying US2-specific UFMylation events. As direct ubiquitination of ERAD substrates is a hallmark of proteasomal degradation, we hypothesized that UFM1 might also conjugate to HLA-I. To test this, HLA-A2-HA-StrepII was immunoprecipitated from U937 cells expressing HA-US2 or US2-lacking control cells that were pre-incubated with proteasome inhibitors MG132 or Bortezomib to accumulate ERAD-targeted HLA-I. Although ubiquitination of HLA class I was observed in US2 expressing cells upon proteasome inhibition (Fig. 4B, lower blot, lanes 12 and 13), we did not observe UFMylation of HLA-A2-HA-StrepII (Fig. 4B, middle panel). Vice versa, when StrepII-tagged UFM1 was immunoprecipitated in the presence or absence of US2, no HLA class I was detected either under the conditions used (Fig. 4C). Our results suggest that HLA-I is not directly UFMylated in US2-expressing cells.

In the context of ubiquitination, the activity of de-ubiquitinating enzymes (dUBs) is a notorious obstacle for detecting targets of ubiquitination²¹. Similarly, downregulation of the deUFMylyating protein UfSP2 by RNAi allows for accumulation of UFMylated target proteins²². Along the same lines, a CRISPR/Cas9-induced knockout of UfSP2 resulted in a strong increase of UFMylation conjugates (Fig. 4C, top panel, lanes 1, 4, 7 and 10). However, UFM1-pulldown from UfSP2 knockout cells did not result in the identification of a UFMylated HLA-I species either (Fig. 4C, lower panel, lanes 7 and 10).

Next, we assessed whether US2 could be a target of UFMylation. For this, we immunoprecipitated StrepII-HA-tagged US2 from HLA-A2-eGFP-expressing U937 cells, but could not detect UFMylated US2 molecule in the lysates by Western blot (Fig. 4D). Similarly, p97, which is a target of SUMOylation²³, was not a target for UFMylation in US2 expressing cells, as assessed by immunoprecipitation on either p97 or UFM1 (data not shown). Finally, we assessed whether UFM1 and ubiquitin would influence one another. We hypothesized that, since both modifications occur on lysine residues, the two UBLs may compete with one another. Addition of the proteasome inhibitor Bortezomib or MG132, which accumulates ubiquitinated proteins, did not affect the overall UFMylation pattern or intensity (Fig. 4B, middle panel, lanes 1-7). Vice versa, expression of the UfSP2 CRISPR sgRNA, which accumulates UFMylation on substrates, did not impact ubiquitination (data not shown). These findings suggest that UFM1 and ubiquitin do not compete for the same targets. Also, no ubiquitin was detected in UFM1 immunoprecipitations (data not shown), suggesting that substrates are not simultaneously modified with both UBLs.

Ribosomes are UFMylated in US2-expressing cells

As we did not detect UFMylation of HLA-I, US2, nor p97 in US2 expressing cells, we next used mass spectrometry to identify UFMylated proteins in an unbiased manner. To this end, we transduced US2-expressing HLA-A2-eGFP U937 cells with either StrepII-UFM1, the inactive UFM1 mutant (StrepII-UFM1 Δ VGSC), or StrepII-mCherry, followed by introduction of the UfSP2-targeting sgRNA in all cell lines. Upon immunoprecipitation of the three StrepII-tagged proteins, we analyzed the distribution of UFM1-conjugates by Western blot (Fig. 5A). As expected, we observed increased levels of UFMylated proteins in StrepII-UFM1 cells as compared to control StrepII-UFM1 Δ VGSC and StrepII-mCherry cells. This difference was apparent in both the absence (Fig. 5A, compare lane 7 to lane 6) and presence (lanes 9 and 10

versus lane 8) of US2.

For mass spectrometry, quadruplicate immunoprecipitations were performed on the sgUfSP2-expressing UFM1- and control cell lines in TAP lysis buffer. These were subsequently subjected to mass spectrometry (Fig. 5B). The enrichment of co-precipitated proteins in the UFM1 sample was compared to the negative control cell lines (Fig. 5C). As expected, the strongest hits were

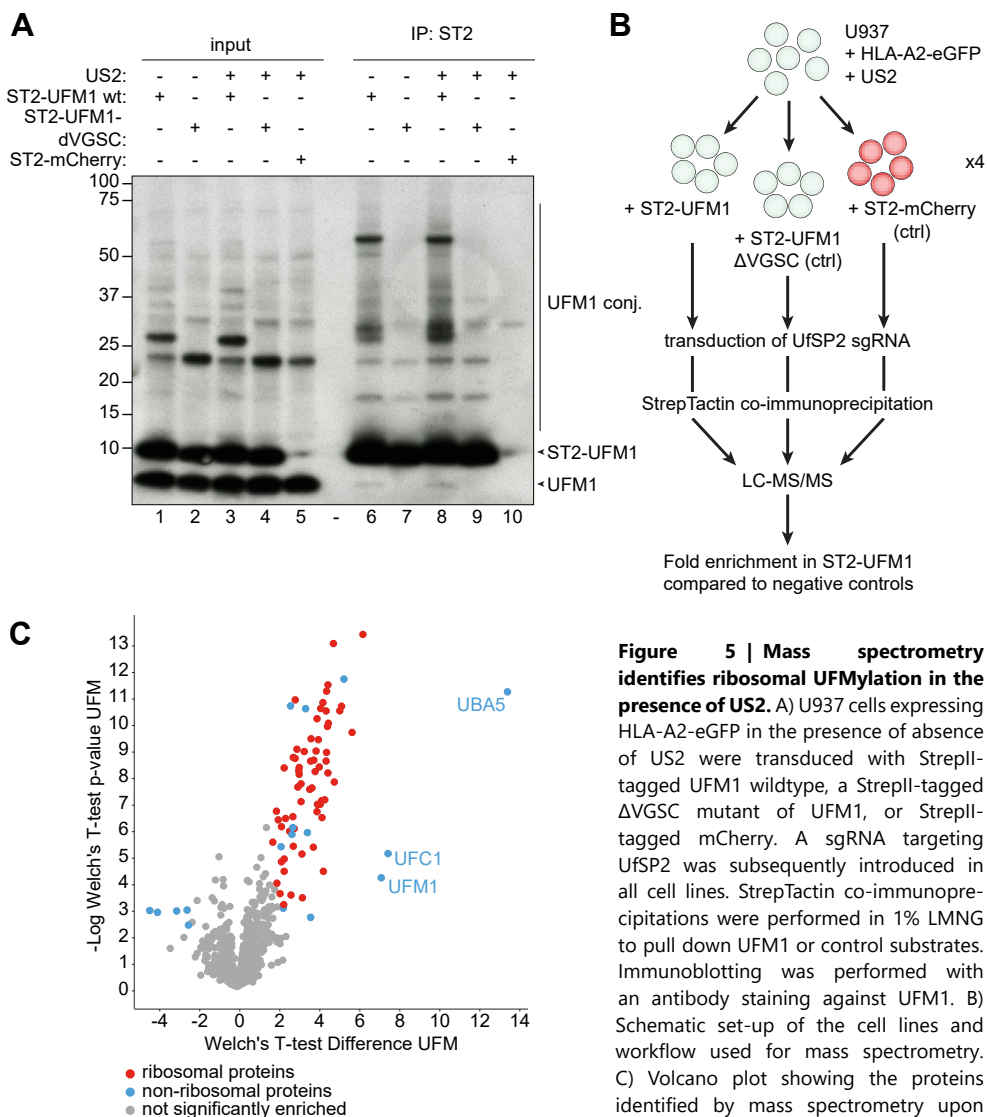


Figure 5 | Mass spectrometry identifies ribosomal UFMylation in the presence of US2. A) U937 cells expressing HLA-A2-eGFP in the presence of absence of US2 were transduced with StrepII-tagged UFM1 wildtype, a StrepII-tagged Δ VGSC mutant of UFM1, or StrepII-tagged mCherry. A sgRNA targeting UfSP2 was subsequently introduced in all cell lines. StrepTactin co-immunoprecipitations were performed in 1% LMNG to pull down UFM1 or control substrates. Immunoblotting was performed with an antibody staining against UFM1. B) Schematic set-up of the cell lines and workflow used for mass spectrometry. C) Volcano plot showing the proteins identified by mass spectrometry upon StrepII-UFM1 immunoprecipitation. The

enrichment per protein was calculated compared to the negative control cell lines. Significantly enriched (top right) or depleted (left) hits are shown in color, while the gray dots show proteins that are not significantly enriched. Red hits represent ribosomal proteins, while all other hits are shown in blue. A complete list with names and functions of the proteins that were significantly enriched, is shown in Supplementary information 2.

directly involved in the UFMylation pathway: UFM1, UBA5 and UFC1, confirming the clear interactions we observed previously (Fig. 4A). Additionally, multiple significantly enriched proteins were detected in the StrepII-UFM1 expressing cells (such as UFP1, GNB2L1 and TXNL1) that were not previously linked to ERAD. Intriguingly, a large number of ribosomal proteins were identified (Fig. 5C, red dots), suggesting that multiple ribosomal subunits are either directly UFMylated, or interact with other UFMylated proteins. Three ribosomal proteins, uS3 (RPS3), uS10 (RPS20) and uL16 (RPL10) have previously been described to be UFMylated²⁴ and are also observed among the ribosomal proteins enriched in our experiment (Supplementary information S2). Even many of the proteins that are not structural components of the ribosome (blue datapoints in Fig. 5C) are related to ribosome function or translation, such as EIF1AX, FAU, and TP53RK (Supplementary information S2). Taken together, we identified a large number of potential UFM1 targets related to the ribosome, strongly suggesting that the effect of UFMylation on HLA class I degradation may occur via a pathway involving the ribosome.

DISCUSSION

Here, we describe a genome-wide CRISPR/Cas9 screen to identify cellular factors involved in HCMV US2-mediated ERAD of HLA-I. We identified multiple genes that were previously linked to US2-mediated HLA-I downregulation, including the ubiquitin ligase TRC8, the E2 enzyme UBE2G2, and p97, the ATPase facilitating dislocation of ERAD substrates. Some genes, such as UBXD8 (FAF2) and the p97 co-factors Npl4 and Ufd1, have previously been described in ERAD, but did not affect US2 function in those studies^{14,17}. Although we have not validated these hits in detail, targeting them with CRISPR sgRNAs results in abrogation of US2-mediated HLA class I. The discrepancy with previous studies may arise from the different techniques used: in contrast to our knockout approach, Npl4 and Ufd1 were previously knocked down using siRNAs¹⁴, while UBXD8 was studied in a pulse-chase approach to assess HLA class I dislocation¹⁷.

We show that knockout of genes involved in the UFM1 pathway moderately, yet consistently, hamper US2-mediated HLA-I degradation. Although a link between UFM1 and the ER has previously been described²⁵, a role in protein degradation has not been reported. UFM1 is a post-translational modifier structurally related to ubiquitin²⁶. Similar to ubiquitin, UFM1 is conjugated to its substrates via an iso-peptide bond between the C-terminal glycine of UFM1 and a lysine residue of the substrate²⁷. For both modifiers, the conjugation to substrates is facilitated by E1, E2 and E3 enzymes. However, UFM1 does not function in ERAD the same way as ubiquitin: where the degradation substrate HLA-I becomes ubiquitinated, UFMylation could not be detected. Similarly, UFMylation did not take place on US2 or proteins directly related to US2-mediated ERAD. Therefore, the mechanism behind UFM1's impact on protein degradation remains to be clarified. This, in combination with the subtle HLA-I rescue phenotypes observed upon knocking out players of the UFMylation pathway, suggests that UFM1 may play an indirect role in protein degradation.

Another recently described genome-wide CRISPR/Cas9 library screen has identified the UFM1 pathway to regulate SQSTM1 expression in an ER-stress-dependent manner²⁸. Several additional studies have attempted to identify targets for UFMylation, mostly by mass spectrometry-based

approaches. Despite these efforts, only few UFM1 substrates have been identified to date. The first-identified UFM1 target²⁰, UFBP1, was later suggested to play a role in the UFMylation pathway itself^{19,25,29}. Other targets include LZAP, a binding partner of UFL1, the ribosome²⁴, and, interestingly, multiple chaperones of the Hsp40 and -70 families, such as DNAJC1, HSPA8, and BiP^{19,29}. While our genome-wide screen also identifies a Hsp70 (HSPA13) and Hsp40 chaperone (SEC63), we did not identify these factors to associate with UFM1 in our mass spectrometry analysis. Although UFM1 is ubiquitously expressed in many tissues²⁰, its target proteins may differ between cell types and the experimental context used.

We identified many ribosome subunits as potential targets for UFMylation in US2-expressing cells. As UFMylation of RPS3, RPS20 and RPL10 has been described previously²⁴, these ribosome subunits are likely genuine targets of UFMylation. Because these three ribosomal proteins are located close to the mRNA entry channel in the large ribosomal subunit, it has been suggested that UFMylation may affect mRNA entry into the ribosome²⁴. In the same study, UFMylation was observed of eIF6, a translation initiation factor that prevents association between the 40S and 60S ribosomal subunits. We identified eIF1AX, another translation initiation factor associated with the 40S ribosome. None of the significantly enriched proteins we identified in mass spectrometry to interact with UFM1 are functionally related to ER-associated degradation. The role of this ubiquitin-like modification in US2-mediated HLA-I degradation therefore remains to be elucidated. Furthermore, it remains unclear whether the UFMylation events we observe are US2-specific.

In immunoprecipitation experiments, we did not observe major differences in UFM1 conjugates when comparing cells with or without US2. This suggests that US2-specific UFMylation events may not occur. However, as UFMylation of the ribosome occurs at subunits that situate close to the mRNA entry channel²⁴, translation efficiency may be hampered. As US2 has an inefficient signal peptide resulting in low protein expression levels (see Chapter 5) it could be particularly sensitive to subtle changes in translational efficiency and therefore cause moderate effects on HLA-I rescue observed upon knocking out UFMylation factors.

Another mechanism by which UFM1 may affect protein degradation is related to ER stress. UFM1 is upregulated via the transcription factor Xbp1s upon chemically-induced ER stress³⁰. UFMylation allows cells to survive ER stress by suppressing apoptosis^{22,25,29,31}. More specifically, UFBP1 (also known as DDRGK1 or C20orf116) is an ER membrane protein that binds the ER stress protein IRE1 α in an UFM1-dependent manner²⁵. IRE1 α in turn cleaves Xbp1, which functions as a transcription factor to activate ER chaperones as well as UFM1³⁰. A positive feedback loop may arise during ER stress, as the elevated expression of UFM1 potentially stabilizes additional IRE1 α molecules. In the absence of UFM1, IRE1 α is a substrate for SEL1/HRD1-mediated ERAD. IRE1 α is not UFMylated, but it is rescued from degradation by binding to UFMylated UFBP1. Hence, depending on the UFMylation status of UFBP1, the protein can rescue ERAD substrates from degradation. Also the ER chaperone BiP has been shown to be an indirect target of UFMylation by interacting with UFBP1²⁹. UFBP1 may thus act as a regulator of protein stability, depending on its UFMylation status. By switching the UFMylation status of a limited number of proteins, such as UFBP1, a far larger number of targets may be regulated via protein-protein interactions without the need for direct UFMylation of these target proteins

themselves. Testing whether UFBP1, rather than UFM1 itself, interacts with HLA-I or US2-mediated ERAD proteins would be an important aspect of future research.

ACKNOWLEDGEMENTS

We would like to thank Addgene for providing the plasmids used for our genome-wide CRISPR/Cas9 library screen. We thank members of the Core Flow cytometry Facility (CFF) and Ger Arkesteijn from the Department of Veterinary Medicine (Utrecht University, The Netherlands) for technical assistance with cell sorting. We also thank Utrecht Sequencing Facility for providing sequencing service and data. Utrecht Sequencing Facility is subsidized by the University Medical Center Utrecht, Hubrecht Institute and Utrecht University.

A.B.C.S. was funded by the Graduate Programme of the Netherlands Organisation for Scientific Research (NWO), project number 022.004.018. R.J.L and M.L.W. were supported by Veni grant 916.10.138 from NWO and Marie Curie Career Integration Grant PCIG-GA-2011-294196.

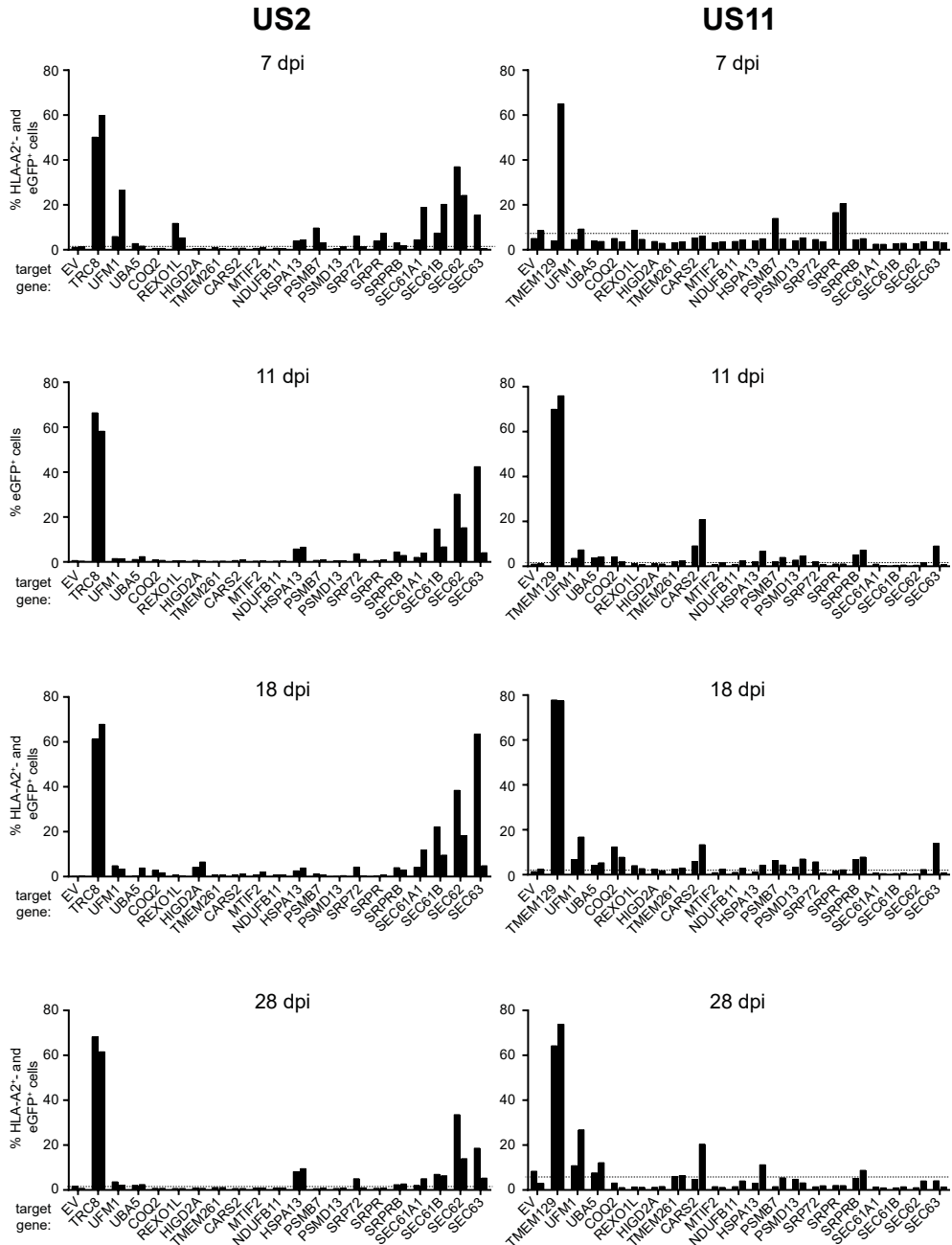
REFERENCES

1. Guerriero, C. J. & Brodsky, J. L. The delicate balance between secreted protein folding and endoplasmic reticulum-associated degradation in human physiology. *Physiol. Rev.* **92**, 537–576 (2012).
2. Zhao, L. & Ackerman, S. L. Endoplasmic reticulum stress in health and disease. *Curr. Opin. Cell Biol.* **18**, 444–452 (2006).
3. Byun, H., Gou, Y., Zook, A., Lozano, M. M. & Dudley, J. P. ERAD and how viruses exploit it. *Front. Microbiol.* **5**, 1–16 (2014).
4. van de Weijer, M. L., Luteijn, R. D. & Wiertz, E. J. H. J. Viral immune evasion: Lessons in MHC class I antigen presentation. *Semin. Immunol.* **27**, 125–137 (2015).
5. Schuren, A. B. C., Costa, A. I. & Wiertz, E. J. H. J. Recent advances in viral evasion of the MHC Class I processing pathway. *Curr. Opin. Immunol.* **40**, 43–50 (2016).
6. Griffiths, P., Baraniak, I. & Reeves, M. The pathogenesis of human cytomegalovirus. *J. Pathol.* **235**, 288–97 (2015).
7. Lilley, B. N. & Ploegh, H. L. A membrane protein required for dislocation of misfolded proteins from the ER. *Nature* **429**, 834–840 (2004).
8. Lilley, B. N. & Ploegh, H. L. Multiprotein complexes that link dislocation, ubiquitination, and extraction of misfolded proteins from the endoplasmic reticulum membrane. *Proc. Natl. Acad. Sci. U. S. A.* **102**, 14296–14301 (2005).
9. Stagg, H. R. *et al.* The TRC8 E3 ligase ubiquitinates MHC class I molecules before dislocation from the ER. *J. Cell Biol.* **186**, 685–692 (2009).
10. Van De Weijer, M. L. *et al.* A high-coverage shRNA screen identifies TMEM129 as an E3 ligase involved in ER-associated protein degradation. *Nat. Commun.* **5**, 1–14 (2014).

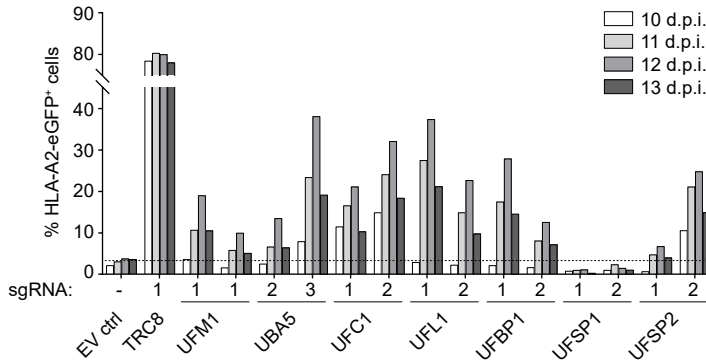
11. van den Boomen, D. J. H. *et al.* TMEM129 is a Derlin-1 associated ERAD E3 ligase essential for virus-induced degradation of MHC-I. *Proc. Natl. Acad. Sci.* **111**, 11425–11430 (2014).
12. van den Boomen, D. J. H. & Lehner, P. J. Identifying the ERAD ubiquitin E3 ligases for viral and cellular targeting of MHC class I. *Mol. Immunol.* **68**, 106–111 (2015).
13. van de Weijer, M. L. *et al.* Multiple E2 ubiquitin-conjugating enzymes regulate human cytomegalovirus US2-mediated immunoreceptor downregulation. *J. Cell Sci.* **130**, 2883–2892 (2017).
14. Soetandyo, N. & Ye, Y. The p97 ATPase dislocates MHC class I heavy chain in US2-expressing cells via a Ufd1-Npl4-independent mechanism. *J. Biol. Chem.* **285**, 32352–32359 (2010).
15. Wiertz, E. J. H. J. *et al.* Sec61-mediated transfer of a membrane protein from the endoplasmic reticulum to the proteasome for destruction. *Nature* **384**, 432–438 (1996).
16. Klemm, E. J., Spooner, E. & Ploegh, H. L. Dual role of Ancient Ubiquitous Protein 1 (AUP1) in lipid droplet accumulation and Endoplasmic Reticulum (ER) protein quality control. *J. Biol. Chem.* **286**, 37602–37614 (2011).
17. Mueller, B., Klemm, E. J., Spooner, E., Claessen, J. H. & Ploegh, H. L. SEL1L nucleates a protein complex required for dislocation of misfolded glycoproteins. *Proc. Natl. Acad. Sci. U. S. A.* **105**, 12325–30 (2008).
18. Christianson, J. C. & Ye, Y. Cleaning up in the endoplasmic reticulum: Ubiquitin in charge. *Nat. Struct. Mol. Biol.* **21**, 325–335 (2014).
19. Yoo, H. M. *et al.* Modification of ASC1 by UFM1 is crucial for ER α transactivation and breast cancer development. *Mol. Cell* **56**, 261–274 (2014).
20. Tatsumi, K. *et al.* A novel type of E3 ligase for the Ufm1 conjugation system. *J. Biol. Chem.* **285**, 5417–5427 (2010).
21. Emmerich, C. H. & Cohen, P. Optimising methods for the preservation, capture and identification of ubiquitin chains and ubiquitylated proteins by immunoblotting. *Biochem. Biophys. Res. Commun.* **466**, 1–14 (2015).
22. Yoo, H. M. *et al.* Modification of ASC1 by UFM1 is crucial for ER α transactivation and breast cancer development. *Mol. Cell* **56**, 261–274 (2014).
23. Wang, T. *et al.* Pathogenic mutations in the valosin-containing protein/p97(VCP) N-domain inhibit the SUMOylation of VCP and lead to impaired stress response. *J. Biol. Chem.* **291**, 14373–14384 (2016).
24. Simsek, D. *et al.* The Mammalian Ribo-interactome Reveals Ribosome Functional Diversity and Heterogeneity. *Cell* **169**, 1051–1065.e18 (2017).
25. Liu, J. *et al.* A critical role of DDRGK1 in endoplasmic reticulum homeostasis via regulation of IRE1 α stability. *Nat. Commun.* **8**, 1–12 (2017).
26. Yoo, H. M., Park, J. H., Jeon, Y. J. & Chung, C. H. Ubiquitin-fold modifier 1 acts as a positive regulator of breast cancer. *Front. Endocrinol. (Lausanne)*. **6**, 1–7 (2015).

27. Komatsu, M. *et al.* A novel protein-conjugating system for Ufm1, a ubiquitin-fold modifier. *EMBO J.* **23**, 1977–1986 (2004).
28. Dejesus, R. *et al.* Functional CRISPR screening identifies the ufmylation pathway as a regulator of SQSTM1/p62. *Elife* **5**, 1–16 (2016).
29. Lemaire, K. *et al.* Ubiquitin fold modifier 1 (UFM1) and its target UFBP1 protect pancreatic beta cells from ER stress-induced apoptosis. *PLoS One* **6**, (2011).
30. Zhang, Y., Zhang, M., Wu, J., Lei, G. & Li, H. Transcriptional Regulation of the Ufm1 Conjugation System in Response to Disturbance of the Endoplasmic Reticulum Homeostasis and Inhibition of Vesicle Trafficking. *PLoS One* **7**, 1–11 (2012).
31. Hu, X. *et al.* Ubiquitin-fold modifier 1 inhibits apoptosis by suppressing the endoplasmic reticulum stress response in Raw264.7 cells. *Int. J. Mol. Med.* **33**, 1539–1546 (2014).
32. Langmead, B. & Salzberg, S. L. Fast gapped-read alignment with Bowtie 2. *Nat. Methods* **9**, 357–359 (2012).
33. Li, W. *et al.* MAGeCK enables robust identification of essential genes from genome-scale CRISPR/Cas9 knockout screens. *Genome Biol.* **15**, 554 (2014).

SUPPLEMENTARY INFORMATION

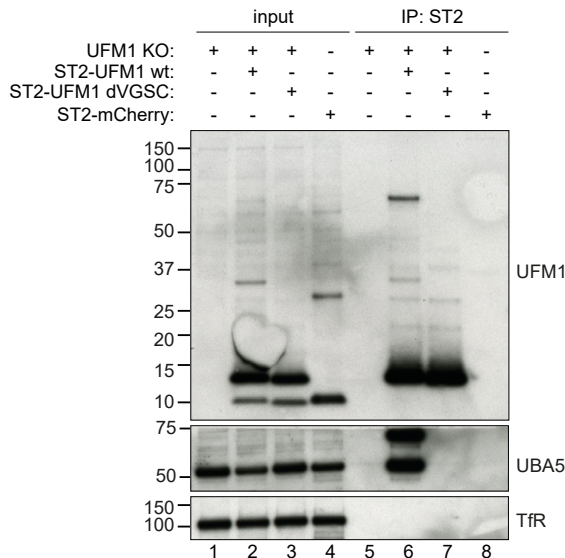


Supplementary figure 1 | Validation of the genome-wide library screen at 7, 11, 18, and 28 days post-infection. Validation of the genome-wide screen was performed as described for figure 1C. At 11 days post-infection only eGFP expression was assessed.



Supplementary figure 2 | Determination of the optimal timepoint for detecting HLA-I rescue. sgRNAs targeting TRC8 or all players of the UFMylation pathway were introduced as described in figure 2. Flow cytometry was performed on multiple days to determine the optimal timepoint for detecting HLA-A2-eGFP rescue. Figure 2B shows a selection of the data from this experiment, with only the 12 d.p.i. timepoint shown.

4



Supplementary figure 3 | Mutant UFM1 lacking its C-terminus is unable to bind UBA5. StrepII-tagged WT UFM1 or a ΔVGSC mutant were expressed in clonal UFM1 knockout cells. As a control, StrepII-mCherry was introduced in UFM1-expressing cells. These StrepII-tagged constructs were immunoprecipitated in 1% LMNG lysis buffer. Input and immunoprecipitation samples were loaded on Western blot and stained for UFM1.

<i>sgRNA name</i>	<i>sgRNA target site</i>		
TRC8_1	AGGAAGATGACAGGCGTCT	HSPA13_1	GATGACCATCGCGTGAACAG
TMEM129_1	GCACACGGCGAACACCAGAT	HSPA13_2	CCAAGTCTATCACCAAGACG
UFM1_1	TACTCACCAGCAGTCTGTGC	PSMB7_1	CCAGCTCATTCTTCCAACC
UFM1_2	ACAAGTGAATTATTACCAA	PSMB7_2	TAATAGGATGGCAGTAGTTCT
UFM1_3	GACGTCAGCGTGATCTTAA	PSMD13_1	CCGCAGAGCATCTTTGTAGT
UFM1_4	gTTTAAGATCACGCTGACGT	PSMD13_2	AATTCAGTTGTTGTGCCTCA
UBA5_1	AGCAGCACTGCCTAAACAAG	SRP72_1	AACTGCCCTGCATTGTAAAG
UBA5_2	AGTGTGATGACAGAAATTGC	SRP72_2	TAACTCTCTCTCCTTTGAAA
UBA5_3	GAGTGTGATGACAGAAATTGC	SRPR_1	ACTGGTTTGCTGGTAGCCAA
UBA5_4	gCCTACTATTGCTACGGCAA	SRPR_2	CTCAAACTCTACCAAACCT
UFC1_1	CCCACAACCTCACGATCTCG	SRPRB_1	GGAAAACGTTGCTCTTTGTC
UFC1_2	CGGTGCTGAAGACTAACGC	SRPRB_2	TACAGCACAGCTGTCTAGTAA
UFL1_1	GTTGGCGCGCGACTTCCAGC	SEC61A1_1	TGTTGTACTGGCCACGGTAG
UFL1_2	gAACCGCTAATCTCTTCCC	SEC61A1_2	ATCAAGTCGGCCCGTACCG
UFBP1_1	GTGGCGCCTGTGTGGTACT	SEC61B_1	TAGTGGCCCTGTTCAGTAT
UFBP1_2	GTAGCGCGGCTCTGCTAGT	SEC61B_2	GTAGAATCGCCACATCCCCC
UFSP1_1	GCTGCCTCGCTCACTTCGGA	SEC62_1	CTGTGGTTGACTACTGCAAC
UFSP1_2	GCCTCTGCCTCGCTCACTT	SEC62_2	GTAGTCAACCACAGACTCCC
UFSP2_1	gTAGCTGAAAAGCCAAATCA	SEC63_1	GTGATGAGGTTATGTTCATG
UFSP2_2	GCTAGCTACTCCTAATGGT	SEC63_2	TTGGTATTCTCGGTCTGTTT
COQ2_1	AGCTCACCCAAGGCTAGTTG		
COQ2_2	GAATAGTCCAGTGCCAAAG		
REXO1L1_1	TGCGAGCCACAGCTCCCTGC		
REXO1L1_2	CTATCTCCTTCAGTTCTGCT		
HIGD2A_1	CACTTACCTATGGGTACCAC		
HIGD2A_2	CTCAGCTCATGATGCGCACC		
TMEM261_1	GCCGATGACCATCTGCGTAA		
TMEM261_2	TCCATGGACCATTACGCAGA		
CARS2_1	TTCCCTCGCCAGTCTTTATG		
CARS2_2	TATGCTGCATCCAAAAACCT		
MTIF2_1	GTTAAAGGGCGATAATCTGA		
MTIF2_2	TCTATTACTGTTCTTCCAC		
NDUFB11_1	TCACAAGCCTCTCAGCTTCG		
NDUFB11_2	TGGCCTATCTGCCTGACTAC		

Supplementary information 1 | sgRNAs used in this study. Target genes and genomic target sites of all sgRNAs used for this study. For validation of the genome-wide library screen, sgRNAs #1 and #2 were used for UFM1 and UBA5.

Depleted

UniProtKB	Gene name	Full name	Function
P12814	ACTN1	Actinin Alpha 1	Actin-binding protein
Q13155	AIMP2	Aminoacyl tRNA Synthetase Complex Interacting Multifunctional Protein 2	Non-enzymatic factor of aminoacyl tRNA-synthetase complex
P01344	IGF2	Insulin-Like Growth Factor 2	Insulin-like growth factor (imprinted gene related to tumorigenesis)
Q95613	PCNT	Pericentrin	Integral component of the pericentriolar material; binds to calmodulin
Q9H4A3	WNK1	WNK Lysine Deficient Protein Kinase 1	Regulation of electrolyte homeostasis

Enriched non-ribosomal proteins (blue)

UniProtKB	Gene name	Full name	Function
P47813	EIF1AX	Eukaryotic Translation Initiation Factor 1A, X-linked	Binding of 40S ribosome, eIF2, GTP, Met-tRNAi and eIF3 to 5' end of capped mRNA
P62861	FAU	Ubiquitin Like and Ribosomal Protein S30 Fusion	Fusion protein of ubiquitin-like protein FUBI (N-term) and ribosomal protein S30 (C-term)
P63244	GNB2L1	Guanidine Nucleotide Binding Protein (G-protein), Beta Polypeptide 2-Like	Scaffolding protein in 40S ribosomal subunit involved in ribosomal quality control
P19338	NCL	Nucleolin	Nucleolar phosphoprotein involved in synthesis and maturation of ribosomes
Q96S44	TP53RK	TP53 Regulating Kinase	Required for the modification of tRNAs that read codons beginning with alanine
P62995	TRA2B	Transformer 2 Beta Homolog	Nuclear protein involved in pre-mRNA splicing
Q8WZ42	TTN	Titin	Key component in the assembly and functioning of vertebrate striated muscle
O43396	TXNL1	Thioredoxin Like 1	Active thioredoxin; component of the 19S regulatory cap of the 26S proteasome
Q9GZZ9	UBA5	Ubiquitin Like Modifier Activating Enzyme 5	E1 activating enzyme for UFM1
Q9Y3C8	UFC1	Ubiquitin-Fold Modifier Conjugating Enzyme 1	E2 conjugating enzyme for UFM1
P61960	UFM1	Ubiquitin Fold Modifier 1	Ubiquitin-like molecule that is conjugated to target proteins in a manner analogous to ubiquitination
Q92900	UPF1	Up-Frameshift Mutation 1 Homolog	nonsense mediated decay of mRNAs; recruited to mRNAs upon translation termination and to stalled ribosomes

Enriched ribosomal proteins (red)

UniProtKB	Gene name	Full name	Function
P62906	RPL10A	Ribosomal Protein L10a	ribosomal protein that is a component of the 60S subunit
P62913	RPL11	Ribosomal P protein L11	ribosomal protein that is a component of the 60S subunit
P30050	RPL12	Ribosomal Protein L12	ribosomal protein that is a component of the 60S subunit
P26373	RPL13	Ribosomal Protein L13	ribosomal protein that is a component of the 60S subunit
P40429	RPL13A	Ribosomal P protein L13A	ribosomal protein that is a component of the 60S subunit
P50914	RPL14	Ribosomal Protein L14	ribosomal protein that is a component of the 60S subunit
P61313	RPL15	Ribosomal P protein L15	ribosomal protein that is a component of the 60S subunit
P18621	RPL17	Ribosomal Protein L17	ribosomal protein that is a component of the 60S subunit
Q07020	RPL18	Ribosomal P protein L18	ribosomal protein that is a component of the 60S subunit
Q02543	RPL18A	Ribosomal P protein L18A	ribosomal protein that is a component of the 60S subunit
P84098	RPL19	Ribosomal Protein L19	ribosomal protein that is a component of the 60S subunit
P46778	RPL21	Ribosomal P protein L21	ribosomal protein that is a component of the 60S subunit
P62750	RPL23A	Ribosomal Protein L23A	ribosomal protein that is a component of the 60S subunit
P83731	RPL24	Ribosomal P protein L24	ribosomal protein that is a component of the 60S subunit
P61254	RPL26	Ribosomal Protein L26	ribosomal protein that is a component of the 60S subunit
P61353	RPL27	Ribosomal Protein L27	ribosomal protein that is a component of the 60S subunit
P46776	RPL27A	Ribosomal P protein L27A	ribosomal protein that is a component of the 60S subunit
P46779	RPL28	Ribosomal Protein L28	ribosomal protein that is a component of the 60S subunit
P47914	RPL29	Ribosomal P protein L29	ribosomal protein that is a component of the 60S subunit
P39023	RPL3	Ribosomal Protein L3	ribosomal protein that is a component of the 60S subunit
P62899	RPL31	Ribosomal Protein L31	ribosomal protein that is a component of the 60S subunit
P62910	RPL32	Ribosomal P protein L32	ribosomal protein that is a component of the 60S subunit
P49207	RPL34	Ribosomal Protein L34	ribosomal protein that is a component of the 60S subunit

P42766	RPL35	Ribosomal P protein L35	ribosomal protein that is a component of the 60S subunit
P18077	RPL35A	Ribosomal Protein L35A	ribosomal protein that is a component of the 60S subunit
Q9Y3U8	RPL36	Ribosomal Protein L36	ribosomal protein that is a component of the 60S subunit
P61513	RPL37A	Ribosomal Protein L37A	ribosomal protein that is a component of the 60S subunit
P62891	RPL39	Ribosomal Protein L39	ribosomal protein that is a component of the 60S subunit
P36578	RPL4	Ribosomal P protein L4	ribosomal protein that is a component of the 60S subunit
P46777	RPL5	Ribosomal Protein L5	ribosomal protein that is a component of the 60S subunit
Q02878	RPL6	Ribosomal P protein L6	ribosomal protein that is a component of the 60S subunit
P18124	RPL7	Ribosomal Protein L7	ribosomal protein that is a component of the 60S subunit
P62424	RPL7A	Ribosomal Protein L7A	ribosomal protein that is a component of the 60S subunit
P62917	RPL8	Ribosomal P protein L8	ribosomal protein that is a component of the 60S subunit
P32969	RPL9	Ribosomal Protein L9	ribosomal protein that is a component of the 60S subunit
P05388	RPLP0	Ribosomal P protein Lateral Stalk Subunit P0	ribosomal protein that is a component of the 60S subunit
P05386	RPLP1	Ribosomal Protein Lateral Stalk Subunit P1	ribosomal protein that is a component of the 60S subunit
P05387	RPLP2	Ribosomal Protein Lateral Stalk Subunit P2	ribosomal protein that is a component of the 60S subunit
P46783	RPS10	Ribosomal P protein S10	ribosomal protein that is a component of the 40S subunit
P62280	RPS11	Ribosomal Protein S11	ribosomal protein that is a component of the 40S subunit
P62277	RPS13	Ribosomal P protein S13	ribosomal protein that is a component of the 40S subunit
P62263	RPS14	Ribosomal Protein S14	ribosomal protein that is a component of the 40S subunit
P62841	RPS15	Ribosomal Protein S15	ribosomal protein that is a component of the 40S subunit
P62249	RPS16	Ribosomal P protein S16	ribosomal protein that is a component of the 40S subunit
P08708	RPS17	Ribosomal Protein S17	ribosomal protein that is a component of the 40S subunit
P39019	RPS19	Ribosomal P protein S19	ribosomal protein that is a component of the 40S subunit
P15880	RPS2	Ribosomal Protein S2	ribosomal protein that is a component of the 40S subunit
P60866	RPS20	Ribosomal P protein S20	ribosomal protein that is a component of the 40S subunit

P63220	RPS21	Ribosomal P protein S21	ribosomal protein that is a component of the 40S subunit
P62266	RPS23	Ribosomal Protein S23	ribosomal protein that is a component of the 40S subunit
P62847	RPS24	Ribosomal Protein S24	ribosomal protein that is a component of the 40S subunit
P62851	RPS25	Ribosomal P protein S25	ribosomal protein that is a component of the 40S subunit
P62854	RPS26	Ribosomal Protein S26	ribosomal protein that is a component of the 40S subunit
Q71UM5	RPS27L	Ribosomal P protein S27L	ribosomal protein that is a component of the 40S subunit
P62857	RPS28	Ribosomal Protein S28	ribosomal protein that is a component of the 40S subunit
P23396	RPS3	Ribosomal P protein S3	ribosomal protein that is a component of the 40S subunit
P61247	RPS3A	Ribosomal Protein S3A	ribosomal protein that is a component of the 40S subunit
P62701	RPS4X	Ribosomal Protein S4X	ribosomal protein that is a component of the 40S subunit
P46782	RPS5	Ribosomal P protein S5	ribosomal protein that is a component of the 40S subunit
P62753	RPS6	Ribosomal Protein S6	ribosomal protein that is a component of the 40S subunit
P62081	RPS7	Ribosomal P protein S7	ribosomal protein that is a component of the 40S subunit
P62241	RPS8	Ribosomal Protein S8	ribosomal protein that is a component of the 40S subunit
P46781	RPS9	Ribosomal Protein S9	ribosomal protein that is a component of the 40S subunit
P08865	RPSA	Ribosomal P protein SA	Required for the assembly and/or stability of the 40S ribosomal subunit and for the processing of the 20S rRNA-precursor to mature 18S rRNA

Supplementary information 2 | List of significantly enriched UFM1-binding proteins. Overview of gene names and protein functions of the hits identified in mass spectrometric analysis of proteins interacting with UFM1. Only significantly enriched proteins (red and blue in figure 5C) are shown.



CHAPTER

5

Genetic editing of SEC61/
-62/63 abrogates HCMV
US2-mediated HLA-I
degradation by regulating
US2 expression

A.B.C. Schuren¹, I.G.J. Boer¹, E.M. Bouma^{1,2}, R.J.
Lebbink¹ and E.J.H.J. Wiertz^{1,*}

1 Dept. Medical Microbiology, University Medical Center Utrecht, 3584CX Utrecht, The Netherlands.

2 Current address: Department of Medical Microbiology, University Medical Center Groningen, Postbus 30001, 9700 RB Groningen, The Netherlands. *Correspondence: E.Wiertz@umcutrecht.nl (E.J.H.J.W.)

submitted

ABSTRACT

Newly translated proteins enter the ER through the SEC61 complex. Proteins that subsequently fail to reach a mature conformation are retro-translocated towards the cytosol and degraded by the ubiquitin-proteasome system, a process called ER-associated protein degradation (ERAD). The channel through which proteins leave the ER is unknown, although the SEC61 complex, which facilitates protein import into the ER, has been implicated in ERAD. The human cytomegalovirus protein US2 induces accelerated ERAD of HLA class I molecules, to prevent immune recognition of virus-infected cells. Here, we targeted all components of the SEC61/62/63 complex by CRISPR/Cas9, creating knock-outs or mutants of the individual subunits of the complex. All subunits affect downregulation of HLA class I. However, because US2 expression is also lowered upon SEC61 knock-out, the HLA class I rescue observed is likely a result of a US2 translocation defect rather than a defect in ERAD.

INTRODUCTION

Up to one-third of all proteins is secreted or expressed in cellular or organelle membranes^{1,2}. These proteins have been translocated into the endoplasmic reticulum (ER) during or after their translation. Translocation of newly translated proteins into the ER is facilitated by the SEC61 complex, which consists of a multimembrane-spanning SEC61 α -subunit associated with smaller SEC61 β and γ subunits³. Depending on the mode of translocation, the complex can be complemented by SEC62 and SEC63⁴⁻⁶.

Translocation of proteins into the ER can occur either co- or post-translationally^{7,8}. The canonical co-translational route is well established in both yeast and mammalian cells. During translation of a signal peptide, the signal recognition particle (SRP) binds the translating ribosome and guides it towards the SRP receptor at the ER membrane. The SRP receptor subsequently interacts with SEC61 α , such that the nascent chain is translocated over the ER membrane as translation continues⁹. Lateral opening of the SEC61 complex allows for release of translated transmembrane domains⁶.

Post-translational translocation remains elusive in higher eukaryotes but is well-studied in yeast. Cytosolic recognition of post-translationally translocated proteins occurs independently of SRP. Instead, cytosolic chaperones of the Hsp70- and Hsp40 families guide fully translated proteins towards the ER¹⁰. In yeast, post-translational translocation occurs mostly for proteins with modestly hydrophobic signal sequences because they interact less strongly with SRP^{11,12}. An auxiliary complex, containing the Sec61 $\alpha/\beta/\gamma$ complex extended with Sec62p, Sec63p, Sec71p and Sec72p is used in this context^{4,7,13}.

Similar to yeast, the homologous SEC62 and SEC63 have been suggested to play a role in mammalian post-translational translocation¹⁴. SEC63 is a Hsp40 chaperone which, via its J-domain, interacts with the ER chaperone BiP to provide the driving force for translocation¹⁵. SEC62 provides an alternative for SRP-mediated translocation. The SEC61 complex can switch from SRP-dependent to SEC62-dependent translocation, when SEC62 outcompetes the SRP receptor for SEC63 binding¹⁶. However, both SEC62 and SEC63 are also implicated in co-translational translocation^{16,17}. In mammals, the post-translational route is thought to play a role mostly for proteins shorter than 110 amino acids in length. It is speculated that transla-

tion of these short proteins occurs too rapidly to allow for co-translational recognition by SRP, suggesting that they are recognized post-translationally^{18,19}. Within this class of small proteins, a positive charge in the signal sequence is conserved and improves translocation efficiency²⁰. Tail-anchored proteins, with their C-terminus anchored in the ER-membrane, are also translocated in a post-translational manner. This translocation is however independent of the SEC61 complex and is instead facilitated by the TRC40/Get3 pathway²¹.

Besides translocation, the SEC61 complex has been suggested to act as a channel for retrograde protein transport in yeast²²⁻³⁰ as well as mammalian cells^{28,31,32}. This so-called retro-translocation (also referred to as dislocation) is a part of the ER-associated protein degradation (ERAD) pathway, a quality control mechanism that prevents cellular damage caused by accumulation of misfolded proteins. In this process, ER proteins that fail to reach their mature conformation are detected by ER chaperones, retro-translocated towards the cytosol, and subsequently degraded by the ubiquitin-proteasome system.

Sec61 α p mutants that are specifically defective in ERAD have been identified in yeast. Temperature-sensitive mutants have shown specific ER export defects³³. Point mutations in^{24,25,31} or deletion of²⁵ the ER-resident loop between SEC61 α transmembrane domains 7 and 8 suggest that this region is of particular importance in ERAD. This loop is also essential for the interaction between SEC61 α and the 19S proteasome³⁴. A SEC61 α mutant deficient in binding the 19S proteasome is import-competent but has a defect in ERAD, suggesting that coupled retro-translocation and degradation may occur³⁴. In higher eukaryotes, the SEC61 complex can also facilitate protein transport towards the cytosol. SEC61 that is recruited from the ER to endosomes provides endosome-to-cytosol transport of peptides destined for cross-presentation on MHC class II³⁵.

Although protein degradation is well-characterized, the retro-translocation step remains elusive. To date, it is unclear whether SEC61 functions as a dislocon to facilitate this step, as other candidates have been suggested as well. These include multimembrane-spanning ubiquitin E3 ligases such as HRD1³⁶ or TMEM129^{37,38}, the ERAD recruiting factor Derlin-1³⁹⁻⁴¹, signal peptide peptidase (SPP)⁴², TRAM1^{43,44} or a combination of E3 ligases, Derlins and cytosolic factors⁴⁵.

The role for SEC61 as a retro-translocon was originally suggested in the context of the human cytomegalovirus (HCMV) protein US2³². HCMV induces accelerated ERAD of HLA class I (HLA-I) molecules to prevent recognition of virus-infected cells by CD8⁺ T lymphocytes. The virus expresses two proteins, US2 and US11, that downregulate HLA-I via ERAD, albeit via different ERAD pathways. Pulse-chase experiments in cells expressing US2 indicated that HLA is degraded within minutes after translocation. As this timeframe is short, HLA may still be associated with the SEC61 complex when US2-mediated ERAD is initiated. SEC61 β and - γ associate with US2 and cytosolic HLA-I, suggesting that SEC61 facilitates retro-translocation of HLA-I in the presence of HCMV US2³². A dual role for the translocation machinery in this context may even be extended to other factors, as the signal peptide peptidase (SPP) and the translocating chain-associated membrane protein 1 (TRAM1) have also been suggested to play a role in US2-mediated ERAD of HLA-I⁴²⁻⁴⁴.

Novel gene-editing techniques, such as CRISPR/Cas9, allow for the generation of gene knockouts in mammalian cells. Using this technology, we re-assessed the role of SEC61 in US2-mediated

HLA-I degradation. We established clonal cell lines with in-frame or out-of-frame indels for each SEC61/62/63 component. We report that SEC61/62/63 components are essential for US2-mediated ERAD of HLA-I, as manipulation of these components rescue the degradation of HLA-I. However, as expression levels of US2 are severely impacted by mutating the SEC61 complex, we speculate that HLA-I rescue is caused by a defect in US2 translocation rather than ERAD.

MATERIALS & METHODS

Cell culture

Human monocytic U937 cells (ATCC) and human embryonic kidney 293T cells (ATCC) were cultured in RPMI 1640 medium (Gibco), supplemented with 5-10% fetal calf serum (BioWest), 100 U/ml Penicillin/Streptomycin (Gibco) and 2 mM Ultraglutamine-1 (Gibco).

Lentivirus production and infection

The day before virus production, 65,000 293T cells were seeded per well in 24-wells plates. For virus production, 250 ng lentiviral vector was co-transfected with a mix of third-generation lentivirus packaging vectors (250 ng total) using Mirus LT-1 transfection reagent (Mirus Bio LLC). Three days post-transfection, the supernatant was harvested and stored at -80 °C. For lentiviral transduction, 100 μ l virus-containing supernatant supplemented with 8 μ g/ml polybrene (Santa Cruz Biotechnology) was added to 30,000 cells. The cells were spin-infected at 1,000G for 1.5 hours at 33 °C.

Generation of clonal knockout cell lines

To generate knock-out cell lines, U937 cells with stable expression of HLA-A2-GFP, HCMV US2 and *S. pyogenes* Cas9 (Addgene #52962) were transduced with a lentiviral vector containing a CRISPR/Cas9 guideRNA (gRNA) and a puromycin resistance gene. Target sequences of the respective CRISPR sgRNAs are shown below (table 1). Three days post transduction, cells were subjected to 2 μ g/ml puromycin to select successfully transduced cells. Single HLA-A2-GFP⁺ cells were FACS-sorted by an Aria3 cell sorter into 96-wells plates containing RPMI 1640 medium supplemented with 50% FCS and allowed to recover. The knock-out status was confirmed by flow cytometric analysis of HLA-I expression, sequencing of the sgRNA target region (table S1), and addback experiments of the respective cDNAs.

Target gene	Target sequence + PAM
SEC61 α 1 (sgRNA 1)	TGTTGTA CTGGCCACGGTAGCGG
SEC61 α 1 (sgRNA 2)	ATCAAGTCGGCCCCGCTACCGTGG
SEC61 α 1 (sgRNA 3)	ATCTCTCCTATTGTCACGTCTGG
SEC61 α 1 (sgRNA 4)	CTGAAGACATGATCCCAACAGG
SEC61 α 2 (sgRNA 1)	TATGTCATGACGGGGATGTATGG
SEC61 α 2 (sgRNA 2)	CCCCGTCATGACATACACAATGG
SEC61 β (sgRNA 1)	TAGTGGCCCTGTTCCAGTATTGG
SEC61 β (sgRNA 2)	GTAGAATCGCCACATCCCCCGG
SEC61 β (sgRNA 3)	GACAGTGGATCCCCGCCCGGG

SEC61 β (sgRNA 4)	GCACTAACGTGGGATCCTCATGG
SEC61 γ (sgRNA 1)	TGTAAAGGACTCCATTCGGCTGG
SEC61 γ (sgRNA 2)	GCATCTTTTAACCAGCCGAATGG
SEC62 (sgRNA 1)	CTGTGGTTGACTACTGCAACAGG
SEC62 (sgRNA 2)	GTAGTCAACCACAGACTCCCTGG
SEC62 (sgRNA 3)	AACCCGGTGACCCATCATATTGG
SEC62 (sgRNA 4)	CACCAATATGATGGGTCACCGGG
SEC63 (sgRNA 1)	GTGATGAGGTTATGTTCATGAGG
SEC63 (sgRNA 2)	TTGGTATTCTCGGTCTGTTTTGG
SEC63 (sgRNA 3)	TCCCGCGACATACTACCTCTGG
SEC63 (sgRNA 4)	TGTTCCCACTGTCATCGTACTGG
TRC8	AGGAAGATGACAGGCGTCTTGG
TMEM129	GCACACGGCGAACACCAGATAGG
P97	GAGGCGCGCCATGGCTTCTGG
Npl4	GATCCGCTTCACTCCATCCGGGG
Ufd1	GATGGAGACCAAACCCGACAGAGG

Table 1 | CRISPR sgRNAs used in this study.

Antibodies

Primary antibodies used for flow cytometry were: PE-conjugated mouse anti-HLA-A2 (clone BB7.2, BD Pharmingen, no. 558570) and human anti-HLA-A3 mAb (clone OK2F3 LUMC, Leiden, The Netherlands).

As secondary antibody for flow cytometry we used PE-conjugated goat anti-human IgG + IgM (H+L) (F(ab')₂) (Jackson ImmunoResearch, no. 109-116-127).

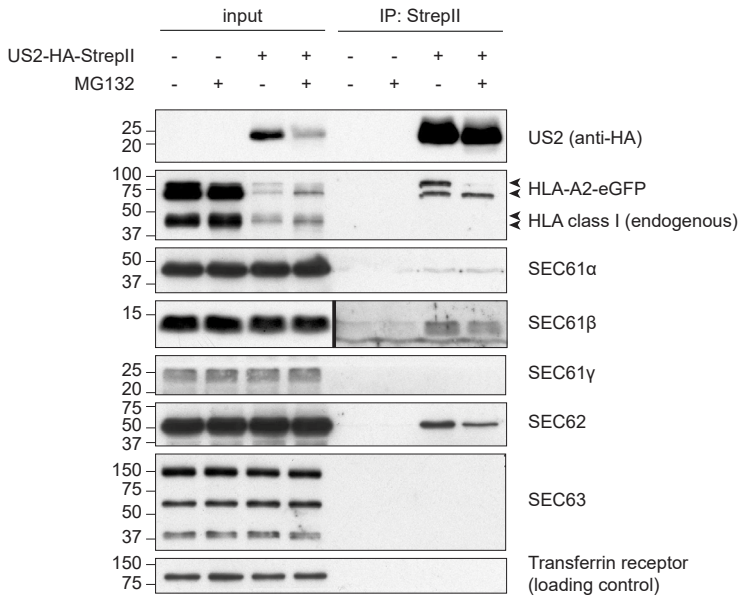
For immunoblotting we used the following primary antibodies: mouse anti-HLA-I HC HCA2 mAb, mouse anti-Transferrin receptor mAb (clone H68.4, Invitrogen, no. 13-6800), rat anti-HA-tag mAb (clone 3F10, Roche, no. 11867423001), rabbit anti-SEC61A mAb (Abcam, ab183046 [EPR14379]), rabbit anti-SEC61B pAb (Abcam, ab15576), rabbit anti-SEC61G pAb (Abcam, ab16843), rabbit anti-SEC62 pAb (Abcam, ab16843), mouse anti-SEC63 pAb (Abcam, ab68550).

Secondary antibodies for immunoblotting were: HRP-conjugated goat anti-mouse IgG (Jackson ImmunoResearch, no. 211-032-171), HRP-conjugated goat anti-rat IgG (Jackson ImmunoResearch, no. 112-035-175), HRP-conjugated goat anti-rabbit IgG (Jackson ImmunoResearch, no. 115-035-174).

Plasmids

The C-terminally GFP-tagged HLA-A2 construct was expressed from a lentiviral pHRSin-cPPT-SGW vector (kindly provided by Dr. Paul Lehner and Dr. Louise Boyle, University of Cambridge). Wildtype HCMV US2 was expressed from an EF1A promoter in a lentiviral plasmid. As this plasmid did not contain a resistance gene for antibiotics selection, US2⁺ cells were FACS-sorted as described before (Chapter 4). A lentiviral vector containing an EFS

A



B

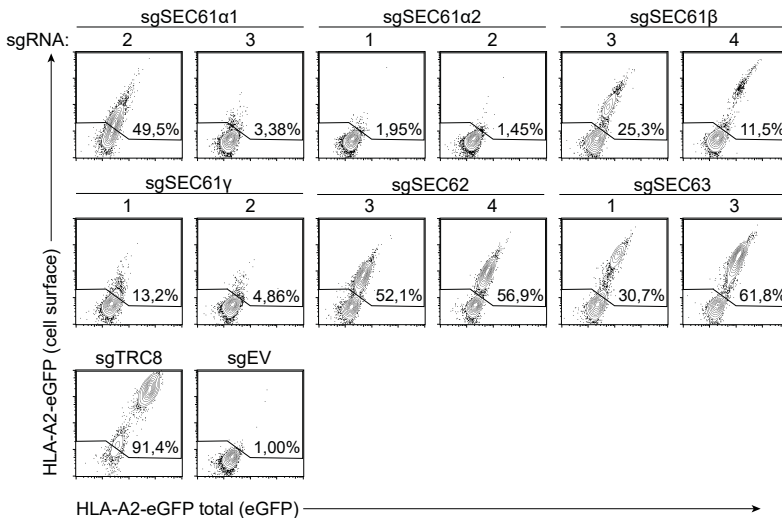


Figure 1 | The SEC61 complex plays a role in US2-mediated degradation of HLA-I. A) StrepII- and HA-tagged US2 containing a CD8 leader (CD8L-ST2-HA-US2) was immunoprecipitated from U937 cells also expressing eGFP-HLA-A2. Co-immunoprecipitation of HLA-I (control), SEC61 β and SEC62 shows that US2 interacts with the SEC61 complex. Each experiment in this study was performed at least twice, unless otherwise stated. One representative experiment is shown in these figures. B) CRISPR/Cas9 sgRNAs targeting SEC61 subunits, or control sgRNAs, were added to U937 cells expressing HLA-A2-eGFP and untagged US2. Four sgRNAs were introduced per gene, of which the two most potent are shown. sgRNA sequences are listed in the materials and methods. All knock-outs of SEC61 subunits, with the exception of SEC61 α 2, rescue HLA-I from US2-mediated degradation.

promoter-driven codon-optimized *S. pyogenes* Cas9 fused to a nuclear localization sequence was purchased via AddGene (lenti-Cas9-Blast, plasmid #52962). This plasmid also contains a Blasticidin resistance cassette. CRISPR sgRNAs were cloned downstream of a human U6 promoter in a BsmBI-linearized pSicoR lentiviral vector also containing an EFS (EF1A short) promoter driving expression of a puromycinR-T2A-Cas9Flag cassette. cDNAs were expressed from an EF1A promoter on a bidirectional lentiviral vector. This vector also contains a human PGK promoter driving expression of a Zeocin resistance gene.

Flow cytometry

Cells were washed in PBS (Gibco) containing 0.5% BSA and 0.02% sodium azide and subsequently fixed 15 min in 0.5% formaldehyde. Cells were stained with the antibodies listed above. Flow cytometry was performed on a FACSCanto II (BD Bioscience) and data was analyzed using FlowJo software.

Immunoblotting

Cells were lysed in Triton X-100 lysis buffer (1% Triton X-100 in TBS, pH 7.5) containing 10 μ M Leupeptin (Roche) and 1 mM Pefabloc SC (Roche). Lysates were spun down at 18,000g for 20 min at 4 °C to remove cellular debris. After addition of Lämmli sample buffer containing DTT, lysates were boiled 5 min at 95 °C and stored at -80 °C until use. SDS-PAGE was performed on 12% polyacryl-amide gels, after which the proteins were transferred to a PVDF membrane (Immobilon-P, Millipore). Primary antibodies were incubated overnight at 4 °C in 1% milk. The secondary antibodies were incubated for 1 hour at room temperature. Each antibody was washed off three times in PBS-T (PBS containing 0.05% Tween20 (Millipore)). Protein bands were detected by incubation with ECL (Thermo Scientific Pierce) and exposed to Amersham Hyperfilm ECL films (GE Healthcare).

Co-immunoprecipitation

Cells were lysed in Digitonin lysis buffer, containing 1% Digitonin (Calbiochem) in 50 mM Tris-HCl, 5 mM MgCl₂ and 150 mM NaCl, at a pH of 7.5. This buffer was supplemented with 10 μ M Leupeptin (Roche) and 1 mM Pefabloc SC (Roche). Lysates were incubated on ice for 30 min, after which they were spun down at 18,000g for 20 min at 4 °C to remove cellular debris. The supernatant was incubated overnight with StrepTactin beads (GE Healthcare) on a rotary wheel at 4 °C. The samples were washed 4 times with 0.1% Digitonin lysis buffer and eluted with d-Desthiobiotin (2.5 mM d-Desthiobiotin, 100 mM Tris-HCl, 150 mM NaCl and 1 mM EDTA, at a pH of 8.0). 0.45 μ M SpinX columns (Corning Costar) were used to collect the eluate. After addition of Lämmli sample buffer with DTT, samples were boiled 5 min at 95 °C and stored at -80 °C until further use. Immunoblotting was performed as described above.

RESULTS

CRISPR/Cas9-mediated editing of all SEC61/62/63 subunits rescues HLA-I from downregulation by HCMV US2

Previously, immunoprecipitations on SEC61 β and γ have shown an interaction between US2,

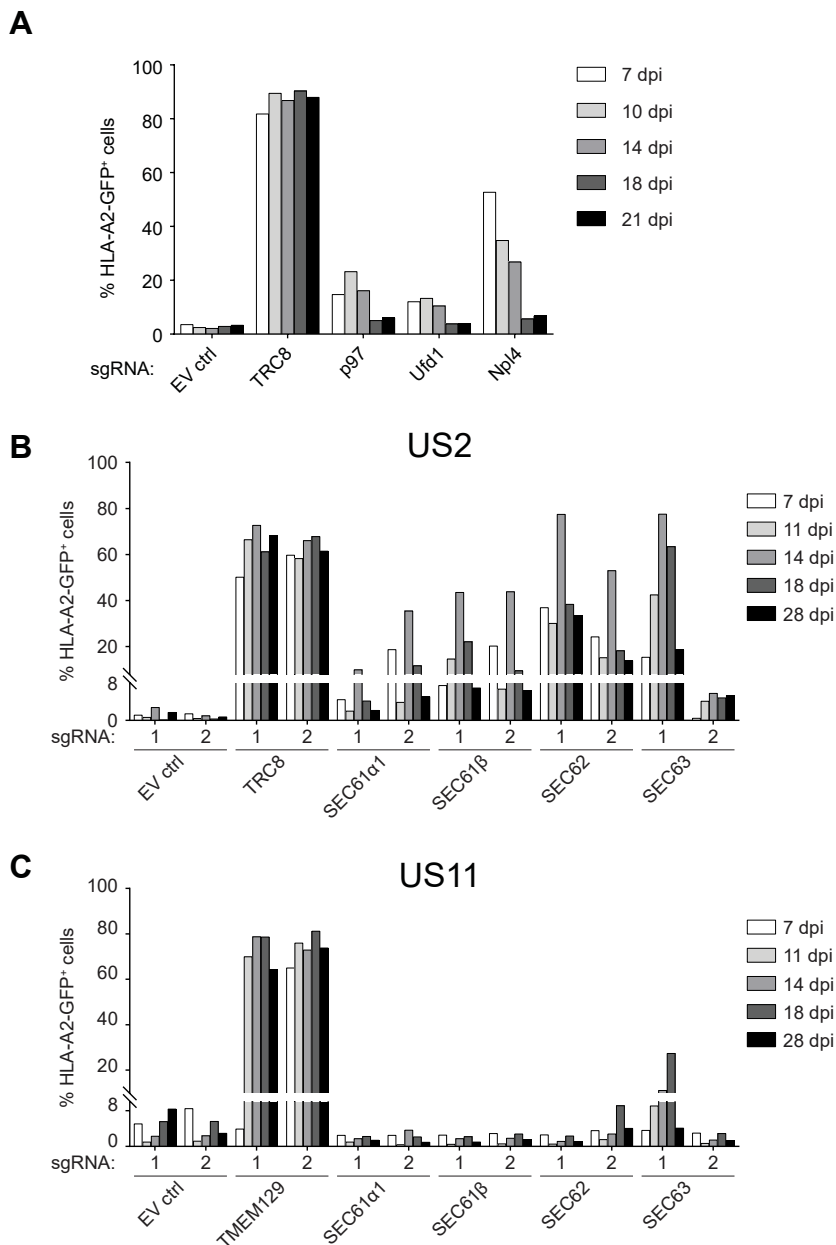


Figure 2 | CRISPR/Cas9 targeting of SEC61 subunits yields stable abrogation of US2-mediated HLA-I degradation. A) Addition of CRISPR/Cas9 sgRNAs targeting essential genes such as p97/VCP or its co-factors Ufd1 and Npl4 leads to a minor and temporary rescue of HLA-I expression which is lost over time due to lethality of the knock-out. B) SEC61 subunit knockout yields a stable HLA-I rescue phenotype over at least 28 days. This phenotype is specific to the HCMV protein US2, since US11 (C), another ERAD-inducing HCMV protein is not sensitive to SEC61 knock-out.

deglycosylated HLA-I and the SEC61 complex³². To more specifically determine which components of the SEC61 complex interact with US2, we reversed the approach. We introduced an N-terminally StrepII-HA-tagged US2 with a cleavable CD8 signal peptide in U937 cells containing HLA-A2-eGFP to efficiently express tagged US2. This US2 construct was pulled out using a StrepTactin immunoprecipitation. Total cell lysates ('input') and immunoprecipitations were immunoblotted and stained for all components of the SEC61/62/63 complex. We confirm the interaction between SEC61 β and US2, but we also find that SEC62 associates with US2. Whether US2 interacts with SEC61 α remains uncertain, as this effect was not reproducible. An interaction between US2 and SEC61 γ or SEC63 was not observed in our hands (fig. 1A). This prompted us to test all the components of the complex for their involvement in US2-mediated HLA-I degradation.

The recent development of CRISPR/Cas9 technology enabled us to study HLA-I downregulation by US2 in the context of genetically mutated SEC61 subunits. CRISPR single guide RNAs (sgRNAs) targeting subunits of the SEC61 complex were introduced in a clonal U937 cell line expressing HLA-A2-eGFP, US2 and Cas9. The HLA-A2 allele was chosen because it is downregulated very effectively by US2⁴⁶. As a control, we CRISPR-targeted the ubiquitin E3 ligase TRC8, which is known to be essential for US2-mediated HLA-I downregulation⁴⁷.

Flow cytometry was used to determine the expression levels of HLA-A2. As it is known that ER-resident HLA-I that is rescued from degradation can escape to the cell surface^{47,48}, we measured both the total (intracellular) HLA-A2 expression by means of its eGFP-tag, as well as cell surface expression using an HLA-A2-specific antibody (Fig. 1B). We tested all subunits of the SEC61/62/32 complex and observed HLA-A2 rescue for SEC61 α 1, SEC61 β , SEC61 γ , SEC62 and SEC63 (fig. 1B), which together comprise the entire SEC61/62/63 complex. Only SEC61 α 2 knock-out did not show rescue of HLA-A2. As no biochemical studies have been performed on SEC61 α 2 to date, it is unclear whether this subunit is in fact part of a functional translocation complex.

The clear HLA-A2 rescue phenotype at 12 days post-transduction with the SEC sgRNAs (fig. 1B) was surprising. Our experience is that knocking out essential ERAD genes, such as p97/VCP and its co-factors Ufd1 and Npl4, yields a minor and transient HLA-I rescue phenotype due to lethality of the knock-out cells and hence loss of the phenotype over time (fig. 2A). By contrast, measuring the SEC61-edited cells over time showed that the HLA-A2 rescue phenotypes were apparent for at least 28 days (fig. 2B), although the effect waned after a peak at 11-14 days post-transduction. The phenotype also seemed specific to the HCMV protein US2, as the activity of another ERAD-inducing HCMV protein, US11, was not sensitive to SEC61 editing (fig. 2C), with the exception of SEC63.

Stable mutant cell lines can be generated for all SEC61 components

Since the HLA-I rescue phenotype in SEC61 knock-out cells declined at later timepoints (fig. 2B) we next assessed whether this was caused by cell death due to SEC61 subunit knockout, or by a growth disadvantage of the mutant cells over non-targeted cells in the polyclonal cell population. In the latter case, clonal cell lines with a SEC61 mutation might survive long-term and enable us to study their effect on US2 functioning. For this we sorted single HLA-A2^{high}

cells from the polyclonal SEC61/62/63 mutant populations by FACS and allowed these to grow out. Surprisingly, we were able to establish clonal lines that displayed stable rescue of HLA-I (fig. 3A). CRISPR/Cas9-induced mutations in these clonal cell lines were assessed by sequencing the sgRNA target regions (table S1). The majority of the clones showed in-frame indels on one

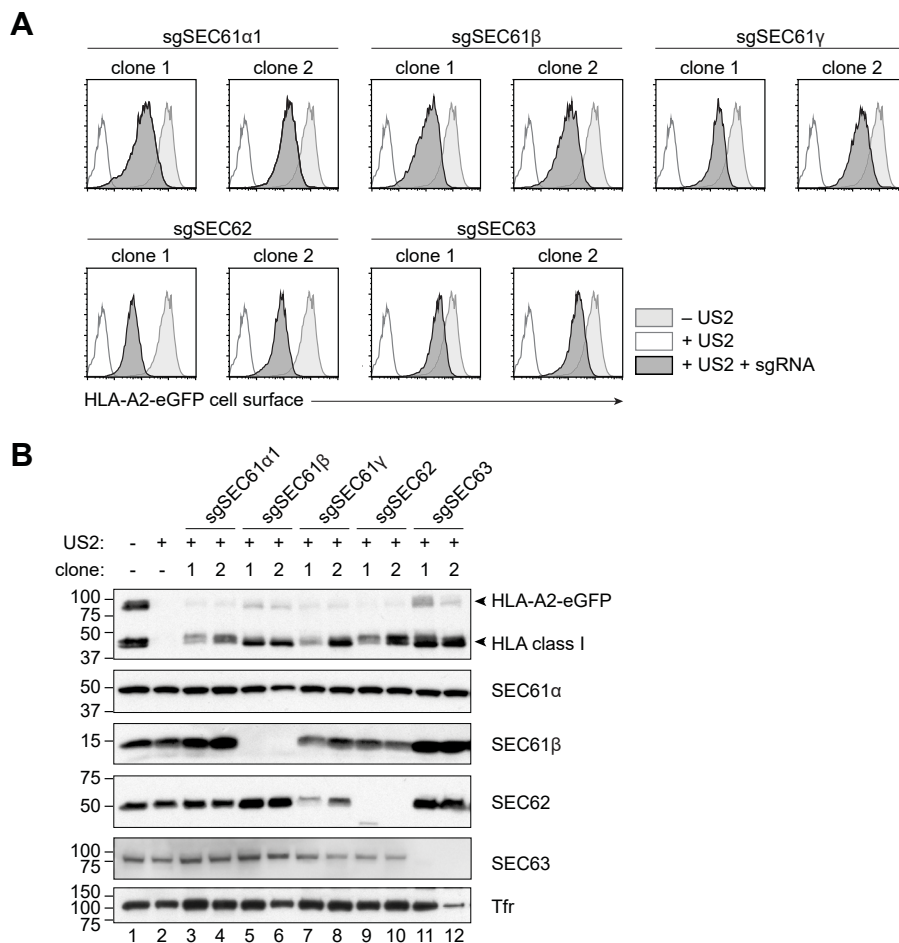
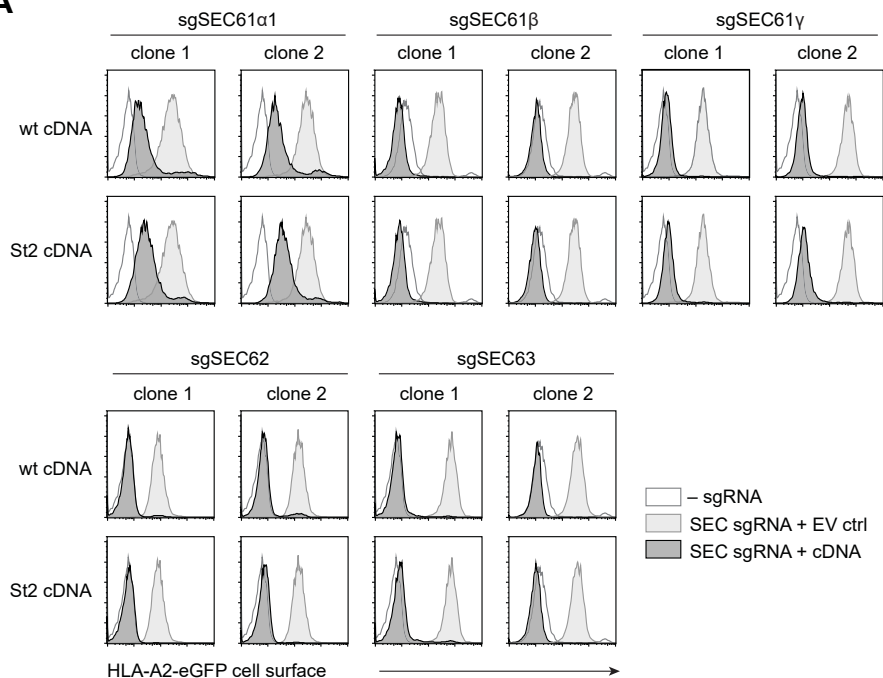


Figure 3 | SEC61/62/63 mutant clonal lines are stable and interfere with US2-mediated HLA-I expression.

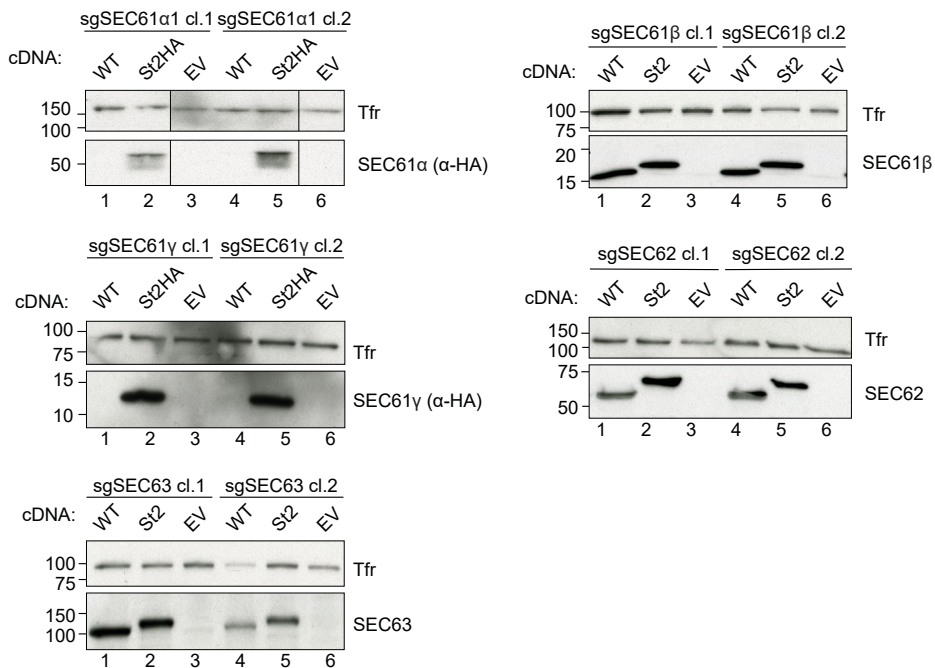
A) Single cells from fig. 2B were isolated by FACS and two clonal lines were selected per edited gene (see also figure S1). Selected clones yield a stable HLA-I rescue phenotype (compare black peaks to non-filled gray peaks). B) Lysates of all selected mutant clones shown in A were immunoblotted and stained against HLA class I and all components of the SEC61/62/63 complex. Addition of CRISPR/Cas9 sgRNAs only affects expression of the targeted SEC61 subunits, but does not impact the stability of the of other subunits, suggesting that editing single subunits does not result in an unstable SEC61/62/63 complex.

Figure 4 | SEC61/62/63 cDNAs revert the mutant phenotype in clonal SEC-edited lines. A) sgRNA-resistant wildtype or StrepII-(HA-)tagged cDNAs were transduced in the respective mutant clones and were selected for using Zeocin treatment. Addition of a sgRNA-resistant cDNA reverts the mutant phenotypes, showing that the HLA-I rescue effects are specific. B) Immunoblots showing the protein expression levels of the respective SEC61 genes after CRISPR/Cas9-mediated editing, and after addition of tagged- and wildtype cDNAs.

A



B



5

or both alleles, although full genetic knock-outs of SEC61 β , SEC61 γ and SEC62 were selected with out-of-frame deletions on both alleles. For each SEC61/62/63 subunit, two clones were selected for further characterization (marked with '1' and '2' in fig. S1). All clones showed stable rescue of HLA-A2 (fig. 3A), although some displayed a decline in growth rate (data not shown).

As many clones showed in-frame deletions, we next assessed whether protein expression was affected of the genes that were targeted (fig. 3B). In clones with a SEC61 β -, SEC62- or SEC63 mutation, the respective proteins were not detectable by Western blot, suggesting that gene-editing resulted in a full knockout of protein expression. SEC61 α expression, however, was not altered upon CRISPR/Cas9-mediated editing of SEC61 α 1. This may be due to the in-frame mutations we identified in the two isolated clones (table S1). Besides the two stable SEC61 α 1-edited genes, we did isolate out-of-frame clones, but these cells were unstable and died within a few weeks (data not shown). This suggests that SEC61 α 1 is essential for cell survival, which is in agreement with RNAi studies reported previously¹⁴. We were unsuccessful to reliably detect SEC61 γ by Western blot.

In agreement with our studies in polyclonal knockout cells, all isolated clones expressed HLA-A2-eGFP as detected by flow cytometry (fig. 3A) and Western blot (fig. 3B). Interestingly, the amount of rescue of endogenous HLA-I was much more pronounced than that of the chimeric HLA-A2-eGFP molecule (fig. 3B, top panel).

We also tested whether the stability of non-targeted subunits was destabilized by CRISPR/Cas9-mediated editing of single subunits. As we did not assess the interactions between the SEC61/62/63 subunits, we cannot distinguish between disintegration of the SEC61/62/63 complex and the stabilization of independent subunits. We do however observe that protein expression of non-targeted subunits remains intact, suggesting that the remaining subunits of the incomplete and potentially aberrantly assembled SEC61/62/63 complex are not degraded by quality-control mechanisms (fig. 3B).

SEC61/62/63 cDNAs revert the HLA-I rescue phenotype of mutant clones

To ascertain that the HLA-I rescue phenotypes we observed were specific to the SEC61/62/63 genes that were edited, we expressed sgRNA-resistant cDNAs of the respective genes in the clonal mutant lines and assessed HLA-I levels by flow cytometry. HLA-I rescue phenotypes as well as

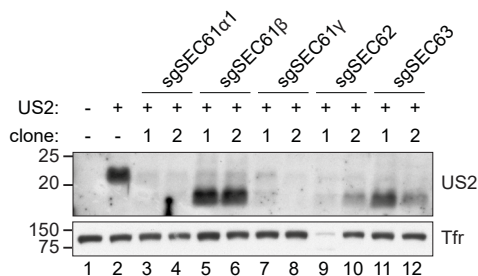


Figure 5 | Mutating SEC61/62/63 components lowers expression of mature US2.

The cell lines shown figure 3B were lysed in Triton X-100 in an experiment separate from the one shown in figure 3B. Lysates were stained with an anti-US2 antibody and an anti-transferrin receptor antibody as a loading control. A decline in US2 expression is observed upon targeting SEC61 α 1, SEC61 γ and SEC62 with sgRNAs. The lower molecular weight band for US2 observed in SEC61 β - and SEC63-targeted cells may represent non-glycosylated US2. The phenotypes observed in this blot are preliminary and should thus be interpreted with caution. Lanes 1-4 are performed twice, while only an n=1 is available for lanes 5-12.

growth defects were reverted by supplementing with either wildtype or StrepII-tagged cDNAs of the genes that were knocked out (fig. 4A). Expression of the cDNAs was confirmed in Western blot (fig. 4B). For SEC61 α 1 and SEC61 γ , a StrepII-HA-tagged cDNA was used to detect the cDNAs via their HA-tags, whereas the expression of SEC61 β , SEC62, and SEC63 were detected using protein-specific antibodies.

Expression of US2 decreases upon SEC61/62/63 editing

SEC61 may act as a two-way transport channel, facilitating HLA retro-translocation from the ER towards the cytosol upon US2 functioning^{28,31,32}. We therefore hypothesized that the rescued expression of HLA-I in the presence of US2 may be caused by a defect in HLA-I retro-translocation. However, we observed a strong downregulation of full-length US2 in clonal SEC61 α 1- and SEC61 γ mutant cells (fig. 5), which suggests that the HLA-I rescue phenotypes are caused by a defect in US2 expression rather than impaired ERAD functioning. The lower molecular weight band that occurs in SEC61 β , SEC62 and SEC63 clones could reflect expression a non-glycosylated form of US2^{32,49}, suggesting that US2 is unable to translocate in these cells. The low baseline expression level of US2, even in control cells that were not targeted by CRISPR/Cas9, posed a technical difficulty that did not allow for validating the US2 expression level nor its glycosylation status. Interestingly, expression of the transferrin receptor, another transmembrane protein that is hence translocated by the SEC61 complex, is not affected in our mutant clones, suggesting that this translocation defect is not a general phenomenon.

The signal peptide determines susceptibility of US2 to SEC61/62/63 editing

Non-glycosylated US2, potentially arising from inefficient translocation, has been described in literature before^{32,49}. As the signal sequence of a protein influences its translocation efficacy⁵⁰, we tested a panel of HA-tagged US2 variants with different signal peptides (figs. 6A, S2 and S3) to study whether a potentially inefficient US2 signal peptide renders US2 susceptible to translocation defects.

First, we wanted to test whether the different US2 variants were able to downregulate the HLA-A2-eGFP construct. All US2 variants were equally able to strongly downregulate HLA-A2-eGFP, as was assessed by flow cytometry (fig. 6B). We next transduced these US2-expressing cells with SEC61/62/63-targeted CRISPR sgRNAs (fig. 6C). Overlays of the flow cytometry data from cells with (red) and without (blue) sgRNAs show that only US2 leader (US2L) expressing US2 variants show significant HLA-A2-eGFP rescue upon SEC61/62/63 editing, whereas US2 with a CD8 or CD11 leader sequence did not. This phenotype was most pronounced when targeting SEC61 α 1, SEC62 and SEC63. In control cells lacking US2, a minor reduction of HLA-I expression is observed only upon sgRNA-targeting of SEC61 α 1 and SEC61 γ (fig. 6C, top panels).

US11 requires functional SEC61/62/63 upon transfer of the US2 signal peptide

We also tested these different signal peptides fused to the HA-tagged HCMV protein US11, which was not sensitive to SEC61/62/63 editing (fig. 2C). To be able to compare the panel of

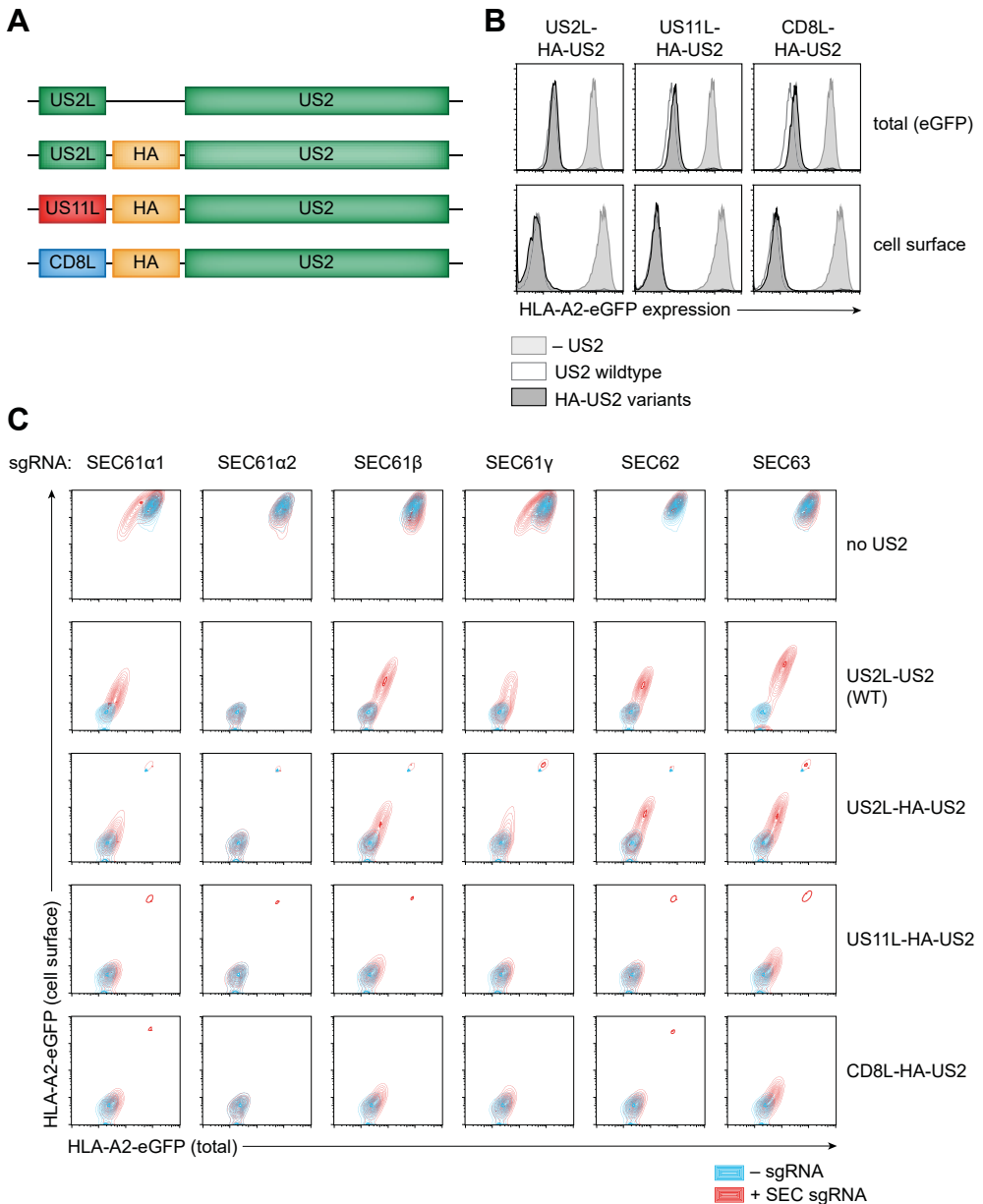


Figure 6 | The signal peptide determines susceptibility to SEC61/62/63 editing. A) Schematic overview of HA-tagged US2-variants with different signal peptides, as compared to wildtype US2 (top). B) U937 cells expressing HLA-A2-eGFP were transduced with the indicated HA-US2 construct or the wildtype (untagged) US2. Subsequently, CRISPR sgRNAs targeting the subunits of the SEC61/62/63 complex were introduced. This polyclonal cell population was subjected to flow cytometry to assess total levels (eGFP, x-axis) and cell-surface levels (antibody stain, Y-axis) of the HLA-A2-eGFP chimera. sgRNAs that were used in this figure are: SEC61 α 1 sgRNA 2; SEC61 α 2 sgRNA 1; SEC61 β sgRNA 2; SEC61 γ sgRNA 1; SEC62 sgRNA 2; SEC63 sgRNA 1.

US2 variants to US11, we stably expressed a non-tagged HLA-A2 molecule in U937 cells using lentiviral transduction, as the C-terminal eGFP-tag on the HLA-A2-eGFP construct renders it insensitive to US11-mediated degradation⁵¹. We subsequently introduced the various HA-tagged US2 and US11 variants and assessed their potential to downregulate HLA-A2 by flow cytometry (Fig. 7A). All US2- and US11 variants were able to downregulate HLA-A2, with US11L- and CD8L-HA-US11 being the most potent (fig. 7A). We observed strong signal peptide-specific differences in the expression levels of the US2- and US11 variants (fig. 7B), which show an inverse correlation with the magnitude of HLA-I downregulation. Subsequently, sgRNAs targeting the SEC61/62/63 subunits were introduced in the six US2- or US11-expressing cell lines, and HLA-A2 expression was assessed by flow cytometry. To be able to compare between cell lines, HLA-A2 rescue was normalized to that in sgRNA-targeted TRC8 (for US2) or TMEM129 (for US11) cells, which were used as positive controls. The US2 variants showed an HLA-A2 rescue pattern that was similar to that observed for the HLA-A2-eGFP construct (fig. 6C), with the US2L-variant showing a substantial HLA-A2 rescue effect upon SEC61/62/63 editing, and the US11L- and CD8L-variants being less strongly affected (fig. 7C, top part). Both US11L-HA-US11 and CD8L-HA-US11 retained their ability to downregulate HLA-A2 in the presence of SEC61/62/63 sgRNAs (fig. 7C, bottom part), as was expected from studies performed in fig. 2C. Interestingly, when the US11 signal peptide was replaced by that of US2, the US11 protein gained sensitivity to SEC61/62/63 editing (fig. 7C, bottom left). The low expression level of proteins containing the US2L signal peptide (fig. 7B) suggests that this signal peptide indeed functions inefficiently, which may result in increased sensitivity to translocation defects. Taken together, HLA-I degradation by HCMV US2 or US2L-containing US11 is decreased when subunits of the SEC61/62/63 complex are edited by CRISPR/Cas9. While previous studies suggest that the SEC61 complex may function as a dislocation complex for ERAD, the HLA-I rescue in our cells may be caused by diminished US2 expression. Our data suggests that this dependence of US2 on the SEC61/62/63 complex is specific to the inefficient signal peptide it bears.

DISCUSSION

In this study we re-evaluated the role of SEC61 in US2-mediated degradation of HLA-I. Our data suggests that mutation of SEC61/62/63 components affects translocation of US2, rather than functioning as a channel for retro-translocation of HLA-I. In agreement with previous studies³², we observed an interaction of US2 with both HLA-I and SEC61 β ³². In an unbiased approach we co-immunoprecipitated components of the SEC61 complex using US2 as a bait. Interestingly, not only SEC61 β , but also SEC62 interacts with US2. However, since all newly made transmembrane proteins interact with SEC61 during translocation, no functional relationship regarding ERAD can be interpreted from this interaction alone.

To study the role of the SEC61 complex in ERAD in a functional way, we established clonal cell lines containing mutants of single subunits of the SEC61 complex. Clonal cell lines provide a well-characterized context to study the effect of protein mutations or deletions. Although knockdown of certain SEC61 subunits is possible¹⁴ and particular mutations in the complex

are compatible with life^{5,52}, it was surprising that CRISPR/Cas9-mediated knock-outs or severe mutation of these important genes yielded stable clonal cell lines. These cell lines could be used in a broader context, such as studying translocation or ERAD of different degradation substrates.

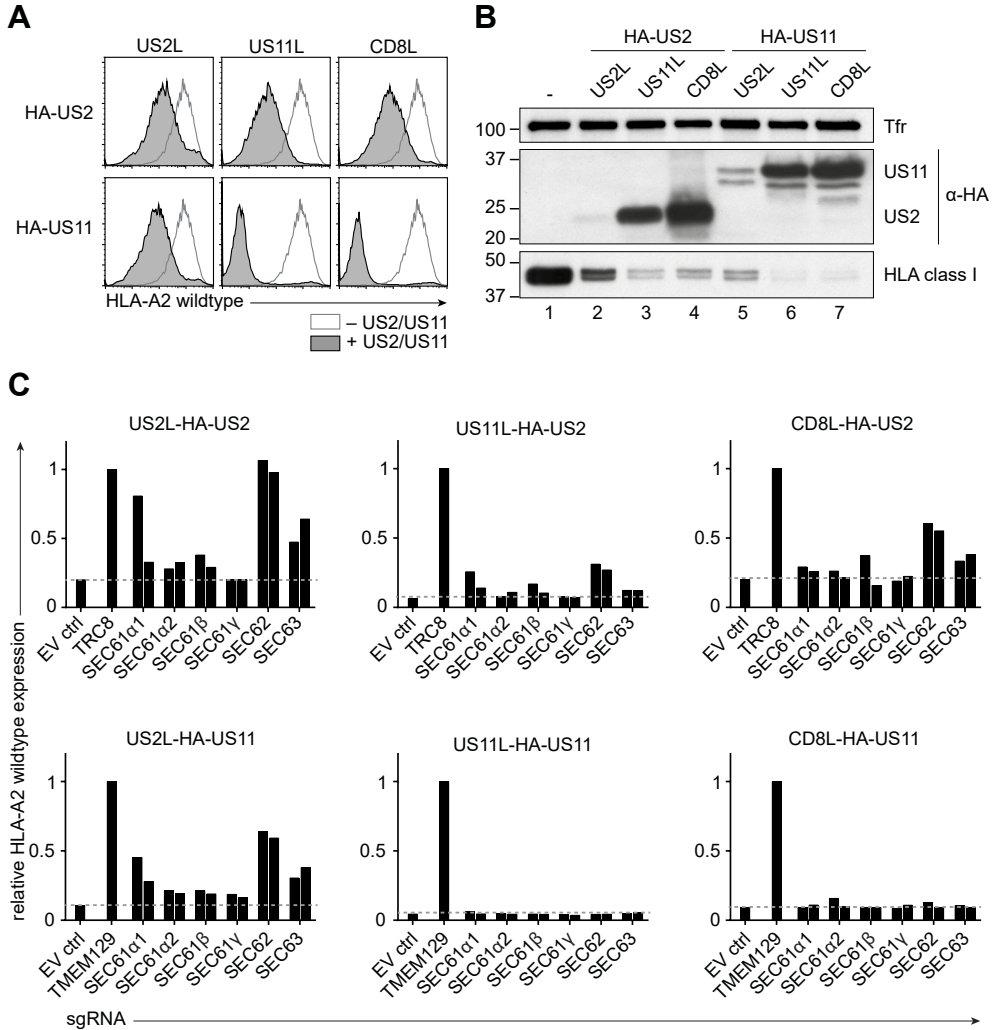


Figure 7 | US11 becomes dependent on functional SEC61/62/63 when fused to the US2 signal peptide.

A) The US2 variants from figure 6A as well as HA-US11 variants containing the three different signal peptides were expressed in U937 cells containing a non-tagged HLA-A2 construct. All HA-tagged US2- and US11-variants downregulate this HLA-A2 molecule, as shown by flow cytometry on cell surface expression of this degradation substrate. B) Western blot on the cells from figure 7A. The expression levels of US2 and US11 are affected by their signal peptides, with US2L leading to a low, US11L to an intermediate and CD8L to a high expression level. C) Relative wildtype HLA-A2 expression in the presence of SEC61/62/63 sgRNAs. This experiment was set up similar to figure 6B, albeit with the untagged HLA-A2 construct. HLA-A2 expression was assessed at the cell surface using an HLA-A2-specific antibody. Flow cytometry data is summarized in bar graphs showing the HLA-A2 expression level (based on mean fluorescence intensity). HLA-A2 fluorescence intensity is shown relative to the positive control (TRC8 for US2, or TMEM129 for US11) to allow comparison between graphs.

The characterization of the mutant clones allows us to hypothesize how they affect US2-mediated HLA-I degradation. For the SEC61 α 1 clones, the mutations are in the cytosolic loop between transmembrane domains 6 and 7. Crystallography studies suggest that the residues deleted in our cell lines would normally interact with the ribosome⁵³, which in our cells might lead to a co-translational translocation defect due to disturbed ribosome interaction. Because SEC61 α comprises the actual translocation channel and a full translocation block may be lethal to any cell, we hypothesize that the SEC61 α 1 mutations must have a mild effect on translocation. By contrast, SEC61 β is not essential in yeast^{54,55}. In line with this, we have been able to create clonal full knockouts of SEC61 β . However, SEC61 β 's non-essential role in translocation suggests that translocation could still occur in our knock-out cells. Because SEC61 β interacts with US2, a yet-to-be-characterized US2-specific effect may take place in these cells. In contrast to SEC61 β , SEC61 γ is essential in yeast⁵⁶, and it was therefore surprising to obtain a clonal cell line with out-of-frame mutations on two alleles, potentially leading to a full knock-out phenotype. The third allele we observe for this clone may arise from aneuploidy, as we use a lymphoma cell line for these experiments. The relatively small HLA-I rescue phenotypes observed upon SEC61 γ editing resemble those of essential genes like SEC61 α 1 and p97, suggesting that SEC61 γ is indeed important for cell survival. Alternatively, SEC61 γ might simply be less important for US2 function. SEC61 γ does however directly interact with US2³², so mutating it may disturb US2 function and therefore explain the HLA-I rescue we observe. SEC62 has previously been knocked down in mammalian cells^{14,57}, suggesting that it is not an essential gene for cell survival. We now confirm this with a full knockout clone of SEC62. The 100-150 amino-terminal residues of SEC62 are required for its interaction with SEC63, through a positively charged domain in SEC62⁵⁸. As our sgRNAs target this N-terminal cytosolic domain, we speculate that even the small in-frame deletion observed in clone 1 (around Cys82) may disturb the interaction with SEC63. The SEC63 sgRNAs we use target the gene within its J-domain. This domain interacts with the ER chaperone BiP⁵⁹. The highly conserved HPD-motif within this domain however remains intact, suggesting that BiP interaction may still occur. Besides being expressed at lower levels, the edited SEC63 in these cells may be less active because of the mutations in the J-domain. Similar to SEC62, a SEC63 knockdown has previously been shown not to be lethal¹⁴.

Our data suggest that a translocation defect of US2 may underlie the rescue of HLA-I in the SEC61/62/63-edited cells, as we observed a downregulation of US2 upon mutating SEC61 subunits. This downregulation appears specific to US2, as the transmembrane transferrin receptor and also HLA-I (in US2-lacking cells) are hardly affected. The sensitivity of US2 to changes in SEC61/62/63 might be two-fold: 1) US2 is inefficiently translocated^{32,49}, making it more sensitive to changes in the translocation process, and 2) as a result of inefficient translocation (even in wildtype cells without SEC61/62/63 editing), US2 is generally expressed at relatively low levels. A further decrease in US2 levels, even when it is minor, may hamper HLA-I degradation when US2 expression falls below a critical threshold. Replacing the signal peptide of US2 by that of US11 or CD8 results in increased US2 expression levels. In cells with highly expressed US2 (or US11) variants, HLA-I degradation is retained even when SEC61/62/63 is edited. This higher protein expression may lead to an excess of US2 or US11, such that minor changes in

protein expression due to translocation defects would potentially not affect HLA-I degradation.

The inefficient translocation of the US2 signal peptide may arise from sequence-specific characteristics. Although signal peptides do not share sequence identity, there is overall homology with regard to their polarity and hydrophobicity⁶⁰. All signal sequences contain an amino-terminal n-region, a central h-region, and a carboxyterminal c-region, containing the cleavage site for removal of the signal peptide. The n- and c-regions contain charged and polar residues, whereas the h-region is hydrophobic⁶⁰. The US2 leader is less hydrophobic than most signal peptides⁴⁹, while this hydrophobicity is crucial for its association with SRP^{61–63}. The low affinity of US2 for SRP may strongly influence the efficiency of co-translational translocation. Another feature that influences translocation efficiency is the usage frequency of amino acid codons in the signal peptide. Signal peptides in general contain a high number of sub-optimal codons. A low concentration of tRNAs binding these rare codons slows down translation, allowing more time for the nascent chain to engage SRP^{64–67}, thereby improving translocation efficiency²⁰. Slowing down translation using a low dose of cycloheximide strongly increases translocation efficiency²⁰, confirming the importance of decelerating translation. Conversely, replacing all sub-optimal codons in a signal sequence by their optimal counterparts, thereby accelerating translation, can lower protein expression at least 20-fold⁶⁸. The US2 signal peptide does not contain any rare codons, which may result in the translating ribosome having an insufficient time window to engage SRP, thereby lowering the chances of successful translocation even further. In mammalian cells, SEC62/63-mediated post-translational translocation has been suggested to act as a back-up mechanism for ER delivery of proteins that fail to translocate via SRP, either because of their short length or because of suboptimal signal sequence functioning^{17,20,69}. A positive charge in the n-region positively affects post-translational translocation²⁰. While this feature is predominantly present in short secretory proteins which are known targets of this post-translational pathway, the US2 signal peptide also contains a positively charged lysine residue in this region. The low hydrophobicity, lack of sub-optimal codons and positive charge in the n-region of its signal peptide make US2 a potential substrate for post-translational translocation.

As post-translational translocation is mediated by SEC62 and SEC63, it was interesting to observe a strong HLA-I rescue phenotype upon CRISPR/Cas9-mediated editing of these genes. Although US2 is an unlikely candidate for SEC62/SEC63-mediated post-translational translocation due to its relatively large size of 199-amino acids, it would be interesting to test whether its sub-optimal signal peptide directs US2 towards post-translational translocation. A similar phenomenon has been described for the preprolactin, a model protein for SRP-mediated co-translational translocation. When the preprolactin signal peptide was mutated, such that it was translocated less efficiently, it suddenly interacted with SEC62 and SEC63¹⁷.

In vitro translation in a co-translational or post-translational translocation context could distinguish the mode of translocation for the translated substrate in an elegant manner. This was shown previously using model substrates for co-translational and post-translational translocation in the context of RNAi-targeted SEC61 α , SEC62 and SEC63¹⁴. A similar approach, in which US2 variants are translated *in vitro* in the presence of semi-permeabilized SEC61 mutant clones

as a membrane source would be very interesting in this regard. This approach allows for testing different signal peptides, or introduction of point mutations within the US2 signal peptide and the effect these have on co-translational or post-translational translocation. This way, translocation defects can be determined very specifically. This experiment is part of our future plans but could not be realized in time to be part of this thesis.

ACKNOWLEDGEMENTS

We thank Prof. Tom Rapoport and Prof. Domenico Tortorella for vital discussions about the SEC61 mutant cell lines, and Dr. Nicholas McCaul for fruitful discussions about the US2 signal peptide and help with the SignalP data. We would also like to thank the Core Facility for Flow Cytometry in the UMCU for sorting the clonal mutant cell lines. A.B.C.S. was funded by the Graduate Programme of the Nederlandse Organisatie voor Wetenschappelijk Onderzoek (Netherlands Organization for Scientific Research; NWO) (project number 022.004.018).

REFERENCES

1. Wallin, E. & Heijne, G. Von. Genome-wide analysis of integral membrane proteins from eubacterial, archaean, and eukaryotic organisms. *Protein Sci.* **7**, 1029–1038 (2008).
2. Chen, X., Karnovsky, A., Sans, M. D., Andrews, P. C. & Williams, J. A. Molecular characterization of the endoplasmic reticulum: Insights from proteomic studies. *Proteomics* **10**, 4040–4052 (2010).
3. Kalies, K. U., Stokes, V. & Hartmann, E. A single Sec61-complex functions as a protein-conducting channel. *Biochim. Biophys. Acta - Mol. Cell Res.* **1783**, 2375–2383 (2008).
4. Deshaies, R. J., Sanders, S. L., Feldheim, D. A. & Schekman, R. Assembly of yeast Sec proteins involved in translocation into the endoplasmic reticulum into a membrane-bound multisubunit complex. *Nature* **349**, 806–808 (1991).
5. Linxweiler, M., Schick, B. & Zimmermann, R. Let's talk about Secs: Sec61, Sec62 and Sec63 in signal transduction, oncology and personalized medicine. *Signal Transduct. Target. Ther.* **2**, 17002 (2017).
6. Johnson, A. E. & van Waes, M. A. The Translocon: A Dynamic Gateway at the ER Membrane. *Annu. Rev. Cell Dev. Biol.* **15**, 799–842 (1999).
7. Zimmermann, R., Eyrich, S., Ahmad, M. & Helms, V. Protein translocation across the ER membrane. *Biochim. Biophys. Acta - Biomembr.* **1808**, 912–924 (2011).
8. Rapoport, T. A. Protein translocation across the eukaryotic endoplasmic reticulum and bacterial plasma membranes. *Nature* **450**, 663–669 (2007).
9. Song, W., Raden, D., Mandon, E. C. & Gilmore, R. Role of Sec61 in the Regulated Transfer of the Ribosome–Nascent Chain Complex from the Signal Recognition Particle to the Translocation Channel. *Cell* **100**, 333–343 (2000).
10. Chirico, W. J., Waters, M. G. & Blobel, G. 70K heat shock related proteins stimulate protein translocation into microsomes. *Nature* **332**, 805–810 (1988).

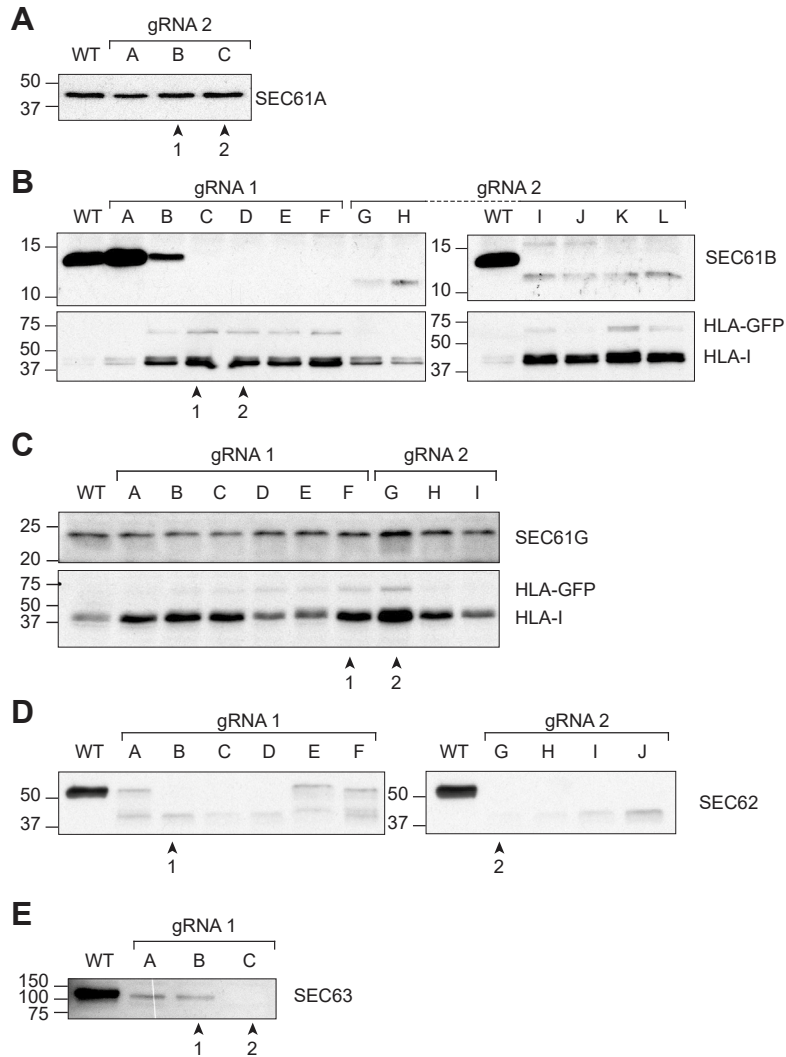
11. Ng, D. T. W., Brown, J. D. & Walter, P. Signal sequences specify the targeting route to the endoplasmic reticulum membrane. *J. Cell Biol.* **134**, 269–278 (1996).
12. Reithinger, J. H., Kim, J. E. H. & Kim, H. Sec62 Protein mediates membrane insertion and orientation of moderately hydrophobic signal anchor proteins in the endoplasmic reticulum (ER). *J. Biol. Chem.* **288**, 18058–18067 (2013).
13. Brodsky, J. L. & Schekman, R. A Sec63p-BiP complex from yeast is required for protein translocation in a reconstituted proteoliposome. *J. Cell Biol.* **123**, 1355–1363 (1993).
14. Lang, S. *et al.* Different effects of Sec61, Sec62 and Sec63 depletion on transport of polypeptides into the endoplasmic reticulum of mammalian cells. *Journal of Cell Science* **125**, 1958–1969 (2012).
15. Lyman, S. K. & Schekman, R. Interaction between BiP and Sec63p is required for the completion of protein translocation into the ER of *Saccharomyces cerevisiae*. *J. Cell Biol.* **131**, 1163–1171 (1995).
16. Jadhav, B. *et al.* Mammalian SRP receptor switches the Sec61 translocase from Sec62 to SRP-dependent translocation. *Nat. Commun.* **6**, 1–11 (2015).
17. Conti, B. J., Devaraneni, P. K., Yang, Z., David, L. L. & Skach, W. R. Cotranslational Stabilization of Sec62/63 within the ER Sec61 Translocon Is Controlled by Distinct Substrate-Driven Translocation Events. *Mol. Cell* **58**, 269–283 (2015).
18. Lakkaraju, A. K. K. *et al.* Efficient secretion of small proteins in mammalian cells relies on Sec62-dependent posttranslational translocation. *Mol. Biol. Cell* **23**, 2712–2722 (2012).
19. Johnson, N., Powis, K. & High, S. Post-translational translocation into the endoplasmic reticulum. *Biochim. Biophys. Acta - Mol. Cell Res.* **1833**, 2403–2409 (2013).
20. Guo, H. *et al.* Positive charge in the n-region of the signal peptide contributes to efficient post-translational translocation of small secretory preproteins. *J. Biol. Chem.* **293**, 1899–1907 (2018).
21. Borgese, N. & Fasana, E. Targeting pathways of C-tail-anchored proteins. *Biochim. Biophys. Acta - Biomembr.* **1808**, 937–946 (2011).
22. Plemper, R. K., Böhmeler, S., Bordallo, J., Sommer, T. & Wolf, D. H. Mutant analysis links the translocon and BiP to retrograde protein transport for ER degradation. *Nature* **388**, 891–895 (1997).
23. Plemper, R. K., Egner, R., Kuchler, K. & Wolf, D. H. Endoplasmic Reticulum Degradation of a Mutated ATP-binding Cassette Transporter Pdr5 Proceeds in a Concerted Action of Sec61 and the Proteasome Endoplasmic Reticulum Degradation of a Mutated ATP-binding Cassette Transporter P. *J Biol Chem* **273**, 32848–32856 (1998).
24. Ng, W., Sergeenko, T., Zeng, N., Brown, J. D. & Romisch, K. Characterization of the proteasome interaction with the Sec61 channel in the endoplasmic reticulum. *J. Cell Sci.* **120**, 682–691 (2007).
25. Tretter, T. *et al.* ERAD and protein import defects in a sec61 mutant lacking ER-luminal loop 7. *BMC Cell Biol.* **14**, 1–14 (2013).

26. Wheeler, M. C. & Gekakis, N. Defective ER associated degradation of a model luminal substrate in yeast carrying a mutation in the 4th ER luminal loop of Sec61p. *Biochem. Biophys. Res. Commun.* **427**, 768–773 (2012).
27. Willer, M., Forte, G. M. A. & Stirling, C. J. Sec61p is required for ERAD-L: Genetic dissection of the translocation and ERAD-L functions of Sec61P using novel derivatives of CPY. *J. Biol. Chem.* **283**, 33883–33888 (2008).
28. Römisch, K. A Case for Sec61 Channel Involvement in ERAD. *Trends Biochem. Sci.* **42**, 171–179 (2017).
29. Scott, D. C. & Schekman, R. Role of Sec61p in the ER-associated degradation of short-lived transmembrane proteins. *J. Cell Biol.* **181**, 1095–1105 (2008).
30. Schäfer, A. & Wolf, D. H. Sec61p is part of the endoplasmic reticulum-associated degradation machinery. *EMBO J.* **28**, 2874–2884 (2009).
31. Lloyd, D. J., Wheeler, M. C. & Gekakis, N. A Point Mutation in Sec61alpha1 Leads to Diabetes and Hepatosteatosis in Mice. *Diabetes* **59**, 460–470 (2010).
32. Wiertz, E. J. H. J. *et al.* Sec61-mediated transfer of a membrane protein from the endoplasmic reticulum to the proteasome for destruction. *Nature* **384**, 432–438 (1996).
33. Pilon, M., Schekman, R. & Römisch, K. Sec61p mediates export of a misfolded secretory protein from the endoplasmic reticulum to the cytosol for degradation. *EMBO J.* **16**, 4540–4548 (1997).
34. Kaiser, M. L. & Römisch, K. Proteasome 19S RP binding to the Sec61 channel plays a key role in ERAD. *PLoS One* **10**, 1–19 (2015).
35. Zehner, M. *et al.* The Translocon Protein Sec61 Mediates Antigen Transport from Endosomes in the Cytosol for Cross-Presentation to CD8+ T Cells. *Immunity* **42**, 850–863 (2015).
36. Baldrige, R. D. & Rapoport, T. A. Autoubiquitination of the Hrd1 Ligase Triggers Protein Retrotranslocation in ERAD. *Cell* **166**, 394–407 (2016).
37. Van De Weijer, M. L. *et al.* A high-coverage shRNA screen identifies TMEM129 as an E3 ligase involved in ER-associated protein degradation. *Nat. Commun.* **5**, 1–14 (2014).
38. van den Boomen, D. J. H. *et al.* TMEM129 is a Derlin-1 associated ERAD E3 ligase essential for virus-induced degradation of MHC-I. *Proc. Natl. Acad. Sci.* **111**, 11425–11430 (2014).
39. Lilley, B. N. & Ploegh, H. L. A membrane protein required for dislocation of misfolded proteins from the ER. *Nature* **429**, 834–840 (2004).
40. Cho, S., Lee, M. & Jun, Y. Forced interaction of cell surface proteins with Derlin-1 in the endoplasmic reticulum is sufficient to induce their dislocation into the cytosol for degradation. *Biochem. Biophys. Res. Commun.* **430**, 787–792 (2013).
41. Suzuki, M. *et al.* Derlin-1 and UBXD8 are engaged in dislocation and degradation of lipidated ApoB-100 at lipid droplets. *Mol. Biol. Cell* **23**, 800–810 (2012).

42. Loureiro, J. *et al.* Signal peptide peptidase is required for dislocation from the endoplasmic reticulum. *Nature* **441**, 894–897 (2006).
43. Ng, C. L., Oresic, K. & Tortorella, D. TRAM1 is involved in disposal of ER membrane degradation substrates. *Exp. Cell Res.* **316**, 2113–2122 (2010).
44. Oresic, K., Ng, C. L. & Tortorella, D. TRAM1 participates in human cytomegalovirus US2- and US11-mediated dislocation of an endoplasmic reticulum membrane glycoprotein. *J. Biol. Chem.* **284**, 5905–5914 (2009).
45. Schulze, A. *et al.* The ubiquitin-domain protein HERP forms a complex with components of the endoplasmic reticulum associated degradation pathway. *J. Mol. Biol.* **354**, 1021–1027 (2005).
46. Barel, M. T. *et al.* Human cytomegalovirus-encoded US2 differentially affects surface expression of MHC class I locus products and targets membrane-bound, but not soluble HLA-G1 for degradation. *J. Immunol.* **171**, 6757–65 (2003).
47. Stagg, H. R. *et al.* The TRC8 E3 ligase ubiquitinates MHC class I molecules before dislocation from the ER. *J. Cell Biol.* **186**, 685–692 (2009).
48. van de Weijer, M. L. *et al.* Multiple E2 ubiquitin-conjugating enzymes regulate human cytomegalovirus US2-mediated immunoreceptor downregulation. *J. Cell Sci.* **130**, 2883–2892 (2017).
49. Gewurz, B. E., Ploegh, H. L. & Tortorella, D. US2, a human cytomegalovirus-encoded type I membrane protein, contains a non-cleavable amino-terminal signal peptide. *J. Biol. Chem.* **277**, 11306–11313 (2002).
50. Kim, S. J., Mitra, D., Salerno, J. R. & Hegde, R. S. Signal sequences control gating of the protein translocation channel in a substrate-specific manner. *Dev. Cell* **2**, 207–217 (2002).
51. Cho, S., Kim, B. Y., Ahn, K. & Jun, Y. The C-Terminal Amino Acid of the MHC-I Heavy Chain Is Critical for Binding to Derlin-1 in Human Cytomegalovirus US11-Induced MHC-I Degradation. *PLoS One* **8**, 1–14 (2013).
52. Haßdenteufel, S., Klein, M., Melnyk, A. & Zimmermann, R. Protein transport into the human ER and related diseases. *Biochem. Cell Biol.* **509**, 499–509 (2014).
53. Voorhees, R. M., Fernández, I. S., Scheres, S. H. W. & Hegde, R. S. Structure of the mammalian ribosome-Sec61 complex to 3.4 Å resolution. *Cell* **157**, 1632–1643 (2014).
54. Görlich, D. & Rapoport, T. A. Protein translocation into proteoliposomes reconstituted from purified components of the endoplasmic reticulum membrane. *Cell* **75**, 615–630 (1993).
55. Finke, K. *et al.* A second trimeric complex containing homologs of the Sec61p complex functions in protein transport across the ER membrane of *S. cerevisiae*. *EMBO J.* **15**, 1482–94 (1996).
56. Falcone, D. *et al.* Stability and Function of the Sec61 Translocation Complex Depends on the Sss1 Tail-Anchor Sequence. *Biochem. J.* **436**, 291–303 (2011).

57. Greiner, M. *et al.* Silencing of the SEC62 gene inhibits migratory and invasive potential of various tumor cells. *Int. J. Cancer* **128**, 2284–2295 (2011).
58. Wittke, S., Dünwald, M. & Johnsson, N. Sec62p, a component of the endoplasmic reticulum protein translocation machinery, contains multiple binding sites for the Sec-complex. *Mol. Biol. Cell* **11**, 3859–71 (2000).
59. Misselwitz, B., Staack, O., Matlack, K. E. S. & Rapoport, T. A. Interaction of BiP with the J-domain of the Sec63p component of the endoplasmic reticulum protein translocation complex. *J. Biol. Chem.* **274**, 20110–20115 (1999).
60. von Heijne, G. Signal sequences. The limits of variation. *J. Mol. Biol.* **184**, 99–105 (1985).
61. Nilsson, I. *et al.* The code for directing proteins for translocation across ER membrane: SRP cotranslationally recognizes specific features of a signal sequence. *J. Mol. Biol.* **427**, 1191–1201 (2015).
62. Karamyshev, A. L. *et al.* Inefficient SRP interaction with a nascent chain triggers a mRNA quality control pathway. *Cell* **156**, 146–157 (2014).
63. Zheng, T. & Nicchitta, C. V. Structural determinants for signal sequence function in the mammalian endoplasmic reticulum. *J Biol Chem* **274**, 36623–36630 (1999).
64. Zalucki, Y. M., Beacham, I. R. & Jennings, M. P. Biased codon usage in signal peptides: a role in protein export. *Trends Microbiol.* **17**, 146–150 (2009).
65. Wang, Y., Mao, Y., Xu, X., Tao, S. & Chen, H. Codon Usage in Signal Sequences Affects Protein Expression and Secretion Using Baculovirus/Insect Cell Expression System. *PLoS One* **10**, 1–15 (2015).
66. Yu, C. *et al.* HHS Public Access. **59**, 744–754 (2016).
67. Pechmann, S., Chartron, J. W. & Frydman, J. Local slowdown of translation by nonoptimal codons promotes nascent-chain recognition by SRP in vivo. *Nat. Struct. Mol. Biol.* **21**, 1100–1105 (2014).
68. Zalucki, Y. M., Jones, C. E., Ng, P. S. K., Schulz, B. L. & Jennings, M. P. Signal sequence non-optimal codons are required for the correct folding of mature maltose binding protein. *Biochim. Biophys. Acta - Biomembr.* **1798**, 1244–1249 (2010).
69. Kriegler, T., Magoulopoulou, A., Amate Marchal, R. & Hessa, T. Measuring Endoplasmic Reticulum Signal Sequences Translocation Efficiency Using the Xbp1 Arrest Peptide. *Cell Chem. Biol.* **25**, 880–890.e3 (2018).
70. Kane, J. F. Effects of rare codon clusters on high-level expression of heterologous proteins in Escherichia coli. *Curr. Opin. Biotechnol.* **6**, 494–500 (1995).

SUPPLEMENTARY INFORMATION



Supplementary figure 1 | Protein expression of the targeted SEC61/62/63 subunits in clonal mutant cell lines. Immunoblotting was performed for all clonal mutant cell lines generated. Two clones were selected for each target gene, based on non-detectable protein levels in Western blot, the level of HLA-I rescue, or sequencing of the sgRNA target sites in the genomic DNA (table S1). Selected clones are indicated by '1' and '2'. Panel A) shows clonal SEC61 α 1-targeted cells; panel B) those for SEC61 β ; C) SEC61 γ ; D) SEC62; E) SEC63.

gene	gRNA	allele	target sequence incl. PAM	indels
SEC61A1		WT	CTGCCAATCAAGTCGGCCCGTACCCTGGCCAGTA...TGTCCAACCTTTATGTCATCT	
		1	CTGCCAATCAAGTCGGCCCG-----TGGCCAGTA...TGTCCAACCTTTATGTCATCT	-6
cl.1	2	2	CTGCCAATCAAGTCGGCCCG-----TGGCCAGTA...TGTCCAACCTTTATGTCATCT	-90
SEC61A1		WT	CTGCCAATCAAGTCGGCCCGTACCCTGGCCAGTACAACACCTATCCCATCAAGCTCTT	
		1	CTGCCAATCAAGTCGGCCCG-----TGGCCAGTACAACACCTATCCCATCAAGCTCTT	-6
cl.2	2	2	CTGCCAATCAAGTCGGCCCG-----TGGCCAGTACAACACCTATCCCATCAAGCTCTT	-12
SEC61B		WT	TCTAGTGGCCCTGTTCAGTATGGTTATGAGTC...TGAGGAATCAGTTTTTTCTAT	
		1	TCTAGTGGCC-----TGGTTATGAGTC...TGAGGAATCAGTTTTTTCTAT	-11
cl.1	1	2	TCTAGTGGCCCTGTTCAGTATGGTTATGAGTC...TGAGGAATCAGTTTTTTCTAT	-232*
SEC61B		WT	TATTTCTAGTGGCCCTGTTCAG-----TATGGTTATGA...CAGTTTTTTTC	
		1	TATTTCTAGTGGCCCTGTTCAGGGGTTATGGTTATGGTTATGA...CAGTTTTTTTC	+10
cl.2	1	2	TATTTCTAGTGGCCCTGTTCAG-----TATGGTTATGA...CAGTTTTTTTC	-226#
SEC61G		WT	ATCTTTTAAACAAGCCGAATGGAGTCCCTTACAAACTGCCGACTGGCTCAACAAACTGC	
		1	ATCTTTTAAACCAGCCGA-----CTGGCTCAACAAACTGC	-24
cl.1	1	2	ATCTTTTAAACCAGCC-A-----AAACTGCCGACTGGCTCAACAAACTGC	-15
SEC61G		WT	TTCTATCAGGTTTAGTGCATCTTTTAAACCAGCC--GAATGGAGTCCCTTTACAAACTGCCG	
		1	TTCTATCAGGTTTAGTGCATCTTTTAAACCAGC--GAATGGAGTCCCTTTACAAACTGCCG	-1
		2	TTCTATCAGGTTTAGTGCATCTTTTAAACCAGCCGAATGGAGTCCCTTTACAAACTGCCG	+1
cl.2	2	3	TTCTATCAGGTTTAGTGCATCTTTTAA--A-----AAAGGAGTCCCTTTACAAACTGCCG	-6
SEC62		WT	AACCAGGGAGTCTGTGGTTGACTACTGC-----AA---...CAGGTACTGTTT	
		1	AACCAGGGAGTCTGTGGTTGACTACTGGTTGAATAA---...CAGGTACTGTTT	+8
cl.1	1	2	AACCAGGGAGTCTGTGGTTGACTACTGC-----AAATAA...AAGCAGGTACTGTTT	+27§
SEC62		WT	AAGCTTTATTTACAACAAGGAGTCTGTGGTTGACTACTGCAACAGGTACTGTTTATTT	
		1	AAGCTTTATTTACAACC-----AGTCTGTGGTTGACTACTGCAACAGGTACTGTTTATTT	-4
cl.2	2	2	AAGCTTTATTTACAACCAGG--GTCTGTGGTTGACTACTGCAACAGGTACTGTTTATTT	-2
SEC63		WT	GCATAAGCTTTTGCTATCCTCATGAACATAAACCCTATCACCTCTTTATCTGGATGATAT	
		1	GCATAAGCTTTTGG--AT-----AT-----CCTCATCACCTCTTTATCTGGATGATAT	-14
cl.1	1	2	GCATAAGCTTTTGCTATCCTCAT-----AACCTCATCACCTCTTTATCTGGATGATAT	-6
SEC63		WT	GCTATCCTCATG-----...-----AACATAACCTCATCACCTCCTTT	
		1	GCTATCCTCATG-----...-----CACCTCCTTT	-13
cl.2	1	2	GCTATCCTCATAACTAACCTC...CCTATCCTCATAACATAACCTCATCACCTCCTTT	+57 [§]

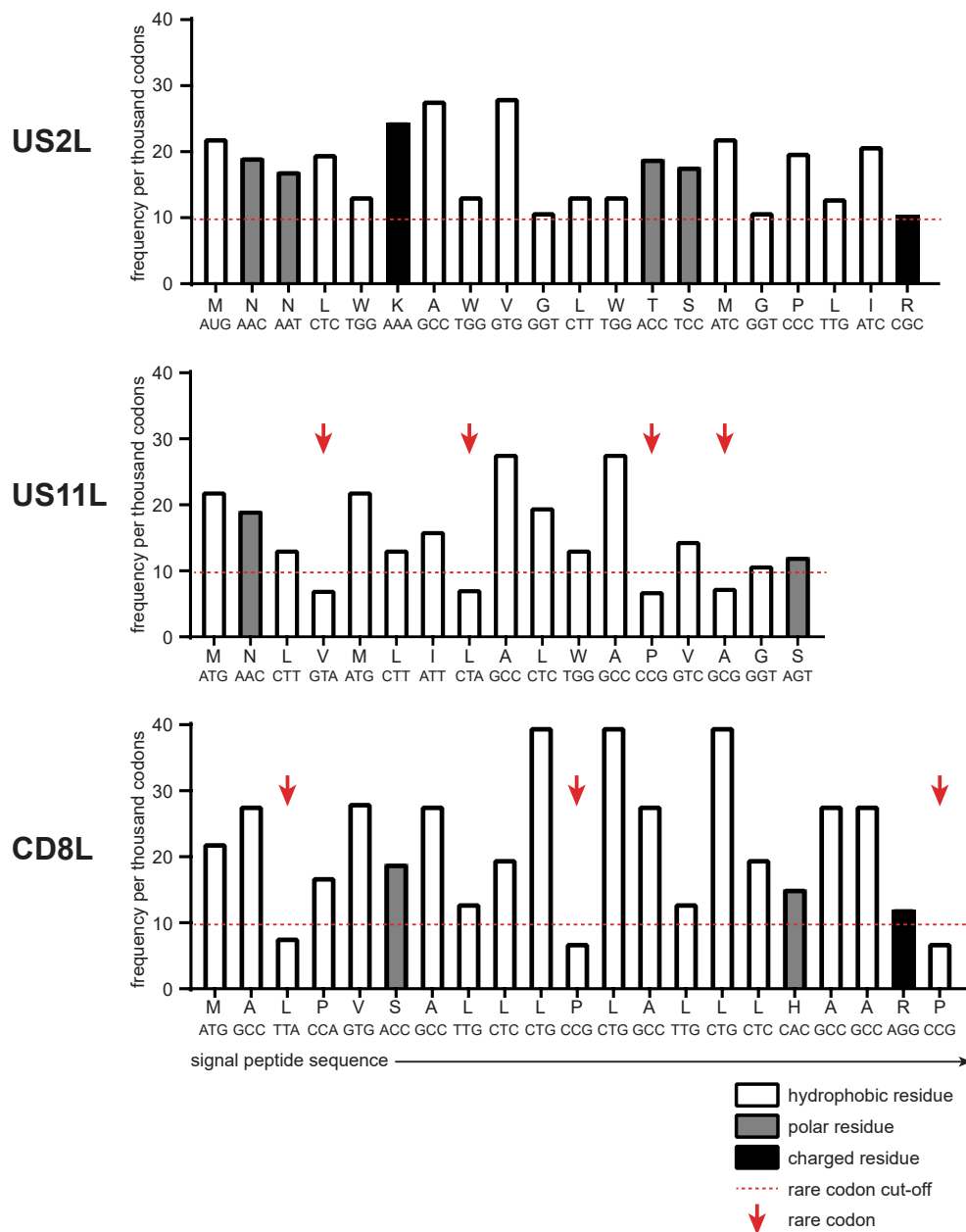
* -78 in coding sequence; rest in 3' UTR

-74 in coding sequence; rest in 3' UTR

§ rest of insertion = TAATAAATAATAATAAATAA

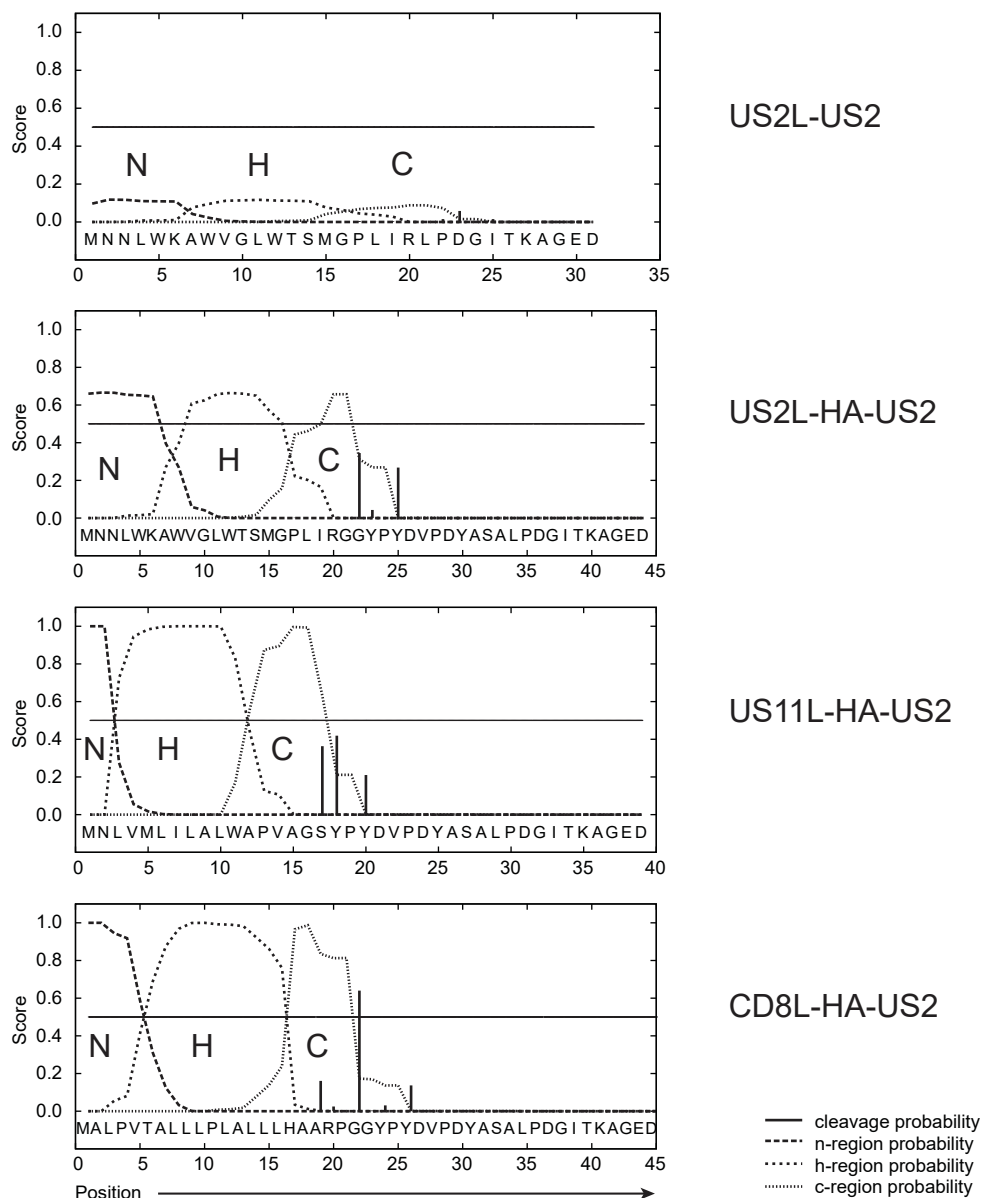
§ rest of insertion = ATAAGGATAGCTTTTGTATCCTCATAACCTTATAA

Supplementary table 1 | Sequence analysis of clonal mutant SEC61/62/63 cell lines. From all SEC61/62/63 mutant clones, genomic DNA was isolated and the sgRNA-target site was amplified by PCR. Editing of sgRNA target sites was analyzed by standard Sanger DNA sequencing. Only the two selected clones per target gene are shown. SEC61β was edited at the 3' end of the gene, resulting in a deletion of the C-terminus. A large part of this deletion was in the DNA encoding the 3' UTR, and did therefore not impact the protein directly. The large insertions observed in SEC62 clone 1 and SEC63 clone 2 are shown only partially. The remaining part of these insertions are listed below the table.



Supplementary figure 2 | Amino acid and codon properties of the US2-, US11- and CD8 signal peptide.

Signal peptide properties of the US2-, US11-, and CD8 leader respectively. On the X-axis, the amino acids and corresponding codons of the signal peptides are shown. The residues are color-coded in the bar graph to show their characteristics with regards to hydrophobicity, polarity or charge. As multiple codons exist for most amino acids, the height of the bars indicates the frequency at which these codons are used (per 1000 codons). These frequencies were derived from <https://www.biologicscorp.com/tools/CodonUsage>. A cut-off was set at 1% (10 out of 1000 codons), below which the codons are indicated as rare⁷⁰.



Supplementary figure 3 | The US2 signal peptide has weak signal peptide characteristics. The N-terminal portions of wildtype US2 or the HA-tagged US2 versions were analyzed using the hidden Markov model (HMM) in SignalP prediction software. This model calculated the probability of the submitted sequence being a signal peptide, including the n-, h-, and c-regions and the predicted cleavage site. For wildtype US2, the signal peptide and part of the protein are shown. For the HA-tagged variants, the signal peptide, HA-tag and the same n-terminal part of the US2 protein are shown. The US2 signal peptide has a low score in this prediction model, suggesting that it bears few of the characteristics of a signal peptide. The HA-tag downstream of the US2 leader may affect signal sequence cleavage, but it is unclear how this impacts the overall HMM score of the signal peptide.



An aerial photograph of a dry, hilly landscape with terraced fields. The fields are arranged in concentric, curved patterns, and the soil is a light brown color. The background shows a hazy, distant horizon.

CHAPTER

6

P97 association with
UBXD8 is essential for
HCMV US11-mediated HLA
class I degradation

Michael L. van de Weijer^{1,2,#}, Anouk B.C. Schuren^{1,#},
Ingrid G.J. Boer¹, Robert Jan Lebbink^{1,*†}, and
Emmanuel J.H.J. Wiertz^{1,*†}

^{#,†} These authors contributed equally

1 Dept. Medical Microbiology, University Medical Center Utrecht, 3584CX Utrecht, The Netherlands.

2 Current address: Cambridge Institute for Medical Research, University of Cambridge, Cambridge

CB2 0XY, UK. *Correspondence: E.Wiertz@umcutrecht.nl (E.J.H.J.W.); R.J.Lebbink-2@umcutrecht.nl (R.J.L.).

submitted

ABSTRACT

Misfolded ER proteins are dislocated to the cytosol and degraded by the ubiquitin–proteasome system in a process called ER-associated protein degradation (ERAD). During infection with human cytomegalovirus, the viral protein US11 efficiently downregulates HLA class I molecules (HLA-I) via ERAD to avoid recognition of infected cells by the immune system. Using US11-mediated HLA-I degradation as a model, p97 was previously identified as a factor critical for ERAD, although the mode of p97 recruitment remains elusive. In this study, we identified the p97 co-factor UBXD8 to be essential for HLA-I degradation. We show that the UBXD8 UBA domain is dispensable for HLA-I degradation, whereas deletion of the UBX domain abrogates p97 recruitment to the dislocation complex and impairs HLA-I degradation. Being part of the US11 dislocation complex, UBXD8 interacts with Derlin-1 and TMEM129 in the absence or presence of US11. Our results suggest that UBXD8 is an essential component of dislocation complexes, and may mediate the recruitment of p97.

INTRODUCTION

Newly synthesized secretory or transmembrane proteins are translocated into the ER, where they undergo quality control by ER chaperones to ensure that they are properly folded. Accumulation of misfolded proteins causes cell damage and should therefore be prevented. Proteins that fail ER quality control are retrogradely transported towards the cytosol for proteasomal degradation, a process called ER-associated protein degradation (ERAD) (Brodsky 2012; Olzmann et al. 2013; Wu & Rapoport 2018). Multiprotein complexes at or near the ER membrane facilitate the steps required for ERAD: substrate recognition, retro-translocation, ubiquitination, and degradation (Olzmann et al. 2013; Christianson et al. 2011).

Manipulation of cellular pathways by viral proteins can be used to gain insight into cellular mechanisms, including ERAD. Human cytomegalovirus (HCMV) is a β -herpesvirus and is the most common infectious cause of congenital defects (Griffiths et al. 2015). Co-evolution between the family of herpesviruses and their hosts has resulted in extensive evasion mechanisms to escape their host's immune system. HCMV expresses two proteins, US2 and US11, that induce accelerated ERAD of HLA class I molecules (HLA-I) (Wiertz, Tortorella, et al. 1996; Wiertz, Jones, et al. 1996; Hsu et al. 2015). As HLA-I presents antigenic peptides to cytotoxic CD8⁺ T lymphocytes, targeting this molecule for degradation is an effective viral mechanism to prevent recognition by the immune system (Schuren et al. 2016; van de Weijer et al. 2015). US2- and US11-mediated degradation of HLA-I is rapid and efficient. These protein degradation pathways are therefore commonly used as a model to study ERAD (Wiertz, Tortorella, et al. 1996; Wiertz, Jones, et al. 1996).

The ER-resident HCMV glycoproteins US2 and US11 bind newly synthesized HLA-I heavy chains and cause their degradation within minutes (Wiertz, Jones, et al. 1996; Wiertz, Tortorella, et al. 1996). Although US2 and US11 both target HLA-I for ERAD, they employ distinct protein complexes. US2 co-opts the ubiquitin ligase TRC8 (Stagg et al. 2009) and the E2 enzyme UBE2G2 (van de Weijer et al. 2017), whereas US11 relies on the E3 enzyme TMEM129 (Van De Weijer et al. 2014; van den Boomen et al. 2014), in conjunction with the ubiquitin-conjugating enzymes UBE2J2 (Van De Weijer et al. 2014) and UBE2JK (Flierman et al. 2006).

Derlin-1 is essential for HLA-I degradation by US11, but not US2 (Lilley & Ploegh 2004). On the cytosolic side, both US2 and US11 require the AAA-ATPase p97 (also known as VCP) to provide the driving force for HLA-I extraction from the ER membrane (Soetandyo & Ye 2010). p97 is a ubiquitin-selective ATPase that is involved in proteasomal degradation of protein quality control substrates as well as a large class of ubiquitin-controlled proteins such as transcription factors, cell cycle regulators, and DNA damage repair proteins (Ye et al. 2001; Buchberger et al. 2015). The protein contains an N-terminal (N) domain, two ATPase domains called D1 and D2, and an unstructured carboxy-terminal extension. The ATPase domains form a stacked homo-hexameric ring with a central pore. It is believed that p97 extracts polyubiquitinated substrates from the ER membrane through this pore (N. Bodnar & Rapoport 2017). The energy for this reaction is provided by ATP hydrolysis in the D2 ATPase domains, while the D1 domains are required for initial substrate unfolding and its eventual release (N. O. Bodnar & Rapoport 2017). p97 itself contains little substrate specificity, but instead relies on a large number of co-factors that control p97 recruitment to specific ubiquitinated target proteins (Buchberger et al. 2015).

Among the co-factors for p97 are several ERAD-related proteins, such as ubiquitin ligases (Ye et al. 2005), Derlins (Ye et al. 2004; Greenblatt et al. 2011), and dedicated p97 co-factors (Buchberger et al. 2015). Various p97-interacting domains have been described, including the VCP-interacting motif (VIM), which is found in VIMP and in the ERAD ubiquitin ligase gp78. The ubiquitin ligase HRD1 contains a VCP-binding motif (VBM). Derlins, which are also present in ERAD complexes at the ER membrane, contain an SHP box that potentially interacts with the N-domain of p97. The UBX proteins comprise the largest group of p97 co-factors. All members of the UBX family, with the exception of UBXD1, can interact with p97 by means of their UBX (ubiquitin regulatory X) domain (Buchberger et al. 2015).

Despite the evident contribution of p97 to US11-mediated HLA-I degradation (Ye et al. 2001), the mechanism of p97 recruitment remains unknown. Multiple potential p97-recruiting factors, such as Derlin-1, VIMP and UBXD8, are part of the US11 ERAD complex (Van De Weijer et al. 2014; Ye et al. 2004; Lilley & Ploegh 2005; Mueller et al. 2008). Also the recently discovered E3 enzyme TMEM129 interacts with p97 (Van De Weijer et al. 2014; van den Boomen et al. 2014), suggesting that it could recruit this ATPase, similar to other ubiquitin ligases such as gp78 and HRD1.

Here, we constructed a lentiviral CRISPR/Cas9-based library targeting known human p97 co-factors and used this resource to screen for p97 co-factors essential for US11-mediated HLA-I downregulation. We identified UBXD8 (also known as ETEA or FAF2) as an essential p97 co-factor for degradation of HLA-I by US11. UBXD8 depletion rescues HLA class I from US11-mediated degradation and retains HLA class I in the US11/Derlin-1/TMEM129 complex. In the absence of US11, UBXD8 is also present in a complex with Derlin-1 and TMEM129. The p97-interacting UBX domain of UBXD8 is essential for US11-mediated HLA-I downregulation, whereas the UBA domain is dispensable, suggesting that the p97-recruiting capacity of UBXD8 is essential for HLA class I degradation by US11.

MATERIALS AND METHODS

Cell culture

U937 human monocytic cells and 293T human embryonic kidney cells were obtained from ATCC (American Type Culture Collection, Manassas, VA, USA) and grown in RPMI medium (Lonza, Breda, The Netherlands) supplemented with glutamine (Gibco, Dublin, Ireland), penicillin/streptomycin (Gibco) and 10% fetal bovine serum (Biowest, Nuaille, France). In the experiments indicated, cells were incubated with 1-3 μM of the p97 inhibitor CB-5083 (Cayman Chemical, Ann Arbor, MI, USA).

Lentiviral transduction

For individual transductions using lentiviruses, virus was produced in 293T cells in 24-well plates using standard lentiviral production protocols and third-generation packaging vectors. The supernatant containing virus was harvested 3 days post transfection and stored at -80°C . For lentiviral transductions, 50 μl supernatant containing virus supplemented with 8 $\mu\text{g}/\text{mL}$ polybrene (Santa Cruz Biotechnology, Heidelberg, Germany) was used to infect approximately 20,000 U937 cells by spin infection at 1,000 g for 2 h at 33°C . Complete medium was added after centrifugation to reduce polybrene concentration. Three days post-infection the cells were subjected to antibiotics to select the successfully transduced cells.

Generation of clonal CRISPR/Cas9-mediated knockout cells

U937 cells stably co-expressing eGFP-Myc-HLA-A2 and HA-US11 or 3xST2-HA-US11 were transduced with a lentiviral CRISPR/Cas9 system, in which a single lentiviral vector co-expresses a Cas9, puromycin and a single guide RNA (sgRNA) sequence (Van De Weijer et al. 2014). Two days post infection (d.p.i.), transduced cells were selected by using 2 $\mu\text{g}/\text{mL}$ puromycin and allowed to recover. Cells were single-cell sorted by fluorescence-activated cell sorting (FACS Aria II, BD Biosciences, Vianen, The Netherlands). The knockout status of the clonal cell lines was confirmed by flow cytometry and immunoblotting. For the generation of double knock-out cells, the sgRNAs listed in Supplementary Information 1 were expressed from a U6 promoter on a vector also containing a neomycin resistance cassette for antibiotic selection.

Antibodies

Primary antibodies used in our studies were: mouse α -HLA class I HC HCA2 mAb; mouse α -TfR H68.4 mAb (no. 13-68xx, Invitrogen, Landsmeer, The Netherlands); mouse α -FLAG-M2 mAb (no. F1804, Sigma-Aldrich, Zwijndrecht, The Netherlands); rat α -HA 3F10 mAb (no. 11867423001, Roche, Woerden, The Netherlands); rabbit α -ETEA/UBXD8 (D8H6D) mAb (no. 34945S, Cell Signaling Technology, Leiden, The Netherlands); mouse α -TMEM129 8D7 mAb (E. Kremmer, Helmholtz Zentrum München, Germany); rabbit α -Derlin-1 pAb (no. PM018, MBL, Woburn, MA, USA); mouse α -VCP/p97 18/VCP mAb (no. 612183, BD Transduction laboratories); rabbit α -VIMP (D1D1M) mAb (no. 15160, Cell Signaling Technology).

Secondary antibodies used in our studies were: goat α -mouse IgG(H+L)-HRP (no. 170-6516, Bio-Rad, Veenendaal, The Netherlands); goat α -rabbit IgG(H+L)-HRP (no. 4030-05, Southern

Biotech, Birmingham, AL, USA); mouse α -rabbit IgG(L)-HRP (no. 211-032-171, Jackson Immunoresearch, Ely, UK); goat α -mouse IgG(L)-HRP (no. 115-035-174, Jackson Immunoresearch); goat α -rat IgG(L)-HRP (no. 112-035-175, Jackson Immunoresearch).

Plasmids and cDNAs

Several different lentiviral vectors were used in the present studies. The N-terminally eGFP and Myc-tagged human HLA-A2 vector present in the lentiviral pHRSincPPT-SGW vector was kindly provided by Dr Paul Lehner and Dr Louise Boyle (University of Cambridge, Cambridge, UK). HCMV US11 was N-terminally tagged with either an HA-tag only, or three Strep(II) tags followed by an HA-tag. The original leader was replaced by the hCD8 leader sequence in the tagged US11 constructs. US11 and tagged variants were expressed from a dual promoter lentiviral vector, which also included expression of BlastR-T2A-mAmetrine via the hPGK promoter. For rescue and ectopic expression experiments, sgRNA-resistant N-terminally FLAG-tagged UBXD8 was generated and cloned into a dual promoter lentiviral vector, which also included expression of ZeoR-T2A-mAmetrine via the hPGK promoter (BIC-PGK-Zeo-T2a-mAmetrine) (Van De Weijer et al. 2014). UBXD8 deletion mutants UBXD8 Δ UBA and UBXD8 Δ UBX were generated by respectively deleting amino acids 12–48 and 357–439. UBXD8 and mutants were N-terminally tagged with either a FLAG tag or a Strep(II)-tag followed by a FLAG tag. Derlin-1 Δ SHP was generated by deleting the last 11 amino acids. sgRNA-resistant Derlin-1 and Derlin-1 Δ SHP were cloned into the BIC-PGK-Zeo-T2a-mAmetrine vector.

Generation of CRISPR/Cas9-based screen targeting known p97 co-factors

A lentiviral CRISPR/Cas9 vector carrying a puromycin resistance cassette was used to facilitate efficient and selectable expression of a nuclear-localized Cas9 gene that was N-terminally fused to a puromycin resistance cassette using a T2A sequence, and a sgRNA regulated by a U6 promoter, as described previously (Van De Weijer et al. 2014). The region immediately downstream of the U6 promoter contains a cassette with a BsmBI restriction site on each side to allow cloning of sgRNA target sites followed by the sgRNA scaffold and a terminator consisting of 5 T-residues. sgRNAs targeting all known human E2s were designed using an online CRISPR Design Tool (<http://crispr.mit.edu/>). sgRNA sequences are listed in Supplementary Information S1.

Flow cytometry

Cells were washed in FACS buffer (PBS containing 0.5% BSA and 0.02% sodium azide). Total eGFP-Myc-HLA-A2 expression was analyzed by assessment of the eGFP signal via flow cytometry acquisition on a FACSCanto II (BD Bioscience). Flow cytometry data were analyzed using FlowJo software.

Immunoblotting

Cells were lysed in 1% Triton X-100 lysis buffer (1.0% Triton X-100, 100 mM NaCl, 50 mM Tris, pH 7.5) containing 1 mM Pefabloc SC (11429876001, Roche) and 10 μ M Leupeptin (Roche). Nuclei and cell debris were pelleted at 12,000g for 20 min at 4 °C. Post-nuclear lysates were denatured in Laemmli sample buffer, heated to 70 °C for 10 minutes and then frozen at

-80 °C. Proteins were separated by SDS-PAGE and transferred to either PVDF membranes (Immobilon-P, Millipore) or the Biorad Transblot Turbo system. Membranes were probed with indicated antibodies. Reactive bands were detected by ECL (Thermo Scientific Pierce), and exposed to Amersham Hyperfilm ECL films (GE Healthcare, Eindhoven, The Netherlands).

Co-immunoprecipitations

Cells were lysed in either Digitonin or LMNG lysis buffer (50 mM Tris-HCl, 5 mM MgCl₂, 150 mM NaCl; pH 7.5, supplemented with either 1% Digitonin (Calbiochem, San Diego, CA, USA), or 1% LMNG (NG310, Anatrace, Maumee, OH, USA) containing 1 mM Pefabloc SC (Roche) and 10 μM Leupeptin (Roche). Lysates were incubated for 90 min at 4 °C. Nuclei and cell debris were pelleted 12,000g for 20 min at 4 °C. Post-nuclear supernatants were incubated overnight with StrepTactin beads (GE Healthcare). After four washes in 0.1% digitonin lysis buffer, proteins were eluted in elution buffer (2.5 mM desthiobiotin, 150 mM NaCl, 100 mM Tris-HCl, 1 mM EDTA, pH 8) for 30 min on ice. The eluate was separated from the beads using 0.45 μm Spin-X filter column (Corning Costar, Corning, NY, USA), and subsequently denatured in Laemmli sample buffer containing DTT. Immunoblotting was performed as described above.

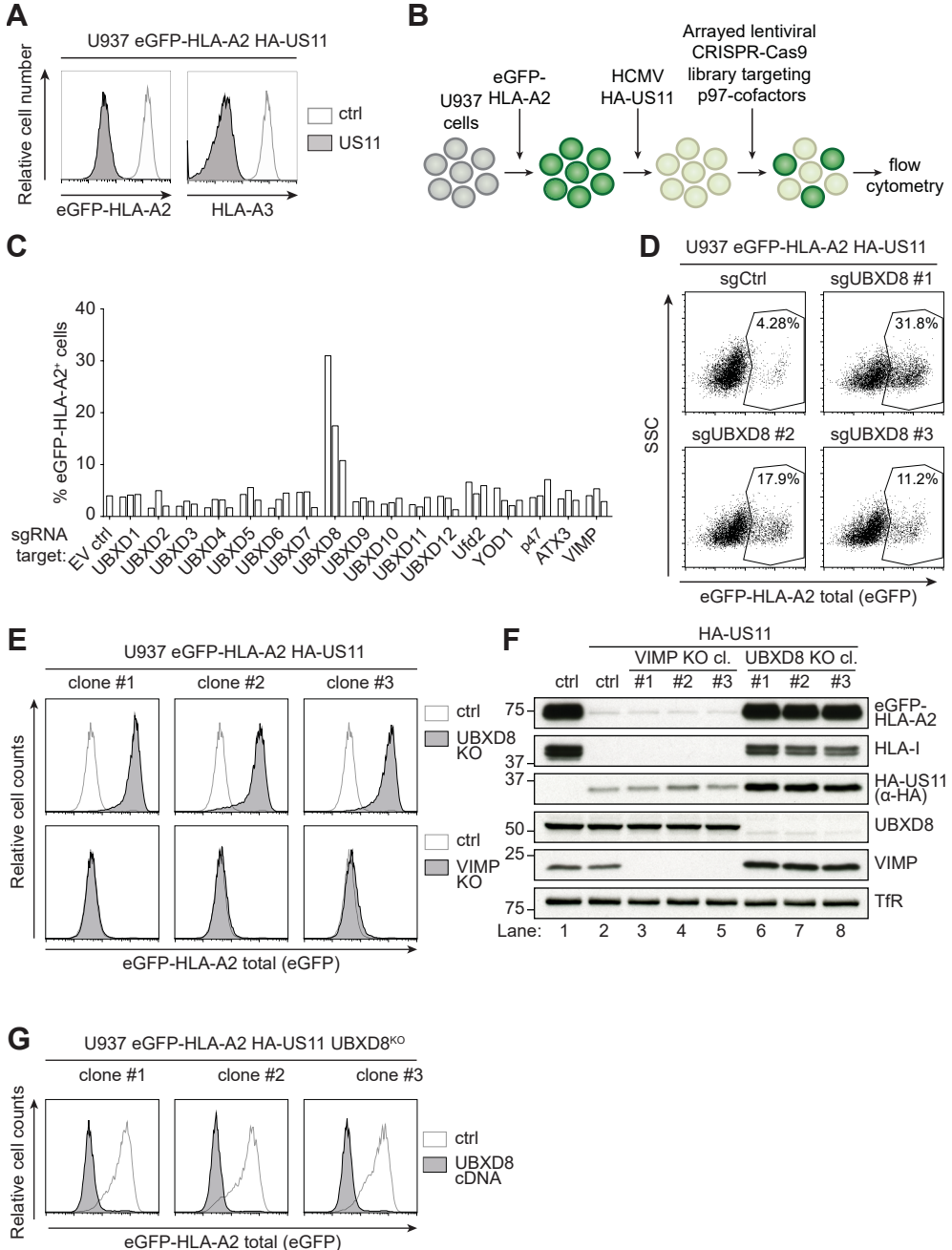
RESULTS

A CRISPR/Cas9 library screen identifies UBXD8 as an essential player in US11-mediated HLA-I downregulation

To identify p97 co-factors required for US11-mediated degradation of HLA-I molecules, we constructed an arrayed lentiviral CRISPR/Cas9-based library targeting 17 known p97 co-factors using approximately three single guideRNAs (sgRNAs) per gene (Supplementary Information S1). U937 monocytic cells stably expressing an HLA-A2 molecule with an N-terminal eGFP tag were generated to allow monitoring of total HLA-I expression levels by flow cytometry.

Figure 1 | UBXD8 is essential for US11-mediated HLA class I downregulation. A) Downregulation of eGFP-HLA-A2 and endogenous HLA-A3 by HA-US11 in U937 cells stably transduced with eGFP-HLA-A2. eGFP levels and cell surface HLA-A3 expression were assessed by flow cytometry. B) Schematic overview of the lentiviral CRISPR/Cas9-based screen for p97 cofactors that regulate US11-mediated MHC-I downregulation. U937 cells were transduced with a chimeric eGFP-HLA-A2 molecule and subsequently transduced with an HCMV US11-expression vector. As a result, cells displayed low total eGFP-HLA-A2 expression levels as assessed by quantification of the eGFP signal. Cells were subsequently transduced with lentiviral CRISPR/Cas9 constructs targeting individual p97 cofactors. Two days after infection, cells were selected using puromycin and the percentage of eGFP-positive (eGFP-HLA-A2 rescued cells) was assessed by flow cytometry at 15 days post-infection (d.p.i.). C) Quantification of the percentage of eGFP-HLA-A2-positive cells after transduction with CRISPR/Cas9 constructs targeting individual p97 co-factors (see also Supplementary Information S1). The empty vector (EV) was used as negative control. D) CRISPR/Cas9-mediated knockout of UBXD8 using three distinct sgRNAs induces rescue of eGFP-HLA-A2 in US11-expressing cells. eGFP-HLA-A2 levels were assessed by flow cytometry 15 d p.i.. Percentages of eGFP-HLA-A2-positive cells are indicated. Side scatter (SSC) is plotted on the Y-axis. E. Three independent knockout clones of either UBXD8 (top panels) or VIMP (lower panels) were established, after which flow cytometric analysis was performed to assess eGFP-HLA-A2 levels. F) Triton X-100 cell lysates of the knockout cells in E) were prepared and subjected to immunoblot analysis to assess expression levels of the indicated proteins. In lane 1, control cells lacking US11 are shown. Lane 2 shows US11-expressing cells lentivirally transduced with an empty vector control. Transferrin receptor (TfR) was used as loading control. G) To validate the involvement of UBXD8 in US11-induced HLA-I degradation, UBXD8 was reintroduced into the UBXD8 knockout clones used in (E), after which flow cytometric analysis was performed to assess eGFP-HLA-A2 levels.

Upon stable introduction of HCMV US11, the chimeric HLA-I molecule as well as endogenous HLA-A3 were degraded efficiently (Fig. 1A). These cells were then transduced with the lentiviral CRISPR/Cas9 library. Disruption of an essential p97 co-factor would result in rescue of the chimeric eGFP-HLA-A2 molecule from degradation, thereby increasing eGFP levels in the



cell that can be assessed by flow cytometry (Fig. 1B). Of all sgRNAs tested, only anti-UBXD8 sgRNAs induced rescue of eGFP-HLA-A2 in US11-expressing cells (Fig. 1C and D).

We established three clonal UBXD8 knockout lines, which all displayed increased eGFP-HLA-A2 levels (Fig. 1E, upper panels). In contrast, US11-mediated HLA-I downregulation was not affected in clonal VIMP knockout cells (Fig. 1E, lower panels). Western blot analysis of UBXD8 clonal cell lines showed that both eGFP-HLA-A2 and endogenous HLA-I expression levels were strongly upregulated (Fig. 1F). Additionally, US11 levels were increased in UBXD8-null cells, an effect often observed upon knockout of genes essential for US11 functioning. The increased US11 levels may have been caused by stabilization of dislocation complexes in the absence of UBXD8. To validate the involvement of UBXD8 in US11-mediated HLA-I degradation, we rescued UBXD8 expression in the clonal UBXD8 knockout cells by means of a sgRNA-resistant UBXD8 cDNA. This resulted in restoration of US11-mediated HLA-I downregulation (Fig. 1G). Our results show that UBXD8 is essential for US11-mediated HLA-I degradation.

UBXD8 is located in a complex with US11, Derlin-1, and TMEM129

To assess whether UBXD8 is present in the US11 dislocation complex, we generated N-terminally Strep(II)- and HA-tagged US11 molecules (ST2-HA-US11) and used these in co-immunoprecipitation experiments. Upon pull-down of ST2-HA-US11, we co-isolated UBXD8, Derlin-1, and TMEM129 (Fig. 2A, lane 4). To test whether UBXD8 is part of dislocation complexes centered around the E3 enzyme TMEM129 (Van De Weijer et al. 2014), TMEM129 complexes were isolated from cells by TMEM129-FLAG-ST2 pulldown experiments. We observed that both UBXD8 and Derlin-1 were co-precipitated with TMEM129-FLAG-ST2 in either the absence or presence of US11 (Fig. 2B, lane 6 and 8 respectively). US11 (lane 8) was also part of this complex. These data show that UBXD8 can associate with Derlin-1- and TMEM129-containing dislocation complexes in an US11-independent manner.

The UBX domain of UBXD8 is essential for HCMV US11-mediated HLA-I degradation

Next, we investigated which domains of UBXD8 are essential for US11-mediated HLA-I degradation. UBXD8 is inserted into the outer leaflet of the ER lipid bilayer via a hydrophobic patch (HP), thereby exposing both the N- and C-terminus of the protein to the cytosol (Lee et al. 2010; Schrul & Kopito 2016). The N-terminal part of UBXD8 contains a UBA domain, responsible for the interaction with poly-ubiquitinated proteins, whereas the C-terminal part contains a UBX domain, facilitating interaction with p97 and cofactors (Buchberger 2002). To investigate the requirement of the UBA and UBX domain in US11-mediated HLA-I degradation, we generated UBA- and UBX-deletion mutants of UBXD8 (Fig. 3A). These deletion mutants were introduced into clonal US11-expressing UBXD8 knockout cells and the eGFP-HLA-A2 expression levels were subsequently assessed by flow cytometry (Fig. 3B). Introduction of full-length (FL) UBXD8 reverted the knockout phenotype, resulting in restored HLA-I degradation. The UBA-deletion mutant (Δ UBA) restored HLA-I degradation by US11 comparable to full length (FL) UBXD8, whereas introduction of the UBX-deletion mutant (Δ UBX) did not. Thus, the UBA domain of UBXD8 is dispensable for US11-mediated HLA-I degradation, whereas the

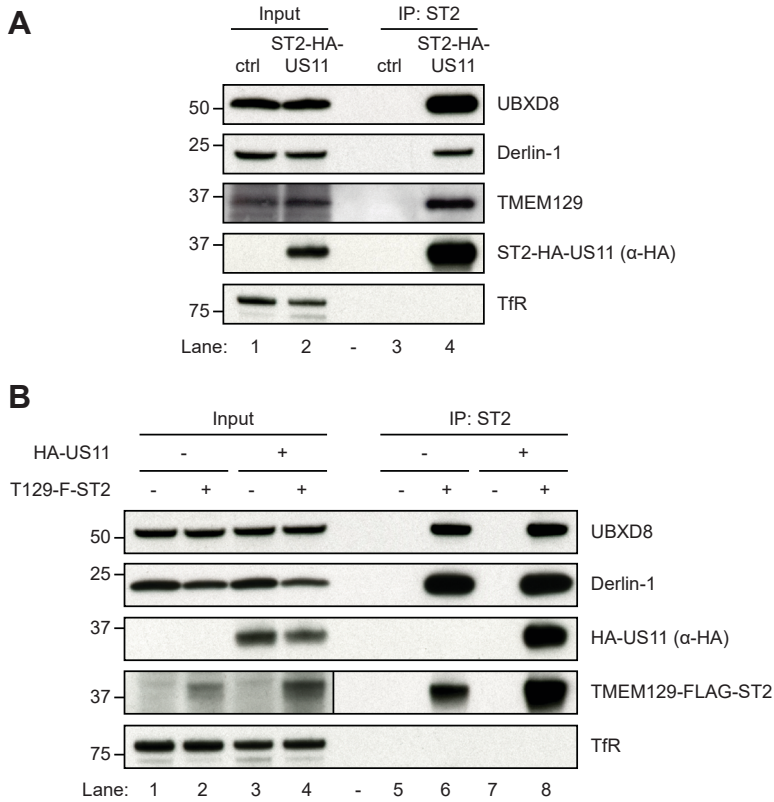


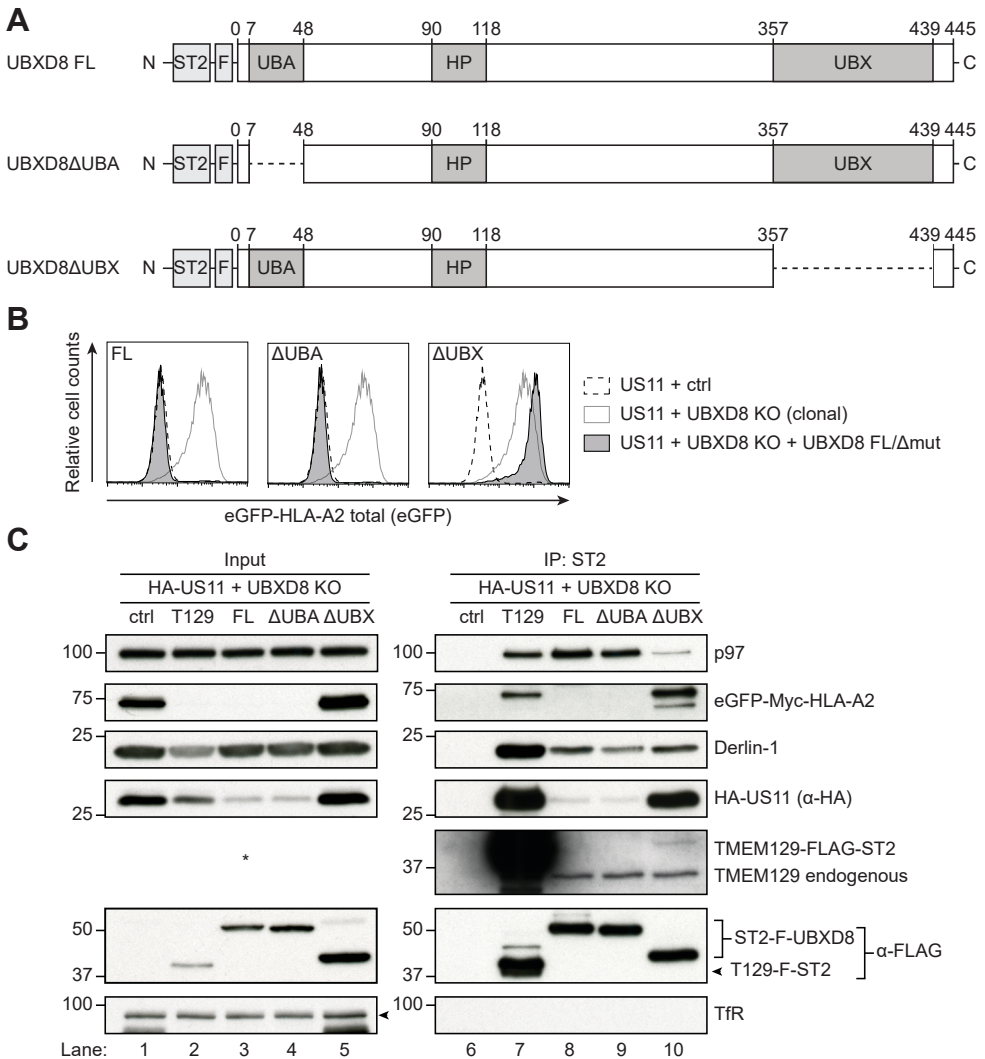
Figure 2 | UBXD8 is in complex with US11, TMEM129 and Derlin-1. A) UBXD8 occurs in a complex with Derlin-1, TMEM129, and US11. Strep(II)-HA-tagged US11 was immunoprecipitated from 1.0% digitonin lysates of ST2-HA-US11-negative and -positive U937 eGFP- HLA-A2 cells using StrepTactin beads. Immunoprecipitated proteins were eluted using d-Desthiobiotin. Immunoblot analysis was performed on post-nuclear cell lysate (Input) and immunoprecipitated material (IP) for the proteins indicated. TfR was used as a loading control for the input samples. B) UBXD8 is part of TMEM129- and Derlin-1-containing dislocation complexes in the presence and absence of US11. Strep(II)-FLAG-tagged TMEM129 was immunoprecipitated from 1.0% digitonin lysates of HA-US11-negative and -positive U937 eGFP- HLA-A2 cells using StrepTactin beads. Immunoprecipitated proteins were eluted using d-Desthiobiotin. Immunoblot analysis was performed on post-nuclear cell lysate (Input) and immunoprecipitated material (IP) for the proteins indicated. Immunoblot analysis of TMEM129-FLAG-ST2 input and immunoprecipitated levels is composed of a long and a shorter exposure, respectively. TfR was used as a loading control for the input samples.

UBX domain is essential.

We next subjected these deletion mutants to co-immunoprecipitation experiments to investigate their association to p97, US11, Derlin-1, and TMEM129 (Fig. 3C). A combined StrepII-FLAG-tag on the UBXD8 cDNA variants allowed for their immunoprecipitation by means of their StrepII-tag, followed by detection via the FLAG-tag. A StrepII-FLAG-tagged TMEM129 construct served as a control for detecting the interactions with components of the US11 dislocation complex. As expected, the Δ UBX mutant showed reduced p97 association compared to

full length UBXD8 and the UBA deletion mutant (compare lane 10 to lanes 8 and 9 in Fig. 3C). Association of UBXD8 with TMEM129 and Derlin-1 was not affected by deletion of either the UBA nor UBX domains (compare lanes 9 and 10 to lane 8).

The expression of US11 varied strongly upon expression of the different UBXD8 variants (lanes 3-5). This could be related to the previously observed increase in the expression of US11 upon knocking out of UBXD8 (Fig. 1F). The Δ UBX showed an increase in US11 expression similar to UBXD8 KO cells (compare lane 5 to lane 1 in Fig. 3C), while the lower US11 expression in FL and Δ UBA cells may reflect its normal expression levels (lanes 3 and 4). All UBXD8 constructs were able to interact with US11 (lanes 8-10). Full length UBXD8 and Δ UBA associated with equal amounts of US11 (lanes 8 and 9). Δ UBX (lane 10) showed increased association with US11 compared to the other UBXD8 constructs, even when the differences US11 expression are



considered (lane 5). HLA-I was co-precipitated only with Δ UBX mutant (lane 10). However, as HLA-I is degraded in FL and Δ UBA cells (Fig. 3B, and lanes 3 and 4 of Fig. 3C), the Δ UBX-specific HLA-I interaction may be a consequence of the HLA-I degradation defect in these cells.

As a positive control for p97 interaction, we expressed TMEM129-FLAG-ST2 (Fig. 3C, lane 2) and immunoprecipitated the protein (lane 7) from these cells. Surprisingly, TMEM129-FLAG-ST2 expression bypassed the requirement of UBXD8 in US11-mediated HLA-I degradation, as HLA-I was efficiently degraded in TMEM129-FLAG-ST2-expressing UBXD8 knockout cells (lane 2). Some TMEM129-associated HLA-I was however observed (lane 7), confirming that HLA-I is degraded via this TMEM129-containing complex.

Taken together, we conclude that UBXD8 is a part of the US11 dislocation complex, even when its UBA- or UBX-domain are lacking. The Δ UBX mutant cannot facilitate HLA-I degradation. As this mutant is unable to bind p97, our data suggests that UBXD8 is responsible for recruiting p97 to the dislocation complex.

UBXD8 knockout lowers p97 recruitment to US11 dislocation complexes

To test whether UBXD8 is responsible for p97 recruitment to the US11 dislocation complex, we assessed the interaction between US11 and p97. We compared this interaction in UBXD8 wildtype cells *versus* a UBXD8 knockout cell line, or UBXD8 KO cells expressing the Δ UBX mutant. The comparison between ERAD-proficient (UBXD8-expressing) and ERAD-deficient cells (UBXD8 KO or Δ UBX-expressing cells) could however not be readily made, as ERAD complexes often accumulate at the ER membrane when protein degradation is blocked (Van De Weijer et al. 2014). Increased US11 expression is another feature of this accumulation, as turnover of US11 is hampered in dislocation-incompetent conditions (van den Boomen et al. 2014). The increased expression of US11 in the context of UBXD8 KO (Fig. 1F) suggests that such accumulation of ERAD complexes also occurs in UBXD8 KO cells.

To reliably compare p97 recruitment to US11 in cells expressing functional UBXD8 and those with compromised UBXD8 function, we stalled dislocation in all cells by incubating them with the p97 inhibitor CB-5083 (Zhou et al. 2015). This inhibitor potently inhibits ATPase activity of the p97 D2 domain. Indeed, incubating WT UBXD8- and US11-expressing control cells

- ◀ **Figure 3 | The UBX domain of UBXD8 is essential for US11-mediated HLA-I degradation.** A) Domain organisation of human UBXD8, and domain-deletion mutants Δ UBA and Δ UBX. FL, Full length; UBA, ubiquitin-associated; HP, hydrophobic patch; UBX, ubiquitin regulatory X. The constructs used in this figure contain an N-terminal StrepII (ST2) and FLAG (F) tag. Residue numbers indicate the position of the domains in the wildtype protein. B) The p97-recruiting UBX-domain of UBXD8 is essential for US11-mediated HLA class I degradation. Full length UBXD8 (FL) and domain-deletion mutants UBXD8 Δ UBA and UBXD8 Δ UBX were introduced into UBXD8-knockout cells expressing US11 and eGFP-HLA-A2. eGFP-HLA-A2 levels were assessed by flow cytometry seven days post-transduction. C) Deletion of the UBX domain impairs p97 recruitment by UBXD8. Strep(II)-FLAG-tagged UBXD8 and domain-deletion mutants UBXD8 Δ UBA and UBXD8 Δ UBX were immunoprecipitated using StrepTactin beads from 1.0% digitonin lysates of UBXD8-knockout U937 cells co-expressing HA-US11 and eGFP-HLA-A2. As a positive control, TMEM129-FLAG-ST2 was immunoprecipitated. Immunoprecipitated proteins were eluted using d-Desthiobiotin. Immunoblot analysis was performed on post-nuclear cell lysate (input) and immunoprecipitated material (IP) for the proteins indicated. This experiment has been performed twice, of which one representative figure is shown. T129 = TMEM129-StrepII-FLAG; FL = StrepII-FLAG-UBXD8 full-length, Δ UBA = StrepII-FLAG-UBXD8 Δ UBA domain; Δ UBX = StrepII-FLAG-UBXD8 Δ UBX domain. *The TMEM129 antibody could not detect endogenous TMEM129 in digitonin cell lysates.

with CB-5083 resulted in a pronounced rescue of HLA-I (Fig. 4A, upper and lower left panels). This HLA-I rescue effect was observed already after incubation times of only 2 to 4 hours. These short incubation times yielded strong inhibition of p97, yet resulted in very low cell toxicity in

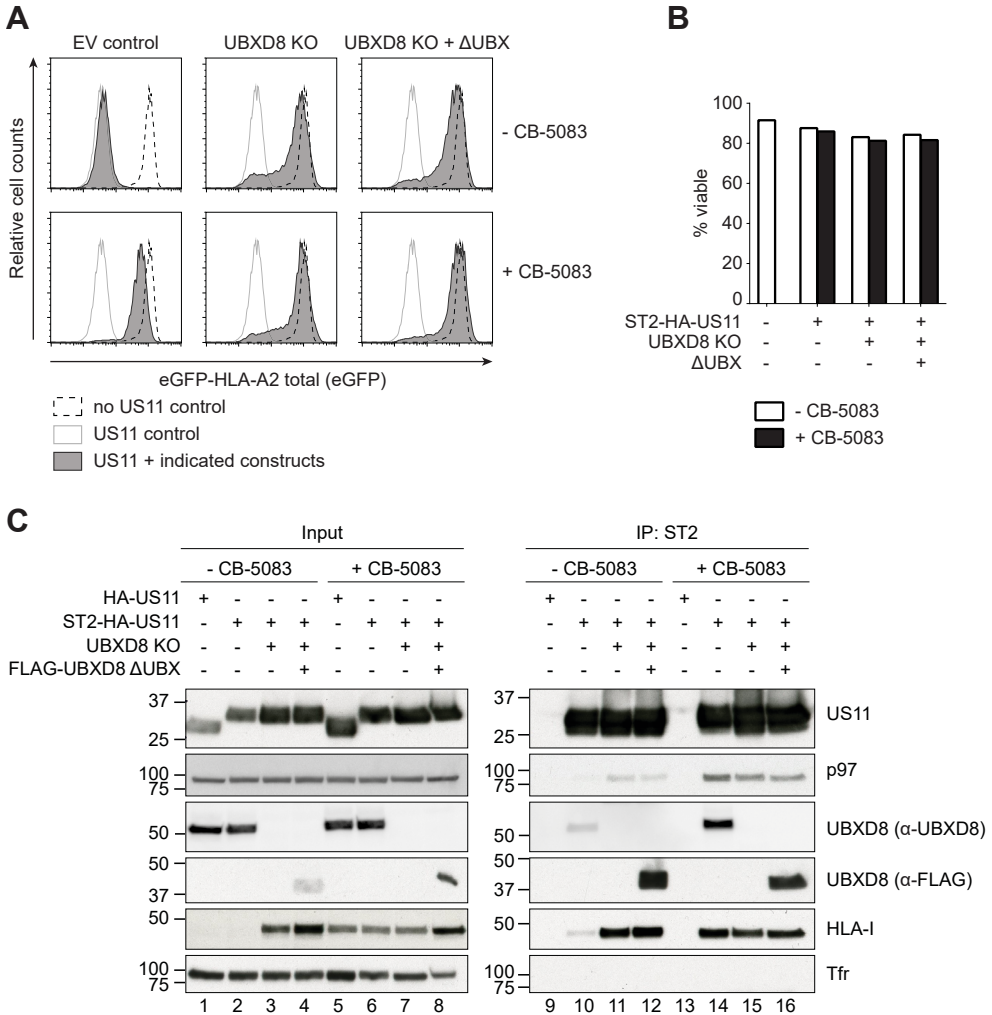


Figure 4 | UBXD8 knockout reduces p97 recruitment to the dislocation complex. A) eGFP-HLA-A2 expression increases upon a 4-hour incubation with 1 μ M CB-5083. Flow cytometry analysis of eGFP expression of the indicated samples is shown. B) Viability of the cells shown in A. C) Strep(II)-HA-tagged US11 was immunoprecipitated using StrepTactin beads from 1.0% LMNG lysates of US11-expressing U937 eGFP-HLA-A2 cells (lanes 2, 6, 10, and 14), US11-expressing U937 eGFP-HLA-A2 cells with a UBXD8 knockout (lanes 3, 7, 11 and 15), or UBXD8 knockout cells expressing a FLAG-tagged Δ UBX UBXD8 cDNA (lanes 4, 8, 12 and 16). HA-US11-expressing eGFP-HLA-A2 cells were used as a negative control for the immunoprecipitation (lanes 1, 5, 9, and 13). The cells were treated with 1 μ M CB-5083 (lanes 5-8 and 13-16) or DMSO control (lanes 1-4 and 9-12) for 4 hours. Tfr was used as a loading control for the input samples.

U937 cells (Fig. 4B). These data confirm that CB-5083 can be used to block HLA-I degradation in both UBXD8-proficient and -deficient cells. We next assessed whether UBXD8 is responsible for p97 recruitment to US11-exploited dislocation complexes. To test this, StrepII-HA-tagged US11 (ST2-HA-US11)-expressing UBXD8 knockout cells with or without FLAG-tagged UBXD8 Δ UBX were incubated with CB-5083 or DMSO control for 4 hours. We also included WT UBXD8 U937 cells expressing an HA-tagged version of US11. Subsequently, the cells were lysed and subjected to StrepTactin co-immunoprecipitation in 1% LMNG buffer to pull-down US11 (Fig. 4C). The HA-US11 construct lacking a StrepII-tag was used as a negative control for the immunoprecipitation (lanes 1, 5, 9, and 13). UBXD8 expression was assessed directly using an anti-UBXD8 antibody. However, as this antibody is directed against the UBX-domain, the UBXD8 Δ UBX protein could not be detected. Therefore, anti-FLAG was used to confirm the presence of UBXD8 Δ UBX. As expected, both full-length UBXD8 and UBXD8 Δ UBX associated with US11. HLA-I was rescued from US11-mediated degradation in cells with a UBXD8 knockout, UBXD8 KO cells expressing the Δ UBX mutant, as well as all cells treated with CB-5083 (lanes 3-8).

Recruitment of p97 to US11 was assessed by staining for p97 in US11-precipitated samples. While p97 is expressed at equal levels in all cells (lanes 1-8), the amount associating with US11 differs between the cell lines. In the absence of CB-5083, hardly any p97 was detected in cells that displayed functional dislocation (lane 10). Knocking out UBXD8 or expressing UBXD8 Δ UBX increased the amount of p97 associated with US11 (lanes 11-12), probably as a consequence of accumulating the stalled dislocation complexes. Incubation with CB-5083 therefore allowed for a more reliable comparison between the cell lines. Upon CB-5083 treatment, US11-associated p97 strongly increased (compare lane 14 to lane 10). UBXD8 KO cells displayed a decrease in US11-associated p97 compared to their UBXD8-expressing counterpart (compare lane 15 to lane 14). To rule out that the absence of UBXD8 influences p97 binding to US11 indirectly due to improper arrangement of the UBXD8-lacking dislocation complex, we expressed the Δ UBX mutant as well (lane 16). Similar to the UBXD8 knockout cells, a decline in p97 was observed, confirming that UBXD8 is involved in recruitment of p97 to the dislocation complex.

Derlin-1 knockout lowers p97 levels in the dislocation complex via an indirect mechanism

The reduction of p97 co-precipitation upon US11 IP was less pronounced compared to that observed for UBXD8 itself (compare Fig. 3C with 4C). This finding suggests that other factors can facilitate p97 recruitment to the US11 dislocation complex as well. We hypothesized that Derlin-1 could act as a potential p97-recruiter, as the protein contains a p97-interacting SHP box. Another candidate is E3 enzyme TMEM129, as p97 can be co-precipitated with this ubiquitin ligase (Van De Weijer et al. 2014). To test whether Derlin-1 or TMEM129 function as p97-recruiters, we performed co-immunoprecipitation experiments on StrepII-HA-US11, this time in clonal Derlin-1-, TMEM129- or UBXD8 KO cells (Fig. 5A). The knockout of these genes completely disrupted HLA-I degradation by US11 (lanes 3-5). However, the HLA-I rescue phenotypes may have not been caused by a p97 recruitment defect, as p97 was still detected in complex with US11 in all cell lines tested (lanes 7-10).

as other factors of the dislocation complex (van den Boomen et al. 2014). Therefore, a Derlin-1 knockout may hamper recruitment of p97 indirectly, by disturbing assembly of the dislocation complex. To investigate this possibility, a Derlin-1 recombinant lacking the p97-interacting SHP domain (Greenblatt et al. 2011) was expressed in clonal Derlin-1 knockout cells. We observed that HLA-I degradation continues in Derlin-1 Δ SHP-expressing cells (Fig. 5B), suggesting that Derlin-1 is not an essential p97 recruiter in this context.

DISCUSSION

The ATPase p97 is indispensable for US11-mediated HLA-I degradation, although the mechanism of its recruitment to the dislocation complex remains elusive. Previously it has been suggested that either Derlin-1 and VIMP (Ye et al. 2004) or UBXD8 (Mueller et al. 2008) are responsible for p97 recruitment during US11-mediated HLA-I degradation, but convincing evidence confirming their essential involvement in US11-mediated HLA-I degradation is lacking. Other Derlin proteins as well as E3 ubiquitin ligases can also directly interact with p97 (Lilley & Ploegh 2005; Ye et al. 2005; Greenblatt et al. 2011; Stolz et al. 2011). This plethora of p97 recruitment possibilities may reflect a requirement for different p97 configurations at different steps of the dislocation complex.

Using a focused lentiviral CRISPR/Cas9 screen, we identified the p97 co-factor UBXD8, but not VIMP, to be essential for US11-mediated HLA-I degradation. This is in agreement with the previous finding that VIMP is dispensable for p97 binding to Derlin-1 (Lilley & Ploegh 2005). Pull-down experiments on US11 revealed that UBXD8 is present in dislocation complexes in the presence of US11. In the absence of US11, pull-down experiments have shown that TMEM129 is also in complex with Derlin-1 and UBXD8. A constitutive, US11-independent dislocation complex containing UBXD8, TMEM129 and Derlin-1 may thus exist.

The UBA domain of UBXD8 is dispensable for US11-mediated HLA-I degradation. UBA domains in general interact with polyubiquitinated proteins (Buchberger 2002). In addition, the UBA domain of UBXD8 is able to recruit BAG6, a cytosolic chaperone involved in ERAD, through the UBL domain of BAG6 (Xu et al. 2013). While BAG6 is essential for US11-mediated HLA-I degradation (Wang et al. 2011), the non-essentiality of the UBXD8 UBA domain for HLA-I degradation suggests that UBXD8 is not responsible for BAG6 recruitment during US11-mediated HLA-I degradation. Alternatively, redundancy may exist for recruiting BAG6.

In contrast to the UBA-domain, the UBXD8 UBX-domain is essential for US11-mediated HLA-I degradation. This domain is required for p97 recruitment (Suzuki et al. 2012; Alexandru et al. 2008; Mueller et al. 2008) and for the degradation of at least one ERAD substrate, i.e. lipidated ApoB-100 (Suzuki et al. 2012). Here, we found that the UBX domain of UBXD8 is also essential for degradation of HLA-I by US11. UBXD8 pull-down experiments showed that the capacity to recruit p97 is severely reduced in a UBX-deletion mutant. The inability of UBXD8 to bind p97 results in diminished p97 levels in the dislocation complex. Our data confirm the phenotype observed in a previous publication, where GFP-tagged UBXD8 rendered HLA-I insensitive to US11-mediated degradation (Mueller et al. 2008).

Defects in protein dislocation can stabilize ERAD complexes. As ERAD is a dynamic process,

dislocation complexes are likely assembled and dismantled continuously. If dislocation is stalled due to a defect in ERAD, dislocation complexes may not disassemble because substrate dislocation cannot be completed. Because the half-life of HLA-I in the context of US11 is less than one minute (Wiertz, Jones, et al. 1996), the transient nature of the functional dislocation complex likely results in low steady-state expression and interaction levels. Stabilization of dislocation-incompetent complexes may therefore accumulate these complexes at the ER membrane. Such accumulation of US11 dislocation complexes has previously been described when expressing an inactive form of the E3 ligase TMEM129, or when TMEM129 is knocked down (Van De Weijer et al. 2014). While the total expression of Derlins, VIMP, p97 and SEL1L is not affected in these cells, far larger amounts of these factors are associated to US11 in the absence of functional TMEM129. Stabilization of dysfunctional dislocation complexes hinders a reliable comparison of p97 recruitment between ERAD-proficient cells and those knocked out for a crucial ERAD factor. Previous studies have successfully blocked dislocation using an ATPase-defective p97 mutant (p97KA) (Ye et al. 2004; Ye et al. 2003). We used a similar approach by treating the cells with the potent and specific p97 inhibitor CB-5083. Using this drug, we could block dislocation in all cell lines, allowing us to compare p97 recruitment in wildtype cells *versus* those lacking functional UBXD8. This way, we could observe that a UBXD8 knockout, or expression of a Δ UBX mutant, hampers p97 recruitment. Despite the inability of UBXD8 Δ UBX to bind p97, some interaction between p97 and US11 remained visible upon UBXD8 knockout or expression of Δ UBX. As p97 recruitment to US11 is not fully eliminated by disrupting UBXD8 expression, additional p97-recruiting factors may exist. We therefore hypothesized that Derlin-1 or TMEM129 may recruit p97.

In the presence of functional UBXD8, a knockout of Derlin-1 results in a minor decrease of p97 recruitment to the ERAD complex. Derlin-1 contains a C-terminal SHP domain which is essential for p97 recruitment and subsequent membrane extraction of the soluble ERAD substrate NHK, a constitutively degraded truncated variant of α -1 antitrypsin (Greenblatt et al. 2011). However, an SHP-deletion mutant of Derlin-1 was still able to drive US11-mediated HLA-I degradation in Derlin-1 knockout cells. As Derlin-1 has a bridging function between US11 and the TMEM129-containing dislocation complex (van den Boomen et al. 2014), we hypothesize that the decreased amount of p97 co-precipitating with US11 arises from a defect in the recruitment of TMEM129 and other potential p97-recruiting co-factors into the ERAD complex. TMEM129 does not contain any known p97 recruitment domains and TMEM129 knockout (in the presence of functional UBXD8) did not diminish p97 recruitment to the US11 complex. It is therefore unlikely that TMEM129 can directly recruit p97.

Because HLA-I is almost fully rescued upon UBXD8 knockout, while approximately half of p97 is still present in the dislocation complex, this suggests that a critical threshold of p97 is required for HLA-I degradation, which is no longer reached in UBXD8 knockout cells. Alternatively, UBXD8 may be responsible for proper positioning of p97 within the dislocation complex. We conclude that UBXD8 is a crucial factor for US11-mediated HLA-I degradation via ERAD, and is involved in the recruitment of p97 to the dislocation complex.

ACKNOWLEDGEMENTS

We thank Tomàs Aguirre Gonzalez for his contribution to setting up the experiments shown in figure 4. We are grateful to the Core Flow cytometry Facility (CFF) at the UMCU for technical assistance with cell sorting.

COMPETING INTERESTS

The authors declare no competing or financial interests. This study was funded by the Graduate Programme of the Netherlands Organisation for Scientific Research (NWO), project number 022.004.018, to A.B.C.S., R.J.L and M.L.W. were supported by Veni grant 916.10.138 from NWO and Marie Curie Career Integration Grant PCIG-GA-2011-294196.

REFERENCES

- Alexandru, G. et al., 2008. UBXD7 binds multiple ubiquitin ligases and implicates p97 in HIF1 α turnover. *Cell*, 134(5), pp.804–16.
- Bodnar, N. & Rapoport, T., 2017. Toward an understanding of the Cdc48/p97 ATPase. *F1000Research*, 6(0), p.1318. Available at: <https://f1000research.com/articles/6-1318/v1>.
- Bodnar, N.O. & Rapoport, T.A., 2017. Molecular Mechanism of Substrate Processing by the Cdc48 ATPase Complex. *Cell*, 169(4), p.722–735.e9. Available at: <http://dx.doi.org/10.1016/j.cell.2017.04.020>.
- van den Boomen, D.J.H. et al., 2014. TMEM129 is a Derlin-1 associated ERAD E3 ligase essential for virus-induced degradation of MHC-I. *Proceedings of the National Academy of Sciences of the United States of America*, 111(31), pp.11425–30.
- Brodsky, J.L., 2012. Cleaning Up: ER-associated degradation to the rescue. *Cell*, 151(6), pp.1163–1167. Available at: <http://dx.doi.org/10.1016/j.cell.2012.11.012>.
- Buchberger, A., 2002. From UBA to UBX: new words in the ubiquitin vocabulary. *Trends in cell biology*, 12(5), pp.216–21.
- Buchberger, A., Schindelin, H. & Hänzelmann, P., 2015. Control of p97 function by cofactor binding. *FEBS Letters*, 589(19PartA), pp.2578–2589.
- Christianson, J.C. et al., 2011. Defining human ERAD networks through an integrative mapping strategy. *Nature Cell Biology*, 14(1), pp.93–105. Available at: <http://dx.doi.org/10.1038/ncb2383>.
- Flierman, D. et al., 2006. E2-25K mediates US11-triggered retro-translocation of MHC class I heavy chains in a permeabilized cell system. *Proceedings of the National Academy of Sciences of the United States of America*, 103(31), pp.11589–11594.
- Greenblatt, E.J., Olzmann, J.A. & Kopito, R.R., 2011. Derlin-1 is a rhomboid pseudoprotease required for the dislocation of mutant α -1 antitrypsin from the endoplasmic reticulum. *Nature*

structural & molecular biology, 18(10), pp.1147–52.

Griffiths, P., Baraniak, I. & Reeves, M., 2015. The pathogenesis of human cytomegalovirus. *The Journal of pathology*, 235(2), pp.288–97.

Hsu, J.-L. et al., 2015. Plasma Membrane Profiling Defines an Expanded Class of Cell Surface Proteins Selectively Targeted for Degradation by HCMV US2 in Cooperation with UL141. *PLOS Pathogens*, 11(4), p.e1004811. Available at: <http://dx.plos.org/10.1371/journal.ppat.1004811>.

Lee, J.N. et al., 2010. Identification of Ubxd8 protein as a sensor for unsaturated fatty acids and regulator of triglyceride synthesis. *Proceedings of the National Academy of Sciences of the United States of America*, 107(50), pp.21424–9.

Lilley, B.N. & Ploegh, H.L., 2004. A membrane protein required for dislocation of misfolded proteins from the ER. *Nature*, 429(6994), pp.834–840.

Lilley, B.N. & Ploegh, H.L., 2005. Multiprotein complexes that link dislocation, ubiquitination, and extraction of misfolded proteins from the endoplasmic reticulum membrane. *Proceedings of the National Academy of Sciences of the United States of America*, 102(40), pp.14296–14301.

Mueller, B. et al., 2008. SEL1L nucleates a protein complex required for dislocation of misfolded glycoproteins. *Proceedings of the National Academy of Sciences of the United States of America*, 105(34), pp.12325–30.

Olzmann, J.A., Kopito, R.R. & Christianson, J.C., 2013. The mammalian endoplasmic reticulum-associated degradation system. *Cold Spring Harbor perspectives in biology*, 5(9), pp.1–16.

Schrul, B. & Kopito, R.R., 2016. Peroxin-dependent targeting of a lipid-droplet-destined membrane protein to ER subdomains. *Nature Cell Biology*, 18(7), pp.740–51.

Schuren, A.B.C., Costa, A.I. & Wiertz, E.J.H.J., 2016. Recent advances in viral evasion of the MHC Class I processing pathway. *Current Opinion in Immunology*, 40, pp.43–50. Available at: <http://dx.doi.org/10.1016/j.coi.2016.02.007>.

Soetandyo, N. & Ye, Y., 2010. The p97 ATPase dislocates MHC class I heavy chain in US2-expressing cells via a Ufd1-Npl4-independent mechanism. *Journal of Biological Chemistry*, 285(42), pp.32352–32359.

Stagg, H.R. et al., 2009. The TRC8 E3 ligase ubiquitinates MHC class I molecules before dislocation from the ER. *Journal of Cell Biology*, 186(5), pp.685–692.

Stolz, A. et al., 2011. Cdc48: a power machine in protein degradation. *Trends in Biochemical Sciences*, 36(10), pp.515–523.

Suzuki, M. et al., 2012. Derlin-1 and UBXD8 are engaged in dislocation and degradation of

lipidated ApoB-100 at lipid droplets. *Molecular biology of the cell*, 23(5), pp.800–10.

Wang, Q. et al., 2011. A ubiquitin ligase-associated chaperone holdase maintains polypeptides in soluble states for proteasome degradation. *Molecular cell*, 42(6), pp.758–70.

van de Weijer, M.L. et al., 2017. Multiple E2 ubiquitin-conjugating enzymes regulate human cytomegalovirus US2-mediated immunoreceptor downregulation. *Journal of Cell Science*, 130(17), pp.2883–2892. Available at: <http://jcs.biologists.org/lookup/doi/10.1242/jcs.206839>.

van De Weijer, M.L. et al., 2014. A high-coverage shrna screen identifies TMEM129 as an E3 ligase involved in ER-associated protein degradation. *Nature Communications*, 5(May), pp.1–14. Available at: <http://dx.doi.org/10.1038/ncomms4832>.

van de Weijer, M.L., Luteijn, R.D. & Wiertz, E.J.H.J., 2015. Viral immune evasion: Lessons in MHC class I antigen presentation. *Seminars in Immunology*, 27(2), pp.125–137. Available at: <http://www.sciencedirect.com/science/article/pii/S1044532315000184>.

Wiertz, E.J.H.J., Tortorella, D., et al., 1996. Sec61-mediated transfer of a membrane protein from the endoplasmic reticulum to the proteasome for destruction. *Nature*, 384(6608), pp.432–438.

Wiertz, E.J.H.J., Jones, T.R., et al., 1996. The human cytomegalovirus US11 gene product dislocates MHC class I heavy chains from the endoplasmic reticulum to the cytosol. *Cell*, 84(5), pp.769–779.

Wu, X. & Rapoport, T.A., 2018. Mechanistic insights into ER-associated protein degradation. *Current Opinion in Cell Biology*, 53, pp.22–28. Available at: <https://doi.org/10.1016/j.ceb.2018.04.004>.

Xu, Y. et al., 2013. A Ubiquitin-like Domain Recruits an Oligomeric Chaperone to a Retrotranslocation Complex in Endoplasmic Reticulum-associated Degradation. *Journal of Biological Chemistry*, 288(25), pp.18068–18076.

Ye, Y. et al., 2004. A membrane protein complex mediates retro-translocation from the ER lumen into the cytosol. *Nature*, 429(6994), pp.841–847.

Ye, Y. et al., 2005. Recruitment of the p97 ATPase and ubiquitin ligases to the site of retrotranslocation at the endoplasmic reticulum membrane. *Proceedings of the National Academy of Sciences of the United States of America*, 102(40), pp.14132–8.

Ye, Y., Meyer, H.H. & Rapoport, T. a, 2001. The AAA ATPase Cdc48/p97 and its partners transport proteins from the ER into the cytosol. *Nature*, 414(6864), pp.652–656.

Ye, Y., Meyer, H.H. & Rapoport, T.A., 2003. Function of the p97-Ufd1-Npl4 complex in retrotranslocation from the ER to the cytosol: Dual recognition of nonubiquitinated polypeptide segments and polyubiquitin chains. *Journal of Cell Biology*, 162(1), pp.71–84.

Zhou, H.J. et al., 2015. Discovery of a First-in-Class, Potent, Selective, and Orally Bioavailable Inhibitor of the p97 AAA ATPase (CB-5083). *Journal of Medicinal Chemistry*, 58(24), pp.9480–9497.

ABBREVIATIONS

CRISPR = clustered regularly interspaced short palindromic repeats

ER = endoplasmic reticulum

ERAD = ER-associated protein degradation

HCMV = human cytomegalovirus

HLA-I = human leukocyte antigen class I

UBA = ubiquitin-associating

UBX = ubiquitin-regulatory X

VBM = VCP-binding motif

VCP = valosin-containing protein

VIM = VCP-interacting motif

SUPPLEMENTARY DATA

#	Name	Alternative names	target site incl PAM
1	gCtrl		n/a
2	UBXD1_1		TCGGATGGTGTCTCGCATG <u>TGG</u>
3	UBXD1_2	UBXN6	CTTCTGCTCCAGCCGGGCTA <u>GGG</u>
4	UBXD1_3		GGCCTGGGGCCCCACATCGC <u>AGG</u>
5	UBXD2_1		GCTCCTTTTGGCCGTCGCGA <u>TGG</u>
6	UBXD2_2	UBXN4	CATTCCGGCCGCCATCGCGA <u>CGG</u>
7	UBXD2_3		CGGCCATCGCGACGGCCAAA <u>AGG</u>
8	UBXD3_1		CTGACAACAGTGTACTACTC <u>AGG</u>
9	UBXD3_2	UBXN10	TCAGGTGGTGTATATTAC <u>AGG</u>
10	UBXD3_3		CAGCAGTTGACAGCCTCATT <u>TGG</u>
11	UBXD4_1		ATTCTTCTTTTATACTTTT <u>AGG</u>
12	UBXD4_2	UBXN2A	GGATCTGATAATCAACCTCT <u>TGG</u>
13	UBXD4_3		GATTGTGATTATTACCAAG <u>AGG</u>
14	UBXD4_4		ACTTCTGAAATCGTCGTGA <u>CGG</u>
15	UBXD5_1		GCACTTTTCGGGTCTTGCTA <u>AGG</u>
16	UBXD5_2	UBXN11	GATTCATAGGCTCCGAGGGC <u>AGG</u>
17	UBXD5_3		ATTCATAGGCTCCGAGGGCAG <u>GGG</u>
18	UBXD6_1		TGTGTCTGGAGCTCCGGCGT <u>GGG</u>
19	UBXD6_2	UBXN8	ATGGCTTACAGTGGGGTTGT <u>TGG</u>
20	UBXD6_3		TGCTGTCCCCCTGTGTGTCT <u>TGG</u>
21	UBXD7_1		AATTAACCCCTTCAGCGCCG <u>AGG</u>
22	UBXD7_2	UBXN7	GCGGCGTCTCGGCGTGAA <u>GGG</u>
23	UBXD7_3		CGGCGTCTCGGCGTGAA <u>GGG</u>
24	UBXD8_1		TGGGTTAGATCCCCTCCTC <u>AGG</u>
25	UBXD8_2	FAF2, KIAA0887, UBXN3B	TGAGGAGCGGGATCTAACCC <u>AGG</u>
26	UBXD8_3		GGATCAGTGTGCCATACCT <u>TGG</u>
27	UBXD9_1		CGTGTGGCGCCGGCGTT <u>GGG</u>
28	UBXD9_2	ASPSR1, UBXN9	CCCGAACGGCCGGCGCCACA <u>CGG</u>
29	UBXD9_3		TCACCTTACCCTGTGGCGC <u>CGG</u>
30	UBXD10_1		CTTGAGAGTCTCATCGAGAT <u>GGG</u>
31	UBXD10_2	SAKS1, UBXN1	TCATCGAGATGGGCTTCCCC <u>AGG</u>
32	UBXD10_3		CCATCGCAGCCTCGATGCC <u>TGG</u>

33	UBXD11_1		TGCAAATCCCGCGCGCTCGG <u>AGG</u>
34	UBXD11_2	p37, UBXN2B	AGAGGAGGTCTCCGGGCCG <u>CGG</u>
35	UBXD11_3		TCCCGCGCGCTCGGAGGCCG <u>CGG</u>
36	UBXD12_1		GATCATCTCCCGGTCCATGT <u>TGG</u>
37	UBXD12_2	FAF1, UBXN3A	CATGGACCGGGAGATGATCC <u>TGG</u>
38	UBXD12_3		AATCCGCCAGGATCATCTCC <u>CGG</u>
39	Ufd2_1		AGGCGCCTTGACAGACTTGC <u>TGG</u>
40	Ufd2_2	UBE4A / UBE4B	CCTGGGGCTGATGCCGCTAT <u>GGG</u>
41	Ufd2_3		GTCCACCAGCAAGTCGTGCA <u>AGG</u>
42	YOD1_1		ACTCGGGAGGGTATCCGACG <u>AGG</u>
43	YOD1_2	YOD1, DUBA8, OTUD2	GGCGGTGAGCGAATCCTCGT <u>CGG</u>
44	YOD1_3		ATCACCGGGATCGCCCCGG <u>CGG</u>
45	YOD1_4		GACGAGGATTGCTGACCGC <u>CGG</u>
46	p47_1	NSFL1C, UBXN2C, Shp1	TCTTTCTCGAGTCGGCCGGC <u>TGG</u>
47	p47_2		CGCTTCTTTCTCGAGTCGGC <u>CGG</u>
48	p47_3		GGCCCGCTTCTTTCTCGAGT <u>CGG</u>
49	ATX3_1		TTGCTTCTAACACTCGTTCC <u>AGG</u>
50	ATX3_2	ATX3	ATGAGGAAGCAGATCTCCGC <u>AGG</u>
54	ATX3_3		AGGAATGTTAGACGAAGATG <u>AGG</u>
55	VIMP_1		GACGATGTACCAGCCATAGG <u>TGG</u>
56	VIMP_2	SELS	GCCCCGCAACGACTCACCCG <u>TGG</u>
57	VIMP_3		GTGCAGGAAGCGCAGCCCT <u>CGG</u>

Supplementary information 1 | CRISPR sgRNAs used in this study.



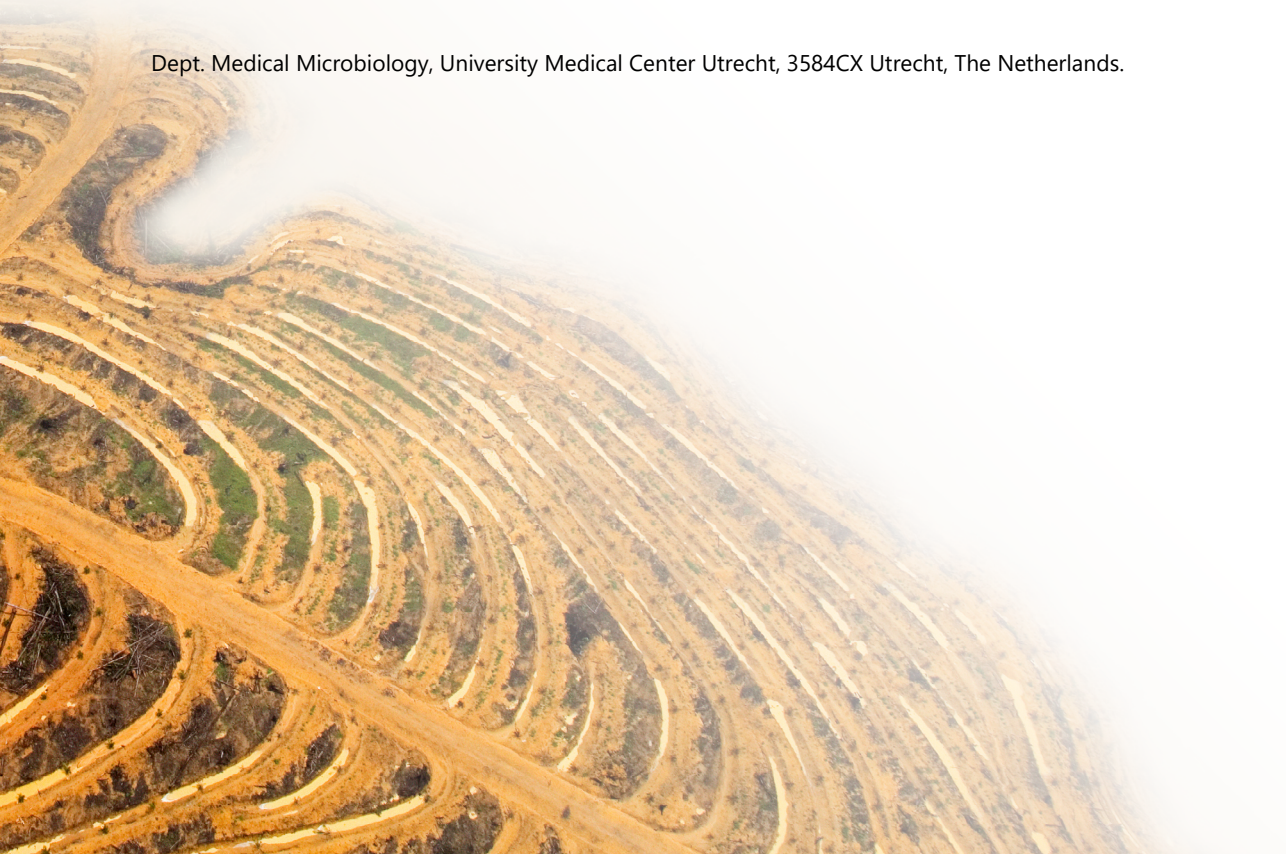
CHAPTER

7

Summarizing discussion

Anouk B.C. Schuren

Dept. Medical Microbiology, University Medical Center Utrecht, 3584CX Utrecht, The Netherlands.



Immune-modulatory mechanisms have allowed herpesviruses to become the successful viruses they are today. Downregulation of MHC (or in humans: HLA) class I plays a central role in herpesviral immune-evasive strategies. In this thesis, we studied HLA class I (HLA-I) degradation by human cytomegalovirus (HCMV), one of the herpesvirus family members. ER-resident HLA class I is degraded by HCMV via two different pathways, mediated by the viral proteins US2 and US11. Both US2 and US11 hijack the cellular ER-associated protein degradation (ERAD) pathway, which causes proteasomal degradation of proteins that fail quality control. These and other HLA class I downregulatory mechanisms hamper conventional antigen presentation so successfully that cross-presentation of HCMV antigens is the major pathway to activate CD8⁺ T cells¹.

ERAD's Next Top Model

In the studies described in this thesis, we used the HLA-targeting proteins US2 and US11 as a model to study ER-associated protein degradation (ERAD). We focused on multiple steps of ERAD, including substrate ubiquitination (**Chapter 3**) and dislocation towards the cytosol (**Chapters 5 and 6**). Using a genome-wide CRISPR/Cas9 screen we also identified another ubiquitin-like modification, UFM1, to potentially play a role in HLA class I degradation (**Chapter 4**).

Using a CRISPR/Cas9 library targeting all human ubiquitin E2 enzymes, we identified UBE2G2 as a crucial ubiquitin-conjugating enzyme for US2-mediated ERAD (**Chapter 3**). The E2 enzymes for US11 have previously been identified to be UBE2J2 and UBE2K^{2,3}. Strikingly, we observed that while UBE2J2 is crucial for US11 function, it counteracts US2. Most likely, UBE2J2 is involved in the turnover of TRC8, the E3 ubiquitin ligase for US2. As TRC8 is a limiting factor for US2-mediated HLA class I degradation, increased TRC8 expression in UBE2J2 knockout cells may cause this additional HLA class I downregulation.

Genome-wide screening techniques using CRISPR/Cas9 have allowed us to screen for essential cellular players in US2- or US11-mediated downregulation of HLA class I molecules. A previous approach, using RNAi, successfully identified TMEM129 as the crucial ubiquitin ligase for US11². We now screened for novel factors in the context of US2 and identify that the entire pathway of UFM1, a ubiquitin-like molecule, affects HLA class I downregulation (**Chapter 4**). As the ubiquitin-proteasome system is an essential part of ERAD, the identification of a novel ubiquitin-like modification is an interesting finding. However, UFM1 may function in a different way than ubiquitin, as it is involved in different cellular pathways and we did not detect UFMylation of the ubiquitin substrate HLA class I. Instead, it seems that the ribosome is UFMylated, which may point towards an indirect way in which UFM1 modulates ERAD.

Utilizing US2 as a model for ERAD has already proven useful in the past to discover that SEC61 plays a role in this protein degradation pathway⁴. However, its particular mechanism of action has remained elusive to date. In **Chapter 5** we took a closer look at the SEC61 complex and its function in the context of US2-mediated HLA class I downregulation. By creating clonal mutant cell lines of all SEC61/62/63 components, we could assess HLA class I dislocation in great detail. However, we noticed that the HLA-I rescue we observed in these cells was caused not by a defect in ERAD, but by an expression defect in US2. We cannot rule out that SEC61

does facilitate substrate dislocation, but that this effect is overshadowed by the US2 expression defect in the mutant cell lines. As SEC61 facilitates protein import into the ER, and potentially also plays a role in ERAD, these mechanisms have to be carefully distinguished biochemically. If further research confirms that a US2-specific translocation block occurs, potentially caused by US2's inefficient signal peptide, US2 may in the future also be used as a substrate for studies in the field of protein translation and translocation into the ER.

In **Chapter 6** we studied the HCMV protein US11 as a model for ERAD and showed that UBXD8 is involved in recruitment of the essential ATPase p97 to the US11 dislocation complex. While the p97-recruiting UBX domain of UBXD8 lowers p97 recruitment to the ERAD complex, recruitment of the ATPase is not fully eliminated. Additional p97-recruiting factors may therefore play a role as well. As p97 is essential for ER extraction of all known ERAD substrates, insights in its function and recruitment could, with caution, be extrapolated to other ERAD substrates.

Genetic editing and ERAD: holy grail or destined to fail?

CRISPR/Cas9 has opened the door to a new generation of genetic research. While previous attempts to disrupt gene function were often limited to knocking down the expression, CRISPR/Cas9 can fully knock out a gene in a stable manner. This is a promising development in the light of the variable potency of siRNAs and shRNAs and of proteins that are expressed in excess amounts. In the case of siRNAs and shRNAs, knockdown protein populations can remain sufficiently active to fulfill their role, thereby lacking a knockdown phenotype. While CRISPR/Cas9 obviously has its limitations, such as potential off-targets of the CRISPR gRNAs, the potency of this novel technique is indisputable.

In the long term, CRISPR/Cas9 could be used for example to repair mutated genes underlying hereditary diseases. Infectious diseases that were long thought to be incurable, such as HIV- or herpes simplex virus infection, are now re-investigated in the light of a potential cure based on CRISPR/Cas9^{5,6}. The applications of this technique are wider than medicine. Agricultural applications for crop development are currently being tested^{7,8}, which hold the potential to raise resistance against common plant pathogens. The ethics of applying gene editing, whether for medical or agricultural applications, are widely discussed. Ethical decisions as well as technical improvements need to be developed before CRISPR/Cas9 can be applied widely outside a laboratory context. This has become evident at the very moment of submitting this thesis, with the media storm following the notion that a Chinese scientist may have created genetically edited human twin babies⁹. In the field of life sciences research, CRISPR/Cas9 has already caused a revolution in the way research is being performed. Beside the original gene disruption approach, novel applications are developed regularly, ranging from knock-ins to expression control to visual applications with fluorescent Cas9 and countless other experimental applications¹⁰.

CRISPR/Cas9 has allowed for an easier way to disrupt gene function. When interpreting knockout phenotypes, it is important to consider that other knockout-related side effects may occur as well, and actually justify the observed phenotype. One such an unexpected effect observed in our genome-wide CRISPR/Cas9 screen is the SEC61 complex. Previous biochemical approaches have shown that SEC61 is associated with deglycosylated HLA class I when US2 is

present⁴. In addition, the SEC61 complex has been suggested as a candidate channel for protein dislocation¹¹⁻¹⁴. Therefore, and as would be expected, HLA class I surface expression is rescued upon CRISPR/Cas9 targeting of SEC61 (**Chapters 4 and 5**). However, this rescue did not result from a defect in dislocation step of ERAD, but from an unrelated underlying mechanism. Genetic editing of the SEC61 complex, which also facilitates protein translocation into the ER, likely caused a translocation defect resulting in the decline in US2 expression. The diminished US2 expression is the underlying cause of HLA class I rescue, which does however provide interesting information about the function of the SEC complex.

Similarly, the HLA rescue observed in the context of CRISPR/Cas9-targeting of the UFM1 pathway may be an indirect consequence of an unrelated event, as we did not observe UFMylation of factors known to be involved in US2-mediated ERAD. On the other hand, we did observe ribosomal UFMylation. If the UFMylation status of the ribosome affects translation efficacy, this may again cause a US2 expression defect. However, as the HLA rescue effects for UFM1 are not comparable to those observed for SEC61, and as UFM1 may affect ER homeostasis in the context of ER-stress¹⁵⁻¹⁸, a different and yet-uncharacterized mechanism may underlie the HLA rescue phenotype just as well. Extensive biochemical validation in a context different from knocking out the genes, is therefore always crucial not to misinterpret findings from CRISPR/Cas9 knockout screens.

Despite the new possibilities of genetic editing, CRISPR/Cas9 allowed only for the identification of a very limited number of players new to ERAD. This could mean either that all ERAD factors in the context of US2-mediated ERAD have already been identified, or that CRISPR/Cas9 may not be the optimal tool to study this process. Especially when it comes to studying essential cell biological processes, knocking out the responsible genes is not always possible. As a consequence, genes essential for HLA class I downregulation may have remained unidentified in the screen if their knockouts were lethal.

Also when a gene knockout does not have a lethal effect, it may lack a phenotype even when it is involved in the process of interest. The view that knocking out a certain gene will uncover its function because of the gap it leaves, is too simplistic. Interestingly, when studies using gene-disruptive approaches such as CRISPR/Cas9 are compared to those studying the same gene using knockdowns, phenotypes are often seen only in the knockdown cells^{19,20}. This seems counterintuitive, as a cleaner and stronger phenotype is expected upon fully disrupting a gene. However, as these mutations may impact cell survival more severely than a mere knockdown, the lack of phenotype in knockout cells presumably arises from compensatory mechanisms.

In all organisms, a sense of genetic robustness is present, which increases their chances of survival. Upon the occurrence of genetic mutations, compensatory effects occur rapidly as a part of this robustness. This may present itself in the form of gene redundancy, where multiple genes can take over when one becomes dysfunctional, or the alteration of expression of other genes in the same gene network. The latter may occur on the transcriptional level, or genomically, by accumulating mutations in related genes, duplicating these genes or even duplicating whole chromosomes²¹. By changing the entire network's function, the knockout phenotype is often compensated^{19,22}. Essential cellular networks, such as those related to transcription, metabolism or signaling, are

tightly regulated and often compensate disruptive mutations¹⁹. ER-associated protein degradation, being an essential process to prevent the accumulation of potentially aggregating proteins, may be assigned to this category as well.

A lack of phenotype in CRISPR/Cas9 screens therefore does not necessarily mean that the targeted gene is irrelevant to the process. When assessing the role of UBXD8 in HCMV US11 function, we encountered the limitations of knockout phenotypes. While UBXD8 is clearly crucial for US11-mediated HLA-I degradation, UBXD8 knockout cells started to lose their HLA class I rescue phenotype after 1-2 months of culturing. Interestingly, the presence of the Δ UBX mutant, which cannot recruit p97, does provide a stable HLA rescue phenotype, suggesting that it functions as a dominant-negative UBXD8. As we hypothesized that Derlin-1 or TMEM129 may take over p97 recruitment in the absence of functional UBXD8, we tried to create double knockouts of these genes on top of a clonal UBXD8 mutation. However, these cells lost their HLA rescue phenotype before they could be selected fully for the second mutation.

For UFM1, we also observed only a temporary HLA-I rescue, although this was mostly due to the targeted cells slowing down their growth rate and being overgrown in a polyclonal cell population. In a clonal cell population, the phenotype remained intact over long periods of time. Similarly, for the SEC61 complex we could obtain a stable mutant cell population – although half of our clonal lines expressed in-frame mutant alleles rather than containing fully disrupted genes. For our genome-wide CRISPR/Cas9 screen we considered the limitations of CRISPR/Cas9 related to toxicity and compensatory mechanisms. To overcome these limitations, we performed the screen on both an early and a late timepoint (7 and 18 days post-transduction with the gRNA). Potentially, the early timepoint would prevent the loss of cells with a lethal knockout, or the development of compensatory mechanisms, while the late timepoint may identify those genes of which protein turnover is slow. With a median half-life of 40-46 hours for mammalian proteins^{23,24}, most of the original protein pool should have disappeared after 18 days. This approach allowed us to identify a wider range of hits, most of which were identified at only one of the two timepoints.

In search of the way out

SEC61 has long been considered as a retro-translocon (or dislocon) through which ERAD substrates leave the ER to be degraded by the proteasome. As SEC61 also facilitates import of newly translated proteins into the ER, this would mean it could function as a two-way channel. The fact that we observed an expression defect of US2 underlying HLA rescue in SEC61 mutant clones does not rule out that SEC61 may also function as a dislocon.

SEC61 was initially suggested as a dislocon due to the rapid degradation of HLA class I by US2⁴, leaving HLA molecules little time to exit SEC61. This rapid degradation of HLA class I resembles another ER-related protein degradation pathway: ER-stress-induced pre-emptive quality control, or ERpQC^{25,26}. In this pathway, ER proteins are targeted for degradation already co-translationally as a way to alleviate ER stress. Interestingly, the factors involved in ERpQC overlap with those of ERAD: HRD1, Derlin-1, SEC61, p97, Bag6 as well as the proteasome are all involved^{25,26}. ERpQC acts upstream of ERAD, by extracting proteins as they are translocating, rather than relocating fully translocated ER proteins. It can however be envisioned that US2 and

US11 induce a somewhat similar process as they are able to downregulate HLA heavy chains before these reach their mature conformation^{4,27,28}. As a non-glycosylated HLA degradation intermediate was observed in the presence of US11²⁷, this molecule could either be dislocated, or have been targeted for degradation without having ever fully entered the ER in the first place. However, when taking into account the kinetics of protein translocation, it is uncertain whether US2 and US11 target HLA molecules for degradation while they are still associated with the SEC61 complex. After studies in the 1990's suggesting that HLA may not be released from SEC61 before engaging US2, the molecular rates of translation ($\sim 4\text{-}6$ aa/sec on average)²⁹⁻³² and translocation (~ 8 aa/sec)³³ have become available. As translation is the rate-limiting factor during translocation into the ER, the duration of HLA class I insertion can be calculated. With a length of 365 residues and a translation speed of approximately 5 residues per second, insertion of this molecule would take ~ 75 seconds. Dislocated HLA class I molecules occur in the cytosol within 5 minutes when US2 is present⁴. Degradation may start even earlier, but as shorter pulse-chase experiments are not available, nor technically feasible, this cannot easily be determined in detail. Would dislocation occur at the same rate as translocation (8 residues/second), then HLA would require another ~ 45 seconds to return to the cytosol completely. As rapidly as HLA is degraded by US2, a five-minute timeframe may provide sufficient time for the HLA molecule to engage a different protein complex through which dislocation occurs. While SEC61 may certainly function as a dislocon, as is underlined by dislocation-incompetent Sec61 α mutants in yeast^{12,13,34-40}, as well as SEC61-containing ERAD-like complexes for ERpQC^{25,26}, other candidates remain possible, even in the context of the rapid US2- or US11-mediated HLA class I downregulation.

Strikingly, no clear dislocon candidates were identified (besides the SEC61 complex) in our genome-wide CRISPR/Cas9 screen for factors involved in US2-mediated HLA class I degradation. As described above, this can be interpreted in multiple ways: the dislocon could be formed out of known components of US2-mediated degradation, or it could simply not be identified using CRISPR/Cas9 due to lethality of a knockout or redundancy with other gene(s).

Other candidates for the dislocation complex have been suggested previously, such as the E3 ubiquitin ligase Hrd1 or Derlin proteins^{26,41-47}. Dimeric yeast Hrd1 forms a funnel-like ER-transmembrane channel in complex with Hrd3, which may function as a dislocon⁴¹. Neither HRD1 nor Derlin-1 however play a role in the context of US2. Interestingly, the E3 ubiquitin ligase TRC8, which is essential for US2 function, spans the ER membrane with 12 transmembrane domains. As the C-terminal portion of TRC8 closely resembles the dislocon-like structure of yeast Hrd1⁴¹, it is well possible that this E3 ligase can also function as a dislocation complex. Moreover, while Hrd1, containing 8 transmembrane domains, forms a dimeric ER-membrane complex, TRC8's 12 transmembrane domains may allow it to form a channel by itself. For comparison, the trimeric translocon, consisting of SEC61 $\alpha/\beta/\gamma$, also contains 12 transmembrane helices in total, suggesting that TRC8 is potentially large enough to form a pore through which peptide chains can pass.

The identification of the translocon may provide insights for the definitive identification of the dislocon. A genetic screen by the Schekman lab in 1979, using *S. cerevisiae*, identified the first mutants with a defective 'Sec'retory pathway⁴⁸, coining the first Sec family member Sec1-1. In

the late 1980's and early 1990's, further genetic screens in yeast identified initially that Sec61, and later also Sec62 and Sec63 mutants were deficient in protein translocation into the ER⁴⁹⁻⁵¹. A mechanistic approach, using purified Sec proteins *in vitro* to identify the minimal requirements for translocation, finally showed that the Sec complex is essential and sufficient for translocation of proteins into the ER^{52,53}. These genome-wide screening approaches resemble our current methods, where genetic screens are used initially for identification of potential candidates, followed by a biochemical approach. However, biochemical identification of the dislocon is potentially more challenging than that of the translocon. In case of protein import into the ER, detection of ER-resident proteins directly confirms the presence of a functional translocation complex. For protein export however, a two-step process is required: proteins first need to be accumulated inside ER vesicles, followed by their removal from the vesicles. As translocation and dislocation may be coupled or be functioning simultaneously, major technical hurdles have to be taken in such an approach. Particularly testing the SEC61 complex this way would be challenging, as it may affect protein transport in both directions. The yeast mutants of SEC61 with 'one-way defects' are very interesting in this regard.

Yeast models with purified ERAD components have recently been employed successfully to prove that Hrd1 can facilitate dislocation of ERAD-L substrates in yeast. Two types of ERAD-L substrates were tested in this regard: the ER-luminal CPY*⁴² and a CPY* fused to a transmembrane domain⁴³. In both cases, homo-oligomerized Hrd1 could function as dislocon, ubiquitinase of CPY*, as well as recruiter of Cdc48, the yeast homolog of p97. However, as only Hrd1 but no other candidates were tested as a dislocon, it remains unclear whether Hrd1 is the only dislocon in *S. cerevisiae*, or whether multiple different complexes may exist. Moreover, the *in vitro* approach used in these studies was based on overexpressed Hrd1, which may potentially cause artificial effects: ERAD-M substrates that are normally not dislocated by Hrd1, but instead use the Derlin-like protein Dfm1, become a target of Hrd1 upon overexpression of this ubiquitin ligase. *ΔDfm1* cells accumulate ERAD-M substrates due to a defect in dislocation. This knockout is compensated naturally, by a gene duplication of Hrd1. When Hrd1 expression is raised in a *ΔDfm1* context as a result of this gene duplication, it takes over Dfm1's function⁵⁴.

Nonetheless, an approach with purified components provides an elegant way to test the substrate dislocation ability and sufficiency of dislocon candidates. Assuming that Hrd1 does not show artificial phenotypes *in vitro*, a speculative mechanism for dislocation can be deduced from these findings. Hrd1 auto-ubiquitination is crucial for substrate dislocation, but ubiquitinated Hrd1 cannot bind a substrate itself⁵⁵. As Hrd3 stabilizes Hrd1 *in vivo* by preventing its auto-ubiquitination⁵⁶, one could speculate that Hrd3 keeps Hrd1 in a conformation capable of interacting with a substrate. Once bound, Hrd3 may release Hrd1, which would then auto-ubiquitinate and cause dislocation. However, as ubiquitinated Hrd1 is also subject to proteasomal degradation itself, it might even dislocate along with the ERAD substrate into the cytosol.

While homologs of Hrd1 and Hrd3 exist in mammals as well (called HRD1 and SEL1L respectively), and both factors are crucial for dislocation, the mammalian system seems to function in a different way. In contrast to yeast, SEL1L does not stabilize HRD1. Instead, HRD1 stabilizes SEL1L. Moreover, mammalian ERAD requires many other factors for dislocation. Curiously, overexpression of SEL1L and HRD1 together lowers dislocation efficiency, perhaps because

the stoichiometry with endogenous ERAD components is disrupted upon overexpression of HRD1 and SEL1L, which also interact with one another outside the context of the other ERAD factors⁵⁷.

Taking advantage of the manipulators

As US2 and US11 are viral proteins, knowing their mechanism of action as well as how to block it sounds, at first sight, as a good way to treat HCMV infection. Although a recombinant rhesus CMV that lacks its HLA-downregulating evasins is still able to cause persistent infection⁵⁸, this lack of HLA class I evasion does result in immunological memory, in contrast to natural CMV strains. As a result of this immunological memory, evasion-incompetent CMV protects rhesus macaques against superinfection with novel CMV strains⁵⁸. If the same holds true for human cytomegalovirus, prophylactic ‘vaccination’ with an evasion-incompetent HCMV may theoretically be used to protect against subsequent natural infection. This would be particularly interesting at a pre-pregnancy age. The benefits of such prophylaxis may however not outweigh the risks. In most adults, HCMV infection is relatively mild. The priority for protecting against the virus is therefore low. Importantly however, the prophylactic virus may be transmitted to non-vaccinated neonates or pregnant women, to whom it may cause serious adverse effects. Antiviral therapy may therefore not be the most promising application of the knowledge provided by this thesis. A broader and more promising clinical application would be to use the knowledge that US2 and US11 provide about ERAD. This can aid the development of treatments against the large number of diseases related to protein degradation (**Chapter 1**). Recently, the first clinical drugs targeting protein degradation have become available for treating malignancies. In these cancer types, aberrant or excessive degradation of cell cycle-regulating proteins is prevented as a treatment. Proteasome inhibitors such as bortezomib, carfilzomib and ixazomib are now used for treating multiple myeloma and non-Hodgkin lymphomas⁵⁹⁻⁶¹. In an experimental *ex vivo* approach in mice, the common cystic fibrosis-causing CFTR mutant $\Delta F508$ was also successfully rescued from ERAD using proteasome inhibitors⁶², which underlines how the proteasome could be a drug target for a wider range of diseases than malignancies alone. Another drug, the p97 inhibitor CB-5083 that was used in this thesis, shows promising results in multiple myeloma model systems⁶¹. The heat shock proteins (HSPs) upstream of ERAD are also interesting drug targets. Besides regulation of apoptosis, HSPs are involved in regulating cell cycle progression and immune surveillance against cancer⁶³. Multiple HSP90 antagonists, such as Ganetespib, Luminespib and Retaspimycin have been or are being tested in clinical trials as antineoplastic drugs, although many did not meet the expectations in phase III trials⁶⁴⁻⁶⁶. As these ERAD-targeting drugs are still being tested or have entered the market only recently, this may be only the beginning of a new class of drugs. A better understanding of ERAD may eventually allow for the development of novel and improved drugs, targeting a broader range of diseases related to protein degradation, such as cystic fibrosis, muscle dystrophies and neurological disorders such as Parkinson’s disease^{67,68}.

Combatting one virus with another

The immune-modulatory features of CMV may also provide a clinical application in a completely

different setting. A primate model testing a vaccine against simian immunodeficiency virus (SIV, the primate variant of HIV), showed that the use of a CMV vector as vaccine backbone elicited an unconventional but highly protective immune response⁶⁹. A T-cell response is normally limited to a specific set of epitopes determined by the individual's MHC alleles. This narrow set of epitopes that are targeted limits an appropriate response against genetically flexible viruses like SIV or HIV, especially since many dominant CD8⁺ T cell epitopes are contained in non-essential and hence variable regions of the HIV or SIV genome. CMV's immune-modulatory features that downregulate MHC class I block the development of a classic MHC class I immune response. This allows the development of an unconventional, subdominant response beneficial for combating SIV infection. The absence of the CMV proteins UL128, UL130 and UL131 enhanced the potency of this immune response by inducing promiscuity in antigen presentation.

The unconventional immune response that was developed as a consequence of the vaccination was based on a number of antigens more than three times as broad as conventional CD8⁺ T cell immunity. Among the antigens of this response were highly promiscuous 'supertopes', which can be presented across disparate MHC alleles. These antigens are not presented in naturally SIV-infected primates or those vaccinated with a different backbone. Moreover, 70% of these 'supertopes' were presented on MHC class II and recognized by a rare set of MHC class II-specific CD8⁺ T cells. Although recognizing MHC II, these CD8⁺ T cells are not confined to a specific allotype. This immune response protected 50% of vaccinated rhesus macaques against the establishment of SIV infection, even when mucosal infection was bypassed by direct intravenous injection. Most strikingly, when vaccinated rhesus macaques were followed over longer periods of time (up to 3.5 years), SIV became undetectable in all animals after 70 weeks⁷⁰. This suggests the macaques are cured of SIV, a concept in stark contrast with the paradigm that SIV or HIV infections can be suppressed but are impossible to cure.

Concluding remarks

The rapid and effective induction of ER-associated HLA class I degradation by US2 and US11 is a useful model to study ER protein quality control and -turnover. Many factors involved in ERAD have been identified using US2 and US11, and with technical developments, this number may increase even further. A better knowledge of ERAD allows for the identification of novel drug targets in this pathway, and thereby a potential treatment for a wide range of protein degradation-related diseases.

REFERENCES

1. Busche, a. *et al.* Priming of CD8⁺ T Cells against Cytomegalovirus-Encoded Antigens Is Dominated by Cross-Presentation. *J. Immunol.* **190**, 2767–2777 (2013).
2. Van De Weijer, M. L. *et al.* A high-coverage shRNA screen identifies TMEM129 as an E3 ligase involved in ER-associated protein degradation. *Nat. Commun.* **5**, 1–14 (2014).

3. Flierman, D., Coleman, C. S., Pickart, C. M., Rapoport, T. a & Chau, V. E2-25K mediates US11-triggered retro-translocation of MHC class I heavy chains in a permeabilized cell system. *Proc. Natl. Acad. Sci. U. S. A.* **103**, 11589–11594 (2006).
4. Wiertz, E. J. H. J. *et al.* Sec61-mediated transfer of a membrane protein from the endoplasmic reticulum to the proteasome for destruction. *Nature* **384**, 432–438 (1996).
5. van Diemen, F. R. *et al.* CRISPR/Cas9-Mediated Genome Editing of Herpesviruses Limits Productive and Latent Infections. *PLoS Pathog.* **12**, 1–29 (2016).
6. Lebbink, R. J. *et al.* A combinational CRISPR/Cas9 gene-editing approach can halt HIV replication and prevent viral escape. *Sci. Rep.* **7**, 1–10 (2017).
7. Liang, Z. *et al.* Efficient DNA-free genome editing of bread wheat using CRISPR/Cas9 ribonucleoprotein complexes. *Nat. Commun.* **8**, 1–5 (2017).
8. Shan, Q. *et al.* Targeted genome modification of crop plants using a CRISPR-Cas systems. *Nat. Biotechnol.* **31**, 686–688 (2013).
9. Saey, T. H. Chinese scientists raise ethical questions with first gene-edited babies. *Science News* Available at: <https://www.sciencenews.org/article/chinese-scientists-raise-ethical-questions-first-crispr-gene-edited-babies>. (Accessed: 30th November 2018)
10. Zhang, Z. *et al.* CRISPR/Cas9 Genome-Editing System in Human Stem Cells: Current Status and Future Prospects. *Mol. Ther. - Nucleic Acids* **9**, 230–241 (2017).
11. Lloyd, D. J., Wheeler, M. C. & Gekakis, N. A Point Mutation in Sec61alpha1 Leads to Diabetes and Hepatosteatosis in Mice. *Diabetes* **59**, 460–470 (2010).
12. Ng, W., Sergeyenko, T., Zeng, N., Brown, J. D. & Romisch, K. Characterization of the proteasome interaction with the Sec61 channel in the endoplasmic reticulum. *J. Cell Sci.* **120**, 682–691 (2007).
13. Tretter, T. *et al.* ERAD and protein import defects in a sec61 mutant lacking ER-luminal loop 7. *BMC Cell Biol.* **14**, 1–14 (2013).
14. Pilon, M., Schekman, R. & Römisch, K. Sec61p mediates export of a misfolded secretory protein from the endoplasmic reticulum to the cytosol for degradation. *EMBO J.* **16**, 4540–4548 (1997).
15. Liu, J. *et al.* A critical role of DDRGK1 in endoplasmic reticulum homeostasis via regulation of IRE1 α stability. *Nat. Commun.* **8**, 1–12 (2017).
16. Hu, X. *et al.* Ubiquitin-fold modifier 1 inhibits apoptosis by suppressing the endoplasmic reticulum stress response in Raw264.7 cells. *Int. J. Mol. Med.* **33**, 1539–1546 (2014).
17. Yoo, H. M. *et al.* Modification of ASC1 by UFM1 is crucial for ER α transactivation and breast cancer development. *Mol. Cell* **56**, 261–274 (2014).
18. Lemaire, K. *et al.* Ubiquitin fold modifier 1 (UFM1) and its target UFBP1 protect pancreatic beta cells from ER stress-induced apoptosis. *PLoS One* **6**, (2011).
19. El-Brolosy, M. A. & Stainier, D. Y. R. Genetic compensation: A phenomenon in search of mechanisms. *PLoS Genet.* **13**, 1–17 (2017).

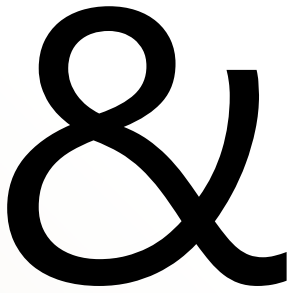
20. Rossi, A. *et al.* Genetic compensation induced by deleterious mutations but not gene knockdowns. *Nature* **524**, 230–233 (2015).
21. Ryu, H. Y., Wilson, N. R., Mehta, S., Hwang, S. S. & Hochstrasser, M. Loss of the SUMO protease ULP2 triggers a specific multichromosome aneuploidy. *Genes Dev.* **30**, 1881–1894 (2016).
22. Teng, X. *et al.* Genome-wide consequences of deleting any single gene. *Mol. Cell* **52**, 485–494 (2013).
23. Schwanhüsser, B. *et al.* Global quantification of mammalian gene expression control. *Nature* **473**, 337–342 (2011).
24. Milo, R. & Phillips, R. in *Cell Biology by the Numbers* (eds. Milo, R. & Phillips, R.) 294–298 (2015).
25. Kadowaki, H. *et al.* Pre-emptive Quality Control Protects the ER from Protein Overload via the Proximity of ERAD Components and SRP. *Cell Rep.* **13**, 944–956 (2015).
26. Kadowaki, H., Satrimafitrah, P., Takami, Y. & Nishitoh, H. Molecular mechanism of ER stress-induced pre-emptive quality control involving association of the translocon, Derlin-1, and HRD1. *Sci. Rep.* **8**, 1–11 (2018).
27. Wiertz, E. J. H. J. *et al.* The human cytomegalovirus US11 gene product dislocates MHC class I heavy chains from the endoplasmic reticulum to the cytosol. *Cell* **84**, 769–79 (1996).
28. Barel, M. T., Hassink, G. C., Voorden, S. Van & Wiertz, E. J. H. J. Human cytomegalovirus-encoded US2 and US11 target unassembled MHC class I heavy chains for degradation. *Mol. Immunol.* **43**, 1258–1266 (2006).
29. Hartl, F. U. & Hayer-Hartl, M. Converging concepts of protein folding in vitro and in vivo. *Nat. Struct. Mol. Biol.* **16**, 574–581 (2009).
30. Kim, Y. E., Hipp, M. S., Bracher, A., Hayer-Hartl, M. & Hartl, U. F. *Molecular chaperones in protein folding and proteostasis.* *Nature* **475**, (2011).
31. Ingolia, N. T., Lareau, L. F. & Weissman, J. S. Ribosome Profiling of Mouse Embryonic Stem Cells Reveals the Complexity and Dynamics of Mammalian Proteomes. *Cell* **147**, 789–802 (2011).
32. Uri, M. B10NUMB3R5 - Rate at which ribosomes progress from 5' ends of transcripts. Available at: <http://bionumbers.hms.harvard.edu/bionumber.aspx?&id=107952>. (Accessed: 29th October 2018)
33. Goder, V., Crottet, P. & Spiess, M. In vivo kinetics of protein targeting to the endoplasmic reticulum determined by site-specific phosphorylation. *EMBO J.* **19**, 6704–6712 (2000).
34. Plemper, R. K., Böhmmler, S., Bordallo, J., Sommer, T. & Wolf, D. H. Mutant analysis links the translocon and BIP to retrograde protein transport for ER degradation. *Nature* **388**, 891–895 (1997).

35. Plemper, R. K., Egner, R., Kuchler, K. & Wolf, D. H. Endoplasmic Reticulum Degradation of a Mutated ATP-binding Cassette Transporter Pdr5 Proceeds in a Concerted Action of Sec61 and the Proteasome Endoplasmic Reticulum Degradation of a Mutated ATP-binding Cassette Transporter P. *J Biol Chem* **273**, 32848–32856 (1998).
36. Wheeler, M. C. & Gekakis, N. Defective ER associated degradation of a model luminal substrate in yeast carrying a mutation in the 4th ER luminal loop of Sec61p. *Biochem. Biophys. Res. Commun.* **427**, 768–773 (2012).
37. Willer, M., Forte, G. M. A. & Stirling, C. J. Sec61p is required for ERAD-L: Genetic dissection of the translocation and ERAD-L functions of Sec61P using novel derivatives of CPY. *J. Biol. Chem.* **283**, 33883–33888 (2008).
38. Römisch, K. A Case for Sec61 Channel Involvement in ERAD. *Trends Biochem. Sci.* **42**, 171–179 (2017).
39. Scott, D. C. & Schekman, R. Role of Sec61p in the ER-associated degradation of short-lived transmembrane proteins. *J. Cell Biol.* **181**, 1095–1105 (2008).
40. Schäfer, A. & Wolf, D. H. Sec61p is part of the endoplasmic reticulum-associated degradation machinery. *EMBO J.* **28**, 2874–2884 (2009).
41. Schoebel, S. *et al.* Cryo-EM structure of the protein-conducting ERAD channel Hrd1 in complex with Hrd3. *Nature* **548**, 352–355 (2017).
42. Stein, A., Ruggiano, A., Carvalho, P. & Rapoport, T. a. Key Steps in ERAD of Luminal ER Proteins Reconstituted with Purified Components. *Cell* **158**, 1375–1388 (2014).
43. Baldrige, R. D. & Rapoport, T. A. Autoubiquitination of the Hrd1 Ligase Triggers Protein Retrotranslocation in ERAD. *Cell* **166**, 394–407 (2016).
44. Lilley, B. N. & Ploegh, H. L. A membrane protein required for dislocation of misfolded proteins from the ER. *Nature* **429**, 834–840 (2004).
45. Lilley, B. N. & Ploegh, H. L. Multiprotein complexes that link dislocation, ubiquitination, and extraction of misfolded proteins from the endoplasmic reticulum membrane. *Proc. Natl. Acad. Sci. U. S. A.* **102**, 14296–14301 (2005).
46. Claessen, J. H. L., Mueller, B., Spooner, E., Pivorunas, V. L. & Ploegh, H. L. The transmembrane segment of a tail-anchored protein determines its degradative fate through dislocation from the endoplasmic reticulum. *J. Biol. Chem.* **285**, 20732–20739 (2010).
47. Carvalho, P., Stanley, A. M. & Rapoport, T. a. Retrotranslocation of a misfolded luminal ER protein by the ubiquitin-ligase Hrd1p. *Cell* **143**, 579–591 (2010).
48. Novick, P. & Schekman, R. Secretion and cell-surface growth are blocked in a temperature-sensitive mutant of *Saccharomyces cerevisiae*. *Proc. Natl. Acad. Sci.* **76**, 1858–1862 (1979).
49. Deshaies, R. J. & Schekman, R. A yeast mutant defective at an early stage in import of secretory protein precursors into the endoplasmic reticulum. *J. Cell Biol.* **105**, 633–645 (1987).

50. Rothblatt, J. A., Deshaies, R. J., Sanders, S. L., Daum, G. & Schekman, R. Multiple genes are required for proper insertion of secretory proteins into the endoplasmic reticulum in yeast. *J. Cell Biol.* **109**, 2641–2652 (1989).
51. Deshaies, R. J., Sanders, S. L., Feldheim, D. A. & Schekman, R. Assembly of yeast Sec proteins involved in translocation into the endoplasmic reticulum into a membrane-bound multisubunit complex. *Nature* **349**, 806–808 (1991).
52. Görlich, D. & Rapoport, T. A. Protein translocation into proteoliposomes reconstituted from purified components of the endoplasmic reticulum membrane. *Cell* **75**, 615–630 (1993).
53. Oliver, J., Jungnickel, B., Görlich, D., Rapoport, T. & High, S. The Sec61 complex is essential for the insertion of proteins into the membrane of the endoplasmic reticulum. *FEBS Lett.* **362**, 126–130 (1995).
54. Neal, S. *et al.* The Dfm1 Derlin Is Required for ERAD Retrotranslocation of Integral Membrane Proteins. *Mol. Cell* **69**, 306–320.e4 (2018).
55. Baldrige, R. D. & Rapoport, T. A. Autoubiquitination of the Hrd1 Ligase Triggers Protein Retrotranslocation in ERAD. *Cell* **166**, 394–407 (2016).
56. Plemper, R. K. *et al.* Genetic interactions of Hrd3p and Der3p/Hrd1p with Sec61p suggest a retro-translocation complex mediating protein transport for ER degradation. *J. Cell Sci.* **112**, 4123–34 (1999).
57. Iida, Y. *et al.* SEL1L protein critically determines the stability of the HRD1-SEL1L Endoplasmic Reticulum-associated Degradation (ERAD) complex to optimize the degradation kinetics of ERAD substrates. *J. Biol. Chem.* **286**, 16929–16939 (2011).
58. Hansen, S. G. *et al.* Evasion of CD8+ T cells is critical for superinfection by cytomegalovirus. *Science* **328**, 102–6 (2010).
59. Reinstein, E. & Ciechanover, A. Narrative Review: Protein Degradation and Human Diseases: The Ubiquitin Connection. *Ann. Intern. Med.* **145**, 676 (2006).
60. Field-Smith, A., Morgan, G. J. & Davies, F. E. Bortezomib (Velcade/trade mark) in the Treatment of Multiple Myeloma. *Ther. Clin. Risk Manag.* **2**, 271–9 (2006).
61. Le Moigne, R. *et al.* The p97 inhibitor CB-5083 is a unique disrupter of protein homeostasis in models of Multiple Myeloma. *Mol. Cancer Ther.* **16**, 2375–2386 (2017).
62. Wilke, M., Bot, A., Jorna, H., Scholte, B. J. & de Jonge, H. R. Rescue of Murine F508del CFTR Activity in Native Intestine by Low Temperature and Proteasome Inhibitors. *PLoS One* **7**, e52070 (2012).
63. Romanucci, M., Bastow, T. & Della Salda, L. Heat shock proteins in animal neoplasms and human tumours - A comparison. *Cell Stress Chaperones* **13**, 253–262 (2008).
64. Medicine, T. U. N. L. of. A Phase 3 Study of Ganetespib in Combination With Docetaxel Versus Docetaxel Alone in Patients With Advanced NSCLC (Galaxy 2). Available at: <https://clinicaltrials.gov/ct2/show/results/NCT01798485>. (Accessed: 2nd November 2018)

65. Piotrowska, Z. *et al.* Activity of the Hsp90 inhibitor Luminespib Among Non-Small Cell Lung Cancers Harboring EGFR Exon 20 Insertions. *Ann. Oncol. Off. J. Eur. Soc. Med. Oncol.* **90**, 1–6 (2018).
66. Reuters. Infinity Pharma's cancer drug fails mid-stage trial goals. Available at: <https://www.reuters.com/article/infinity-cancerdrug-idUSL4N0HL2S220130925>. (Accessed: 2nd November 2018)
67. Guerriero, C. J. & Brodsky, J. L. The delicate balance between secreted protein folding and endoplasmic reticulum-associated degradation in human physiology. *Physiol. Rev.* **92**, 537–576 (2012).
68. Zhao, L. & Ackerman, S. L. Endoplasmic reticulum stress in health and disease. *Curr. Opin. Cell Biol.* **18**, 444–452 (2006).
69. Hansen, S. G. *et al.* Cytomegalovirus Vectors Violate CD8+ T Cell Epitope Recognition Paradigms. *Science (80-.)*. **340**, 1237874–1237874 (2013).
70. Hansen, S. G. *et al.* Immune clearance of highly pathogenic SIV infection. *Nature* **502**, 100–104 (2013).





Appendices

- Nederlandse samenvatting voor niet-ingewijden
- Dankwoord
- Publicaties
- Curriculum vitae

A.B.C. Schuren

Dept. Medical Microbiology, University Medical Center Utrecht, 3584CX Utrecht, The Netherlands.



NEDERLANDSE SAMENVATTING VOOR NIET- INGEWIJDEN

Gedeeltelijk gepubliceerd op [Scientias.nl](https://www.scientias.nl)

IN HET KORT

Kwaliteitscontrole is enorm belangrijk voor het goed functioneren en zelfs de veiligheid van de spullen om ons heen. Ook in de cellen van ons lichaam vindt constant kwaliteitscontrole plaats. Wanneer deze controle faalt, ontstaan er ernstige ziektes zoals taaislijmziekte, Parkinson of diabetes.

In dit proefschrift heb ik de kwaliteitscontrole in cellen onderzocht. Hiervoor heb ik gebruik gemaakt van een virus dat dit systeem manipuleert. Virussen worden normaal gesproken herkend en opgeruimd door het immuunsysteem. Dit virus, CMV (cytomegalovirus), weet echter te ontkomen aan het immuunsysteem. Het zorgt er namelijk voor dat componenten van het immuunsysteem, waarmee een virusinfectie normaal zou worden herkend, worden afgebroken door de kwaliteitscontrole, zelfs wanneer hun kwaliteit in orde is. Omdat de werking van het immuunsysteem wordt verstoord, kan het virus onzichtbaar blijven en zich levenslang vestigen in het lichaam.

Heb je wel eens een koortslip gehad? Dan is het je misschien opgevallen dat deze vervelende zweertjes vaak terugkomen wanneer je afweer is verzwakt. Dat komt omdat het soort virus dat een koortslip veroorzaakt ongezien in het lichaam aanwezig blijft. Deze virussen manipuleren namelijk het immuunsysteem om te voorkomen dat ze worden opgeruimd. Wanneer de afweer verzwakt is, grijpen dit soort virussen hun kans en veroorzaken bijvoorbeeld een nieuwe koortslip.

Er zijn verschillende soorten herpesvirussen die aan elkaar gerelateerd zijn. Niet alleen het virus dat een koortslip veroorzaakt, Herpes Simplex Virus type 1, maar ook de virussen die waterpokken of de ziekte van Pfeiffer veroorzaken zijn lid van deze familie van virussen. Deze virussen, samen de herpesvirussen genaamd, komen erg vaak voor: vrijwel iedereen is geïnfecteerd met één of meerdere herpesvirussen, meestal zonder zich hiervan bewust te zijn.

Type herpesvirus	Symptomen	% geïnfecteerd
Herpes Simplex Virus-1 (HSV-1)	koortslip, soms genitale herpes, oogontsteking	~50-70%
Herpes Simplex Virus-2 (HSV-2)	genitale herpes, soms koortslip	~20-30%
Varicella Zoster Virus (VZV)	waterpokken, gordelroos	~95%
Epstein-Barr Virus (EBV)	Meestal geen symptomen, anders ziekte van Pfeiffer. In zeldzame gevallen kan dit virus kanker veroorzaken.	~90%
Humaan Cytomegalovirus (HCMV)	Meestal geen symptomen of Pfeiffer-achtige symptomen, anders aangeboren afwijkingen, longontsteking, maagontsteking of afstoting van getransplanteerde organen.	~40-60%
Humaan Herpesvirus-6 (HHV-6)	Zesde ziekte (kinderziekte)	> 90%
Humaan Herpesvirus-7 (HHV-7)	Zesde ziekte (kinderziekte)	onbekend
Kaposi's Sarcoma-geassocieerd Herpesvirus (KSHV)	Kaposi's sarcoma (zeldzame vorm van huidkanker)	< 5%

Tabel 1 | Overzicht van de verschillende herpesvirussen en hoe vaak ze voorkomen. Het percentage geïnfecteerde personen is gebaseerd op de Nederlandse situatie, waarbij is gekeken naar of diegene op dat moment een actieve infectie doormaakt, of in het verleden met het virus is geïnfecteerd en het virus in inactieve vorm bij zich draagt. Cijfers afkomstig van het RIVM.

CMV, moeder der geboortefwijkingen

In dit proefschrift heb ik gewerkt aan een virus dat nauw verwant is aan dat van de koortslip. Dit virus, cytomegalovirus (CMV) genaamd, geniet maar weinig bekendheid. Toch is ongeveer de helft van de Nederlandse bevolking ermee besmet, meestal zonder dat mensen het zelf weten. Van een infectie met CMV merk je meestal dan ook maar weinig. In sommige gevallen kan het virus echter veel schade toebrengen. Wanneer een vrouw tijdens de zwangerschap geïnfecteerd raakt met CMV, kan dit resulteren in ernstige afwijkingen aan het ongeboren kind. Ook vrouwen die



al vóór hun zwangerschap geïnfecteerd zijn geweest met CMV lopen een risico: net als bij een koortslip blijft ook CMV levenslang in het lichaam aanwezig. Wanneer het virus opnieuw actief wordt tijdens de zwangerschap, kan het kind geïnfecteerd worden.

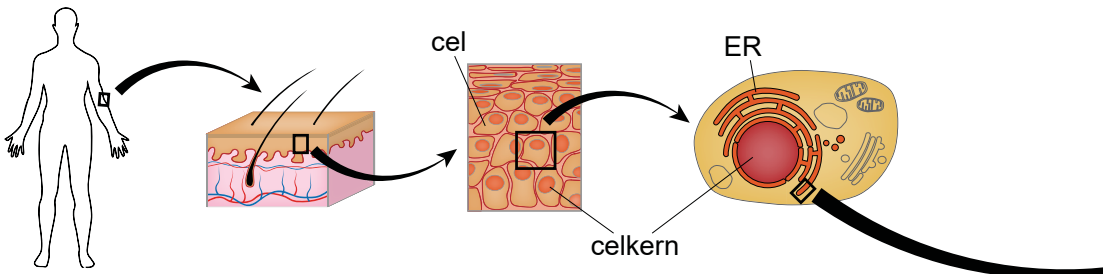
CMV is de meest voorkomende infectieuze oorzaak van aangeboren afwijkingen. Eén op de 50 tot 100 vrouwen raakt tijdens de zwangerschap geïnfecteerd met CMV, wat in eenderde van de gevallen leidt tot symptomen bij de baby. Het aantal vrouwen bij wie reeds aanwezig virus opnieuw actief wordt en vervolgens het kind infecteert, ligt nog hoger. Ieder jaar worden in Nederland rond de 1000 baby's geboren met een CMV-infectie. Ongeveer 180 van hen ontwikkelen symptomen zoals een laag geboortegewicht, blind- of doofheid, epilepsie of een ontwikkelingsachterstand. Ook bij mensen met een lage afweer, zoals ouderen of mensen die een orgaandonatie hebben ondergaan, kan het virus ernstige klachten veroorzaken.

Er is geen vaccin beschikbaar tegen CMV, en ook behandeling van het kind tijdens de zwangerschap is moeilijk tot onmogelijk. Mocht er een behandeling van aangeboren CMV worden ontwikkeld, dan is het belangrijk om meer kennis op te doen over dit virus.

Evasie van de antivirale afweer

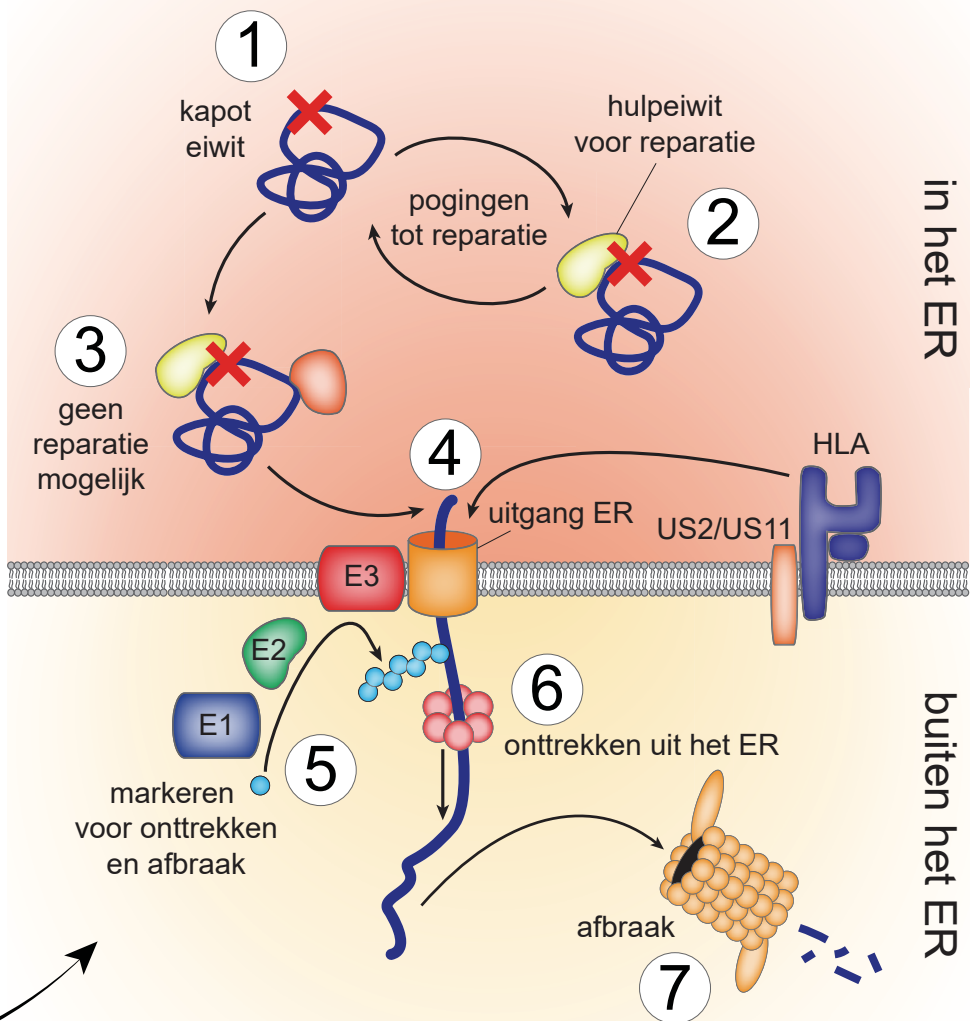
Hét kenmerk van niet alleen CMV, maar ook alle daaraan verwante virussen, is dat deze zogenaamde herpesvirussen een groot repertoire aan mechanismen hebben waarmee ze herkenning door het immuunsysteem kunnen omzeilen. Dit zorgt ervoor dat deze virussen levenslang in het lichaam aanwezig kunnen blijven en opnieuw actief kunnen worden. Andere virussen, zoals bijvoorbeeld bij een verkoudheid, worden meestal binnen korte tijd opgeruimd door het immuunsysteem.

Dit alles vindt plaats op het niveau van cellen, de bouwstenen van het lichaam (zie afbeelding hieronder). Ieder weefsel van een lichaam, zoals bijvoorbeeld de huid, is opgebouwd uit cellen. Virussen zijn veel kleiner en simpeler dan cellen en kunnen zichzelf niet onderhouden. Toch wil een virus – net als ieder wezen – zichzelf graag voortplanten. Een virus is daarvoor afhankelijk van lichaamscellen: het dringt er binnen en maakt gebruik van de lopende processen in een cel om zich voort te planten. Een virus kan cellen zodanig in zijn macht krijgen dat ze zich alleen nog kunnen richten op het produceren van nieuwe virusdeeltjes en zichzelf verwaarlozen. Veel cellen gaan dan ook dood als ze zijn geïnfecteerd met een virus, wat schade aan het lichaam tot gevolg kan hebben. Nieuw gemaakte virussen verspreiden zich vervolgens door het lichaam of naar andere mensen, waar ze de infectie zullen uitbreiden en nog meer schade aanrichten. Het lichaam gaat dit tegen door virussen op te sporen met behulp van het immuunsysteem.



In mijn proefschrift heb ik me gericht op twee componenten van CMV, genaamd US2 en US11. Deze virus-eiwitten zorgen ervoor dat een cruciaal onderdeel van het immuunsysteem wordt afgebroken.

Omdat virussen binnenin geïnfecteerde cellen zitten en immuuncellen alleen aan de buitenkant kunnen patrouilleren, heeft de afweer een handig systeem ontwikkeld: iedere cel bevat een soort grijp-armen die fragmenten van de binnenkant van de cel vangen en deze mee naar buiten nemen, vergelijkbaar met de grijpmachines op de kermis. In tegenstelling tot grijpmachines gaan de grijp-armen in cellen (ook wel HLA genoemd) mee naar de buitenkant van de cel, waar ze de celfragmenten tonen. Patrouillerende immuuncellen kunnen zo detecteren wat er binnenin cellen gebeurt. Wanneer de er een fragment van een virus getoond wordt op het celoppervlak, zal



het immuunsysteem herkennen dat deze cel geïnfecteerd is. Afweercellen doden de geïnfecteerde cel dan om verdere verspreiding van de infectie tegen te gaan. De virus-eiwitten US2 en US11 zorgen ervoor dat het HLA op hoge snelheid wordt afgebroken, nog voordat het cel- of virusfragmenten aan zich kan binden. Zo wordt voorkomen dat CMV-besmette cellen verslag uitbrengen aan het immuuncellen, waardoor de infectie onzichtbaar blijft voor het immuunsysteem.

Het remmen van US2 en US11 kan een aanknopingspunt zijn voor behandeling van CMV. De HLA-afbraak die deze virus-eiwitten in gang zetten, biedt echter inzichten die voor veel meer ziektes relevant kunnen zijn. Meer dan 70 ziektes zijn gerelateerd aan het type eiwitafbraak dat US2 en US11 in gang zetten. Zo vindt er bij taaislijmziekte te veel afbraak plaats, terwijl bij hersenziektes zoals Parkinson juist kapotte eiwitten ophopen. Ook bij kanker is de afbraak van eiwitten vaak verstoord.

Van cel tot eiwit tot afbraak

Om beter te begrijpen hoe de afbraak van HLA plaatsvindt, is het belangrijk om te begrijpen hoe een cel aan de binnenkant werkt. De cellen van ons lichaam bevatten allerlei compartimenten, zoals de celkern, waarin zich het DNA bevindt. Het DNA is een handleiding om eiwitten mee te maken. Deze eiwitten, waarvan er duizenden verschillenden bestaan, voeren alle processen uit die in een cel plaatsvinden. Ongeveer eenderde van alle eiwitten wordt naar hun plaats van bestemming gestuurd via het logistieke centrum van de cel, het ER (endoplasmatisch reticulum). Aangekomen in het ER worden eiwitten aan uitgebreide kwaliteitscontrole onderworpen, omdat kapotte eiwitten ernstige gevolgen kunnen hebben, zoals de eerdergenoemde ziektes.

Normaal gesproken vindt afbraak van eiwitten alleen plaats na kwaliteitscontrole. Functioneert een eiwit niet goed (stap 1 in de rechter afbeelding), dan wordt eerst geprobeerd het te repareren (stap 2). Een eiwit dat niet meer te repareren valt, wordt herkend door de opruimingsdienst (3), die het kapotte eiwit uit het ER verwijdert (4). Eenmaal buiten het ER, waar zich de andere tweederde van alle eiwitten bevindt, moet het signaal worden doorgegeven dat dit eiwit kapot is. Daarom wordt er door een samenwerking van E1-, E2- en E3-eiwitten een markering aan gehangen (5). Eenmaal gemarkeerd wordt het eiwit herkend door een pomp die het kapotte eiwit uit het ER trekt (6). Uiteindelijk komt het kapotte eiwit terecht in de vuilverbrander van de cel (7), die eiwitten kapot knipt zodat de bouwstenen opnieuw gebruikt kunnen worden om nieuwe eiwitten mee te maken.

US2 en US11 manipuleren dit proces, door ervoor te zorgen dat normaal functionerend HLA uit het ER wordt verwijderd (stap 4). Door het overslaan van de kwaliteitscontrole (stap 1 t/m 3) vindt de afbraak van HLA heel snel en effectief plaats. Daarom hebben we deze HLA-afbraak gebruikt als model voor eiwitafbraak in het algemeen, zodat met deze kennis misschien ook inzichten voor de 70 andere ziektes opgedaan kan worden.

Dit promotie-onderzoek

In dit proefschrift heb ik de HLA-afbraak door US2 en US11 bestudeerd. Hoofdstuk 2 geeft een overzicht van de verschillende manieren waarop virussen de werking van HLA dwarsbomen. Niet alleen CMV, maar alle herpesvirussen én sommige andere virussen hebben namelijk manieren

om op deze manier onzichtbaar te blijven voor het immuunsysteem. Afbraak, zoals US2 en US11 veroorzaken, is maar één van de strategieën. Andere virussen houden HLA bijvoorbeeld gevangen binnen in de cel of zorgen ervoor dat HLA wordt afgeschermd voor het immuunsysteem zodra het het celoppervlak bereikt.

De verschillende onderzoeksprojecten binnen mijn promotieonderzoek gingen in op stappen die in de figuur geschreven staan. Zo hebben we in hoofdstuk 3 opgehelderd welk E2 eiwit uit stap 5 betrokken is bij de afbraak van HLA door US2.

Het geïdentificeerde E2-eiwit was een duidelijke 'missing link' waar we naar konden zoeken, maar we vermoedden dat er meer onbekende spelers waren die minder gemakkelijk te vinden zouden zijn. Daarom hebben we in hoofdstuk 4 systematisch de productie van alle eiwitten in de cel verstoord om te zien welke een rol zouden spelen bij de afbraak van HLA. Hiermee zijn we een proces op het spoor gekomen dat nauw verwant is aan de markering van kapotte eiwitten (stap 5), maar een heel andere rol lijkt te spelen bij de afbraak van HLA.

Ook vonden we met deze systematische aanpak een kanaal dat als de uitgang van het ER zou kunnen functioneren (stap 4). Toen we hier beter naar keken in hoofdstuk 5, zagen we echter dat dit kanaal de productie van US2 beïnvloedt. Deze onverwachte vinding kan voor een andere tak van wetenschap, die zich richt op de productie van eiwitten, een belangrijke rol spelen.

Ten slotte hebben we in hoofdstuk 6 onderzocht hoe de pomp (stap 6) naar het ER wordt gerekruteerd in cellen met US11.

Dankzij deze inzichten hebben we een beter begrip gekregen van de afbraak van HLA door de CMV-eiwitten US2 en US11.

DANKWOORD

Daar is hij dan: de dag die ik dacht dat nooit zou komen. (Eerlijk gezegd had ik ook nooit gedacht dat ik dat vreselijke Koningslied hier zou citeren...) Het aantal momenten waarop ik heb overwogen om te stoppen met mijn promotie is niet op één hand te tellen. Zonder de steun van vrienden, familie, collega's en anderen had ik hier vandaag niet gestaan. Er is dan ook een groot aantal mensen dat ik graag wil bedanken voor hun hulp en steun de afgelopen jaren.

Emmanuel, toen ik bij je langskwam omdat ik een beursaanvraag voor NWO mocht gaan schrijven, was ik al snel om. Niet alleen vond ik virale immuunevasië een fascinerend onderwerp, je enthousiasme werkte ook aanstekelijk. Dat grenzeloze optimisme bleek soms toch een tikje onrealistisch, maar het werkte altijd opbeurend als ik het na een reeks mislukte experimenten even niet meer zag zitten. Bedankt voor je steun en oprechte betrokkenheid op de momenten dat het met mij op persoonlijk vlak wat minder ging. Dankzij jouw flexibele insteek kon ik vier dagen per week gaan werken en kreeg ik de kans me te ontplooien op andere gebieden. Natuurlijk wil ik je ook heel erg bedanken voor je begeleiding. Met name in de laatste maanden hebben we veel samen gezeten en zijn er nog goede ideeën voor de projecten bijgekomen.

Robert Jan, na je intensieve begeleiding bij de screen in mijn eerste jaar is het contact helaas wat verwaterd. Toch ben ik altijd blijven waarderen hoe je op de achtergrond meedacht met mijn projecten, ook toen die steeds verder van jouw expertise af kwamen te staan. De dagen waarop we de daadwerkelijke screen hebben gesort, zijn een paar van de intensiefste geweest van mijn hele promotie. Het schepte een bijzondere band om die lange dagen samen met jou te doorstaan. Bedankt ook voor de onmisbare rol die je speelt in de onderzoeksgroep. Je brengt een stuk ervaring en realisme mee die mijn begeleiding altijd in balans hebben gehouden.

Ingrid, zonder jouw pipetteerskills was dit boekje maar half zo dik geworden. Niet alleen weet je in drie dagen per week bergen aan experimenten uit te voeren, er was ook genoeg tijd voor koffie tussendoor. Op de momenten dat ik mezelf weer eens dreigde te verliezen in het werk, was jij er altijd om me er even tussenuit te trekken en samen naar de Koffiecorner te gaan. We hebben veel goede gesprekken gevoerd en je bent een fantastische, betrokken en lieve collega. Je organiseertalent wordt wel eens ondergewaardeerd in de groep, maar tijdens onze samenwerking ben ik gaan inzien hoe essentieel een goede administratie is om je data ooit nog terug te kunnen vinden. Ik denk dat er niemand is die zoveel van mijn proefschrift heeft gelezen als jij, en ik sta nog steeds perplex hoe je uit je hoofd sgRNA-sequenties en productnummers van antilichamen wist te verbeteren. Super leuk dat je op deze bijzondere dag naast me wilt staan als paranimf!

Jery, of Jerybaan, de dinsdag is lang onze vaste klimavond geweest (en laten we onze goede voornemens vooral waarmaken om dat door te zetten!). Met al die klimavonden, entetjes vooraf en fietstochten heen en terug hebben we elkaar goed leren kennen. Ik heb groot respect voor je doorzettingsvermogen als je weer eens 'een rondje IJsselmeer' wist te skaten of andere fysieke uitdagingen aanging. Je woordgrappen en Photoshop-skills waren altijd een geniale inbreng in de MMB aio app. Ook jij hebt niet de gemakkelijkste periode gehad tijdens je promotie, maar ik vond het fijn om onze ervaringen te kunnen delen. Het maakt het des te bijzonderder dat ook

jij als paranimf aan mijn zijde staat op 2 april. Na een onderbreking ben ook jij weer vol aan de bak. Heel veel succes met de laatste loodjes van je eigen promotie – ik heb er alle vertrouwen in dat je dat binnenkort ook tot een mooi einde weet te brengen!

Als een van de weinige aio's heb ik het geluk mogen hebben om vanaf dag 1 op hetzelfde kantoor te kunnen blijven. Room dinners (inmiddels toch wat in de vergetelheid geraakt...) en gezamenlijke Koepel-kostuums schepten altijd een goede band. Nooit gedacht dat mijn krav maga-verleden ons nog eens de kostuumprijs op zou leveren! In de jaren dat ik op de kamer zat, zijn er heel wat roomies gekomen en gegaan, en ik wil jullie allemaal bedanken voor de fijne sfeer die er altijd op de kamer is geweest:

Kirsten, wat bijzonder om een collega te vinden die in zoveel opzichten op mezelf lijkt. Lange tijd ben je mijn buurvrouw geweest op kantoor, en het was wel even slikken toen je de kamer moest verlaten. Gelukkig loop je nog steeds op de afdeling rond, zodat we toch nog af en toe kunnen bijkletsen over onze nieuwe huizen en banen (oh, wat zijn we burgerlijk geworden!) onder het genot van een cappuccino. Laten we dat vooral voortzetten nu we toch nog semi-collega's zijn bij de BMW Bachelor!

Wouter, op dezelfde dag begonnen als ik, en lekker voortvarend je promotie afgerond - echt knap gedaan! In een ver verleden hebben we nog een Russische kerstborrel georganiseerd, dat zou ik alweer bijna zijn vergeten. Als dokter moest je wel even wennen aan de afdeling, maar je hebt het fantastisch gedaan hier. Samen met **Steven** en **Kobus** waren jullie een fantastisch trio dat altijd leven in de brouwerij bracht. Kobus, jij ook veel succes bij je eigen promotie, een paar dagen na de mijne!

Mike, koning co-IP, bedankt voor alle technische skills die me hebt geleerd. Ook jij hebt niet het gemakkelijkste einde van je promotie gehad, maar ik denk dat je er een mooier mens door bent geworden. Heel veel succes in Oxford en met je verdere loopbaan!

Manouk, oud-buurvrouw in Couwenhoven en kamergenoot, bedankt voor het water geven van onze plantjes tijdens vakanties, en voor je bemoedigende woorden vanuit Edinburgh toen het met mij even wat minder ging! Ik ben blij om te merken dat jij er zo goed bovenop bent gekomen en het naar je zin hebt in de Schotse bergen.

Samantha, samen hebben wij heel wat Illustrator skills geleerd waarmee we onze figuren naar een hoger niveau konden tillen. Met onze koophuizen hebben we de burgerlijkheidspunten van de kamer samen flink opgekrikt. Leuk om de spannende periode van een huizenzoektocht met elkaar te kunnen delen. Je hebt mijn stekje gezien, nu ik het jouwe nog! Samen waren we aan het afronden en ook dat schepte een goede band. Wat een gek idee dat je er niet meer was de laatste maanden, omdat ik er op het laatst toch wat langer over bleek te doen dan jij. Ik wens je heel veel succes met je post-doc bij het Hubrecht!

Yuxi, or Dr. van Hensbergen-Zhao by the time I graduate, thank you for the amazing food during room dinners and other random moments in the office! From a somewhat shy girl you gradually developed into the fun and teasing colleague you are now. We will all miss you when you return to China with Vincent van H. after your graduation, but I hope you will also enjoy being back in your home country!

Rob, voor jou ook de allerlaatste loodjes op het moment dat je dit proefschrift ontvangt. Het was

erg leuk om nog een klimmer in de kamer te hebben en te horen over je vele buiten-avonturen met Annemarie. Met Jerry als mijn plaatsvervanger blijft het aantal klimmers in de kamer toch nog even op peil! Heel veel succes met je eigen verdediging!

Vincent de M., bedankt voor je hulp als ik als digibeeet weer eens iets niet voor elkaar kreeg. Je was de rustige, stille kracht in onze kamer, maar altijd betrokken. Ook jij heel veel succes met schrijven en afronden!

Gosia, Stephanie, Dennis, Lianne en Janneke, vanwege het wat rommelige einde van mijn promotie heb ik jullie helaas maar weinig mee mogen maken. Wel hebben we nog goede gesprekken gevoerd in mijn laatste weken op de afdeling, waardoor ik jullie op de valreep toch wat beter heb leren kennen. Ik wens ook jullie allemaal veel succes de komende jaren. Als kamer-oma wil ik jullie meegeven dat je altijd op je grenzen moet letten. Maak niet te lange dagen (dat kan altijd nog in de laatste maanden van je promotie...)!

Ferdy, als ik jou in de gang tegenkwam, was het zo vier uur later! Wat hebben wij een boel goede gesprekken gevoerd over politiek, geschiedenis, klimaat, en wat niet. Samen hebben we de wereldproblemen allang opgelost. Waar ik zelf niet kon wachten tot het afronden van mijn promotie, wilde jij het liefst nog even blijven hangen vanwege de onzekerheid erna. Super knap dat je je schouders eronder hebt gezet en zelfs al vlak na mij gaat promoveren. Ik vind het een eer om je paranimf te mogen zijn in juni!

Hanneke, het is alweer even geleden dat je de afdeling hebt verlaten voor een baan die zoveel beter bij je bleek te passen. Wat hebben we veel goede gesprekken gevoerd voordat je ging, en zelfs nog daarna (onder het genot van een pizzaból). Onze manier van denken over wetenschap bleek erg op elkaar te lijken en ik waardeer nog steeds de inzichten die ik aan het begin van mijn promotie van jou heb gekregen.

Jasper, veel succes met je eigen verdediging kort na de mijne. ‘Work hard, play hard’ was duidelijk jouw motto tijdens je promotie. Hoe je het volhield is me een raadsel, maar het is je gelukt om vrijwel binnen de normale tijd een prachtig boekje af te leveren. De laatste keer dat ik je sprak was je je actief aan het oriënteren op een baan in het bedrijfsleven. Dat moet zeker goedkomen met jouw arbeidsethos!

The others from the Wiertz/Lebbink group, **Patrique, Hendrik, Shu and Anouk E.**, I wish you all the best with your research projects!

Over the years I was honored to supervise such talented and enthusiastic students. Thank you **Daan, Ellen, Louella and Tomás**. I really enjoyed supervising you and I’m proud to see how you are continuing your professional lives.

Piet, mijn oud-achterbuurman op het lab, bedankt voor je onuitputtelijke kennis van al wat labgerelateerd is! Natuurlijk zijn er nog veel meer **MMB collega’s** die ik hier niet heb genoemd. Uiteraard wil ik jullie ook allemaal bedanken voor de fijne sfeer op de afdeling en de vele sociale

activiteiten die de collegiale band versterken! Ik ben er zelf niet altijd bij geweest, maar heb ook genoten van de verslagen over de app.

Ineke, als aio-begeleidingscommissie was je een fantastische steun in mijn rug. Het was inspirerend om ook eens op een heel andere manier over onderzoek te brainstormen en ik heb het enorm gewaardeerd dat je ondanks je drukke agenda ook over mij wilde ontfermen. Ik voelde me bijna een van je eigen aio's toen ik bij je thuis aan de keukentafel mijn project mocht bespreken omdat je eigenlijk met sabbatical was. Heel erg leuk dat je bij mijn promotie aan de andere kant van de tafel zit!

Ik mag dan wel weg zijn bij de MMB, toch loop ik nog steeds rond in het UMC. Ook mijn nieuwe **28+ brothers on the 4th floor** wil ik bedanken voor de fijne sfeer op mijn nieuwe werkplek. Hoewel ik er pas kort rondloop, voelt het als één grote familie. Super leuk hoe jullie al meteen op mijn eerste werkdag vroegen wanneer mijn promotie zou zijn, zodat hij meteen in de agenda's kon!

Natuurlijk zijn er ook een boel mensen buiten het werk die veel voor me hebben betekend tijdens mijn promotie. **Astrid** en **Kelly**, jullie hebben mij al heel wat jaartjes meegemaakt en ik vind het heel erg leuk dat we nog altijd contact hebben. Juist omdat jullie me al zo lang kennen, was het soms vast ook duidelijk dat het niet altijd even leuk was tijdens mijn promotie, maar gelukkig had ik daarbij veel steun aan jullie en hebben we ook altijd zát andere (leukere) dingen om over te praten. Hopelijk wordt het de komende tijd gemakkelijker om etentjes te plannen, wanneer mijn promotie achter de rug is en Astrid (hopelijk!) de opleiding Kindergeneeskunde in is gekomen. Dat er nog maar vele jaren van vriendschap mogen volgen!

Hester, ondanks alle spookverhalen van mijn kant ben je zelf ook aan een promotietraject begonnen. Hoewel jouw type onderzoek totaal anders is dan het mijne was, heb je inmiddels wel door waar ik nou altijd over zeurde... Ondanks de tegenslagen die erbij horen, heb je een heel bewuste keuze gemaakt voor dit onderzoek en dat vind ik erg knap. Ik heb groot respect voor de omscholing die je hebt gevolgd en die je nu hier heeft gebracht. Met jouw doorzettingsvermogen en unieke blik vanuit twee disciplines weet ik zeker dat er veel kansen voor je gaan zijn als je het weet af te ronden. Nog even doorbijten!

Lione, Susanne, Daniëlle en **Albert**, mijn BMW-vriend(innet)jes uit groepje 9 en 10. Van al mijn vrienden weten jullie toch het beste wat het inhoudt om in de biomedische wetenschappen te promoveren. Met de helft van jullie kon ik mijn smart delen over de obstakels in een promotieonderzoek; de andere helft van jullie heeft de verstandige keuze gemaakt om er nooit aan te beginnen... Tijdens het Ardennen-weekendje vorig jaar heb ik jullie op een nieuwe manier leren kennen. Het komt niet vaak voor dat je met een groep zo op één lijn zit, dus dat geplande weekend na het afronden van onze promoties moeten we zeker ook nog maar gaan prikken binnenkort!

Ook het **bestuur van KlimaatGesprekken** wil ik graag bedanken. Bij de quote voorin dit proefschrift (*'Not in our heads but in our hearts lies the power that leads us to the greatest deeds'*) denk ik ook nadrukkelijk aan jullie. Jullie mogen dan misschien inhoudelijk niet betrokken zijn geweest bij mijn onderzoek; ik denk dat de inhoud slechts een klein deel is van wat een promotietraject behelst. De uiteindelijke waarde zit hem in de persoonlijke ontwikkeling die je doormaakt in deze snelkookpan. Niet alleen wil ik jullie bedanken voor de rol die jullie hebben gespeeld bij het oplossen van mijn eigen cognitieve dissonantie op het gebied van klimaat - waar ik voorheen toch wel erg lang mijn kop voor in het zand heb gestoken, - ook wil ik jullie bedanken voor jullie warme, vriendelijke houding die ik ook voor mezelf nog meer eigen hoop te maken. Ik zie ernaar uit om, nu ik mijn onderzoek eindelijk af heb weten te ronden én hopelijk wat beter met mijn work/life balance om kan gaan, eindelijk als klimaatcoach bij jullie aan de slag te gaan!

Een zelfde vriendelijke houding heb ik altijd ervaren bij **Caroline Kraaijvanger** van Scientias. Dankjewel Caroline, dat je zo enthousiast bent geweest over mijn stukken, terwijl ik zelf nog een beetje moest wennen aan de nieuwe toon die zo anders is dan bij een wetenschappelijk artikel. Dankzij jou heb ik mijn levenslange hobby, het schrijven van verhaaltjes, na bijna 20 jaar weer op weten te pakken! Bij vlagen kon ik niet stoppen met schrijven, en dan had ik weer een writer's block of simpelweg geen tijd. Jouw vertrouwen en aanmoedigende woorden hebben me er altijd bovenop geholpen als ik weer een tijdje niks geproduceerd kreeg. Nu al het schrijfwerk voor het proefschrift achter de rug is en ik weer meer tijd zou moeten hebben, hoop ik mijn writer's block voor Scientias ook weer snel te doorbreken!

Not all people in these acknowledgements will be able to actually read these words. Nevertheless, I can't withstand thanking you for the life experiences and insights I gained by you. Thank you **Bharat, Balkrishna & Radhika**, and **Surya & Aamaa**. You have taught me the valuable lesson that compassion will always be more important than ambition, and that pursuing an ambitious career is a very limited goal in life. Nepal will always be in my mind. मुरी मुरी धन्यवाद.

Lieve **Theo** en **Marion**, op zulke lieve schoonouders als jullie had ik nooit durven hopen. Ik wil jullie bedanken voor de onwaardelijke liefde en acceptatie die ik bij jullie ervaar en de openheid waarmee we over alles kunnen praten. Jullie vriendelijke, open en ontspannen levenshouding is voor mij een bron van inspiratie op weg naar een gelukkiger leven.

Gijs en **Kim**, de schoonfamilie is natuurlijk niet compleet zonder jullie. Het is fijn om de levenslessen die ik in Nepal heb opgedaan met jullie te kunnen delen. Met al jullie reizen hebben jullie waarschijnlijk al een veelvoud hiervan ervaren. Het feit dat we qua promoveren ook in hetzelfde schuitje zaten, elk op onze eigen manier, heeft me steun en relativeringsvermogen gegeven. Bij dezen kan ik zeggen dat er een last van je schouders valt wanneer je het weet af te ronden - dus ik kijk uit naar jullie promoties!

Manon, ik heb zoveel respect gekregen voor hoe jij jaren geleden je eigen crisis te boven bent gekomen. Op mijn eigen dieptepunt is dat een bron van hoop geweest. Omdat we niet bij elkaar

om de hoek wonen, zien we elkaar minder vaak dan ik zou willen. Maar jouw bezoekjes aan mij op je vrije dag of voorafgaand aan een late dienst hebben me veel goed gedaan toen ik thuis zat. Ook **Nander** wil ik bedanken voor zijn bijdrage aan de familie, en natuurlijk in het bijzonder voor de rol die je speelt in Manon's leven. Het scheidt een band om een mede-biomedicus in de familie te hebben, die ook nog eens geïnteresseerd is in wetenschapscommunicatie en schrijven. Tegelijkertijd zijn we op zoek geweest naar een nieuwe baan en die hebben we ook nog bijna op hetzelfde moment gevonden. Ik hoop dat het je goed bevalt bij de RVO tegen de tijd dat je dit proefschrift ontvangt!

Yosca, met een beetje geluk lukt het je om je ogen open te houden op 2 april, jetlagged als je zal zijn zo net na je terugkomst uit Zuid-Amerika. Ik ben trots dat je deze reis alleen hebt durven ondernemen (en als grote zus toch ook wel een beetje bezorgd geweest) en hoop dat het je naast mooie ervaringen ook even afstand heeft kunnen geven van de situatie hier. Ik vind het mooi om te zien hoe je bent gegrepen door je werk en hoe je vanuit je studie al stappen hebt gezet om te komen waar je nu bent. Maar het meeste ben ik onder de indruk van de sterke jonge vrouw die je bent geworden. Niemand heeft verdiend wat jij moest meemaken, maar ik heb groot ontzag voor de kracht die je het afgelopen jaar hebt getoond. Ik hoop dat je ons altijd weet te vinden als je daar behoefte aan hebt.

Maurits, hoeveel mensen er ook aanwezig zijn bij mijn promotie, het feit dat jij er niet meer bij kunt zijn laat een leegte achter die voor ons allemaal moeilijk en pijnlijk blijft. Bedankt voor de mooie jaren die je Yosca hebt kunnen geven voordat je ons, veel en veel te vroeg, moest verlaten.

Lieve **pap en mam**, dankjulliewel voor de steun die jullie altijd voor mij zijn geweest. Interesse in biologie heb ik met de paplepel ingegoten gekregen en het was leuk om met jullie te kunnen delen waar mijn onderzoek over ging. Nu we dichterbij jullie wonen is het wat vaker gelukt om op woensdag bij elkaar langs te gaan, en daar heb ik erg van genoten. Ik heb veel steun gehad aan jullie telefoontjes toen ik op mijn dieptepunt zat en ik ben blij dat we zo open hebben kunnen praten. Ik blijf toch meer op jullie te lijken dan ik altijd dacht, nu ik zelf ook een tuin en huis heb waar ik in los kan gaan... Ik vind het leuk dat ik ook op die vlakken met jullie kan sparren en hoop nog veel van jullie te kunnen leren!

Lieve **Marc**, op mijn promotiedag is het precies 6 jaar geleden dat we onze onovertroffen 'eerste date' in New York afsloten met de musical Chicago. Wie had gedacht dat 'een oud- en nieuw feestje met vrijgezelle mannen' bij Ruben en Annemiek ertoe zou leiden dat wij, bijna zes en half jaar en 2 huisjes, 50 (haag)boompjes en 2 beestjes verder, nog steeds bij elkaar zouden zijn? Met jouw kalmte ben je voor mij absoluut een rots in de branding geweest tijdens de emotionele achtbaan van de afgelopen jaren. Ik heb ontzettend veel van je geleerd, van meditatie en kalmte bewaren tot kennis van geschiedenis, de maatschappij en willekeurige 'Quite Interesting' feitjes. Je hebt van mij een mooier mens gemaakt. De gebeurtenissen van het afgelopen jaar hebben me doen inzien dat een gelukkig samenzijn niet vanzelfsprekend is. Het heeft me nog meer doen beseffen dat we alle mooie momenten samen moeten koesteren, en ik hoop dat die er nog veel mogen komen. Ik hou van je!

CURRICULUM VITAE

Anouk Schuren was born on August 19, 1990 in Haren (Gn.), The Netherlands. In 2008, she graduated *cum laude* from her pre-university education (VWO, Nature & Technology and Nature & Health, with German as additional subject) at the Rembrandt College in Veenendaal. She continued her studies at Utrecht University, with a Bachelor's degree in Biomedical Sciences, from which she graduated *cum laude* in 2011. During her Bachelor, Anouk was admitted to the Honours Programme, for which she performed an extracurricular internship at the University of Cambridge (UK) in 2010. Her Bachelor thesis 'An antiviral immune response turning against the host in pathogenic HIV infection' was awarded with the Suzanne Hovinga thesis award.



In 2011, she started the Master's programme Infection & Immunity at Utrecht University. During this Master, she performed internships at the Wilhelmina Children's Hospital (Utrecht, The Netherlands) under supervision of Dr. José Borghans and Dr. Kiki Tesselaar (2011-2012), and at the Icahn School of Medicine at Mount Sinai (New York City, USA) in the group of Prof. Adolfo García-Sastre (2013). Her Master's thesis was written in collaboration with the University Medical Center St. Radboud (Nijmegen, The Netherlands) under supervision of Prof. Robert Sauerwein.

When Anouk graduated her Master of Science in 2013, she obtained a research grant from the NWO Graduate Programme to fund her PhD research at the University Medical Center Utrecht. This research was supervised by Prof. Emmanuel Wiertz and Dr. Robert Jan Lebbink, and focused on the human cytomegalovirus immune evasion proteins US2 and US11. The results of this research are described in this thesis and have partly been published in scientific journals. During her PhD, Anouk has worked as a primary school teacher in Banasthali (Kathmandu area, Nepal; 2014) and as a freelance science journalist for Scientias.nl since 2016. She has also volunteered for environmental foundations, including a position as board secretary for Stichting KlimaatGesprekken (2017-2018).

In January 2019, Anouk continued her career as a policy officer for the Biomedical Sciences Bachelor education at Utrecht University/UMC Utrecht. She combines this job with volunteering as a climate coach, coaching group workshops by Stichting KlimaatGesprekken.

SCIENTIFIC PUBLICATIONS

A.B.C. Schuren, I.G.J. Boer, E.M. Bouma, M.L. van de Weijer *et al.* The UFM1 pathway impacts HCMV US2-mediated degradation of HLA class I. (*submitted*)

A.B.C. Schuren, G.J. Brak-Boer, E.M. Bouma *et al.* Genetic editing of SEC61/62/63 abrogates HCMV US2-mediated HLA-I degradation by regulating US2 expression. (*submitted*)

M.L. van de Weijer*, A.B.C. Schuren*, G.J. Brak-Boer *et al.* P97 association with UBXD8 is essential for HCMV US11-mediated HLA class I degradation. (*submitted*)

M.L. van de Weijer*, A.B.C. Schuren*, D.H.J. van den Boomen *et al.* Multiple E2 ubiquitin-conjugating enzymes regulate human cytomegalovirus US2-mediated immunoreceptor downregulation. *J Cell Sci* (2017) 130:2883-2892

A.B.C. Schuren*, A.I. Costa* and E.J.H.J. Wiertz. Recent advances in viral evasion of the MHC class I processing pathway. *Curr Opin Immunol* (2016) 40:43-50

A.B.C. Schuren and K. Tesselaar. Plasmacytoïde dendritische cellen in de strijd tegen HIV: vloek of zegen? *HIV Bulletin* (2012) 2:27-29

* *Shared first co-authorship.*

POPULAR-SCIENTIFIC PUBLICATIONS

A.B.C. Schuren. Het einde van gas is pas het begin van de toekomst. Scientias.nl (2018)

A.B.C. Schuren. De antibioticaresistentie te lijf: dag antibiotica, hallo fagen! Scientias.nl (2017)

A.B.C. Schuren. De grootste bedreiging voor het klimaat? Jouw brein! Scientias.nl (2017)

A.B.C. Schuren. Vaccineren: levensgevaarlijk of levensreddend? Scientias.nl (2017)

A.B.C. Schuren. De grieprik: levensreddend of levensgevaarlijk? Scientias.nl (2016)

A.B.C. Schuren. Een wereld zonder plastic is dichterbij dan je denkt. Scientias.nl (2016)

A.B.C. Schuren. Herpes: een slim virus dat terugvecht. Scientias.nl (2016)